University of Wollongong

Research Online

University of Wollongong Thesis Collection 2017+

University of Wollongong Thesis Collections

2017

Coordinated Voltage Control in Modern Distribution Systems

Dothinka Ranamuka Rallage
University of Wollongong

Follow this and additional works at: https://ro.uow.edu.au/theses1

University of Wollongong

Copyright Warning

You may print or download ONE copy of this document for the purpose of your own research or study. The University does not authorise you to copy, communicate or otherwise make available electronically to any other person any copyright material contained on this site.

You are reminded of the following: This work is copyright. Apart from any use permitted under the Copyright Act 1968, no part of this work may be reproduced by any process, nor may any other exclusive right be exercised, without the permission of the author. Copyright owners are entitled to take legal action against persons who infringe their copyright. A reproduction of material that is protected by copyright may be a copyright infringement. A court may impose penalties and award damages in relation to offences and infringements relating to copyright material. Higher penalties may apply, and higher damages may be awarded, for offences and infringements involving the conversion of material into digital or electronic form.

Unless otherwise indicated, the views expressed in this thesis are those of the author and do not necessarily represent the views of the University of Wollongong.

Recommended Citation

Rallage, Dothinka Ranamuka, Coordinated Voltage Control in Modern Distribution Systems, Doctor of Philosophy thesis, School of Electrical, Computer and Telecommunications Engineering, University of Wollongong, 2017. https://ro.uow.edu.au/theses1/142

Research Online is the open access institutional repository for the University of Wollongong. For further information contact the UOW Library: research-pubs@uow.edu.au

UNIVERSITY
OF WOLLONGONG
AUSTRALIA

School of Electrical, Computer and Telecommunications Engineering

Faculty of Engineering and Information Sciences

Coordinated Voltage Control in Modern Distribution Systems

Dothinka Ranamuka Rallage (MEng)

This thesis is presented as part of the requirements for the

Award of the Degree of

Doctor of Philosophy

of the

University of Wollongong

November 2017

Dedicated to My Wife, Menaka Subhashini and Son,
Aushada Ranamuka Rallage …

CERTIFICATION

I, Dothinka Ranamuka Rallage, declare that this thesis, submitted in partial fulfilment of the requirements for the award of Doctor of Philosophy, in the School of Electrical, Computer and Telecommunications Engineering, Faculty of Engineering and Information Sciences, University of Wollongong, is wholly my own work unless otherwise referenced or acknowledged. This manuscript has not been submitted for qualifications at any other academic institution.

Dothinka Ranamuka Rallage
Date: 01 November 2017

ACKNOWLEDGEMENT

It is my responsibility to extend sincere appreciation to all who rendered support in numerous ways to make my research project a success. First and foremost, I wish to express my sincere gratitude and respect to my supervisors Professor Kashem Muttaqi and Dr. Ashish Agalgaonkar of the University of Wollongong, for the excellent guidance throughout my postgraduate study period in many ways. You both have always been more than supervisors to me. Your knowledge, experience, dedication and patience inspired me to become an independent researcher and helped me realise the power of critical thinking. I really admire all of your encouragement, insightful comments, guidance and kind support given to complete my research.

I gratefully acknowledge the support by the personnel at Endeavour Energy distribution utility company, New South Wales Australia in providing data and relevant information for the distribution system test feeders.

I wish to convey my heartiest appreciation and special thanks to Illawarra Coal-BHP Billiton Ltd and Teleo Engineering Pvt Ltd for the financial support given to me by a project electrical engineer employment. Without this rare and valuable support, starting this PhD research had to be a night mare for me. Also, I gratefully acknowledge the kind support given by Valerie Williams in proof-reading my thesis.

My heartiest gratitude goes to my wife Menaka Subhashini for her honest support and love given to me during this research project. Also, I am indebted to my mother Olga Malathi Vidanage, my farther Somadasa Ranamuka Rallage, my sister Upulwan Indira Ranamuka Rallage, brother in law Sarath Wimalathunga and my sister's daughter Kavindya Wethmini for their continuous encouragement, loving words and mental care given to me during my studies.

My heartiest love goes to my special son Aushada Ranamuka Rallage. Almost all the new ideas in this thesis came into my mind, when I hugged him and slept on our small bed with our cat. Once he was in deep sleep, I jumped out from the bed

and jotted down those ideas in a piece of a paper, and next day I made them into reality deserving many barriers. During this research project, our story was almost similar to the story in Walt Disney movie Bambi, which is about a farther and his son Bambi. My loving Bambi, I believe that your innocence face, loving words, heart beat and secrets were my strength behind this work. At last, I hope nature will support me to wait until you are also doing something new for this wonderful world. I have already proved you that human beings can do good things at any time of their lives.

ABSTRACT

Modern distribution systems, especially with the presence of distributed generation (DG) and distribution automation are evolving as smart distribution systems. Distribution management systems (DMSs) with communication infrastructure and associated software and hardware developments are integral parts of the smart distribution systems. With such advancement in distribution systems, distribution system voltage and reactive power control are dominant by Volt/VAr (voltage and reactive power) optimisation and utilisation of DG for system Volt/VAr support. It is to be noted that the respective controls and optimisation formulations are typically adopted from primary, secondary and tertiary voltage and reactive power controls at upstream system level. However, the characteristics of modern distribution systems embedded with high penetration of DG are different from transmission systems and the former distribution systems with uni-directional power flow. Also, coordinated control of multiple Volt/VAr support DG units with other voltage control devices such as on-load tap changer (OLTC), line voltage regulators (VRs) and capacitor banks (CBs) is one of the challenging tasks. It is mainly because reverse power flow, caused predominantly by DG units, can influence the operation of conventional voltage control devices. Some of the adverse effects include control interactions, operational conflicts, voltage drop and rise cases at different buses in a network, and oscillatory transients. This research project aimed to carry out in-depth study on coordinated voltage control in modern MV distribution systems utilising DG for system Volt/VAr support.

In the initial phase of the research project, an in-depth literature review is conducted and the specific research gaps are identified. The design considerations of the proposed coordinated voltage control, which also uses the *concept of virtual time delay*, are identified through comprehensive investigations. It emphasises on examining and analysing both steady-state and dynamic phenomena associated with the control interactions among multiple Volt/VAr support DG units and voltage control devices. It would be essential for ensuring effective coordinated

voltage control in modern distribution systems. In this thesis, the interactions among multiple DG units and voltage control devices are identified using their *simultaneous and non-simultaneous responses* for voltage control through time domain simulations. For this task, an analytical technique is proposed and small signal modelling studies have also been conducted. The proposed methodology could be beneficial to distribution network planners and operators to ensure seamless network operation from voltage control perspective with increasing penetration of DG units. Notably, it has been found that the significant interactions among multiple DG units and voltage control devices are possible under conventional standalone, rule-based, and analytics based control strategies as well as with real-time optimal control under certain system conditions.

In the second phase of the research project, the proposed coordinated voltage control strategy is elaborated. The control design considerations are fundamentally based on eliminating the adverse effects, which can distinctly be caused by the *simultaneous and non-simultaneous responses* of multiple Volt/VAr support DG units and voltage control devices. First, the *concept of virtual time delay* is applied for dynamically managing the control variables of Volt/VAr support DG units and voltage control devices through the proposed *control parameter tuning algorithm*. Because it has been found that the conventional time-graded operation cannot eliminate the adverse effects of DG-voltage control device interactions under certain system conditions. Secondly, the distinct control strategies are designed and tested for effectively and efficiently coordinating the operation of multiple Volt/VAr support DG units and voltage control devices in real-time. The test results have demonstrated that the proposed coordinated voltage control strategy for modern MV distribution systems can effectively be implemented in real-time using advanced substation centred DMS. The proposed coordinated voltage control strategy presented in this thesis may trigger paradigm shift in the context of voltage control in smart distribution systems.

In the final phase of the research project, short-term and/or long-term oscillations which can be possible for a MV distribution system operation embedded with

Volt/VAr support DG are discussed. Typically, the short-term oscillations are occurred due to interactions among different DG units and their controllers (i.e., inter-unit electro-mechanical oscillations in synchronous machine based DG units) while the long-term oscillations occurred due to DG-voltage control device interactions. Also, sustained oscillations may occur due to tap changer limit cycle phenomenon. The concept of *alert-state voltage control* is introduced for mitigating the sustained oscillations subjected to OLTC limit cycles in the presence of high penetration of DG. The investigative studies in this thesis further emphasise the requirements of supplementary control and other mitigating strategies for damping the oscillations in modern active MV distribution systems. The proposed research will pave the way for managing increasing penetration of DG units, with different types, technologies and operational modes, from distribution system voltage control perspective.

"Since reactive power cannot be transmitted over long distances, voltage control has to be affected by using special devices dispersed throughout the power system. The proper selection and coordination of equipment for controlling reactive power and voltage are among the major challenges of power system engineering".

Prabha Kundur (Power System Stability and Control/Section 11.2)

LIST OF PRINCIPAL SYMBOLS AND ABBREVIATIONS

[A]	state matrix
a	tap ratio
a, b, c	phase-a, b and c of a three phase system
ABS	Air break switch
B	susceptance
$\underline{c}$	intercept of a linear variation
CHP	combined heat and power
CM-BSO	control module for blocking simultaneous responses
CT	current transformer
CVR	conservation voltage reduction
DB	dead-band
DFIG	doubly-fed induction generator
DG	distributed generation
DG-VCM	DG voltage control module
DMS	distribution management system
DNO	distribution network operator
D_{sij}	electrical distance between nodes i and j
DSCADA	distribution level SCADA
DSTATCOM	distribution static compensator
E'	voltage behind the sub-transient inductance
E_f	exciter field voltage
F	magnetomotive force (*mmf*)
H	inertia coefficient
HV	high voltage
I	current magnitude
i	current phasor value
[I]	identity matrix
IEEE	Institution of Electrical and Electronics Engineers
J	objective function
k_L	load factor

L'	sub-transient inductance
LDC	line drop compensator
LG	Local Generation
LV	low voltage
$\underline{m}$	gradient of a linear variation
MINLP	mixed integer non-linear programming
MV	medium voltage
OLTC	on-load tap changer, also denoted as load tap changer (LTC)
P	active power
$P^{\wedge}$	number of poles
PV	photovoltaic
Q	reactive power
QP	quadratic programming
R	resistance
ref	reference value
RER	renewable energy resource
S	apparent power
s	state of any system configuration
SCADA	supervisory control and data acquisition
SVR	step voltage regulator, also denoted as voltage regulator (VR)
T	time delay
t	time
T_{em}	electro-mechanical torque
T_m	mechanical torque produced by turbine
V	voltage magnitude
v	voltage phasor value
VAr	reactive power
Volt	voltage
VT	voltage transformer
X	reactance
x	state variable
Y	admittance magnitude

Z	impedance magnitude
ε_t	hysteresis tolerance value
α	phasor angles, α of nodal voltages
λ	steady state flux linkage
λ'	sub-transient flux linkage
μ_{sij}	attenuation of voltage variation between node *i* and *j*
δ	rotor angle
Ψ	resultant of the vector addition of stator and rotor *mmf*s
ω	rotary speed
ω_e	synchronous speed
ω_{rm}	prime mover speed

PUBLICATIONS ARISING FROM THIS THESIS

Journal Publications:

1. D. Ranamuka, A. P. Agalgaonkar, and K. M. Muttaqi, "Examining the Interactions between DG Units and Voltage Regulating Devices for Effective Voltage Control in Distribution Systems," *IEEE Transactions on Industrial Applications*, vol. 53, no. 2, pp. 1485-1496, Mar. 2017.

2. D. Ranamuka, A. P. Agalgaonkar, and K. M. Muttaqi, "Online Voltage Control in Distribution Systems with Multiple Voltage Regulating Devices," *IEEE Transactions on Sustainable Energy*, vol. 5, no. 2, pp. 617-628, Apr. 2014.

3. D. Ranamuka, A. P. Agalgaonkar, and K. M. Muttaqi, "Online Coordinated Voltage Control in Distribution Systems Subjected to Structural Changes and DG Availability," *IEEE Transactions on Smart Grid*, vol. 7, no. 2, pp. 580-591, Mar. 2016.

4. D. Ranamuka, A. P. Agalgaonkar, K. M. Muttaqi, and M. J. E. Alam "Mitigating Tap Changer Limit Cycles in Modern Electricity Networks Embedded with Local Generation Units," *IEEE Transactions on Industrial Applications*, vol. 52, no. 1, pp. 455-465, Jan./Feb. 2016.

5. D. Ranamuka, A. P. Agalgaonkar, and K. M. Muttaqi, "Investigating the Operation of Multiple Voltage Regulators and DG in a Distribution Feeder", *ELSEVIER Energy Procedia,* vol. 14, pp. 1945-1950, 2012.

Conference Publications:

1. D. Ranamuka, A. P. Agalgaonkar, and K. M. Muttaqi, "Dynamic Adjustment of OLTC Parameters using Voltage Sensitivity while utilising DG for Volt/VAr Support", in *Proc. 2014 IEEE Power Engineering Society (PES) Conf.*, pp. 1-5.

2. D. Ranamuka, A. P. Agalgaonkar, and K. M. Muttaqi, "Mitigating Tap-changer

Limit Cycles in Modern Electricity Networks Embedded with Local Generation Units," in *Proc. 2014 IEEE Industrial Applications Society (IAS) Conf*., pp. 1-8.

3. D. Ranamuka, A. P. Agalgaonkar, and K. M. Muttaqi, "Examining the Interactions between DG Units and Voltage Regulating Devices for Effective Voltage Control in Distribution Systems," in *Proc. 2015 IEEE Industrial Applications Society (IAS) Conf*., pp. 1-8.

4. D. Ranamuka, A. P. Agalgaonkar, and K. M. Muttaqi, "Simulink Model for Examining Dynamic Interactions Involving Electro-Mechanical Oscillations in Distribution Systems, in *Proc. 2015 Australasia Power Engineering Conf. (AUPEC)*, pp. 1-5.

Publications under Review:

1. D. Ranamuka, A. P. Agalgaonkar, and K. M. Muttaqi, "Dynamic Adjustment of Volt/VAr Control Set-points for Minimising Interactions and Power Losses in Distribution Grids," *Applied Energy Journal*.

2. D. Ranamuka, A. P. Agalgaonkar, and K. M. Muttaqi, "Novel Volt/VAr Control Scheme using Voltage Regulating Devices and Renewable DG Units for Modern Distribution Systems," *IEEE Transactions on Smart Grid*.

3. D. Ranamuka, A. P. Agalgaonkar, and K. M. Muttaqi, "Conservation Voltage Reduction and VAr Management Considering Urban Distribution System Operation with Solar-PV," *Renewable Energy Journal*.

TABLE OF CONTENTS

LIST OF FIGURES

LIST OF TABLES

CHAPTER 1: GENERAL INTRODUCTION

1.1 Statement of the Problem

The need for in-depth research on the planning and operation of electric power distribution systems cannot be underestimated because of the following main reasons. The investment in distribution systems is normally around 40% whereas for electric power generation, and hence greater than transmission systems. Customers are directly affected as approximately 80% of interruptions are due to outages in distribution systems. In addition, very little field information is available in distribution systems barring low related information from selected customers. On the other hand, most of the distribution system operations are based on heuristics, with 10-20 daily switching operations. Furthermore, electrical variables such as voltage in modern distribution system are subjected to inherently and frequently varying conditions.

In modern medium voltage (MV) distribution systems, both renewable and non-renewable distributed generation (DG) units, located close to load centres, play an important role. The potential positive techno-economic impacts include voltage and reactive power support, energy loss reduction, reliability improvement, emission reduction and cost deferral, usually in terms of system infrastructure investment. The associated technological advancement, economic savings and environmental concerns promote the integration of private and utility-owned DG units as one of the attractive alternative options for distribution system planning. However, ongoing challenges are faced in the successful operation of distribution systems embedded with renewable and non-renewable DG units. The conventional operational practices are mainly based on the consideration of unidirectional power flow from transmission systems to distribution systems through to consumer loads; however, it is not the case in the presence of DG. This emphasises the need to devise new tools, practices and control mechanisms for distribution system operation which, in the presence of variability of DG power output, can indeed be challenged. This thesis aims to address the challenges

associated with voltage control in distribution systems embedded with DG, while utilising DG's reactive power capability for Volt/VAr (voltage and reactive power) support in the system.

By its nature, voltage magnitude typically demonstrates the health of an electric power system. Hence, voltage control is the fundamental operating requirement of all electricity distribution systems to maintain voltages within stipulated limits. A well designed voltage control mechanism can improve utilities' revenue and goodwill. Many types of electrical equipment operate at a poor power factor and draw more than their rated current without any increase in power consumption for lower voltages, thus causing more loss of power for a utility, and low efficiency and a decrement in the lifetime of customers' equipment. On the other hand, the modern distribution system voltage profile is inherently subjected to steady-state and dynamic variations. These phenomena are mainly caused by small and large perturbations associated with the system; the operation of conventional voltage control devices such as on-load tap changers (OLTCs), voltage regulators (VRs) and capacitor banks (CBs); and the responses of DG units considering associated dynamics. In case of MV distribution systems embedded with conventional voltage control devices, the integration of DG can introduce adverse effects such as: (a) control interactions; (b) operational conflicts causing rapid wear and tear in voltage control devices; (c) rises and drops in voltage at different locations; (d) transient and sustained oscillations; and (e) a decrement in the voltage stability margin. The worst impacts are expected under low loading conditions especially for long distribution feeders with high penetration of DG. Another issue is the occurrence of voltage swings (up and down) along the feeder systems. Typically, these are caused by the intermittent power generation by renewable DG units and variability in power output of non-renewable DG units during the built-in time delays associated with voltage control devices. Therefore, in the presence of DG, conventional voltage control practices need to be reviewed and updated.

The voltage control objectives in MV distribution systems differ according to the policies laid out by distribution network service providers and are commonly based on: (a) maintaining the voltage at the consumer end within stipulated limits;

(b) minimising system losses; and (c) increasing the distribution area voltage stability margin. The level of achievement for these objectives mainly depends on: (a) strong and steady voltage support by the local transmission network; (b) adequate Volt/VAr control devices; and (c) control coordination strategies for operating voltage control devices and DG units by minimising the number of manoeuvres. In general, the aim of an ideal normal-state voltage controller is to maintain the steady-state voltage magnitude at each bus within the stipulated limits while eliminating the interactions between DG and the voltage control devices. The aim of an ideal dynamic voltage controller is to instantly and fully damp out the associated oscillatory and non-oscillatory impacts on the distribution system. In reality, due to the inherent operational performance and unpredictable nature of modern distribution systems embedded with various DG technologies, none of the conventional voltage control devices can achieve these ideal characteristics.

The voltage control strategies used in industry and proposed in the literature for active distribution systems can be classified as (a) decentralised voltage control and (b) centralised voltage control. In decentralised voltage control, commonly season-based tuning for the local control parameters of voltage control devices and DG controllers is accomplished using optimisation, rule and analytics based formulations. Coordination of the operation is accomplished using time-graded operation by assigning appropriate time delays based on experience and/or rules of thumb. In centralised voltage control, the coordination of voltage control devices and DG units is accomplished by short-term tuning of the control parameters and by updating control actions with or without centrally dispatching the DG power output (or updating the DG Volt/VAr control mode). The decisions at a particular control state are enacted using a centralised distribution management system (DMS) where the common time interval of a control state is 1 hour or 15 or 10 minutes. The most suitable time periods for practically dispatching DG and updating voltage controllers are determined based on their construction and operation. In addition, optimisation, rule and analytics based formulations are widely adopted where time-graded operation is fine-tuned or

adaptive as compared to the decentralised voltage control. However, in the case of decentralised voltage control, there is no mechanism to operationally eliminate or minimise the adverse effects caused by interactions between DG units and voltage control devices during a period of two consecutive seasons during which modern distribution systems are subjected to inherently and randomly varying characteristics. Therefore, under decentralised voltage control, there is a higher possibility of DG and voltage control device interactions leading to adverse effects such as conflicting operations and resultant voltage variations and transients. In the case of centralised voltage control, there is still some possibility of control interactions between multiple DG units and voltage control devices leading to adverse effects under certain system operating conditions. The main reason is that there is no guarantee of operationally eliminating or minimising the adverse effects caused by the interactions between DG units and voltage control devices during the time interval of a control state. The rationale is provided by the following four major phenomena: (a) the modern distribution system electric variables (e.g., voltage) are subjected to inherently and frequently varying conditions compared to those in transmission and distribution systems without DG; (b) the DG impacts are dynamic in nature and they grow as proliferation increases; (c) it is very difficult to forecast power generation from renewable sources due to the high level of uncertainty associated with their intermittent power output even with stochastic modelling; and (d) the prioritised operation of different voltage control devices depends on the network topology and the associated system characteristics. Table 1.1 summarises the important technical aspects associated with centralised and decentralised voltage control in modern distribution systems.

A well designed control framework is therefore necessary to address the above issues in order to achieve effective voltage control in modern distribution systems. However, this would require control mechanisms which may differ from the voltage control strategies used in transmission systems and passive distribution systems, as the modern distribution system characteristics are different. Hence, in this context, the first requirement is a unique classification for DG and voltage

control device interactions to enable the required control modules to be designed. Furthermore, to coordinate the DG and voltage control devices, the associated controller parameters have to be appropriately tuned with pre-defined time delays updated in such a way that the distribution system characteristics and operational objectives are followed by the controllers without any operational delay. However, in practical terms, this may not be feasible as no human-made controller can operate without any operational delay. The time interval associated with control states still has to be maintained equal or greater than the 10-minute level, as this is the most practical and feasible time frame for dispatching DG and updating the voltage control devices. Therefore, the problem of enabling effective voltage control still exists in relation to modern distribution system operation.

1.2 Research Objectives and Methodologies

The main objectives of the research work presented in this thesis are to tackle voltage control in modern distribution systems, while incorporating the DG reactive power capabilities for Volt/VAr support thereby enhancing the overall voltage regulation performance.

The main aims of this thesis are achieved through:

- In-depth literature review on voltage control in conventional and modern distribution systems
- Detailed modelling of realistic distribution systems derived from the electricity network of New South Wales (NSW), Australia, considering both normal-state and dynamic-state operational aspects related to voltage control
- Establishment of theoretical analysis to examine the impact of DG on voltage control performance
- Investigative case studies for examining the interactions between DG units and voltage control devices
- Classifying DG units and voltage control device interactions using simultaneous and non-simultaneous responses for correcting target node voltages

- Introducing the concept of virtual time delay to coordinate the operations of DG units and voltage control devices in order to minimise the adverse effects of interactions
- Development of an algorithm for tuning the control parameters of voltage control devices and Volt/VAr support DG units in modern distribution systems
- Development of a comprehensive coordinated voltage control strategy for improving voltage control performance of a modern distribution system
- Investigating oscillations, which can be induced due to the operation of voltage control devices and Volt/VAr support DG units in modern distribution systems, and examining tap changer limit cycle phenomenon

In the case of normal-state voltage control, the main basis for developing the proposed algorithm for tuning the local controller parameters of multiple voltage control devices and DG units was to alleviate the following technical issues: (a) numerous and erroneous operations in controllers and resultant voltage variations; (b) steady state voltage variations on a feeder; and (c) significant voltage swings (up and down) especially on a feeder embedded with DG units during time-delayed operation of conventional voltage control devices. Moreover, the techniques incorporated in the proposed optimisation formulation and search method lead to a new strategy of optimal Volt/VAr control in modern distribution systems. The developed tuning algorithm can be implemented in a substation-centred advanced DMS as a separate module for online voltage control. The proposed optimisation formulation is invaluable as it has the flexibility to adopt any network philosophy such as conservation voltage reduction and loss minimisation.

In the case of normal-state voltage control, the proposed coordinated voltage control strategy encountered issues associated with structural changes and DG availability in the distribution system. In the case of distribution systems with multiple DG units and voltage control devices, the interactions between the DG units and voltage control devices were defined using their simultaneous and non-simultaneous responses. To eliminate the adverse effects of interactions, the concept of virtual time delay was then applied with the aid of mathematical

models and associated control logic to achieve effective coordinated voltage control in a modern distribution system embedded with Volt/VAr support DG units. This can improve the system voltage profile by eliminating the uncoordinated operation of voltage control devices and DG units, thereby reducing possible conflicting operations and consequent voltage variations in the system during online voltage control.

In the investigative case studies, interactions between Volt/VAr support DG units involving electro-mechanical oscillations in the distribution system were observed. Long-term oscillations in the distribution system induced by interactions between voltage control devices and DG units were also observed. Furthermore, analyses highlighting tap changer limit cycle phenomenon and the resultant sustained oscillations were conducted on a realistic distribution network. Also, a strategy for mitigating limit cycle induced oscillations is proposed. These studies highlight the requirement for supplementary control and alert-state control to effectively operate modern distribution systems and improve dynamic voltage control performance.

1.3 Outline of the Thesis

A brief description of the contents of the remaining chapters is provided in this section.

Chapter 2 summarises and presents the literature detailing research work aligned to this research project. An introduction of electric power distribution systems, Australian MV distribution systems and modern distribution systems, and a detailed description of voltage control devices in distribution systems and DG are also included.

Chapter 3 presents detailed investigation of interactions between multiple DG units and voltage control devices in the context of optimal Volt/VAr control in modern distribution systems. It discusses optimal Volt/VAr control strategies adopted for modern distribution systems. In addition, this chapter presents preliminary case studies, simulation results and findings.

Chapter 4 presents the examination of interactions between multiple DG units and voltage control devices of different control actions. It includes a comprehensive introduction and a discussion on classification for effective voltage control in modern distribution systems. In addition, the chapter presents preliminary case studies and simulation results taking into consideration small perturbations in the distribution system. Furthermore, discussions are presented on the research gap, the concept of simultaneous/non-simultaneous responses and virtual time delay; and the best possibilities for mitigating the adverse effects of interactions between multiple Volt/VAr support DG units and voltage control devices.

Chapter 5 presents the proposed algorithm for tuning the control parameters of voltage control devices and Volt/VAr support DG units in distribution systems. It includes the proposed DMS algorithm, the test case study and simulation results. Furthermore, the chapter discusses the impacts of reactive power generation by renewable DG on system voltage regulation; the proposed solution methodology; the proposed operational guidelines for tap changing devices; and a practical implementation strategy for the proposed online tuning algorithm and the algorithm embedded in each control layer.

Chapter 6 presents the proposed strategy for coordinated voltage control in distribution systems with multiple voltage control devices and DG, taking into consideration the simultaneous responses. It discusses the operation of multiple tap changing devices and DG units in distribution systems. Details associated with the operation of substation OLTC and step voltage regulators (SVRs) are presented. Also, the effect of simultaneous responses of tap changing devices and Volt/VAr support DG units on the nodal voltage profile is discussed. The chapter then presents the practical implementation strategy for the proposed online coordinated voltage control including the DG voltage control module (DG-VCM) and the control module for blocking simultaneous operation (CM-BSO).

Chapter 7 presents the proposed strategy for coordinated voltage control in distribution systems subjected to structural changes and DG availability, taking into consideration the non-simultaneous responses (in addition to simultaneous

responses) of multiple voltage control devices and DG. It includes a detailed description of the mathematical model used to derive the voltage control zones for Volt/VAr support DG in distribution systems; and the mathematical proof for the proposed coordinated voltage control. Also, the chapter presents the proposed coordinated voltage control strategy including algorithm development and determination of the operational sequence of operating Volt/VAr support DG units and voltage control devices, and online implementation of the proposed strategy.

Chapter 8 depicts the oscillations caused by Volt/VAr support DG unit and voltage control device interactions subjected to normal-state voltage control. The chapter elaborates system modelling aspects, case studies and analyses. The chapter specifically outlines the sustained oscillations induced by OLTC limit cycles due to interactions between tap changer control, load and local generation under flat load profiles. Moreover, discussions are presented on the possibilities of mitigating tap changer limit cycles and the associated sustained oscillations in the MV distribution systems.

Chapter 9 presents the concluding remarks. It highlights and summarises the contributions of the research project presented in this thesis and the possible research directions for future.

Appendices: Appendix-I presents possible Volt/VAr management issues under conservation voltage reduction (CVR). Appendix-II presents the proposed static tool for assessing the DG impact on line drop compensation (LDC) in voltage regulating devices. Also, the details of the mathematical model used for deriving the proposed voltage sensitivity-based tool are included. Appendix-III outlines the testing methodology for voltage controllers, while Appendix-IV presents the searching mechanism incorporated in Control Layer-02 for the tuning algorithm proposed in Chapter 5. The Figure 1.1 presents the link between contribution chapters (i.e., Chapter-1 to Chapter-9) of the thesis.

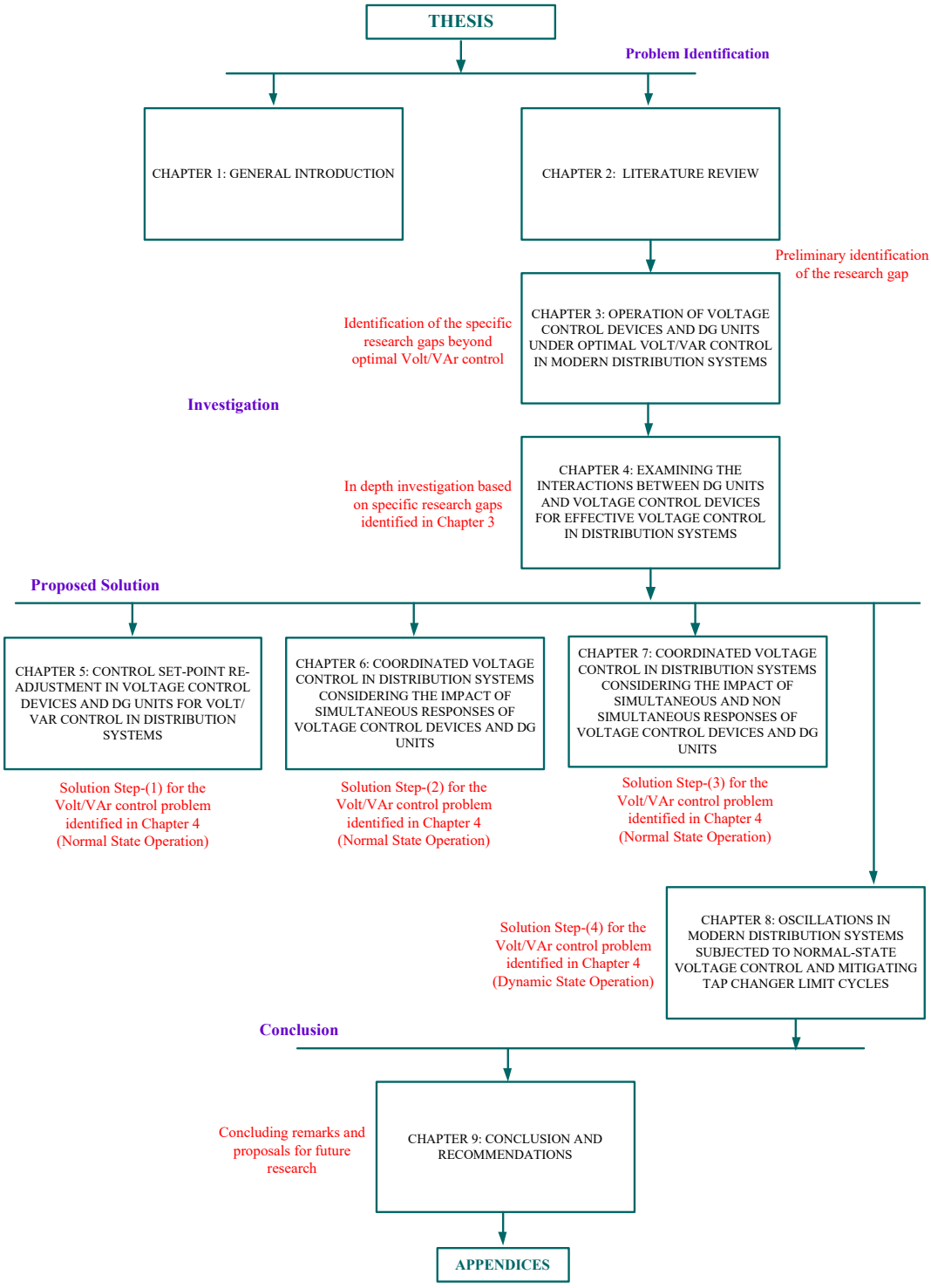

Figure 1.1: Diagrammatic representation showing the link between contributory chapters

CHAPTER 2: LITERATURE REVIEW

2.1 Introduction

This section consists of an overview of distribution systems including specific details highlighting Australian MV distribution systems, characteristics of modern distribution systems, and summary of voltage control in distribution systems.

2.1.1 Overview of Distribution Systems

In centralised large generating stations, the voltage is stepped up to high voltage levels to efficiently transmit the generated power over long distances through interconnected transmission systems as customers are far from these generating stations, which are at a relatively small number of locations. The voltage from the high voltage transmission systems is stepped down to MV distribution systems and then to low voltage (LV) distribution systems, from where the electric power is distributed to customer loads. The distribution systems typically start with a distribution substation fed by a sub-transmission or transmission system, with each distribution substation serving one or more distribution feeder systems. Among the major components of an electric power system (i.e., central generation station, interconnected transmission system, bulk power substation, sub-transmission network, distribution substation and distribution feeders), the overall distribution system has traditionally been characterised as the most unglamorous component [1]. The planning and operation of large interconnected networks are subjected to continuous research and development; meanwhile, with little or no analysis, distribution systems continue to deliver power to customers and, as a direct result, distribution systems have normally been over-designed. However, times have changed, and researchers and engineers have realised the necessity of in-depth research related to modelling and analysis of distribution systems including development of new control strategies for efficient and reliable power delivery to customers. Accordingly, the new voltage control philosophies and strategies are evolving: hierarchically, they can be classified as transmission voltage control, distribution area voltage control, voltage control in MV

distribution systems and voltage control in LV distribution systems. In this research project, the contribution is to develop voltage control strategies in MV distribution systems in which DG is embedded. The penetration level of small-scale generation connected to local distribution systems, which is called DG or dispersed generation or embedded generation, has significantly increased over the last decade. Electricity market liberalisation; environmentally friendly electricity generation; constraints on the construction of transmission lines; reduction of the usage of fossil fuel resources and increasing demand for a highly reliable electricity supply are the main driving forces for this trend in electricity networks. In addition, Volt/VAr correction by DG units using their reactive power capability is one of the promising concepts highly regarded by researchers and engineers, which today is already at the level of implementation. Accordingly, the Institute of Electrical and Electronics Engineers (IEEE) Standard 1547^{TM}: "Standard for Interconnecting Distributed Resources with Electric Power Systems" has recently been amended allowing the utilisation of DG for Volt/VAr support in distribution systems [2]. The penetration of DG into distribution systems has therefore led to the concept of modern distribution systems; however, this has caused more complex distribution planning and operational problems for distribution system planners and operators all over the world. As a remedy for these technical problems, conventional distribution systems are on the verge of restructuring to become modern distribution systems utilising smart grid infrastructure. These sophisticated distribution systems are named 'smart distribution systems'.

A comprehensive discussion on distribution system characteristics and distribution system modelling and analysis can be found in [1].

2.1.2 Australian Medium Voltage Distribution Systems

Long distribution feeder systems can frequently be seen in Australian MV electricity networks. These systems are mainly designed for rural electrification which is normally lightly loaded. The voltage drop is high due to the long length of the feeders. Cascaded multiple SVRs are used for feeder voltage regulation in addition to the substation OLTC. Feeder capacitors are also used locally for Volt/VAr support, if required. Distributed generators are normally connected to

these feeders, if an ancillary power supply is required. The majority of these DG units are dispatchable. Furthermore, the majority of DG units embedded in Australian MV distribution systems are still based on synchronous machine based technologies. Smaller synchronous machine based DG units tend to be operated in constant power factor mode closer to the unity power factor, while other larger units are operated in voltage control mode.

According to Australian Standard (AS) 60038-2012: "Australian Standard for Standard Voltages", the stipulated operating voltage limits for MV distribution systems are within +/– 10% from a nominal voltage. The voltage control devices are still conventionally tuned and operated, and the associated operational problems, that is, control interactions, operational conflicts and associated oscillations are not properly addressed/solved in modern distribution systems. The following feedback provided by a senior engineer working for an Australian distribution company provides evidence in support:

> Our 66/11 kV main transformer tap changers have 1.5% taps; so, to prevent hunting, we set out voltage regulating relays with a bandwidth of a bit more than half a tap. If the voltage stays outside this limit, it starts a timer which we set a bit slower than the upstream 132/66 kV sub-transmission transformer. If our 11 kV voltage has come back within bandwidth, we stop and reset the timer; if it has not, we initiate a tap change after its time delay. If there is a downstream 11 kV voltage regulator, we would use the same methodology, a bandwidth greater than half a tap but now a larger time delay and so on down the line. We do this to minimise wear and tear on the tap changer contacts because some tap changers need overhauls after 10,000 tap changes. Having said that, there are fast acting single-phase voltage regulators that can exceed 100,000 tap changes or more between overhauls and these have 5/8% taps, so we can set these with a much narrower bandwidth and a shorter time delay, and still achieve reasonable operating life between overhauls while giving very close voltage regulation. However, we can still set these with a broad bandwidth so they operate much less often but take

two taps at a time and we can use a higher time delay if we want to. It would be interesting to see how we could optimise the tap operation of these tap changers to give us long life while still maintaining acceptable power quality.

The topology of an example of a MV distribution feeder system derived from the electricity network of NSW, Australia, is shown in Figure 2.1. The feeder system associated with feeder configuration–01 is around 41.6 km long and has 95 (MV to LV) nodes. It is fed by a 132/11 kV, 30 MVA transformer equipped with an OLTC. In addition, two Type-B SVRs, SVR1 and SVR2, are connected in feeder configuration–01 to correct the voltage. Moreover, a synchronous machine based DG unit, DG1, which has capacity of 1.25 MVA, is connected closer to the end of the feeder. There are 69 (MV to LV) nodes in feeder configuration–02, where the total line length is around 30.4 km. In addition to the operation of SVR2 and DG1, another Type-B SVR, SVR3, is connected in feeder configuration–02. Also, the system includes 2 air break switches (ABS) which can be used to improve flexibility of operation for the system.

2.1.3 Modern Distribution Systems

Modern distribution systems, also known as smart or active distribution systems, are characterised by the large penetration of renewable and non-renewable electricity generation; automated infrastructure with the application of DMSs; smart meters at customer locations; real-time pricing of electricity; demand management with smart appliances; customer participation in the buying and selling of electricity; technology savvy customers; and demand for higher power quality and fewer interruptions as well as higher flexibility and resiliency. Therefore, modern distribution systems are equipped with smart grid technologies such as sophisticated measuring devices and advanced sensors; powerful and refined communications equipment; highly advanced computing equipment; advanced power electronics; advanced protection equipment; and automated control with distributed and centralised intelligence [2].

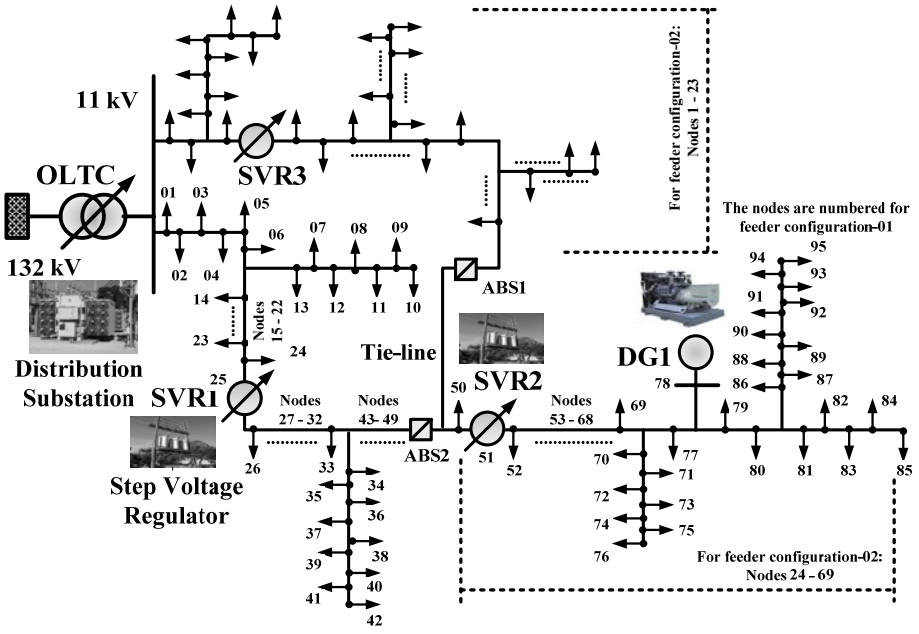

Figure 2.1: Topology of an example of an Australian MV distribution feeder system

The modern distribution control centres are mainly characterised by the integration of supervisory control and data acquisition (SCADA) systems and customer information systems; faster decisions and real-time analysis; big data-bases and analysis; decentralised and centralised intelligent computing; more complex analysis; and cyber security. The critical applications are optimal Volt/VAr control; online power flow and short circuit analysis; adaptive protection; contingency analysis; advanced fault detection and location; advanced fault isolation and service restoration; dynamic de-rating of equipment due to power quality issues; distribution operator training simulator; and real-time pricing and demand response. The main benefits of automation are released capacity; reduced losses; increased service reliability; life extension of equipment, and effective utilisation of assets. Thus, smart distribution applications are being developed for different needs and at different speeds with the aim being to enhance the efficiency, reliability and quality of power delivery by distribution systems. These are detailed in IEEE Guide P1854: “Smart Distribution

Application" [2]. On the other hand, through their application in some utilities, smart distribution systems today have already become realistic. For example, all the MV and LV distribution systems in the state of Alabama, United States of America (USA), have been fully automated, with their respective utility engineers capable of discussing relevant technical advancements and the associated benefits in modern distribution system technology [2]. In this research project, the proposed voltage control strategies are designed for implementation in modern distribution systems.

2.2 Voltage Control Devices in Distribution Systems

This section presents an overview of tap changing devices such as OLTCs, SVRs and CBs. These devices are still commonly utilised for Volt/VAr control in distribution systems all over the world, and they will also serve future distribution systems.

2.2.1 On-load Tap Changers and Step Voltage Regulators

Tap changing devices are the most robust devices invented and widely used for voltage regulation in electricity networks. As stated above, they comprise OLTCs also denoted as load tap changers (LTCs), and SVRs also denoted as voltage regulators (VRs).

Different technologies for OLTC switching are being continuously developed. Tap changers with arcing contacts submerged in insulating oil are already in use. These OLTCs dominate the market; however, due to the long lifetime of power transformers, degradation of this older design is of concern. New developments, like vacuum switching or solid-state (thyristor) technology, are developed with the purpose being to prolong the maintenance interval. Solid-state OLTCs, mostly found in transformers with a low power rating, are expensive, have high no-load losses and have difficulties in handling high short circuit currents. On the other hand, vacuum tap changers transfer the load current using vacuum bottle switches and can handle high power ratings, but are also relatively new, expensive and therefore not yet widely implemented. In addition to these newly installed technologies, manufacturers are continuously improving the design of

conventional oil-filled tap changers. For example, experience with tap changer degradation has led to design improvements using new contact materials, higher contact pressure or wiping contacts. OLTCs that use oil as the arc-quenching medium are still the most frequently installed type due to their cheap and improved design. As a result, the robust mechanical OLTCs will also be in service for future electric power systems [3].

Power transformers equipped with OLTCs are usually defined and specified using an approach based on international standards and the associated test criteria. The design of transformers based on this approach is typically optimised with objectives such as minimising total losses, operating temperatures and noise mainly at the worst case testing or the most common service conditions related to the position of tap changer or ambient temperatures. The common measures are hot-spot gradient and hot-spot temperature rise versus tap position [4]. Therefore, the optimal tap position of an OLTC is a major event in the case of designing transformers. On the other hand, OLTCs contribute to a large number of transformer failures which can be explained by the fact that the OLTC is the only transformer component that contains moving parts. The OLTC factors responsible for transformer failures include: oil quality (particulate contamination); OLTC contact temperature rise; contact coking; carbon film build-up; short circuit mechanical forces; contact wear; and arcing. In addition to these aspects, utility control practices which may cause tap changer hunting and therefore excessive tap changer operations contribute to tap changer aging and failures [3]. The common OLTC failures can be seen in the change-over selector of stator contact blocks, the drive shaft of selector switches and the change-over selector of stator roller contacts. In addition, transformer windings can be destroyed due to an OLTC failure in cases where protective mechanisms do not react quickly enough to prevent transformer damage [3]. Other factors affecting the incidence of transformer failures are those that occur due to tap changer failures and how transformers where tapping is seldom performed are often more problematic due to contact coking and high contact resistances that cause localised heating [3]. Therefore, wear and tear on the tap changer mechanism is one of the most

common reasons for transformer failure and maintenance. It can be more significant at the level of distribution networks that contain large-scale DG, and OLTC controls can lead to conflicting tap operations due to steady-state and dynamic interactions between the OLTC and DG. In addition to the resultant steady-state voltage variations, each additional OLTC tap operation introduces transients to the system. In the case of online tap changing devices, a reactor or high-speed resistance tap changing mechanism bridges the two taps temporarily while changing from one to the other, thus introducing switching transients. Moreover, OLTC limit cycles would be common in modern distribution systems.

In the case of SVRs, the controls, operational issues and network impacts are almost similar to the case of OLTCs. Throughout the Australian electricity network, numbers of SVRs are utilised where further voltage regulation is required in addition to the coarse voltage control by OLTCs. The SVRs can be either single phase or three phase: single-phase regulators can be connected in wye, delta or open delta in addition to operating as a single-phase device. The three-phase SVRs can only be connected in a three-phase wye or closed delta. The SVR connection and number of units depend on the distribution system design. In four-wire, multi-grounded systems, three wye-connected regulators with a grounded neutral are required, with SVRs regulating voltages independently in each phase [1]. In cases where three-phase loads are connected phase-to-phase requiring an open or closed delta-connected SVR, SVRs cannot regulate voltages independently of each other as they would in four-wire, multi-grounded systems. The reason is that by regulating voltages in one phase, voltages in one of the other phases will also change. A SVR is basically an autotransformer with a load tap changing mechanism on the series winding, in which the voltage change is obtained by changing the number of turns (tap changes) of the series winding of the autotransformer. It is noted that an autotransformer can be visualised as a two winding transformer with a solid connection between a terminal on the primary side of the transformer and a terminal on the secondary side. The position of the tap is determined by a control circuit called a line drop compensator which is also available with some OLTCs as an additional option. The LDC models the voltage

drop of the distribution line from the regulator to the defined load centre. The SVRs can be connected in a Type-A or Type-B connection, with the most common type being Type-B [1]. Input to the Type B type step voltage regulators is across the series and shunt windings, where the Type A type step voltage regulators have the load side connected across the series and shunt windings. When a change in taps is required, the autotransformer of the step voltage regulator unit changes the number of turns on the series winding [1]. A three-phase SVR has connections between the single-phase windings internal to the SVR housing, whereas the three-phase SVR is gang-operated with all taps on all windings changing the same and, as a result, only one LDC circuit is required. In this case, it is up to the distribution network operator (DNO) to determine which phase current and voltage will be sampled by the line drop compensator. From recent studies, it has been found that the operation of the LDC can be significantly affected by the reverse power flow of DG under certain system conditions leading to conflicting tap operations [5]. Moreover, in addition to the forward-mode operation, there are three main autonomous operational modes of SVR in which they can potentially interact with DG especially when operated in voltage control mode. These modes are: (i) bi-directional mode, (ii) reactive bi-directional mode (mostly used in loop distribution systems) and (iii) co-generation mode [6]. The evolution of tap changer control in distribution systems is discussed in the following paragraph.

In the evolution of control concepts, the following five main stages are implemented for tap changer control in MV distribution systems in which DG is embedded: (i) local control; (ii) simple control first generation; (iii) simple control second generation; (iv) advanced control; and (v) topology based advanced control [7]. In the case of local control, local controllers control not only tap changers but also DG units and CBs, ensuring that their local voltage limits are in accordance with the relevant standards used. In addition to local control, this stage is the fall-back strategy in case of loss of communication in real-time control. There is no communication between the grid and the voltage control devices of the system. In the case of the first generation of simple control, the enhancement

is the integration of voltage measurements in the network within a simple optimisation algorithm for application prior to tap changer operations. The associated communication infrastructure is used to obtain the information on actual voltage band violations to control the voltage level in the system. There is only a uni-directional communication channel available from the grid to the voltage control devices. Other voltage control devices such as DG units and CBs are still in droop control mode as in the local control stage. In the second generation of simple control, communication to the voltage control devices within the grid is activated. In addition to the integration of voltage measurements in the network, it is possible to provide a system-wide strategy resulting in new control set-points, for example, control settings of CBs and DG controllers enabling the feeding of maximum active power from all DG units. The disadvantage of the associated sub-optimal control action is that DG units with weak influence in critical node voltages start feeding reactive power to increase the voltage and/or hitting reactive power capability limits. In this stage of voltage control, a bi-directional communication infrastructure is available, but what is commonly enabled is only a sub-optimal solution with the goal of maximising the feeding of active power. In advanced control, to enable heterogeneous distribution of DG and e-mobility, different optimisation algorithms based on maximising active power feed in with minimal reactive power flows are introduced and coordinated dynamic controls utilising information and communication infrastructure are adopted. The global control set-points for the actors in the second generation of simple control are replaced by individual fine control set-points which are mostly generated by an optimisation algorithm incorporated in a grid controller. In topology-based advanced control, specific controls which take into consideration information about the network's actual topology in the optimisation are utilised. This allows the global optimum solution to be found in case dynamic changes occur in the network topology, for example, due to network reconfiguration and/or DG availability. This can be done by installing additional smart meter based current guards in all branches and selected nodes. Moreover, an intelligent algorithm for topology estimation based on power snapshot analysis would be utilised [7].

2.2.2 Capacitor Banks

CBs are the most robust devices invented and widely used by human beings for economically supplying reactive power to power systems. A CB is a grouping of several identical capacitors which are commonly inter-connected in parallel with one another. Shunt capacitors capable of supplying reactive power and boosting the voltage are commonly used throughout distribution systems with a wide range of sizes, when local Volt/VAr correction is required. Distribution CBs are usually switched automatically to accomplish the required voltage correction online, and they are called switched shunt CBs. Fixed capacitor banks are also utilised, but mainly for power factor correction in distribution systems [8]. Therefore, it is very clear that there should be a proper coordination mechanism among CBs and other voltage control devices for effective voltage regulation especially in distribution systems.

The early capacitors were made utilising oil as the dielectric; however, their size, weight and cost were very high. Therefore, modern capacitors are constructed by employing cheaper dielectric materials. These advancements in materials engineering and other improvements in capacitor construction have brought a significant reduction in CBs' sizes and prices. The main advantages of modern shunt CBs are their low cost and flexibility in their installation and operation. They can be readily integrated into the system, thereby contributing effective power delivery to customers. The major disadvantage of employing CBs, especially in distribution systems, is that their reactive power output may be reduced at low voltages when it is most needed, as the reactive power output of shunt capacitors is proportional to the voltage [8].

2.3 Distributed Generation

In this section, the common DG technologies and their operational modes are briefly discussed, including the DG embedded in Australian MV distribution feeder systems. DG is the term used to define local power generation (close to end-users), usually in units with sizes up to 10 MVA, connected to the distribution feeder systems and substations. DG can be broadly defined as the utilisation of

modular small-scale generation technologies interconnected to distribution systems. DG units may be owned by a utility or more likely are owned by a customer who may use all of the power on site or who may sell a portion or perhaps all of it to the local utility. When waste heat is available from the generator, the customer may be able to use it for process heating, space heating and air conditioning, thereby increasing the overall efficiency from the primary source to electricity and useful thermal energy [9]. The main advantages of DG integration are: distribution system capacity expansion deferral; power delivery efficiency improvement; reliability improvement; idle capacity cost reduction; as well as less design, authorisation, construction, interconnection and investment return time. According to the output power characteristics, DG can be classified as dispatchable or non-dispatchable. If the DG units are dispatchable, the DG operator can determine their power output by controlling the primary energy sources supplied to the DG units. In the case of non-dispatchable DG units, the DG operator cannot dispatch the DG units because the behaviour of the primary energy sources cannot be controlled. Non-dispatchable DG units are generally the plants driven by renewable energy sources such as wind and solar where the power output depends on the availability of the energy sources, which is indeed variable, intermittent and difficult to forecast.

2.3.1 DG Technologies and Operational Modes

The DG units can be connected to distribution systems using synchronous or induction generators or via a power electronic interface. In the following paragraphs, the common renewable DG technologies are briefly discussed with reference to [5] and [9].

Solar-photovoltaic (PV) systems directly convert sunlight into electricity without any heat engine; in other words, they use a clean energy source. The implementation of solar-PV systems is motivated by the availability of sunlight, long life cycle, high modularity, low operation cost, ability for off-grid application and the short time needed for design and installation. However, the application of solar-PV systems is capital-intensive and exhibits low efficiency thus making solar-PV systems expensive. Without subsidies, solar-PV power remains 2–5

times as expensive as grid power, where grid power exists. Some barriers for solar-PV systems include significant area requirements due to the diffuse nature of the solar resource; higher installation cost than other DG technologies; and intermittent output with a low load factor. As small generating units, solar-PV modules can commonly be seen in LV distribution feeder systems. As large generating units, solar-PV farms can commonly be seen in MV and sub-transmission power networks.

Wind energy today plays a key role in generating clean electricity. Large wind power plants, both off shore and on shore, are competing with fossil fuel-fired power plants by supplying economical clean electric power in many parts of the world. Hence, wind power is more like central generation than DG. Today, the size of commercial wind turbines has increased significantly from 50 kW to 5 MW, thus creating economies of scale for wind power technology. The doubly-fed induction generator (DFIG) based technology is more popular. The main challenges of wind power technology are associated with intermittency in power output and grid reliability. As wind power generation is based on natural forces, it cannot dispatch power on demand but, on the other hand, utilities must supply power closely balanced to demand.

Bio-diesel internal combustion engines convert heat from the combustion of bio-diesel into rotary motion which, in turn, probably drives a synchronous generator. They are one of the most common technologies that represent proven technology with low capital cost; large size range; good efficiency; possible thermal or electrical cogeneration in buildings; and good operating reliability. As internal combustion engines can be quickly started during a power outage and do not require much space for installation, they have become the main choice for standby emergency power supplies. Major barriers for the usage of these internal combustion engines are the high maintenance cost and, sometimes, the bio-diesel cost which is the highest among the DG technologies, with their high emissions and noise also the highest among the DG technologies.

Biomass resources mainly include agricultural waste, animal manure, forest waste, industry waste, municipal waste, sewage sludge and crops. Biomass can be converted into electricity or heat in one of several processes. The majority of biomass electricity is generated using a steam cycle where biomass material is first converted into steam in a boiler. The resulting steam is then used to turn a turbine generator. Biomass can also be used with coal to produce electricity in an existing power plant, with this process called co-firing. Co-firing is the most economical near-term option for introducing new biomass electricity generation and lowers air emissions from coal-fired power plants. Another alternative is to convert the solid biomass into a fuel gas. The fuel gas can then be used in a piston-driven engine or a high-efficiency gas turbine generator. The use of biomass resources for electricity power and combined heat and power (CHP) generation is steadily expanding worldwide. Main barriers to the widespread use of biomass for power generation are cost, low conversion efficiency and feedstock availability. Biomass has a low energy density which makes transportation over long distance costly. In addition, the over-exploitation of biomass sources should be avoided. Certification that biomass feedstock is produced in a sustainable way is needed to improve the acceptance of biomass sourced from public forest and land management. Bio-gas turbines typically consist of a compressor, a combustor and a turbine generator system that convert the rotational energy into electric power output. Gas turbines of all sizes are now widely used in the power industry. Small-scale gas turbines are commonly used in CHP applications. They are normally useful when higher temperature steam is required. The maintenance cost is also slightly lower than for reciprocating engines. Gas turbines can be noisy but emissions are somewhat lower than for combustion engines as cost-effective emission controls are integrated. In combined-cycle gas turbines, the exhaust air–fuel mixture exchanges energy with water in the boiler to produce steam for the steam turbine. The produced steam enters the steam turbine and expands to produce shaft work which is converted into additional electric energy in the generator. The outlet flow from the turbine is condensed and returned to the boiler. Combined-cycle gas turbines are becoming increasingly popular due to their higher efficiency. However, gas turbine installations that are much below 10

MVA are generally not combined cycle due to the scaling inefficiencies of the steam turbine.

Small hydropower turbines are generally hydropower units with a capacity that is normally below 10 MVA. The amount of power generated from small hydropower plants worldwide is quite large.

Geothermal energy is available as heat emitted from within the earth usually in the form of hot water or steam. While this is an abundant source, only a very small fraction can be converted commercially to electricity with the technology available today. Geothermal power plants are normally highly capital-intensive but with low operating costs. These plants are also clean without emissions during operation. Hence, a new and significant opportunity for geothermal development will emerge when the reduction of carbon emission, as a response to greenhouse gas emission concerns, is considered as a credit.

Solar thermal systems generate electricity by concentrating the incoming sunlight and then trapping its heat which can raise the temperature of a working fluid by many degrees to produce steam and then generate electricity, probably by using synchronous generators. Applications for concentrating solar power are now feasible ranging from the level of a few kilowatts to megawatts. Compared to solar-PV systems, the solar thermal system is more economical as it eliminates the need for costly semiconductor cells and associated technologies. Solar thermal plants can be grid-connected for central generation or can operate as stand-alone applications for DG applications. In addition, these units are suitable for fossil-hybrid operation or can include cost-effective thermal storage to meet dispatch requirements. Solar thermal units are the emerging renewable power generation technology in Australian power systems, and they would be the most suitable technology in the context of future Australian renewable power generation.

In terms of operational modes, the DG units can be operated in power factor control mode, reactive power control mode and voltage control mode. The associated Volt/VAr controllers embedded in different DG technologies are detailed in [9]-[10]. In the case of inverter-interface DG units (i.e., solar-PV and

DFIG), the inverter system is utilised to control the power factor, the VAr supply or the voltage. The synchronous machine based DG units can be operated in power factor control mode, reactive power control mode and voltage control mode thus enabling utilisation of an excitation system [10]-[11]. A typical excitation system topology used in synchronous machine based DG applications is shown in Figure 2.2 [11].

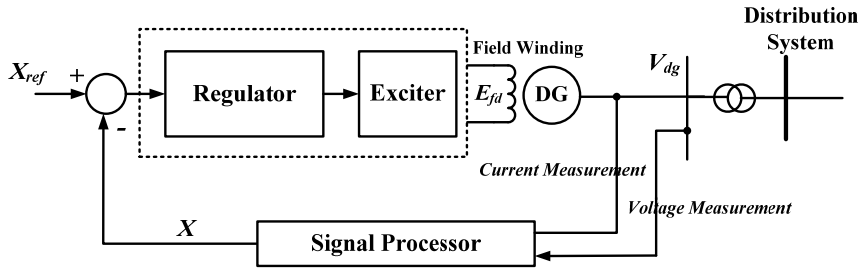

Figure 2.2: Typical excitation system topology used in DG applications

In general, the structure of the excitation system shown in the figure above consists of measurement and signal processing circuit, a regulator circuit and an exciter. LDC is also used in some applications in order to regulate the voltage at a remote bus, which is usually the DG transformer high-voltage bus. The reference value for the system control is X_{ref}, where X is the measured signal provided for the regulator circuit. In the case of DG operation in power factor control mode, the measured signal is the power factor. The DG exciter field voltage, E_{fd}, is then adjusted to maintain the power factor constant according to the defined reference value. Similarly, in the cases of reactive power and voltage control modes of operations, the measured signal is the reactive power and the voltage, respectively. The exciter field voltage, E_{fd}, is accordingly adjusted based on the regulator circuit output with the regulator circuit normally equipped with over and under excitation limiters. These excitation limiters limit the maximum reactive power injected or consumed by the generator according to the reactive power capability of the DG unit. As a result, the DG active power may also have to be controlled, if the DG unit needs to be operated for network Volt/VAr support under all system conditions. These operational modes can also be updated in real-time for enabling Volt/VAr control by the DG units. One of the ways to achieve

this requires designing a strategy based on updating X_{ref} value or making it adaptive based on varying network conditions.

2.3.2 DG Embedded in Australian Medium Voltage Distribution Systems

The DG embedded in Australian MV distribution systems is still commonly based on synchronous machine based technologies. As renewable DG technologies, they can be bio-diesel, biogas, small hydro, geothermal and solar-thermal.

A DG unit with a synchronous generator has the advantage that it can easily be controlled to provide or absorb reactive power and thereby significantly support system Volt/VAr control. It has been shown that synchronous machine based DG has the potential benefit of increasing the voltage stability margin for all kinds of voltage instability mechanisms. The fast response from a DG exciter ensures fast voltage recovery, thus significantly improving the transient voltage stability. DG operation at a constant voltage keeps the distribution system voltages high when major transmission lines trip. This enhances long-term large-disturbance voltage stability. In the case of long-term small-disturbance voltage stability, the larger reactive power generated by DG with the growing load may enhance the stability margin [5]. The synchronous machine based DG increases system fault level and then fault ride-through capability as well as contributing inertia to the system. The majority of these DG units are also dispatchable. Moreover, synchronous machine based DG units are capable of responding instantaneously to meet the system load demand. Furthermore, these DG technologies serve locations where there is no access to adequate renewable energy resources such as wind and solar and work as standby power supplies.

Therefore, this research project gives its main attention to the renewable synchronous machine based DG units, of approximately 1 MVA capacity or higher, which are integrated into MV distribution systems. However, the investigations, analyses and voltage control strategies developed in the project and proposed in this thesis can also be extended to distribution systems embedded with wind and solar-PV units which have adequate reactive power capabilities.

2.4 Optimal Volt/VAr Control in Modern Distribution Systems

Various methodologies have been proposed for tuning the control parameters of OLTCs, SVRs, CBs and DG units for optimal Volt/VAr control in distribution systems. The most common objective is: to minimise the system active power losses while maintaining the system voltage within the stipulated limits. On the other hand, some strategies and algorithms directly minimise the number of OLTC and SVR tap operations and CB switching operations using conventional optimisation methods (single objective or multi-objective) [12], while other strategies reduce the number of operations as a result of the proposed control action [13]. In addition, optimal Volt/VAr control strategies can be based on decentralised control or centralised control mainly through DMSs or a combination of both in a real-world application. In recent proposals, the DG units are also actively utilised for voltage and reactive power control with other voltage control devices. In [14], an optimal coordinated voltage control algorithm is proposed for distribution systems with multiple DG units using different technologies. It mainly utilises an optimisation based approach for voltage control on behalf of both real and reactive power dispatch of multiple DG units in addition to control set-point re-adjustment in substation OLTC operations. However, it also highlights a requirement for modifications to the proposed method in the case of distribution system operations with not only multiple DG units, but also multiple SVRs and CBs. In [15] and [16], a coordinated optimal voltage control and reactive power management schemes are proposed for the efficient utilisation of multiple DG units using different technologies in distribution systems without real-time measurements and smart grids, respectively. The control algorithms also impose constraints on inverter-interfaced DG units for maximising the instant reactive power reserve in steady-state to react against contingency situations in addition to control set-point re-adjustment for voltage regulation including the substation OLTC. In [17], an optimal distributed voltage control strategy is proposed enabling utilisation of a DG unit for voltage regulation in distribution systems based on a linear programming method. The solution methodology is supported by the strategy used for decomposition of the system sensitivity matrix which neglects weak couplings between DG units and

nodes while keeping the strong couplings for the effective utilisation of DG units for voltage regulation by tuning the respective control parameters. In [18], a similar method is proposed, but it is underpinned by power flow sensitivity factors allowing the utilisation of real-time knowledge of power system thermal ratings. This would be of value in situations where distribution network power flows require management as a result of DG proliferation. However, these methodologies do not address the distribution system operation with multiple SVRs, CBs and multiple DG units using different technologies.

The distribution system operation for voltage control with multiple DG units and voltage control devices has also been addressed in the literature. In [19], an optimal distribution Volt/VAr control strategy is proposed for coordinating common voltage control devices such as OLTCs, SVRs, CBs and a static VAr compensator in the presence of DG units. This strategy utilises multi-objective optimisation and a genetic algorithm solver that expedites the approximation of the solution from the feasible area discretely set as a large-scale optimisation problem. Similarly, an optimal control strategy is proposed in which the distributed local generator units are actively utilised for steady-state voltage and reactive power control with other voltage control devices such as OLTCs, SVRs and CBs using a dynamic programming algorithm [12]. These methods are commonly based on dynamically dispatching the DG output reactive power when operating in VAr control mode or the voltage reference value when operating in voltage control mode cooperatively with the control set-point re-adjustment of other voltage control devices one day or one hour in advance by an optimal dispatch schedule and using forecasted load demand and generation profiles. The common objectives of these proposed online multi-objective optimisation-based methods are: to decrease the number of tap and switching operations of OLTCs, SVRs and CBs; to reduce the active power losses in the distribution system; to enhance the distribution system voltage stability margin; and to improve the quality of voltage, while maintaining the system voltage within the stipulated limits. In addition, in case of conventional optimal Volt/VAr control methods, typically, optimisation is undertaken considering the step variations of load

demand and DG power generation as well as the voltage profile within two time-series data sets. However, the control settings need to be updated with a mechanism which accurately considers the correction of voltage profile within two time-series data sets and the variation in reactive power capability of DG units following the variability associated with their active power generation. This mechanism is needed as the variability of the power output of DG units may lead to cases of both voltage rise and drop on a feeder, while causing considerable voltage swings (up and down) especially on the feeder buses close to the DG units during the time-delayed operation of conventional voltage control devices. Moreover, optimal voltage control strategies based on optimisation formulations with weighting factors and penalty functions may not be reliable for practical online voltage control as they can lead to issues associated with accuracy and/or convergence in real-time operations. Furthermore, the application of some search methods such as genetic algorithms, particle swarm optimisation, dynamic programming and interior point techniques may require a complex mathematical formulation of the problem and may not always reach the real optimal solution in case of distribution systems with multiple voltage control devices and DG units. This is further evidenced, for example, by findings in [20]. The associated study concluded that conventional greedy and Tabu search methods may not be suitable for optimal tuning of the control parameters of multiple voltage control devices, especially in the presence of high solar-PV penetration. On the other hand, in the case of online tuning of control parameters, keeping a choice for nodal voltages, rather than assigning a pre-defined multi-objective function, is an added advantage when commercialising DMSs under smart-grid operation as different network operators have different philosophies and practices in voltage control.

2.5 Coordinated Voltage Control in Modern Distribution Systems

In most cases, voltage control by means of the optimal and time-graded operation of multiple voltage control devices such as OLTCs, SVRs and CBs may need to be operationally updated in the presence of DG units for effective voltage regulation in distribution systems. The main reason is that the interactions caused by simultaneous and non-simultaneous operations of Volt/VAr support DG units

and multiple voltage control devices may lead to conflicting operations under certain system conditions within a control state, resulting in voltage variations and voltage rise in the distribution system. More complex phenomena can occur when distribution systems are subjected to structural changes and the availability of DG units. Control coordination is one feasible way of minimising the adverse effects caused by interactions between DG units and voltage control devices. Various methodologies have already been proposed for control coordination of DG units and voltage control devices in distribution systems.

Novel rule and analytics based strategies are proposed in [21] and [22] for maximising DG voltage support and coordinating with voltage control devices. In [17], the ε-decomposition and deep-first search methods are used to identify the network bus voltages which are significantly influenced by DG units in order to utilise multiple DG units for coordinated voltage control. Similarly, power flow sensitivity factor-based strategies for coordinated output control of multiple DG units are detailed in [18]. In [23], online coordinated voltage control strategies are proposed for effective voltage control in distribution systems in a DG-rich environment. However, these methods do not address the coordination of DG units with other voltage control devices in the case of distribution systems with multiple voltage control devices and multiple DG units.

In [19], a strategy is proposed for optimal voltage control and coordination with DG in distribution systems with multiple voltage control devices and DG units. This strategy is formulated as a large-scale optimisation problem, where the amount of operation by each voltage control device is determined using a genetic algorithm-based solver. A strategy is proposed in [12] for coordinated control of DG units and voltage control devices using a dynamic programming algorithm. In [24], a comprehensive decentralised Volt/VAr control strategy is proposed for coordinating the operation of voltage control devices and synchronous machine-based DG units in distribution systems. In [25], the optimal tap settings of the substation OLTC and DG dispatch schemes are derived with the aid of multi-agent systems. In addition, it is reported in [26] that DG participation in voltage control could result in a reduction of tap operations and voltage variations. In [27],

other than the special advantages of the heuristic strategies, the proposed solution methodology eliminates the use of weighing coefficients or penalty terms for optimal coordinated voltage control. In [28], an optimisation-based methodology is proposed for controlling and coordinating DG units with economic considerations and voltage control. A new methodology to reconfigure distribution systems for loss minimisation and thereby optimal voltage control is proposed in [29], whereas coordinated distribution voltage control is achieved by considering DG and load uncertainties in [30]. A multiple LDC based voltage regulation method for under-load tap changer transformers is proposed in [31], where the desired tap positions are determined by solving an integer optimisation problem. In [32], coordinated voltage control methods are proposed based on the statistical analysis considering customer voltage conditions and operational characteristics of DG systems. In [33], a strategy for short-term scheduling of DG units and voltage control devices is proposed for implementing coordinated voltage and reactive power control in distribution systems embedded with renewable DG. The proposed intra-day scheduler is based on a non-linear multi-objective optimisation problem which iteratively applies mixed-integer linear programming to find the solution. However, these studies do not clearly address the way in which the proposed controls perform operationally to minimise the adverse effects of multiple Volt/VAr support DG unit and voltage control device interactions caused by their simultaneous and non-simultaneous operations within a control state, specifically when distribution systems are subjected to structural changes and DG availability. There may also be topology based limitations which are discussed in detail in [14].

CHAPTER 3: OPERATION OF VOLTAGE CONTROL DEVICES AND DG UNITS UNDER OPTIMAL VOLT/VAR CONTROL IN MODERN DISTRIBUTION SYSTEMS

Optimal Volt/VAr formulations are used for tuning the Volt/VAr control parameters of voltage control devices and Volt/VAr support DG units. In this chapter, such a strategy is tested; and the simulation results show that the DG-voltage control device interactions may also be possible even with optimal Volt/VAr control. Section 3.1 provides an introduction to the chapter, while Section 3.2 discusses the problem formulation associated with the proposed optimal Volt/VAr control strategy. Section 3.3 details the test case studies including simulation results and associated discussion is also included. Based on the outcomes of this chapter, a publication titled "Dynamic Adjustment of Volt/VAr Control Set-points for Minimising Interactions and Power Losses in Distribution Grids," authored by D. Ranamuka, A. P. Agalgaonkar, and K. M. Muttaqi, has been submitted to the *Applied Energy Journal.*

3.1 Introduction

Conventional optimisation methods such as linear programming (LP), non-linear programming (NLP), quadratic programming (QP), mixed integer linear programming (MILP), and mixed integer non-linear programming (MINLP) as well as intelligent search methods such as particle swam optimisation (PSO), neural network (NN) and evolutionary algorithms (EA) are widely applied for optimisation of electric power system operation. With the high penetration of renewable energy resources such as wind and solar in electric power systems, the probabilistic optimisation methods considering uncertainties are widely utilised [34]-[36].

NLP methods have higher accuracy and global convergence where the convergence could be guaranteed independent of the starting point. However, in some cases, a slow convergence rate may be experienced due to zigzagging in the search direction [37]. In LP methods, the non-linear optimisation problems are converted to linear optimisation problems in such a way that objective function

and constraints have linear forms. LP methods are reliable considering convergence properties, and infeasibility identification. LP methods can accommodate numerous operational limits of electric power systems. Hence, such methods are widely used for power system optimisation.

QP methods model objective function in quadratic form and the constraints in linear form. QP methods normally have higher accuracy than LP methods, and some electric power system optimisation problems such as distribution system optimal Volt/VAr control problem can directly be formulated in quadratic form [34], [35]. Moreover, electric power system operational problems can be formulated using linear or non-linear mixed integer programming (MIP) based methods by accommodating discrete variables such as OLTC/VR tap operations, CB switching operations and generator unit on and off status. However, MINLP methods are difficult to solve and may require longer computational time and memory space in cases with higher number of discrete variables. Therefore, decomposition techniques are commonly applied with MIP methods to improve the computational efficiency [34].

Distribution system optimal Volt/VAr control strategies, proposed in the literature, can be formulated with the aid of different optimisation methods, while utilising DG for Volt/VAr support. Also, some of the optimal Volt/VAr control strategies are proposed for implementation on real-time basis [27]. The tuned controller parameters are updated simultaneously or based on a desired sequence; whereas the Volt/VAr controllers are operated in accordance with the assigned control logics/algorithms, controller limits and conventional time graded operation [5]. Under conventional time graded operation, the substation OLTC time delay can be set based on constant time variant or inverse time characteristics. In case of constant time variant characteristics, the time delay is constant. With inverse time characteristics, the time delay is inversely proportional to the voltage deviation and can dynamically be updated according to the system conditions. In case of line VRs, VR farther from the substation has longer time delay than the VR closer to the substation. This time delayed operation of VRs is normally based on constant time variant characteristics. Non-

sequential or sequential operational strategies are used for tap operations and to locally coordinate VR operation with the upstream regulators. In non-sequential operation, the time delay is used for all the tap steps, while in sequential operation the time delay is used only for the first tap operation and the subsequent taps are operated with mechanical time delay. However, in [13], it has been investigated that the objectives of the optimisation formulation are not fully achieved under certain system conditions due to conflicting operations resulting into interactions among multiple voltage control devices and the Volt/VAr support DG units. This is an important technical aspect in the context of coordinated voltage control. In this chapter, DG-voltage control device interactions are observed after incorporating optimal Volt/VAr control strategy with an objective of minimising active power losses.

In addition, the conservation voltage reduction (CVR) is emerged as a technique for improving the efficiency of an electrical grid by *optimising voltage* in the distribution system [2]. Accordingly, Volt/VAr management issues under CVR have also been investigated in conjunction with the outcomes reported in this chapter. The case study results are included in Appendix-I for clarity. CVR is one of the viable options for peak-demand reduction and long-term energy savings in densely populated areas or urban power systems. Also, CVR benefits include reduced central generation cost, reduced network losses (both distribution and transmission), improved monitoring, utilisation and performance of distribution assets, deferred investment in transmission and distribution, and potential incentives from regulatory bodies. The associated consumer benefits include reduced energy consumption and electricity bills, improved quality of services, and environmental benefits.

3.2 Problem Formulation of the Proposed Distribution Optimal Volt/VAr Control Strategy

Sequential quadratic programming (SQP) is applied for loss minimisation. Since the substation OLTC deals with voltage regulation at the substation bus-bar level using a coarse control and operates after a prolonged time delay, the substation OLTC operation is not considered as a control variable. The total number of buses

in the distribution system are denoted by n (i.e., $i = 1, \ldots, n$). The generic form of the problem (quadratic sub-problem) is given by (01). It is subjected to deriving the control variables for VRs, DG units and CB; while satisfying equality and inequality constraints denoted by g and h, respectively. The equality constraints are active and reactive power balance equations. The considered inequality constraints include voltage limits, hourly DG reactive power capability limits, distribution line thermal limits, tap limits of VRs, and VAr limits of CBs.

The search-direction at current iterate, k is denoted by $d^{(k)}$. The ∇f denotes respective gradient matrix of the objective function, f of the vector of variables $x^{(k)}$ including control variables; while $\nabla^2 L$ denotes the matrix of *Hessian* of the respective Lagrangian (positive definite approximation). It is a matrix of second order derivatives of the objective function, $f(x^{(k)})$ and the components of equality constraints functions, $g(x^{(k)})$ and non-equality constraints functions, $h(x^{(k)})$ in addition to the Lagrangian multipliers, $\lambda^{(k)}$. The Lagrangian of this problem is given by (02). It is noted that the Lagrangian multipliers of the equality constraints must be non-negative. The Jacobian matrices corresponding to the constraints' vectors of equality and non-equality constraints are J_g and J_h, respectively. Handling discrete control variables is done following the method proposed in [14]. The flow chart of the optimisation process is shown in Figure 3.1. Also, it is worth noting that the discrete control variables related to CB switching operations can also be treated as tap operations. In this chapter, CB switching operations are assumed as continuous control variables in the loss minimisation process. It is mainly because (a) the operational cost associated with a VAr supply from CB is normally very small, and (b) the impact of a CB switching operations on system voltage is localised. The methodology and algorithm proposed in [35] is used for solving the *quadratic sub-problem.*

If the DG units and CBs are operated in voltage control mode, the optimisation problem needs to be re-formulated. Moreover, the voltage control device manoeuvres can be minimised by appropriately maintaining lower values for voltage limits (i.e., V_{min} and V_{max}) compared to the substation secondary bus

voltage. It is assumed that the derivation of hourly DG reactive power capability limits in accordance with the availability of DG active power generation (P_{dgk}) in each hourly control-state is carried out by an algorithm embedded in the DMS, and the loss minimisation algorithm is updated accordingly. The derivation of reactive power capability limits for different types of DG units considering the operational aspects and associated controller limitations is detailed in [36].

$$min_{d^{(k)}} \quad (\nabla f)^{(k)T} d^{(k)} + \frac{1}{2} d^{(k)T} \left(\nabla^2 L\right)^{(k)} d^{(k)}$$

$$\forall \quad g^{(k)} + J_g{}^{(k)} d^{(k)} = 0, \quad h^{(k)} + J_h{}^{(k)} d^{(k)} \leq 0 \tag{01}$$

$$L\left(x^{(k)}, \lambda^{(k)}\right) = f^{(k)} + \sum \lambda_g{}^{(k)} g^{(k)} + \sum \lambda_h{}^{(k)} h^{(k)} \tag{02}$$

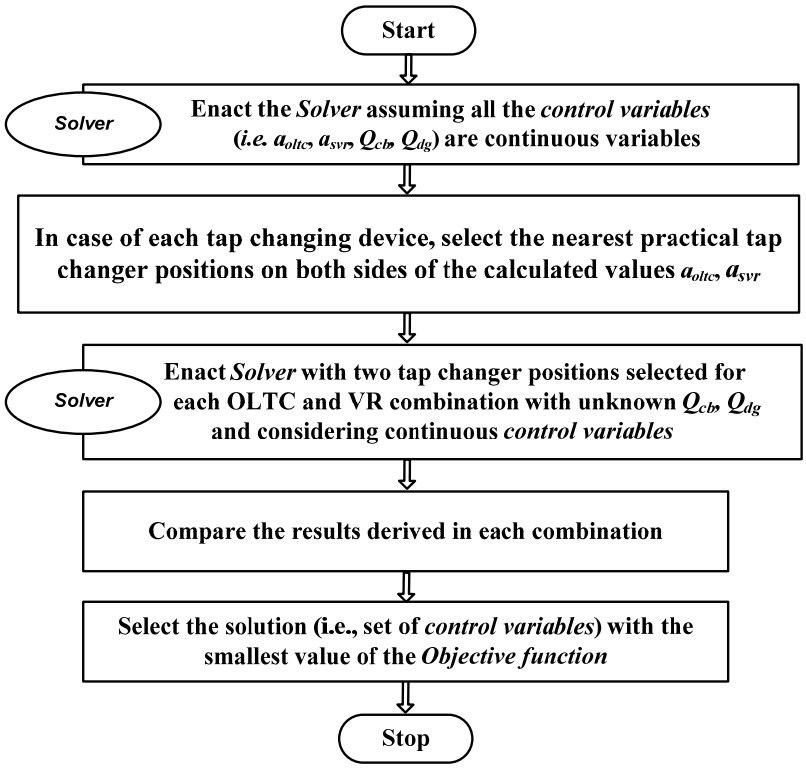

Figure 3.1: Flow chart of the optimisation process for handling discrete variables

3.3 Test Case Study

The test distribution feeder system used in this chapter is modified version of the realistic distribution system topology shown in Figure 2.1 incorporating a switched CB1 of 0.500 MVAr capacity (with 10 equal switching steps) near the end of the feeder, and additional DG units (DG1 and DG2) in the distribution feeder as shown in Figure 3.2. In this section, the balanced distribution feeder system operation i.e., feeder configuration–01 with two synchronous machine based DG units, DG1 and DG2 with 0.750 MVA rated capacity each is used for the simulation purposes. Accordingly, the different system states have been modelled and simulated depicting the distribution system operation. The case study presented in this section is based on a daily operation of the distribution system considering hourly control states. MATLAB software is used for modelling and simulations.

Figure 3.3 (a) depicts the simulated load demand pattern, where the load demand values are in per unit. The per unit active power generation patterns for DG1 and DG2 are shown in Figure 3.3 (b). The optimisation model given by (01) and (02) is adopted for deriving the optimal control parameters of the Volt/VAr control devices. The simulated substation secondary bus voltage is 1.03 pu; while feeder bus voltage limits are maintained within 0.90 pu and 1.04 pu, thereby minimising voltage control device manoeuvres. For VRs, 32 tap positions (+16/-16) are modelled and magnitude of voltage correction for one tap operation equals to 0.00625 pu (to maintain the voltage between 0.90 pu to 1.10 pu) for the VR operation without LDC.

The simulation results obtained using proposed optimal Volt/VAr control strategy are also compared with the results obtained assuming control set-point re-adjustment of Volt/VAr control devices (as mentioned in Table 3.1) based on a conventional method. The conventional Volt/VAr control strategy detailed in [5] is adopted. It mainly considers the critical operational scenarios in the distribution system over a season i.e., (a) maximum load–no generation, (b) maximum load–maximum generation, and (c) minimum load–maximum generation; and

maintains the bus voltages within the stipulated limits. The derived Volt/VAr controller parameters for each hourly operation under proposed optimal Volt/VAr control are shown in Figure 3.4. Moreover, in each case, the variation in system voltage is assessed using the following *voltage variation index*, *VVI* [2]. The maximum and minimum voltages at i^{th} bus are denoted by $Vmax_i$ and $Vmin_i$, respectively.

$$VVI = max\ \left(V\ max_{\,i} - V\ min_{\,i} \right) \quad \forall\ i = 1,\ ...,\ i,\ ...,\ n \ \text{ where } n = \text{total number of busses}$$

Table 3.1: Volt/VAr controller parameters derived using conventional tuning

VR1	VR2
Voltage set value = 1.00 pu	Voltage set value = 0.99 pu
DG1	DG2
VAr setting = 0 MVAr	VAr setting = 0 MVAr
CB	
VAr setting = 0.35 MVAr at 17:00–1:00 hr VAr setting = 0.30 MVAr at 2:00–16:00 hr	

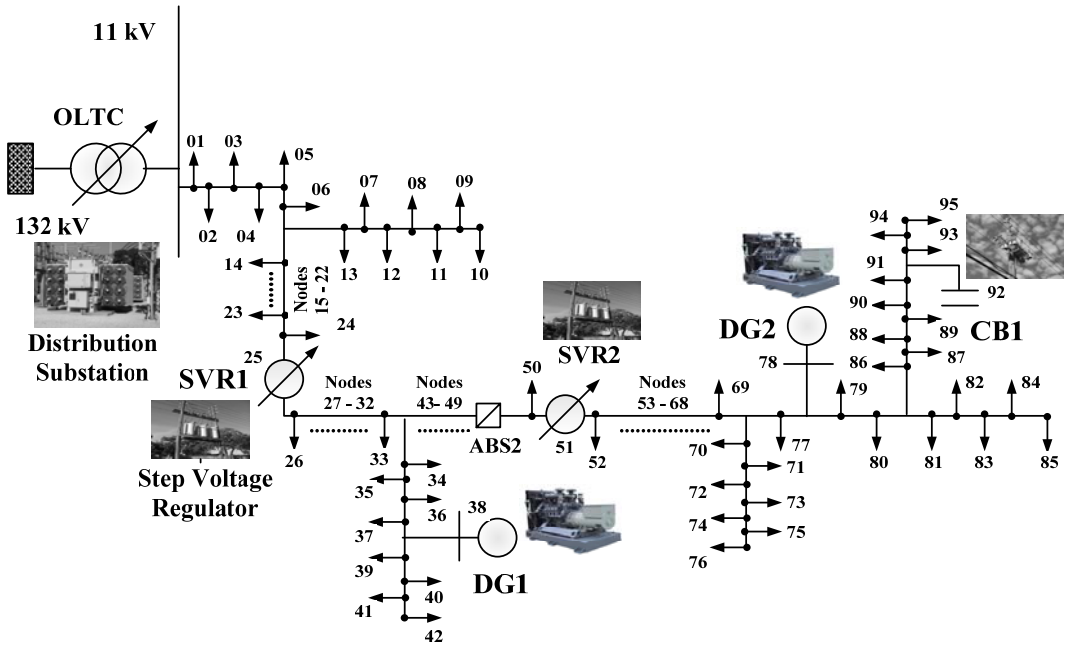

*** Feeder Configuration - 01: System with ABS-1 opened and ABS-2 closed (OLTC, 2 SVRs, DG1, DG2 and CB are in operation)**

Figure 3.2: Topology of MV test distribution feeder system

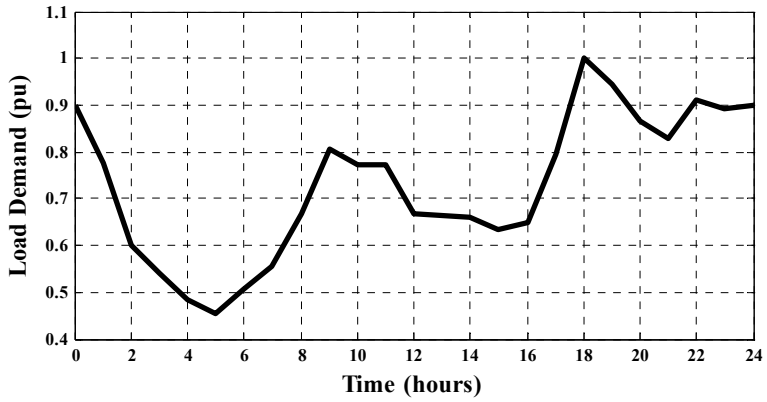

(a)

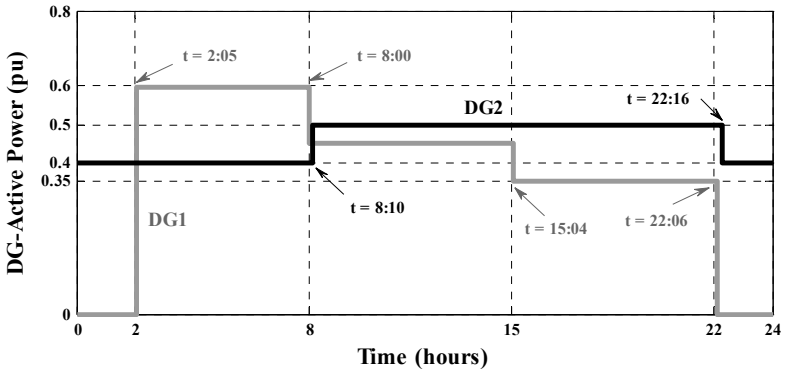

(b)

Figure 3.3: Simulated (a) daily load demand pattern of the test distribution system, and (b) active power generation pattern for DG1 and DG2

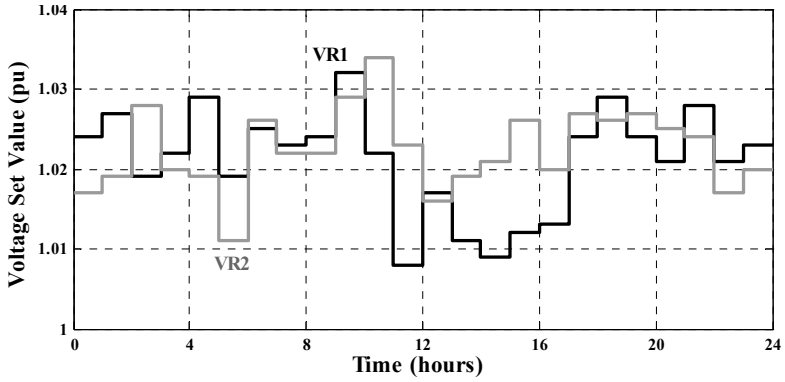

(a)

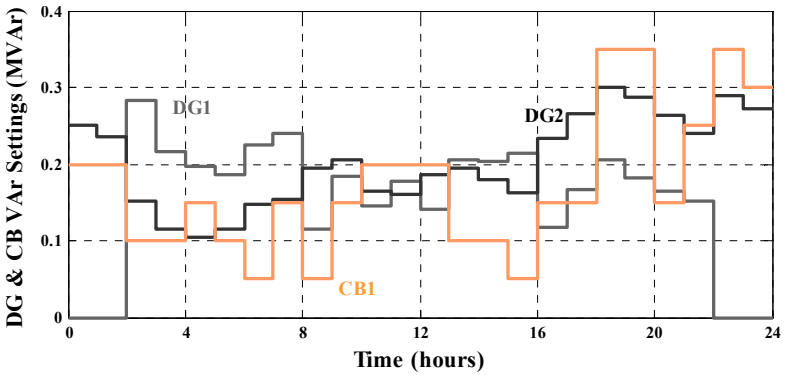

(b)

Figure 3.4: The derived controller parameters under proposed optimal Volt/VAr control for (a) VRs, and (b) DG1, DG2, and CB1

3.3.1 Simulation Results: System Regulated with Optimal Volt/VAr Control Vs Unregulated System

In this section, the simulated results for the test distribution system adopting proposed optimal Volt/VAr control strategy is compared with the simulated results under unregulated system, where VAr support from DG units = 0, VAr supply from CBs = 0 and tap position for VRs = 1. Figure 3.5 (a) shows the active power losses for the unregulated system and for the system operated with the proposed optimal Volt/VAr control; whereas Figures 3.5 (b) and (c) show the voltage at selected buses for unregulated and regulated systems, respectively. The number of *estimated* control actions in each Volt/VAr control device including the DG units in each hourly period for the system regulated with optimal Volt/VAr control is shown in Figure 3.6.

Table 3.2 shows the *VVI* for the unregulated system and system operation under proposed optimal Volt/VAr control. It can be seen that the number of control actions in certain hourly control states are high under optimal Volt/VAr control. However, according to the *VVI* value, the voltage variation in the distribution system is significantly reduced with the implementation of optimal Volt/VAr control.

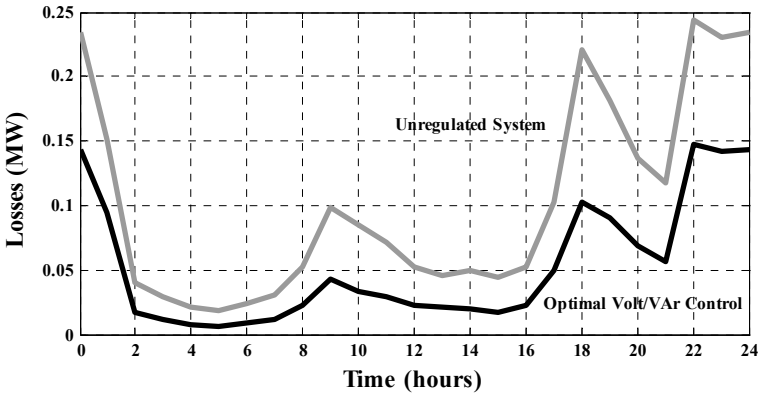

(a)

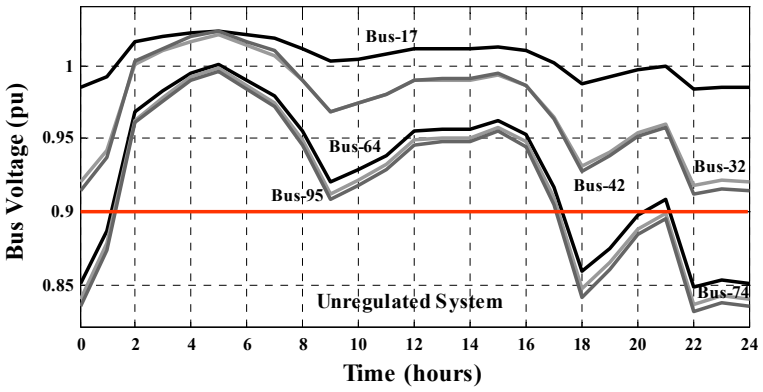

(b)

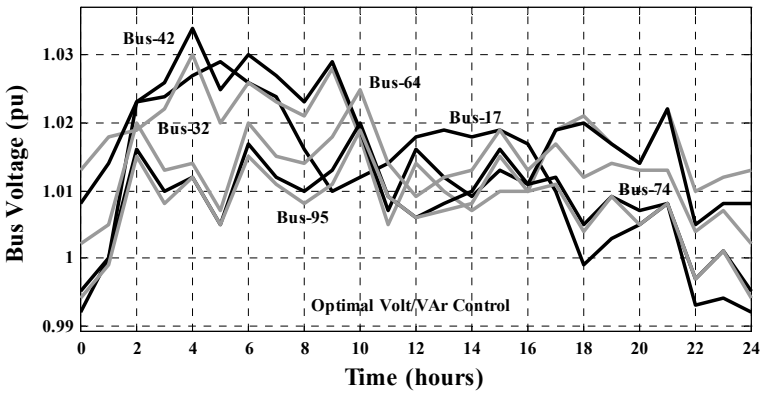

(c)

Figure 3.5: Variation of (a) active power losses, (b) bus voltages for the unregulated system, and (c) bus voltages under optimal Volt/VAr control

– No Volt/VAr control action for the unregulated system –

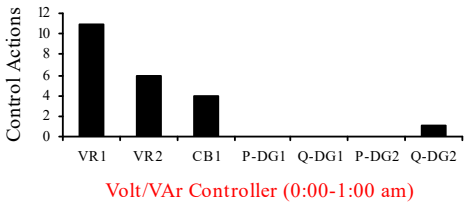

22 control actions

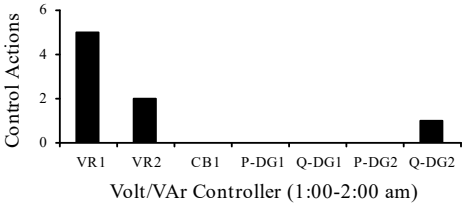

8 control actions

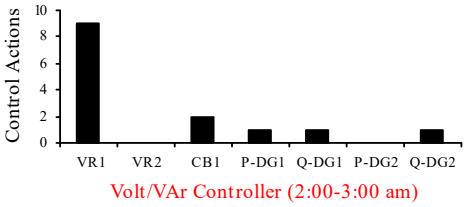

14 control actions

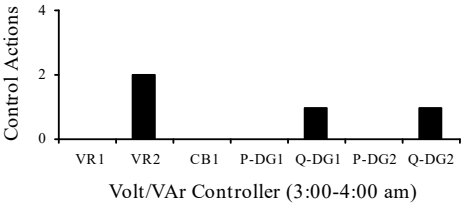

4 control actions

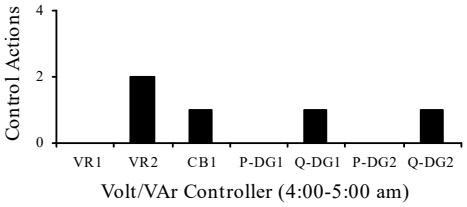

5 control actions

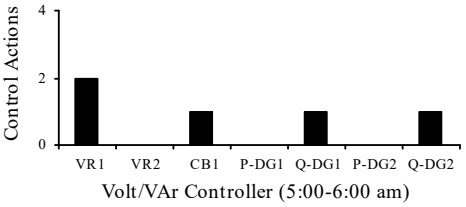

5 control actions

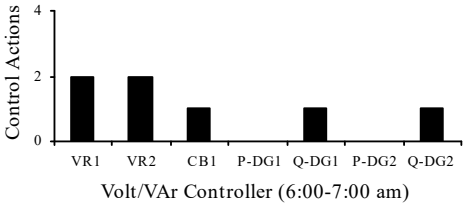

7 control actions

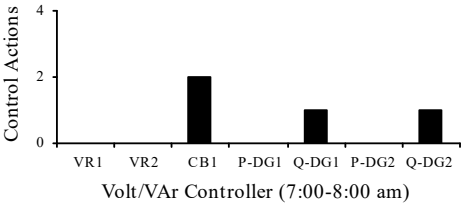

4 control actions

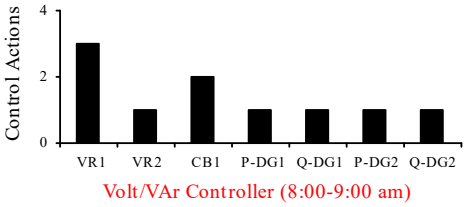

10 control actions

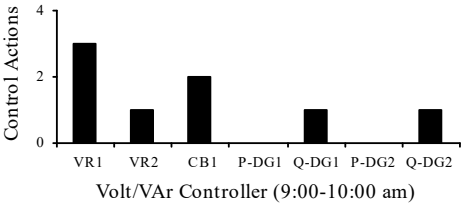

8 control actions

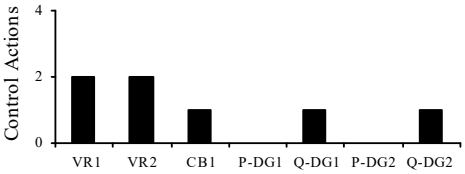

Volt/VAr Controller (10:00-11:00 am)

7 control actions

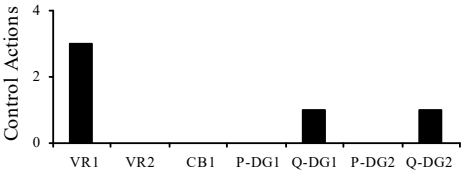

Volt/VAr Controller (11:00-12:00 am)

5 control actions

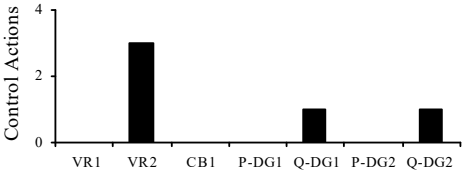

Volt/VAr Controller (12:00-13:00 pm)

5 control actions

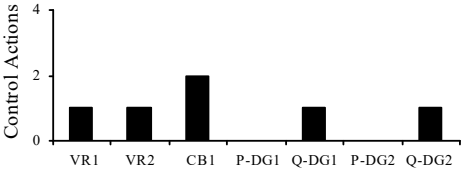

Volt/VAr Controller (13:00-14:00 pm)

6 control actions

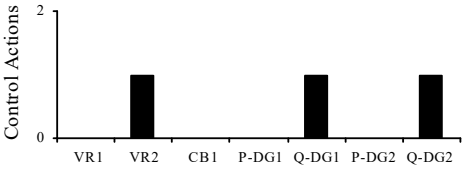

Volt/VAr Controller (14:00-15:00 pm)

3 control actions

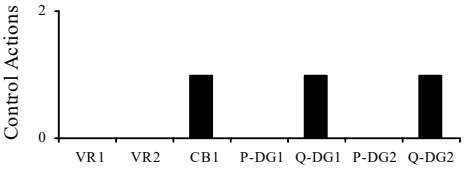

Volt/VAr Controller (15:00-16:00 pm)

3 control actions

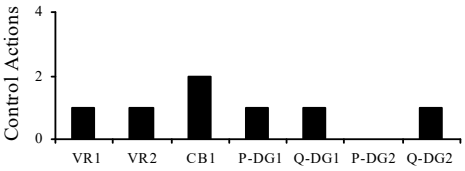

Volt/VAr Controller (16:00-17:00 pm)

7 control actions

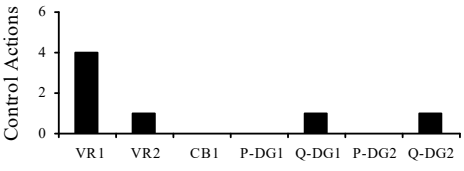

Volt/VAr Controller (17:00-18:00 pm)

7 control actions

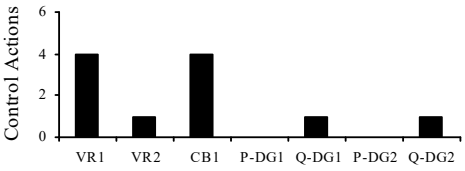

Volt/VAr Controller (18:00-19:00 pm)

11 control actions

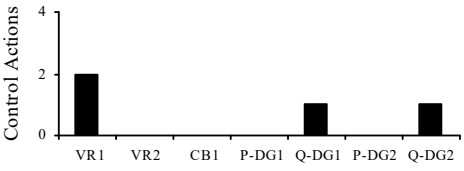

Volt/VAr Controller (19:00-20:00 pm)

4 control actions

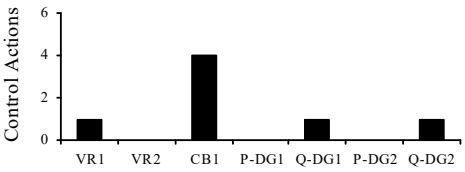

Volt/VAr Controller (20:00-21:00 pm)

7 control actions

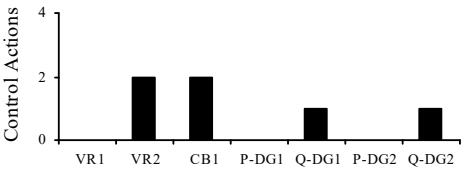

Volt/VAr Controller (21:00-22:00 pm)

6 control actions

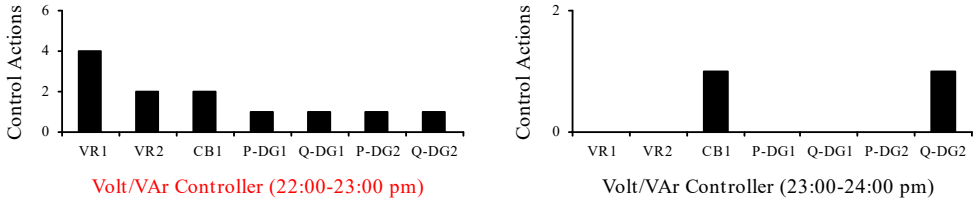

12 control actions

2 control actions

Figure 3.6: Number of estimated control actions in each Volt/VAr control device

Table 3.2: Voltage variation index, *VVI* – case study 3.3.1

Unregulated System	System Regulated with Optimal Volt/VAr Control
0.165	0.073

3.3.2 Simulation Results: Optimal Volt/VAr Control Vs Conventional Volt/VAr Control

In this section, the simulated results under proposed optimal Volt/VAr control strategy are compared with the simulation results obtained for the distribution system assuming conventional method of control set-point re-adjustment (as shown in Table 3.1) for the Volt/VAr control devices. Figure 3.7 (a) shows the active power losses under conventional and proposed optimal Volt/VAr control; while Figures 3.7 (b) and (c) show voltages at the selected buses for the conventional and proposed control strategies. The total number of *estimated* control actions for each Volt/VAr control device during the daily operation is shown in Table 3.3. Table 3.4 shows the respective *VVI* for each system operation. It can be seen that the proposed optimal Volt/VAr control strategy supersedes the conventional method in terms of minimising active power losses in the system. However, it requires additional control actions by the Volt/VAr control devices compared to the conventional Volt/VAr control method within hourly control states under certain system conditions and thereby leading to more number of voltage fluctuations in the system as shown in Figure 3.7. (c). Notably, this is an important observation; because many control-actions may lead to conflicting operations among the Volt/VAr control devices affecting efficiency and effectiveness of the proposed voltage control process, if not properly coordinated in real-time operation. Moreover, it can be seen that the *VVI* values under

conventional Volt/VAr control and optimal Volt/VAr control are almost same for the simulated daily operation of the test system. However, case studies done in [2] have revealed that the *VVI* in presence of significant solar-PV penetration is very much higher than the *VVI* without the solar-PV in the system even with the adoption of optimal Volt/VAr control.

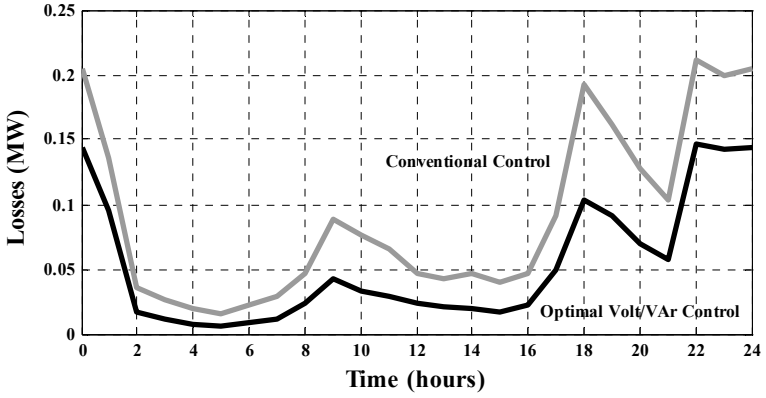

(a)

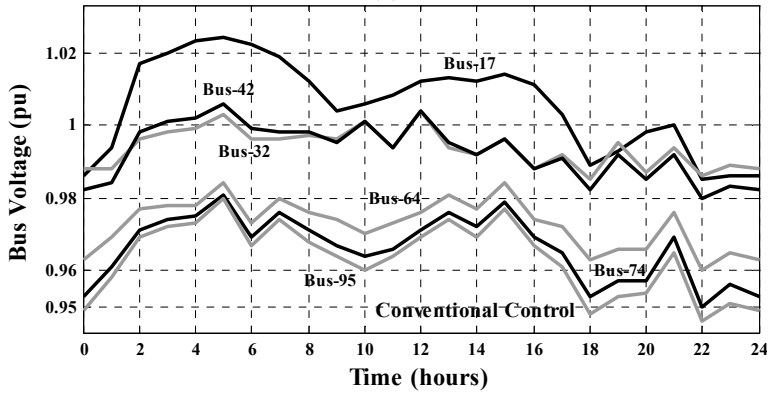

(b)

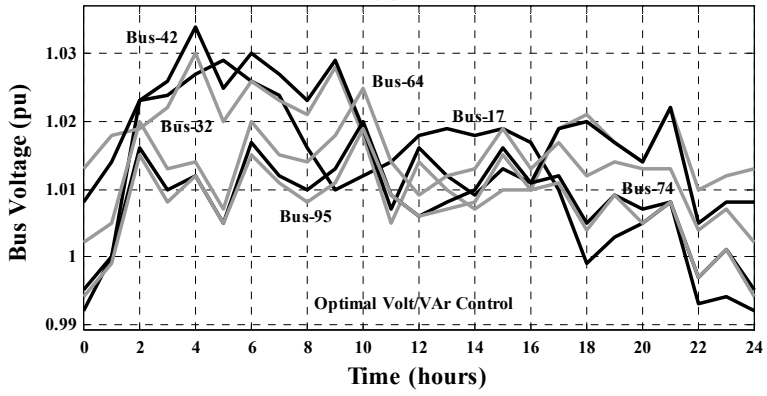

(c)

Figure 3.7: Variation of (a) active power losses, (b) bus voltages under conventional control, and (c) bus voltages under the proposed optimal Volt/VAr control

Table 3.3: Number of estimated control actions in each Volt/VAr control device

Daily Operation | 0:00 am – 24:00 pm					
Conventional Volt/VAr Control			Optimal Volt/VAr Control		
∑ VR Tap Operations	∑ CB Switching Operations	∑ DG Control Actions	∑ VR Tap Operations	∑ CB Switching Operations	∑ DG Control Actions
80	16	6	106	38	51

Table 3.4: Voltage variation index, *VVI*– case study 3.3.2

Conventional Volt/VAr Control	Optimal Volt/VAr Control
0.08	0.07

3.3.3 Simulation Results: Time Domain Simulation under Optimal Volt/VAr Control

In this section, the distribution feeder system operation (i.e., feeder configuration-1 shown in Figure 2.1) under proposed optimal Volt/VAr control is tested in time domain environment using a MATLAB-Simulink simulated detailed model of the test system as shown in Figure 3.8. The main purpose is to observe control actions of tap changing devices under conventional time-graded operation, and the possibilities for tap changing device and DG interactions in steady-state under proposed optimal Volt/VAr control. Hence, only the tap operations are monitored. A separate MATLAB *m-file* is used to load the derived optimal controller parameters into the Simulink model. Load ramping is modelled assuming that the impact of load ramping during a 10-minute (i.e., 600 s) period on the operation of Volt/VAr control devices is negligible. The simulated time delays for VR controllers (assuming Type-B type VRs) are 60 s for VR1 and 90 s for VR2. The substation OLTC is simulated with 30 s time delay and 1.03 pu voltage set-value at the secondary of the associated transformer. For OLTC, 16 tap positions (+8/-8) are modelled and magnitude of voltage correction for one tap operation equals to 0.01250 pu (to maintain the voltage within 0.90 - 1.10 pu). The simulated dead-band of tap changing devices is twice the per unit value of voltage change per tap operation. The total mechanical time delay for substation OLTC, VR1 and VR2

are 5 s, 7 s, and 10 s, respectively. The time delays are not assigned for CB operations and VAr controllers of the DG units, since their time delays are very small compared to the time delays of tap changing devices. The controllers of VRs and CB are updated simultaneously at the beginning of each hourly control state, while VAr controllers of DG1 and DG2 are updated with random sequence i.e., simultaneously and non-simultaneously with VR and CB controller updates depicting the instances of DG operations enforced by the requirements of distribution network operator and operational limitations associated with the modular DG units. It is assumed that the time delay associated with communication channels is negligible.

The selected simulation results showing some of the instances, where there are significant interactions between DG units and VRs, are presented in Figure 3.9. These results are derived and presented on individual 10-minute time spans for clarity purposes. It can be seen that the substation OLTC tap operations have not been altered throughout the simulated daily operation of the test distribution system. It is indicative of the fact that the operation of VRs, the CB and the Volt/VAr support DG units as well as load ramping in the simulated distribution feeder system itself do not have any impact on the OLTC target point voltage i.e., substation secondary voltage. Moreover, it can be seen that the load ramping during 10-minute interval has no significant impact on the operation of line VRs thereby violating there dead-band limits. Consequently, it validates the assumption used for simulating the distribution system operation which says impact of load ramping during a 10-minute (i.e., 600 s) period on the operation of Volt/VAr control devices is negligible. These observations will be useful, when designing coordinated voltage control strategies in presence of Volt/VAr support DG operation in modern distribution systems as detailed in subsequent chapters of the thesis. Furthermore, it is observed that the variability and availability in DG active and reactive power generations, as simulated, lead to additional and/or counteracting VR tap operations by violating the VR dead-band limits under certain system conditions. This is indicative of the fact that interactions among Volt/VAr support DG units and other voltage control devices can be significant

under certain system conditions even with the enforcement of optimal Volt/VAr control; hence, coordinated voltage control strategy is needed for effective voltage control, which can ensure efficient operation of the distribution system.

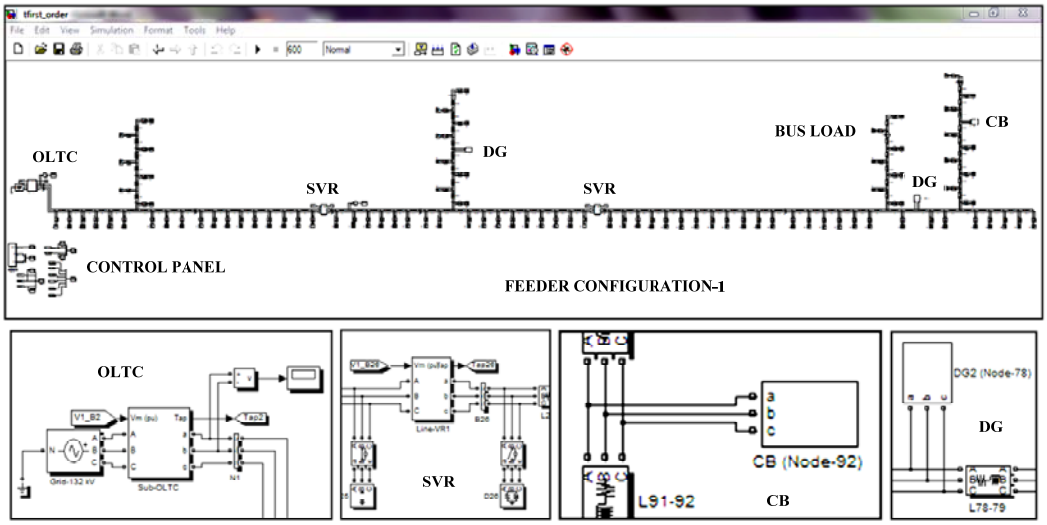

Figure 3.8: Test distribution system modelled in MATLAB-Simulink

In Figure 3.9, the tap operations shown in *blue colour* are for OLTC, while tap operations shown in *green* and *red colours* are of VR1 and VR2, respectively. Also, the voltage profiles shown are for nodes 17 (blue), 32 (red), 42 (green), 64 (light blue), 74 (purple) and 95 (yellow).

Hour | 2:00 – 3:00 am

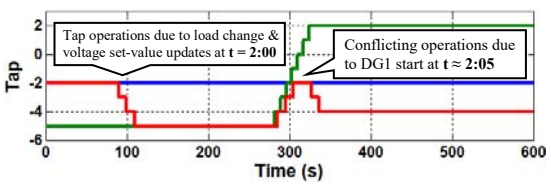

Time | 2:00 – 2:10 am

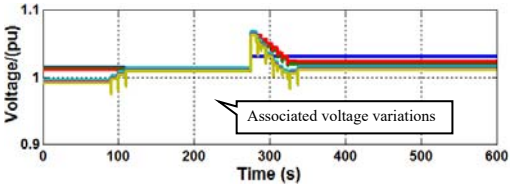

Time | 2:00 – 2:10 am

Hour | 8:00 – 9:00 am

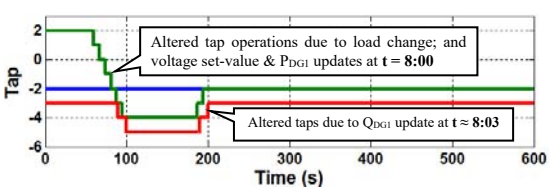

Time | 8:00 – 8:10 am

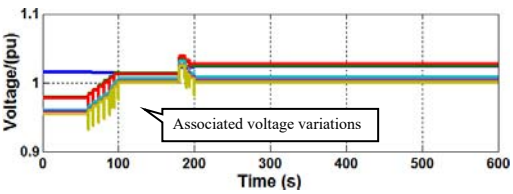

Time | 8:00 – 8:10 am

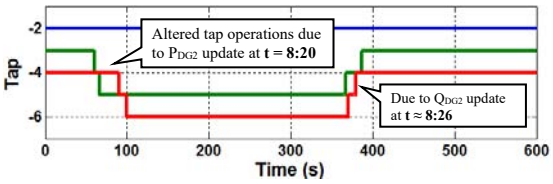

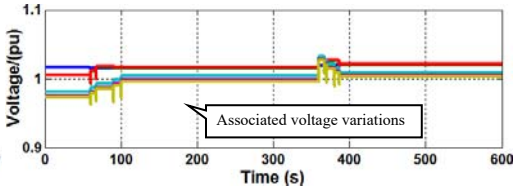

Time | 8:20 – 8:30 am

Time | 8:20 – 8:30 am

Hour | 9:00 – 10:00 am

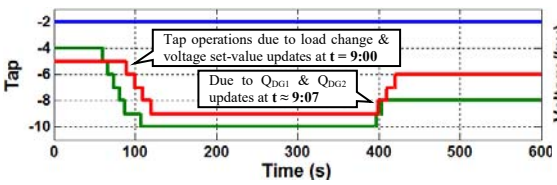

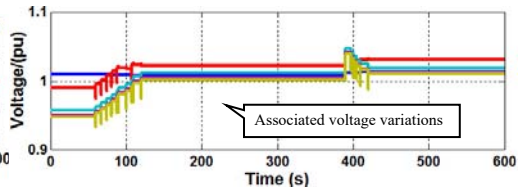

Time | 9:00 – 9:10 am

Time | 9:00 – 9:10

Hour | 11:00 am – 12:00 pm

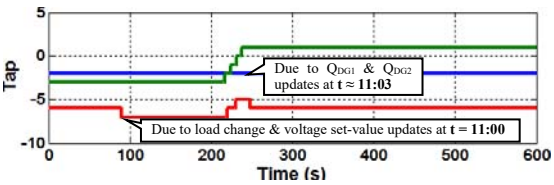

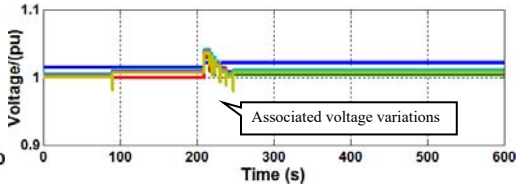

Time | 11:00 – 11:10 am

Time | 11:00 – 11:10 am

Hour | 17:00 – 18:00 pm

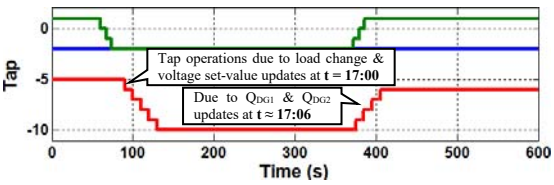

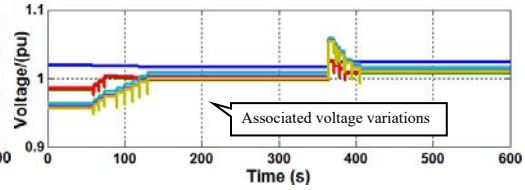

Time | 17:00 – 17:10 pm

Time | 17:00 – 17:10 pm

Hour | 18:00 – 19:00 pm

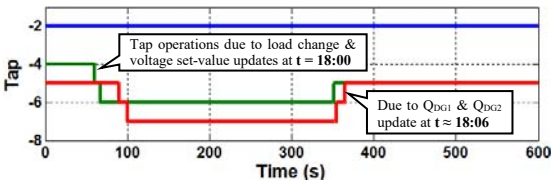

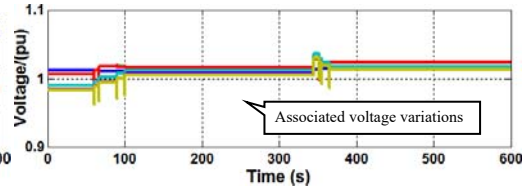

Time | 18:00 – 18:10 pm

Time | 18:00 – 18:10 pm

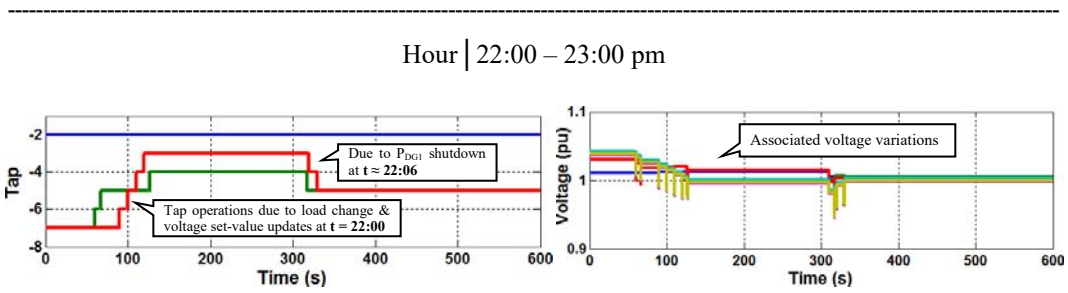

Figure 3.9: Simulated VR and OLTC taps under time -graded operation: selected cases

3.4 Summary

In modern distribution systems, the DG units are utilised for system Volt/VAr support, while achieving the desired objectives of the proposed optimal Volt/VAr control strategy. However, it may introduce additional control actions in the operation of Volt/VAr control devices within certain control states. These control actions may be enacted and updated simultaneously and/or non-simultaneously and continued to operate following an assigned time-graded operation. In such scenario, the operation of multiple Volt/VAr support DG units in conjunction with other voltage control devices (such as OLTC, line VRs and CBs) can lead to significant DG-voltage control device interactions and possible conflicting operations. The outcomes also depend on the objective, mathematical model and search method used in the proposed optimisation, and associated control set-point re-adjustments in the Volt/VAr control devices. This may be a more complicated phenomenon in the presence of multiple DG units with varying power outputs, embedded in the distribution system, wherein multiple CBs and tap changing devices are operated using assigned control logic or algorithm and time delay sequence. Therefore, it is worth examining DG-voltage control device interactions in details, for effective voltage control in modern distribution systems.

CHAPTER 4: EXAMINING THE INTERACTIONS BETWEEN DG UNITS AND VOLTAGE CONTROL DEVICES FOR EFFECTIVE VOLTAGE CONTROL IN DISTRIBUTION SYSTEMS

In this chapter, the proposed modelling and analytical techniques used for examining the interactions between multiple DG units and voltage control devices have been elaborated. Also, some of the important and specific simulation results, obtained using MATLAB, are presented. Section 4.1 provides an introduction to the chapter and Section 4.2 introduces the concept of simultaneous and non-simultaneous responses. Section 4.3 details the test distribution system models used for simulation case studies whereas Section 4.4 outlines the analytical technique used for examining the control interactions. Section 4.5 presents the simulation results and discussion associated with the selected simulation case studies. This chapter is based on the journal publication titled "Examining the Interactions between DG Units and Voltage Regulating Devices for Effective Voltage Control in Distribution Systems," authored by D. Ranamuka, A. P. Agalgaonkar, and K. M. Muttaqi, which has been accepted in the *IEEE Transactions on Industrial Applications* on 21st September 2016.

4.1 Introduction

As discussed earlier, the voltage control strategies proposed in the existing literature for active distribution systems can distinctly be classified as (a) decentralised voltage control and (b) centralised voltage control, based on the control action in space and time. The voltage control mechanisms, which utilise both decentralised and centralised infrastructure may enhance the voltage control performance, however it may not be as sophisticated as centralised voltage control. In cases where downstream distribution feeder systems have not communication infrastructure, the combined decentralised and centralised voltage control can be more robust in presence of renewable DG [13].

In conventional decentralised voltage control, tuning of local control parameters on a seasonal basis is common and is accomplished using optimisation, rule and analytics based formulations. The coordinated operation is achieved using time-

graded operation of different voltage control devices i.e., by assigning appropriate time delays based on experiences and/or commonly used thumb rules. However, there is no mechanism to avoid or minimise the interactions among DG units and voltage control devices during seasonal changes leading to inherent random variations in network conditions. Therefore, it is clear that there are higher possibilities of interactions between DG units (i.e., operated with power factor, reactive power and voltage control modes) and voltage control devices such as OLTC/VRs which are enacted with and without line drop compensation and CBs. It may lead to adverse effects such as conflicting operations and resultant voltage variations, especially under conventional decentralised voltage control.

Under centralised voltage control, coordinated operation of OLTC, VRs and CBs are accomplished by short term tuning with or without centrally dispatching the DG. The control decisions at a particular control state are commonly enacted using a centralised DMS, associated hardware, software and communication infrastructure. The short-term control states are commonly defined with 1 hour, 15 or 10 minute time periods, which are suitable for practically dispatching DG and updating its voltage controller based on the operational capabilities. It is noted that there may be significant control interactions among multiple DG units and voltage control devices as there is no mechanism to operationally eliminate or minimise the control interactions between 2 control states. In case of active distribution systems embedded with DG units, this is reasoned by four major phenomena as below: (a) Network voltages are subjected to inherently and frequently varying operating conditions and perturbations compared to those in transmission systems and distribution systems without DG units; (b) the impact of DG from voltage control perspective cannot be assessed simply under steady state network conditions but dynamic network conditions also need to be examined; (c) it is very difficult to forecast the renewable power generation because of high level of uncertainty associated with their intermittent power output; and (d) the prioritised operation of different voltage control devices depends on the network topology and the associated system characteristics. This emphasises the requirement of a *new voltage control strategy* for effective voltage control in active distribution

systems as outlined in Figure 4.1. It examines the DG-voltage control device interactions based on a generic classification for the interactions and proposed analytical technique, which considers both steady-state and dynamic impacts.

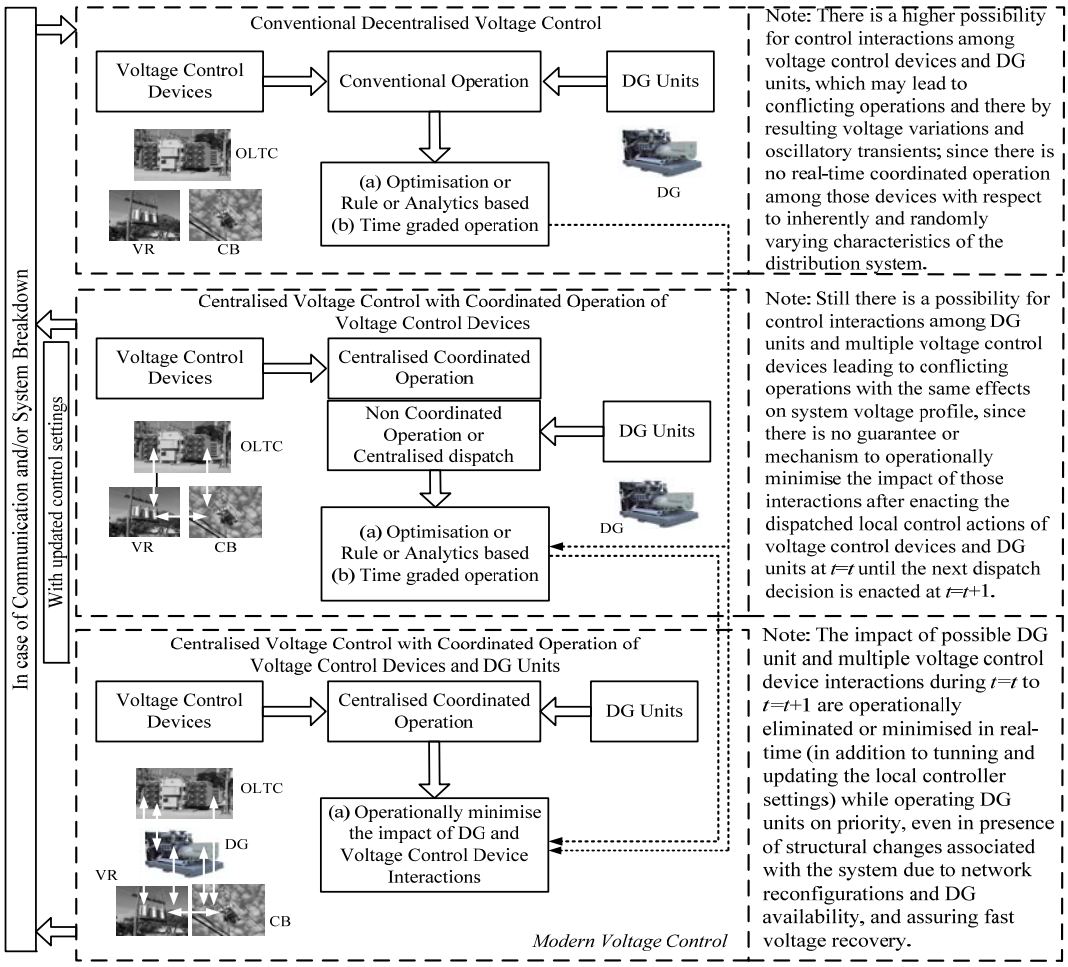

Figure 4.1: Diagrammatic representation classifying coordinated voltage control in active distribution systems

In the published literature, the DG-voltage control device control interactions have been examined using simulation studies and by assessing the conflicting operations and associated voltage variations. In the publication *originated from this research project* [38], DG impact on operation of OLTC and line VRs has been observed using dynamic model, detail time domain simulations and by comparing the number of tap operations with and without availability of DG. However, the impact of DG in each case is not distinctly analysed. In [2], [39]-[40], the impact of DG on operation of OLTC and VRs connected in different

distribution system topologies has been observed using static models and simulation case studies. Accordingly, a classification for DG-voltage control device interactions has been made with respect to different DG operational modes (i.e., unity power factor, reactive power control and voltage control) as well as considering the number of tap operations and resultant voltage variations in the distribution system. In [13], [24], similar investigation studies have been carried out by classifying DG units into synchronous, induction machine and inverter interface based units. However, the dynamic impact is not explicitly analysed in these studies. The dynamics associated with DG and voltage control device operation under large perturbations is discussed in [16]. In [5], the DG-voltage control device interactions and their impact on voltage stability are analysed. However, they do not address the inherent operation of multiple DG units and voltage control device for correcting the normal-state voltage subjected to small perturbations; which require a unique approach for classifying and analysing the interactions among multiple DG units and voltage control devices considering both steady-state and the dynamic impact. The typical time scale of dynamics associated with DG and voltage control device operations is shown in Figure 4.2 [2].

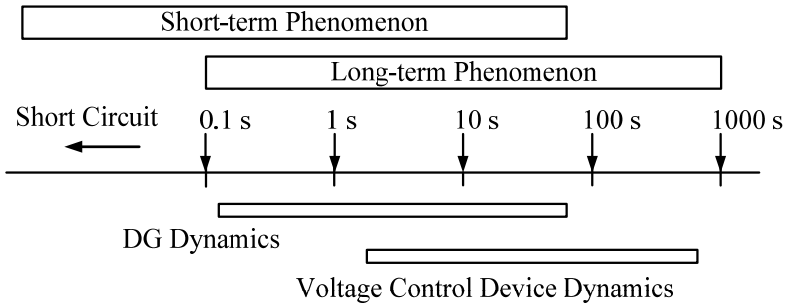

Figure 4.2: Typical time scale of DG and voltage control device dynamics

Therefore, in this chapter, control interactions among multiple voltage control devices, including OLTCs, VRs, and CBs, and Volt/VAr support DG units in a distribution system are examined using the *concept of simultaneous and non-simultaneous responses,* and effectiveness of designing required *voltage control strategy* is discussed.

4.2 Concept of Simultaneous and Non-simultaneous Responses

In this section, the concept of simultaneous and non-simultaneous responses of multiple voltage control devices and DG units is introduced for classifying the DG and voltage control device interactions and analysing their impact on normal-state voltage control.

In the context of normal-state voltage control in active distribution systems, the interactions among DG units and voltage control devices can be classified into interactions caused by two fundamental phenomena namely Simultaneous and Non-simultaneous Responses of DG units and voltage control devices. Typically, these responses are representative of OLTC and VR tap operations, CB switching operations, operation of other voltage control devices and update of X_{ref} value of DG Volt/VAr controllers (as shown in Figure 2.2), which can also vary the DG active and reactive power outputs as outlined in Section 2.3.1. Simultaneous responses are the DG and voltage control device operations which do occur at the same time, where non-simultaneous responses are the DG and voltage control device operations which do not occur at the same time.

In this thesis, it has been identified that this distinct classification for DG-voltage control device interactions subjected to inherent operation of multiple DG units and voltage control devices for correcting the voltage is one of the convenient ways of analysing the impact of the associated interactions. It eventually has led to a versatile approach for mitigating the possible adverse effects on system voltage profile. It is noted that mitigating the impacts of simultaneous and non-simultaneous responses distinctly would lead to a new concept of normal-state voltage control in modern distribution systems as outlined under *Modern Voltage Control* in Figure 4.1 and elaborated further in the Sections 4.6 and 4.7. Also, these concepts are supplemented through specific research studies conducted in Chapters 5, 6, and 7.

4.3 System Modelling

In this section, the test MV distribution system model used in the case studies is explained in detail. A MV distribution feeder system with HV/MV integrated substation system is modelled for examining the possible DG and voltage control device interactions using the concept of simultaneous and non-simultaneous responses of the DG units and the voltage control devices [41], [42].

The test systems are modelled incorporating the steady-state power balance equations and models for OLTC, VRs, CBs and DG units. The details on modelling OLTC, VRs, CBs and their controllers in distribution systems are extracted from [1], [5]. The nodes where DG units operated in power factor or VAr control mode are modelled as *PQ-nodes*, and the nodes where DG units operated in voltage control mode are modelled as *PV-nodes*. The loads are modelled using constant power characteristics, and Newton-Raphson algorithm is applied for obtaining the power flow solutions. The static simulation studies are carried out for selected short-term system states on 10 minute basis related to the test distribution system operation. It is noted that the load ramping is normally negligible within 10 minute intervals. Moreover, a small signal model is developed for distinctly identifying and analysing the dynamic impact of simultaneous and non-simultaneous responses of multiple voltage control devices and DG units in the test distribution systems. The simulation case studies are carried out on the test system for selected operating points.

The proposed small signal model is given by (01), where x, V, δ and u denote the state variables, bus voltage magnitudes, bus voltage phasor angles and discrete events of voltage control devices and DG units, respectively. The associated numerical matrices are [A], [B], [C] and [D], where [A] is the state matrix. The a_{oltc} and a_{vr} denote tap ratio of OLTC and VRs respectively, where B denotes the susceptance value of CBs. Subscripts R and I denote the real and imaginary parts of current, i and nodal voltage, v vectors; respectively.

$$\Delta\dot{x} = [A].\Delta x + [B].\Delta u, \quad \Delta v = [C].\Delta x + [D].\Delta u \tag{01}$$

$$\Delta u = \begin{bmatrix} \Delta a_{oltc} & \Delta a_{vr} & \Delta B_{cb} & \Delta X_{ref} \end{bmatrix}^T - \text{Inputs}$$

$$\Delta v = \begin{bmatrix} \Delta V_R & \Delta V_I \end{bmatrix}^T - \text{Outputs}$$

The loads are modelled as given by (02) and using dynamic parameters which have been derived from field measurements as detailed in [43]. The x_l is state matrix, which models the load active and reactive power recoveries by x_p and x_q respectively. The recovery time constants are T_p and T_q, and α_s, α_t, β_s, β_t are the exponents of the voltage. The steady state nodal voltage dependency of loads is denoted using $P_s(V)$ and $Q_s(V)$, whereas the transient (instantaneous) nodal voltage dependency is denoted using $P_t(V)$ and $Q_t(V)$ respectively. The P_d and Q_d denote actual loads where the rated load values are denoted using P_0 and Q_0. The load scale factor is k_L. The [v_l] (which includes magnitude and phasor angle of the load voltage) and [i_l] (which includes magnitude and phasor angle of the load current) denotes the input and output matrices, respectively.

$$\dot{x}_p = \frac{1}{T_p}\left(-x_p + P_s(V) - P_t(V)\right), \quad P_s(V) = k_L P_0 \left(V_l\right)^{\alpha_s}$$

$$P_t(V) = k_L P_0 \left(V_l\right)^{\alpha_t}, \quad P_d = x_p + P_t(V)$$

$$\dot{x}_q = \frac{1}{T_q}\left(-x_q + Q_s(V) - Q_t(V)\right), \quad Q_s(V) = k_L Q_0 \left(V_l\right)^{\beta_s}$$

$$Q_t(V) = k_L Q_0 \left(V_l\right)^{\beta_t}, \quad Q_d = x_q + Q_t(V)$$

$$\Delta\dot{x}_l = \left[A_l\right]\Delta x_l + \left[B_l\right]\Delta v_l, \quad \Delta i_l = \left[C_l\right]\Delta x_l + \left[D_l\right]\Delta v_l \tag{02}$$

$$\Delta x_l = \begin{bmatrix} \Delta x_p & \Delta x_q \end{bmatrix}^T, \ \Delta v_l = \begin{bmatrix} \Delta V_{lR} & \Delta V_{lI} \end{bmatrix}^T, \ \Delta i_l = \begin{bmatrix} \Delta I_{lR} & \Delta I_{lI} \end{bmatrix}^T$$

Since majority of local generation embedded in MV distribution systems is still based on synchronous machine based technology, such synchronous machine based renewable DG units operated in voltage control mode are modelled and simulated. However, the proposed method can also be applied to the distribution systems embedded with other types of DG technologies. Overall, DG unit model including the models of the controllers can be derived as given by (03). The state

matrix [x_{dg}] includes the sub matrices of synchronous generator, excitation system and prime mover-governor system states, which are represented by [x_m], [x_e] and [x_t] respectively. The [v_{dg}] (magnitude and phasor angle of the DG bus voltage) and [i_{dg}] (magnitude and phasor angle of the current fed by the DG) denoted the input and output matrices, respectively.

$$\begin{aligned}
\Delta\dot{x}_{dg} &= \left[A_{dg}\right]\Delta x_{dg} + \left[E_{dg}\right]\left[\Delta X_{ref}\right] + \left[B_{dg}\right]\Delta v_{dg} \\
\Delta i_{dg} &= \left[C_{dg}\right]\Delta x_{dg} + \left[D_{dg}\right]\Delta v_{dg} \\
\Delta\omega_{ref} &= 0, \quad X_{ref} = V_{ref}, \quad \Delta x_{dg} = \left[\Delta x_m \,|\, \Delta x_e \,|\, \Delta x_t\right]^T \\
\Delta v_{dg} &= \left[\Delta V_{dgR} \;\; \Delta V_{dgI}\right]^T, \quad \Delta i_{dg} = \left[\Delta I_{dgR} \;\; \Delta I_{dgI}\right]^T
\end{aligned} \tag{03}$$

The synchronous generator can be modelled using standard 5th order dynamic representation as given by (04) [8]. The state matrix [x_m] includes the state variables of rotor angle (δ_r), rotor speed (ω_r), *d*-axis field winding flux linkage (φ_{fd}), *d*-axis damper winding flux linkage (φ_{1d}) and *q*-axis damper winding flux linkage (φ_{1q}). The symbols, T_m and E_{fd} denote the mechanical torque produced by the turbine and exciter field voltage, respectively. The [v_m] (magnitude and phasor angle of the machine terminal voltage) and [i_m] (magnitude and phasor angle of the machine current) denote the input and output matrices, respectively.

$$\begin{aligned}
\Delta\dot{x}_m &= \left[A_m\right]\Delta x_m + \left[E_m\right]\left(\Delta T_m \;\; \Delta E_{fd}\right)^T + \left[B_m\right]\Delta v_m \\
\Delta i_m &= \left[C_m\right]\Delta x_m + \left[D_m\right]\Delta v_m \\
\Delta x_m &= \left(\Delta\delta_r \;\; \Delta\omega_r \;\; \Delta\varphi_{fd} \;\; \Delta\varphi_{1d} \;\; \Delta\varphi_{1q}\right)^T \\
\Delta v_m &= \left[\Delta V_{mR} \;\; \Delta V_{mI}\right]^T, \quad \Delta i_m = \left[\Delta I_{mR} \;\; \Delta I_{mI}\right]^T
\end{aligned} \tag{04}$$

The excitation system shown in Figure 4.3 is adopted from [44] for simulating DG excitation control. The associated small signal model is given by (05), wherein x_e is state matrix, which models the internal states x_{e1}, x_{e2}, x_{e3}, x_{e4}, and x_{e5} according to the Figure 4.3. The *T* and *K* values in each block (as depicted in Figure 4.3)

define the respective time delays and gain constants in the circuit, where *s* denotes the Laplace transform operator.

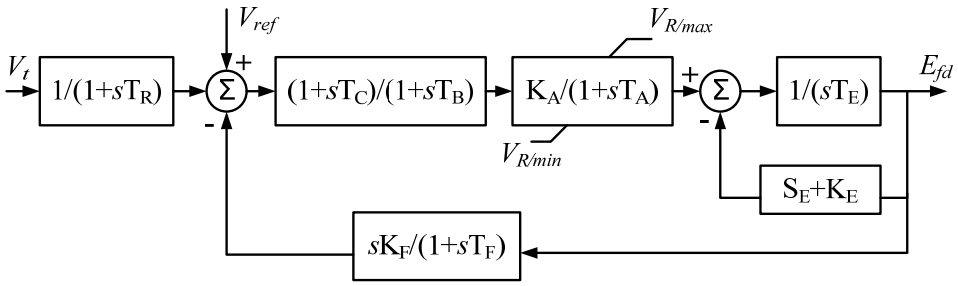

Figure 4.3: Block diagram of excitation system model

$$\Delta\dot{x}_e = \lfloor A_e \rfloor \Delta x_e + \lfloor E_e \rfloor \Delta X_{ref} + \lfloor B_e \rfloor \Delta v_m$$

$$\Delta E_{fd} = \lfloor C_e \rfloor \Delta x_e + \lfloor D_e \rfloor \Delta v_m \qquad (05)$$

$$\Delta X_{ref} = V_{ref}\ , \quad \Delta x_e = \lfloor \Delta x_{e1} \ \ \Delta x_{e2} \ \ \Delta x_{e3} \ \ \Delta x_{e4} \ \ \Delta x_{e5} \rfloor^T$$

$$\Delta v_m = \lfloor \Delta V_{mR} \ \ \Delta V_{mI} \rfloor^T$$

The prime mover system shown in Figure 4.4 is used for simulating bio-diesel DG prime mover control [45]. Its small signal model is given by (06), where x_t is the state matrix which models the internal states x_{t1}, x_{t2}, x_{t3} and x_{t4} according to Figure 4.4. T_e denotes the electro-mechanical torque.

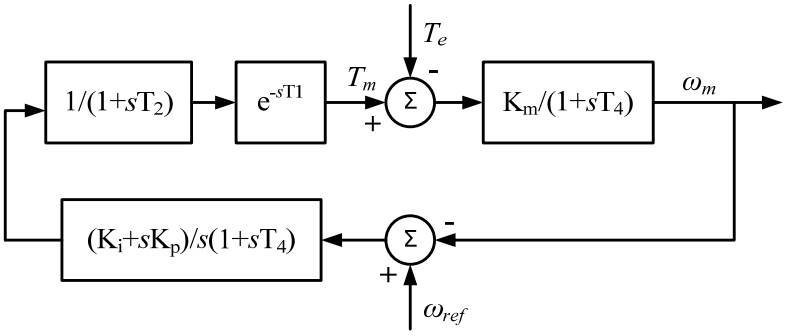

Figure 4.4: Block diagram of bio-diesel prime mover model

$$\Delta\dot{x}_t = \lfloor A_t \rfloor \Delta x_t + \lfloor B_t \rfloor \Delta T_e\ , \quad \Delta T_m = \lfloor C_t \rfloor \Delta x_t + \lfloor D_t \rfloor \Delta T_e \qquad (06)$$

$$\Delta\omega_{ref} = 0\ , \quad e^{-sT_1} \approx \left(1 - sT_1\right), \quad \Delta x_t = \lfloor \Delta x_{t1} \ \ \Delta x_{t2} \ \ \Delta x_{t3} \ \ \Delta x_{t4} \rfloor^T$$

The prime mover system shown in Figure 4.5 [46] is adopted for simulating small-hydro DG prime mover control. The relevant small signal model is given by (07), where x_t is the state matrix which models the internal states x_{t1}, x_{t2} and x_{t3} according to the Figure 4.5. The ω_m denotes the mechanical speed of the turbine.

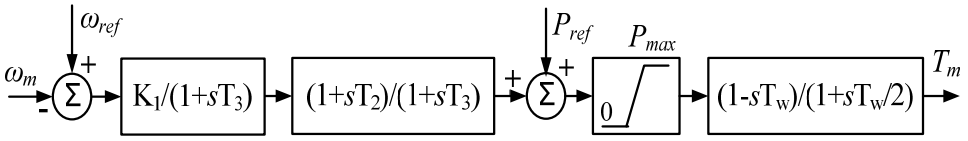

Figure 4.5: Block diagram of small-hydro prime mover model

$$\Delta\dot{x}_t = \lfloor A_t \rfloor \Delta x_t + \lfloor B_t \rfloor \Delta\omega_m \,,\ \Delta T_m = \lfloor C_t \rfloor \Delta x_t + \lfloor D_t \rfloor \Delta\omega_m \tag{07}$$

$$\Delta\omega_{ref} = 0,\quad \Delta P_{ref} = 0,\quad \Delta x_t = \left[\Delta x_{t1}\ \ \Delta x_{t2}\ \ \Delta x_{t3}\right]^T$$

The prime mover system shown in Figure 4.6 is adopted from [47] for simulating bio-gas DG prime mover control. Its small signal model is given by (08), where x_t is the state matrix which models the internal states x_{t1}, x_{t2} and x_{t3} according to the Figure 4.6. The ω_m denotes the mechanical speed of the turbine.

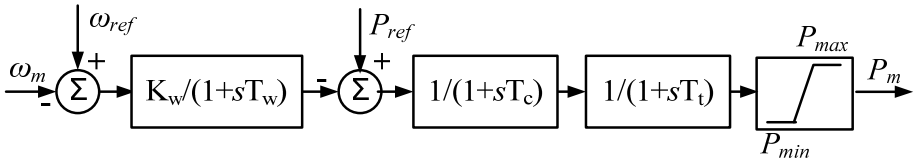

Figure 4.6: Block diagram of bio-gas prime mover model

$$\Delta\dot{x}_t = \lfloor A_t \rfloor \Delta x_t + \lfloor B_t \rfloor \Delta\omega_m \,,\ \Delta T_m = \lfloor C_t \rfloor \Delta x_t + \lfloor D_t \rfloor \Delta\omega_m \tag{08}$$

$$\Delta\omega_{ref} = 0,\quad \Delta P_{ref} = 0, \Delta x_t = \left[\Delta x_{t1}\ \ \Delta x_{t2}\ \ \Delta x_{t3}\right]^T$$

Finally, the overall small signal model of the interconnected system is derived by linking the small signal models of each component with the associated linearised version of the static network model and the linearised version of the power balance equations, $g(x_l, v, a, B) = 0$ mainly at the load buses as in (09) and (10), respectively. Flow chart for deriving the proposed overall small signal model is shown in the Figure 4.7. Small signal version of branch admittance matrix is Y_{bus}.

$$\begin{pmatrix} \Delta I_R \\ \Delta I_I \end{pmatrix} = \left(Y_{bus}\right)\begin{pmatrix} \Delta V_R \\ \Delta V_I \end{pmatrix}, \quad \text{slack bus}: \Delta V_{0R} = \Delta V_{0I} = 0 \tag{09}$$

$$\left(\frac{\partial g}{\partial x_l}\right)\Delta x_l + \left(\frac{\partial g}{\partial v}\right)\Delta v + \left(\frac{\partial g}{\partial a}\right)\Delta a + \left(\frac{\partial g}{\partial B}\right)\Delta B = 0 \tag{10}$$

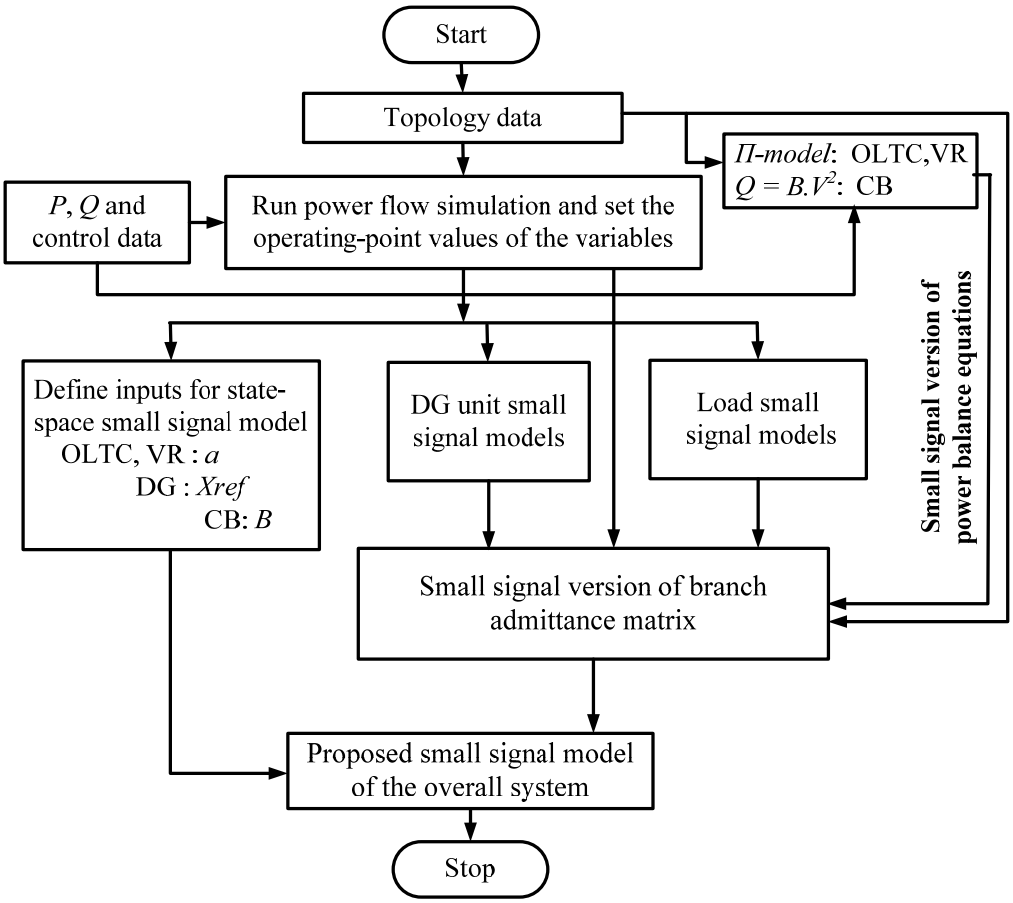

Figure 4.7: Flow chart for deriving the proposed small signal system model

4.4 Analytical Technique for Examining Interactions between Voltage Control Devices and DG Units

In this section, the proposed methodology for examining the interactions between the DG units and voltage control devices in active distribution systems is summarised. In modern distribution systems, the information from DMS can be utilised for assessment of the interactions in short-term system states i.e., on 10 minute interval basis using the steps discussed below.

Step-I: Adopt the concept of simultaneous and non-simultaneous responses for classifying the DG unit and voltage control device interactions.

- Note: As introduced in Section 4.2, the interactions among DG units and voltage control devices are classified into interactions caused by two fundamental phenomena namely simultaneous and non-simultaneous responses of DG units and voltage control devices. Typically, those responses are OLTC and VR tap operations, CB switching operations, operation of other voltage control devices and update of X_{ref} value of DG controllers which eventually leads to varying DG power output.

Step-II: Select the system states including all required data in the test distribution system operation according to the adopted voltage control strategy.

- Note: In this chapter, short-term system states on 10 minute interval basis are selected.

Step-III: Examine the steady-state phenomenon using the static model proposed in Section 4.3.

Step-IV: Identify the adverse effects caused by the DG unit and voltage control device interactions on system voltage control performance.

Step-V: Carryout the investigations using the small signal model proposed in Section 4.3 using selected operating points for the selected system state (Step-II) for distinctly identifying the dynamic impact associated with respective simultaneous and/or non-simultaneous responses of the DG units and the voltage control devices.

- Note: Conduct eigen-value analysis and modal analysis in order to identify the oscillatory modes, non-oscillatory modes, associated participation factors and instability of the voltage control process.
- Note: Derive the Bode plots of transfer functions in order to analyse the dynamic impact of the DG-voltage control device operation on system voltage in detail. In this case, the output matrix of the proposed small signal model is modified using (11), since output to input link (feedback) through each voltage controller to the respective open loop transfer function requires change in voltage

magnitude, V as an input. The β denotes the respective voltage phasor angle. Then, the overall small signal model is given by (12).

$$\begin{pmatrix} \Delta V_R \\ \Delta V_I \end{pmatrix} = \begin{pmatrix} \cos(\beta) & -V\sin(\beta) \\ \sin(\beta) & +V\cos(\beta) \end{pmatrix} \times \begin{pmatrix} \Delta V \\ \Delta \beta \end{pmatrix} \quad (11)$$

$$\Delta \dot{x} = \left[\hat{A}\right] \Delta x + \left[\hat{B}\right] \Delta u, \qquad \Delta v = \left[\hat{C}\right] \Delta x + \left[\hat{D}\right] \Delta u \quad (12)$$

$$\Delta u = \left[\Delta a_{oltc} \;\; \Delta a_{vr} \;\; \Delta B_{cb} \;\; \Delta X_{ref} \right]^T - \text{Inputs}$$

$$\Delta v = \left[\Delta V \;\; \Delta \beta\right]^T - \text{Outputs}$$

- Note: The inter-unit electro mechanical oscillations among different DG units are identified, if the examined oscillatory behaviour is inversely proportional to the impedance between the DG units followed by the mode-shape analysis. In case of inter-unit electro-mechanical oscillations, the mode shape analysis will show the phase angle difference of respective right eigen vectors with respect to the rotor angle states, δ_r of the DG units nearly or exactly equal to 180^0.

The flow chart detailing all the steps of the proposed analytical technique is shown in Figure 4.8. Moreover, the concept of electric distance is applied for identifying and analysing the interactions among DG units and voltage control devices. The term electric distance is defined using different approaches and mathematical models. In this chapter, the sensitivity based method detailed in Chapter 7 is adopted. In the sensitivity based method, the electrical distance is defined using sensitivity matrix $\partial V/\partial Q$ which can be derived from the system Jacobian matrix, where the electrical distance, D_{ij} is calculated as the attenuation of voltage variations between two nodes i.e., i and j, given by (13). The magnitude of voltage coupling between any two buses of a power system can be quantified by the maximum attenuation of voltage variation between the two buses. The electric distance is also represented using the respective logarithmic value and the normalised value. The V_i, V_j, Q_i and Q_j denote the voltage magnitude and reactive power export or import at bus i and j, respectively.

$$D_{ij} = \frac{\partial V_i}{\partial V_j} = \frac{\partial V_i}{\partial Q_j} \Big/ \frac{\partial V_j}{\partial Q_j} \quad (13)$$

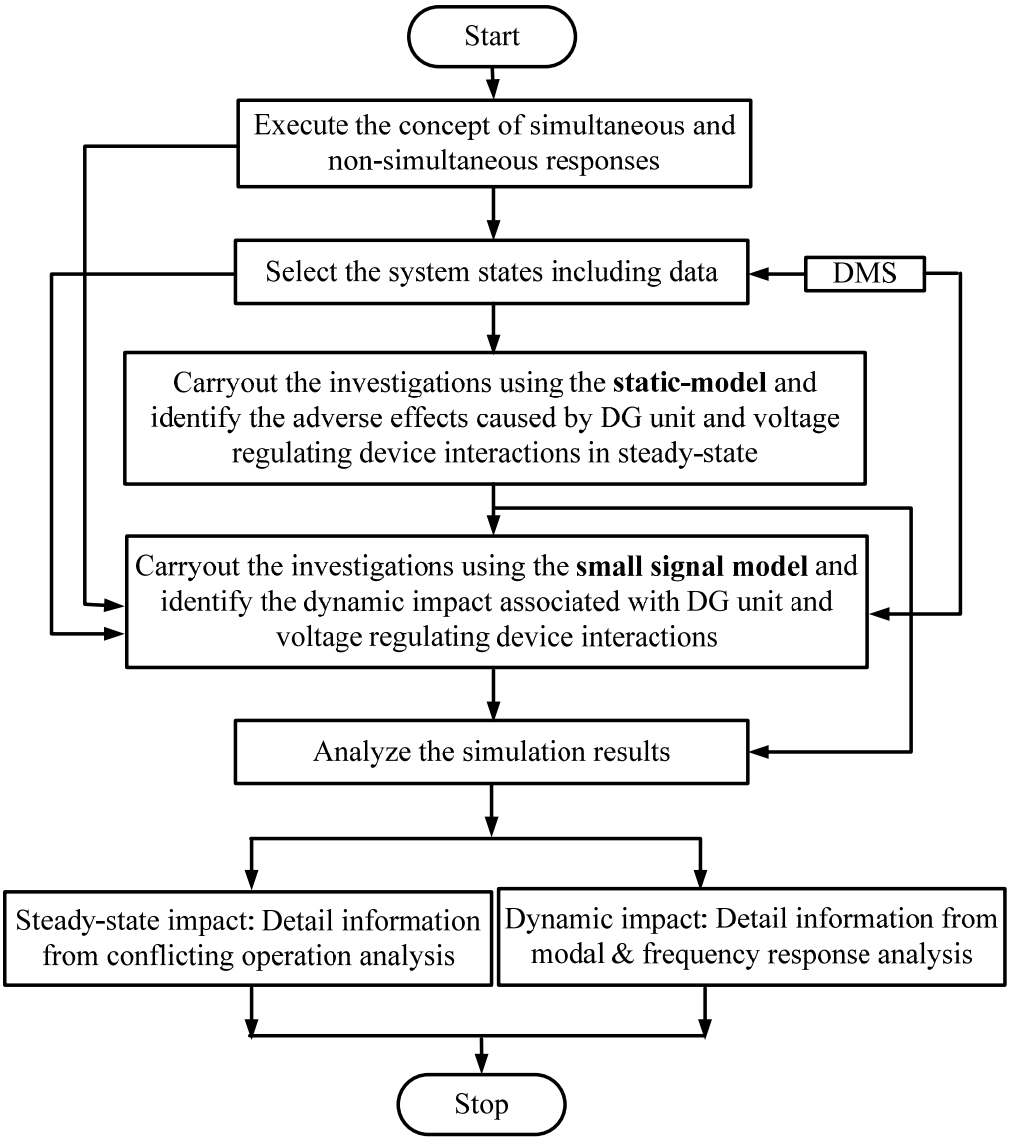

Figure 4.8: Flow chart for examining the DG-voltage control device interactions

4.5 Case Studies and Validations

In this section, the simulation results of the selected case studies are elaborated. The simulation data is also presented. The test system includes (a) model of MV distribution feeder, and (b) model of MV distribution substation. The topology of MV distribution feeder, derived from the realistic network from the state of New South Wales, Australia, is shown in Figure 4.9. The topology of MV distribution substation system is shown in Figure 4.10.

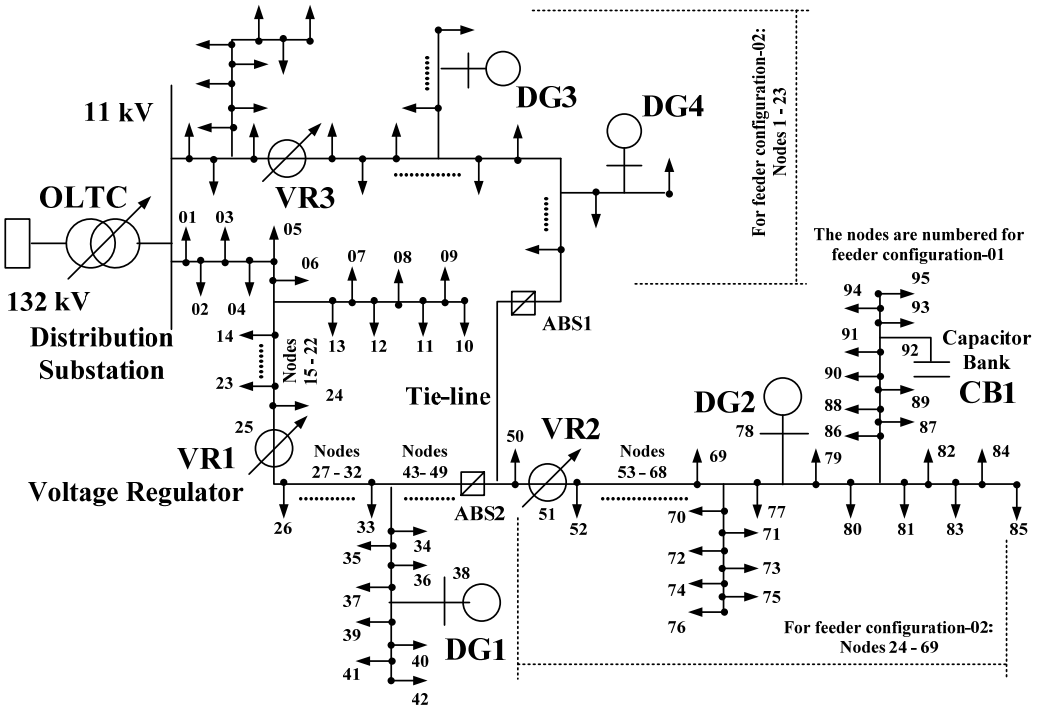

Figure 4.9: Topology of MV distribution feeder test system

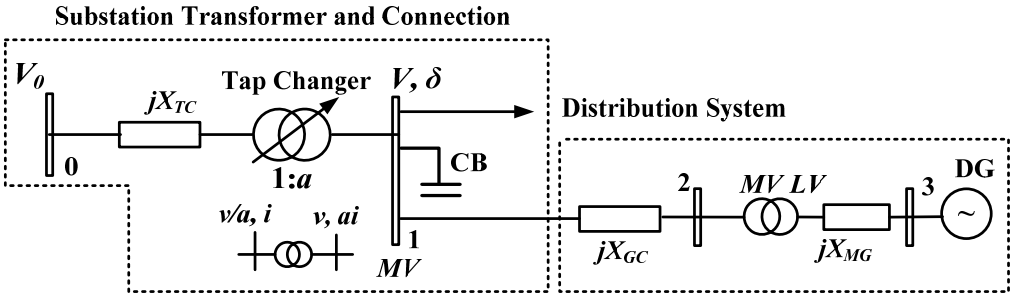

Figure 4.10: Topology of MV substation test system embedded with DG

4.5.1 Simulation Case Studies Conducted on Medium Voltage Distribution Feeder Model

In this sub-section, the simulation results for selected operational states of the MV distribution feeder shown in Figure 4.9 are presented in accordance with the Steps I to IV detailed in Section 4.4. Test distribution feeder system used in this chapter is a modified version of the distribution system topology shown in Figure 2.1. In the modified version, a CB with 0.50 MVAr capacity is connected at the end of

the test feeder system, where additional DG units with 1.000 MVA capacity are connected to the distribution feeders as shown in Figure 4.9. Accordingly, the different system operational states have been selected and simulated. Moreover, the simulation results have been carefully examined considering each voltage control device and DG response, distinctly. In this section, some of the selected results are presented. The simulations are carried out using MATLAB software, and models of the test distribution systems. The simulated voltage limits for the medium voltage test systems are 1.10 pu and 0.90 pu.

In Case Study-1, the balanced distribution feeder system operation i.e., feeder configuration–01 with two DG units, DG1 and DG2 (case-1) and feeder configuration–02 with one DG, DG2 (case-2) are used for the simulation case studies. The short term system states on 10 minute basis with total load demand of 3.0 MVA in case-1 and 3.4 MVA in case-2 with constant power characteristics and DG power injection at unity power factor operation are simulated. It is noted that the *zoomed versions* of simulation figures are presented in order to clearly observe the phenomenon. The simulated test data of voltage control devices and DG units are shown in the Table 4.1.

The simulated results are shown in Figure 4.11 and Figure 4.12. In Figure 4.11 (a) of case-1, at t = 48 s and t = 60 s, there are simultaneous responses due to VR1, VR2 operations and DG2 power output variations. Consequently, all other VR, CB and DG unit operations define non-simultaneous responses. The associated voltage variations in the remote bus of the distribution feeder system are shown in the Figure 4.11 (b), where the operation of voltage control devices in a scenario where there is no variation in the power output of DG units as at t = 48 s and 60 s is shown in the Figure 4.11 (c).

Table 4.1: Simulated data: Case study-1

CB
Number of total switching steps = 5 of 0.1 MVAr
Switching voltage = 0.90 pu (for switch ON)
Switching voltage = 1.01 pu (for switch OFF), Time delay = 0.1 s

OLTC	
The voltage reference value is set at 1.05 pu for OLTC	
VR1 and VR3	VR2
Type = Type-B (32 taps, ± 10 %) Voltage set value = 1.0 pu DB limits = ± 1.0 % Load centre $R_L = X_L = 0$ Initial time delay = 30 s Mechanical time delay = 6.0 s Initial VR1 tap position = -3 Initial VR3 tap position = 0	Type = Type-B (32 taps, ± 10 %) Voltage set value = 1.0 pu DB limits = ± 1.0 % Load centre $R_L = X_L = 0$ Initial time delay = 40 s Mechanical time delay = 4.0 s Initial VR2 tap position = -1
DG1	DG2
Case-1: P_{DG1} = 0.60 MW for t < 60 s P_{DG1} = 0.74 MW for t $\geq$ 60 s Unity power factor Case-2: Not available	Case-1: P_{DG2} = 0.70 MW for t < 48 s P_{DG2} = 0.62 MW for t $\geq$ 48 s Unity power factor Case-2: P_{DG2} = 0.80 MW for t < 64 s P_{DG2} = 0.62 MW for t $\geq$ 64 s Unity power factor

According to Figure 4.11 (a), the interactions caused by simultaneous responses of VRs and DG units at t = 60 s (in addition to the simultaneous responses at t = 48 s) lead to violation in the dead band (DB) limit of VR1, because VR1 is closer to the DG1 in terms of electrical distance where there is a 0.14 MW power output variation in DG1 at t = 60 s. Hence, tap operations (upward) are required for VR1 to correct the voltage with respect to its voltage set value. In case of a light load scenario, this could be more significant. On the other hand, since DG1 is closer to the VR1 and DG2 is closer to the VR2 in terms of electrical distance, the power output variations lead to a lesser number of tap operations in VR1 and significantly a higher number of tap operations in VR2, respectively as shown in the Figure 4.11 (a) including their impact on system voltage as shown in the Figure 4.11 (b) compared to the scenario where there is no change in DG responses at t = 48 s and 60 s as shown in the Figure 4.11 (c). This is an example for assessing the impact of interactions caused by non-simultaneous responses of

DG units and voltage control devices. In the Figure 4.12 (a) of case-2, mainly there are conflicting operations in VR2 and CB due to the power output variation of DG2 at t = 64 s, since DG2 is closer to those devices in terms of electrical distance. It is because of the voltage change (as shown in the voltage profile of the remote end bus) by the DG2 power output variation leads to violation in the DB limit of VR2 and switching voltage of CB in operation opposite directions. These simulation case studies provide basis to the complex nature of DG and voltage control device interactions and their adverse effects under certain system operating conditions.

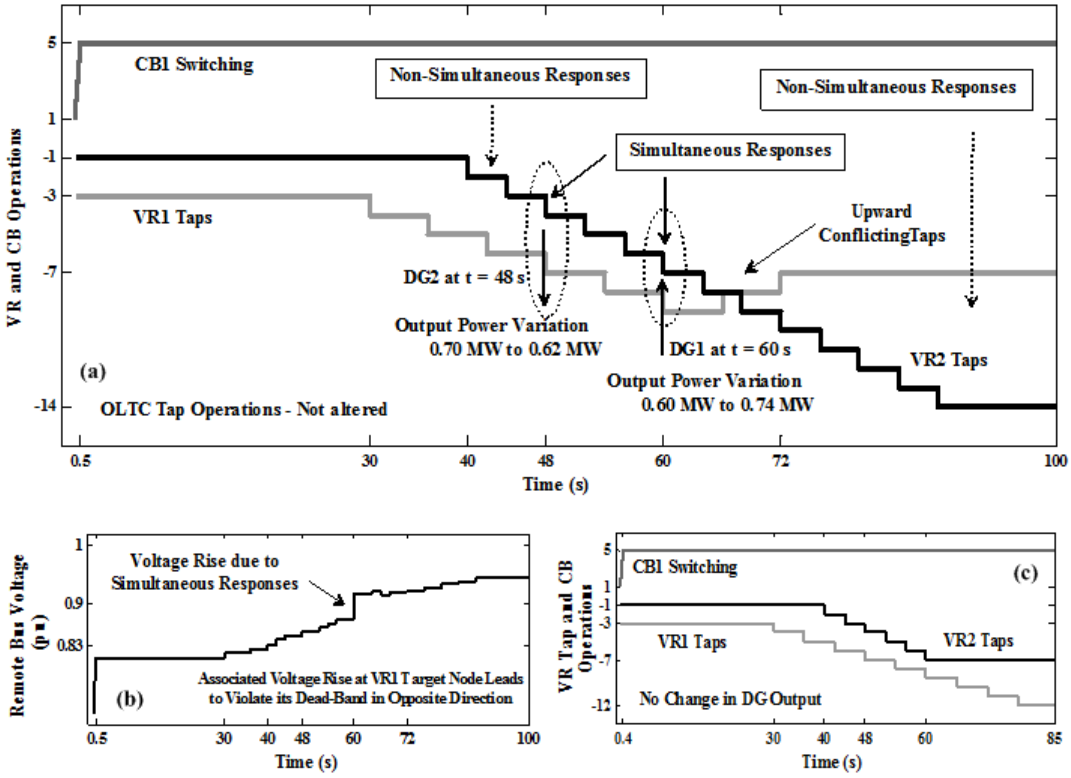

Figure 4.11: Simulation results derived from the distribution feeder system configuration-1 (case-1): (a) VR and CB operations and (b) remote bus voltage, incorporating varying DG responses; and (c) VR and CB operations, without incorporating the varying DG responses

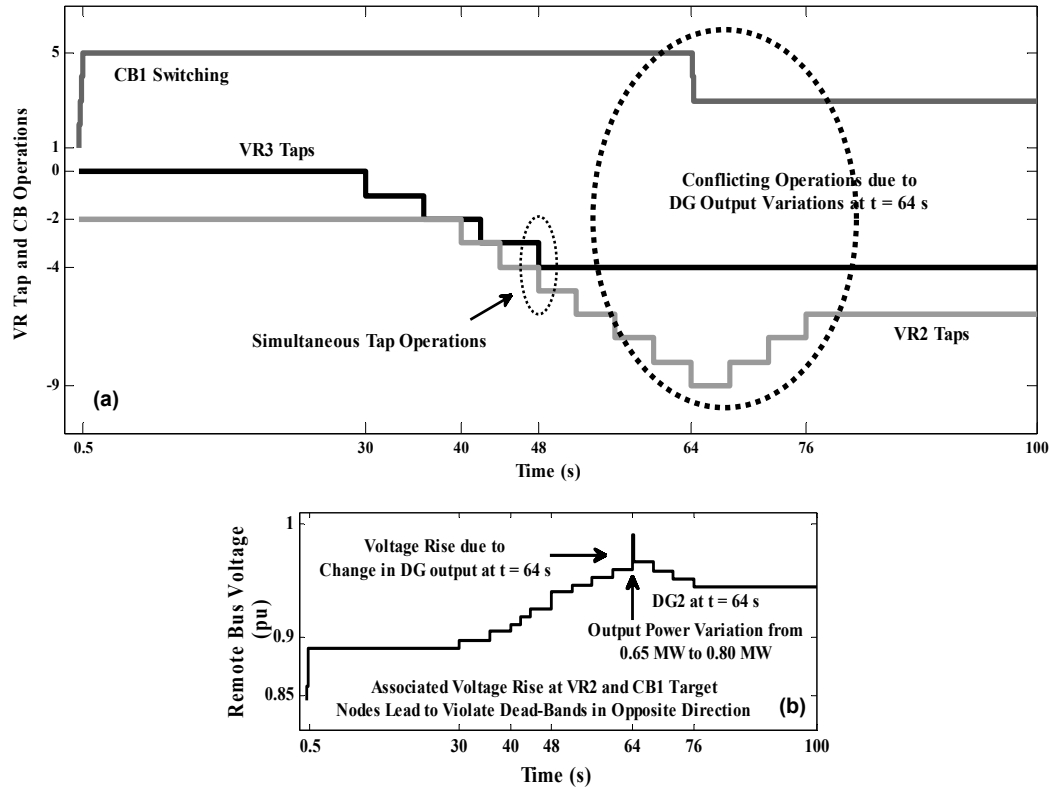

Figure 4.12: Simulation results derived from the model of distribution feeder system configuration-2 (case-2): (a) VR and CB operations and (b) remote bus voltage, incorporating varying DG responses

In Case Study-2, the simulated DG data (active and reactive power injection) is shown in Table 4.2, whereas the other simulated data is similar to Case Study-1, case-1 (case-3). The simulated load demand with constant power characteristics is 3.75 MVA. Figure 4.13 shows the simulation results. In the Figure 4.13 (a), it is shown that the change in DG1 and DG2 *active and reactive power* injections simultaneously at t = 54 s violates the DB limits of both VR1 and VR2 in opposite direction and leads to upward tap operations. However, VR2 managed to correct the target node voltage by 1 tap operation, while VR1 had to operate 5 taps up to nominal position for correcting its target node voltage. The tap operation of VR1 at t = 96 s leads to downward tap operations in VR2. These are conflicting operations, which also lead to simultaneous tap operations in VR1 and VR2 at t = 108 s and additional 5 downward tap operations in VR2. In case of a CB, no switching operation is altered after its initial switching operations up to maximum

limit. The VR tap and CB switching operations are shown in Figure 4.13 (a), while variations in bus 38 and remote end voltage of the test system are shown in Figure 4.13 (b) and Figure 4.13 (c), respectively. This simulation case study further envisages the complex nature of DG and voltage control device interactions.

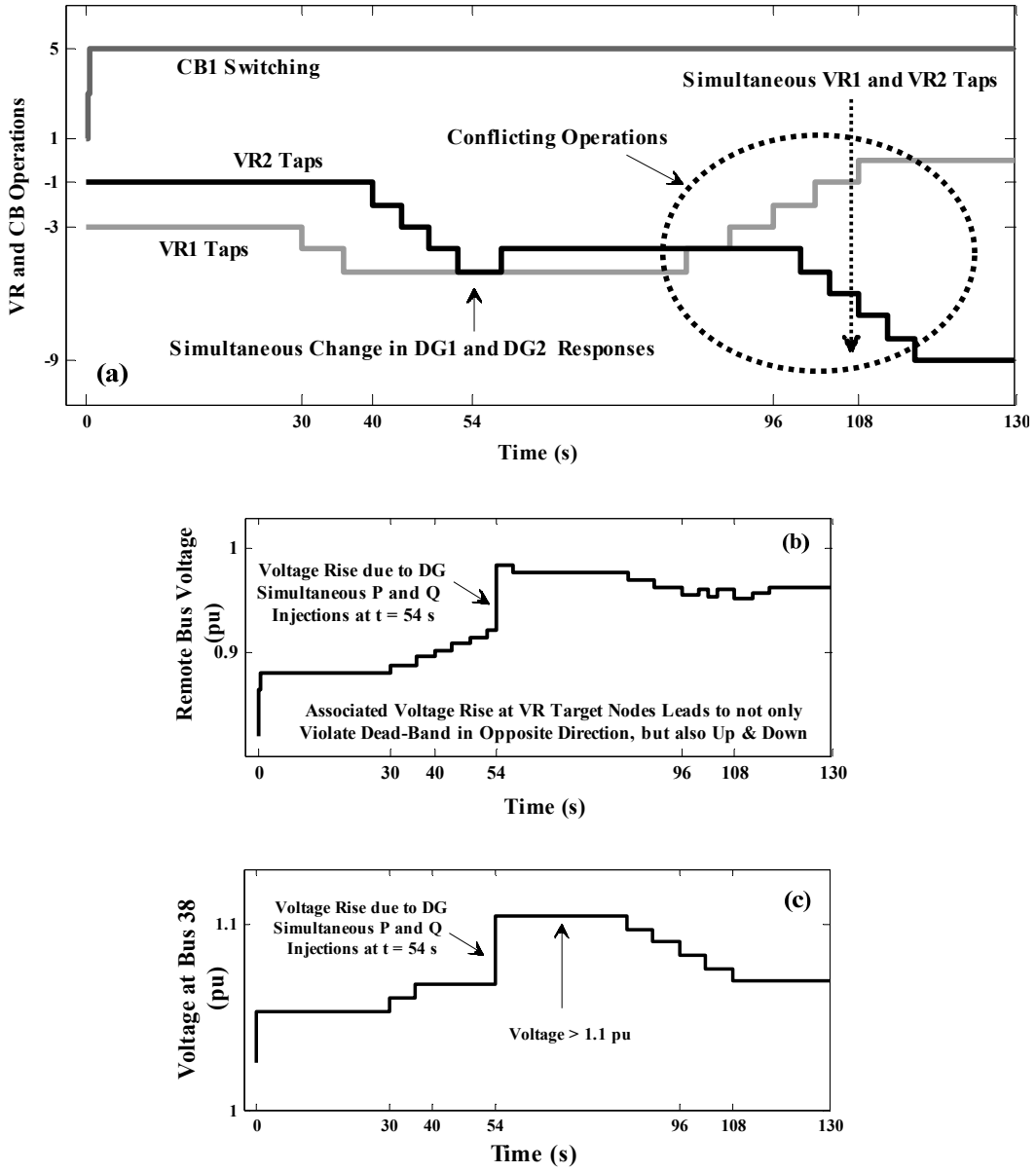

Figure 4.13: Simulation results derived from the model of distribution feeder system configuration-1 (case-3): (a) VR and CB operations, (b) remote bus voltage and (c) voltage at bus-38, incorporating varying DG responses

Table 4.2: Simulated DG data: Case study-2

DG1	DG2
Case-3: P_{DG1} = 0.60 MW for t < 54 s Q_{DG1} = 0.20 MVAr for t < 54 s P_{DG1} = 0.70 MW for t ≥ 54 s Q_{DG1} = 0.30 MVAr for t ≥ 54 s	Case-3: P_{DG2} = 0.75 MW for t < 54 s Q_{DG2} = 0.25 MVAr for t < 54 s P_{DG2} = 0.85 MW for t ≥ 54 s Q_{DG2} = 0.35 MVAr for t ≥ 54 s

In Case Study-3, the simulated DG data (active power injection and voltage reference, V_{ref} following reactive power capability of the DG unit) is shown in Table 4.3, where other simulated data is similar to that of Case Study-1, case-1 (case-4). The simulated load demand with constant power characteristics is 3.80 MVA. Figure 4.14 (a) and Figure 4.14 (b) show the simulation results. In this case, the change in voltage reference value of DG2, $V_{ref/DG2}$ at t = 85 s leads to violate the DB limits of VR1 and VR2 in the same direction. It leads to voltage rise at VR1 target node and voltage drop at VR2 target node as well as additional CB switching operations. Moreover, it has been observed that more tap operations are required in VRs to correct the voltage according to their voltage reference value, since the DG voltage control mode operation and associated V_{ref} values of the DG units dampen the voltage correction by VRs. Also, at the end of the simulation, the tap operations of VR2 are exhausted. Moreover, the tap operations of VRs at nodes 25 and 51 do not significantly affect the remote end voltage (i.e., at node 95), mainly because of the fast and assigned voltage control action of DG2 at node 78. This simulation case study reveals the severity of DG-voltage control device interactions under certain system conditions, when the DG units are operated in *voltage control mode*.

Table 4.3: Simulated DG data: Case study-3

DG1	DG2
Case-4: P_{DG1} = 0.60 MW for t < 56 s $V_{ref/DG1}$ = 1.0000 pu P_{DG1} = 0.60 MW for t ≥ 56 s $V_{ref/DG1}$ = 1.0000 pu (No change)	Case-4: P_{DG2} = 0.75 MW for t < 56 s $V_{ref/DG2}$ = 1.0000 pu P_{DG2} = 0.75 MW for t ≥ 56 s $V_{ref/DG2}$ = 0.9500 pu

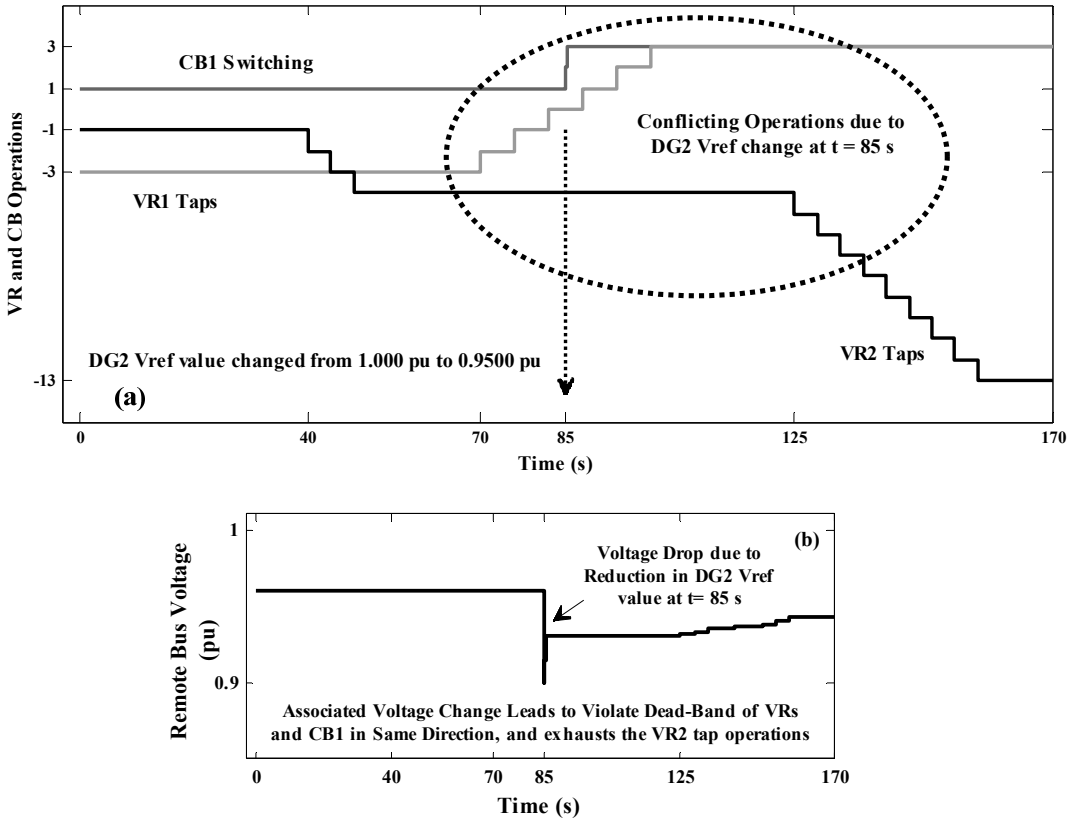

Figure 4.14: Simulation results derived from the model of distribution feeder system configuration-1 (case-4): (a) VR and CB operations and (b) remote bus voltage, incorporating varying DG responses.

In summary, the total numbers of conflicting operations in VRs and CB were calculated for a year assuming the DG-voltage control device interactions within any one system state on 10 minute basis in each hourly period, and the results are presented in Table 4.4. The above simulation results highlight the DG and voltage control device interactions and their possible adverse effects under different system operational conditions.

In the following sub-section, the small signal model proposed in Section 4.1 is applied for identifying the dynamic impact of simultaneous and non-simultaneous responses of DG unit and voltage control device operation at a MV distribution substation, depicted in Figure 4.10.

Table 4.4: Number of conflicting operations associated with DG-voltage control device interactions

Simulated System States	No. of Conflicting Operations in VRs and CBs due to Simultaneous Responses	No. of Conflicting Operations in VRs and CBs due to Non-Simultaneous Responses	Remarks
Case Study-1 (Case-1) Table 4.1 Figure 4.11	VR Tap Operations = 17520 (per year)	VR Tap Operations = 35040 (per year)	* Additional VR, CB operations due to interactions
Case Study-1 (Case-2): Table 4.1 Figure 4.12	N/A	CB1 Switching = 17520 (per year) VR Tap Operations = 26280 (per year)	* Additional VR, CB operations due to interactions
Case Study-2 (Case-3): Table 4.1, 4.2 Figure 4.13	VR Tap Operations = 52560 (per year)	VR Tap Operations = 43800 (per year)	* Additional VR, CB operations & * Voltage rise, due to interactions
Case Study-3 (Case-4): Table 4.1, 4.3 Figure 4.14	N/A	CB1 Switching = 17520 (per year) VR Tap Operations = 105120 (per year)	* Additional VR, CB operations & * Voltage drop, due to interactions

4.5.2 Simulation Studies Involving Medium Voltage Distribution Substation Model

In this sub-section, the simulation results under one of the selected operating conditions depicting worst case control scenario at a MV distribution substation are detailed. In this simulation study, the small signal version of standard 4th order state space representation (i.e., δ_r, ω_r, φ_{fd}, φ_{1d}) is used for modelling the synchronous machine based small hydro generator. The small-hydro governor is modelled with three state variables (i.e., x_{t1} to x_{t3}). According to the Step-V of the proposed analytical technique in Section 4.4, modal analysis has been carried out for identifying the possible oscillatory and non-oscillatory modes as well as the system states which do have dominant participation in each mode. Moreover, frequency response analysis has been carried out for distinctly identifying the dynamic impacts of simultaneous and non-simultaneous responses of voltage control devices and the DG unit on system voltage.

Table 4.5 shows the simulated distribution system data, the data of OLTC, CB, DG, and load demand. The simulated data of synchronous generator, its excitation system and governor models are directly obtained from [47]. The simulated grid voltage is 1.0 pu. The power flow results are shown in Table 4.6, whereas Table 4.7 shows eigen values of the system state matrix $A_{(14x14)}$. The results of the modal analysis including dominant participation factors (magnitude) in each mode are shown in Table 4.8. It can be seen that the modes 03 and 04 are oscillatory modes and the other modes are non-oscillatory in nature. The DG operation can significantly be unstable, if the modes-06 and mode-09 would be excited. Moreover, it can be seen that the load dynamics predominately participates in modes 13 and 14.

Table 4.5: Simulated data: Small signal analysis

Node Number	Branch Impedance/(pu)
0 – 1	0.282835
1 – 2	0.080810
2 – 3	0.114342

DG/(MW & MVAr)	OLTC	CB/(MVAr)
P_{DG} = 2.922 MW	Initial tap = 1 ↓	$Q_{CB/max}$ = 3.000
– 0.800 ≤ Q_{DG} ≤ 0.950	V/tap = 0.00625 pu	Initial Q_{CB} = 2.000
DG V_{ref} = 0.9800 pu	DB = +/– 1.5 %	$Q_{CB/step}$ = 0.1000

Power Flow Load Data	Small Signal Model Load Data
P_L = 10.800 MW	k_L = 1.00, Tp = 60 s, Tq = 90 s
Q_L = 5.400 MVAr	α_s = 2.0, α_t = 1.0, β_s = 1.5, β_t = 0.5
Power factor = 0.9000	P_0 = (P_L x k_L x 1.1)/Base_MVA
Base_MVA = 100 MVA	Q_0 = (Q_L x k_L x 1.1)/Base_MVA

Table 4.6: Results: Power flow analysis

Bus No.	Voltage pu	Load MW	Load MVAr	Gene MW	Gene MVAr	Injected MVAr
1	1.000	0.0000	0.0000	7.8770	4.4030	0.000
2	0.982	10.800	5.4000	0.0000	0.0000	2.000
3	0.981	0.0000	0.0000	0.0000	0.0000	0.000
4	0.980	0.0000	0.0000	2.9220	–0.7520	0.000

Table 4.7: Results: Eigen value analysis

Mode Name	Eigen Value ($1.0000e^{+4}$ *)
Mode – 01	– 1.00000
Mode – 02	– 1.00000
Mode – 03	– 0.00300 + j0.01580
Mode – 04	– 0.00300 – j0.01580
Mode – 05	– 0.00760
Mode – 06	+ 0.00370
Mode – 07	– 0.00300
Mode – 08	– 0.00130
Mode – 09	+ 0.00110
Mode – 10	– 0.00030
Mode – 11	– 0.00020
Mode – 12	– 0.00010
Mode – 13	– 0.00004
Mode – 14	– 0.00003

The dynamic impact of voltage control devices and the DG unit on the system voltage, from operational perspective, has been identified using proposed small signal model and the associated Bode plots. The simulated results are shown in Figure 4.15 (a), 15(b) and 15(c). The Bode plots show that the overall system function (closed loop) with feed-back through each voltage controller is unstable. It is indicative of the fact that operation of each voltage control device including voltage support DG unit can excite the mode-06 and mode-09; which may also lead to instability in the voltage control process.

According to the simulation results and the participation factors, it can also be seen that the control parameters of the DG unit excitation system play a major role. It is indicative of the fact that adaptive tuning of DG excitation system parameters would mainly be required in order to eliminate possible unstable network conditions. However, it may require a different design criteria compared to the conventional design criteria used for transmission systems as the variables in active distribution system are inherently subjected to varying system conditions.

Table 4.8: Results of Modal analysis

Modal Index	Physical Object	State Variable	Participation Factor
Mode – 01	DG – excitation	x_{e2}	0.99970
Mode – 02	DG – excitation	x_{e1}	1.00000
Mode – 03	DG – excitation	x_{e3}	0.50380
Mode – 04	DG – excitation	x_{e3}	0.50380
Mode – 05	DG – machine	δ_r	0.36130
Mode – 06	DG – machine	δ_r	0.76900
Mode – 07	DG – machine	φ_{1d}	0.61110
Mode – 08	DG – governor	x_{t3}	1.00790
Mode – 09	DG – machine	φ_{fd}	0.95820
Mode – 10	DG – governor	x_{t2}	0.99850
Mode – 11	DG – governor	x_{t1}	1.00090
Mode – 12	DG – excitation	x_{e4}	0.68470
Mode – 13	Load at bus – 1	x_p	1.00000
Mode – 14	Load at bus – 1	x_q	1.00000

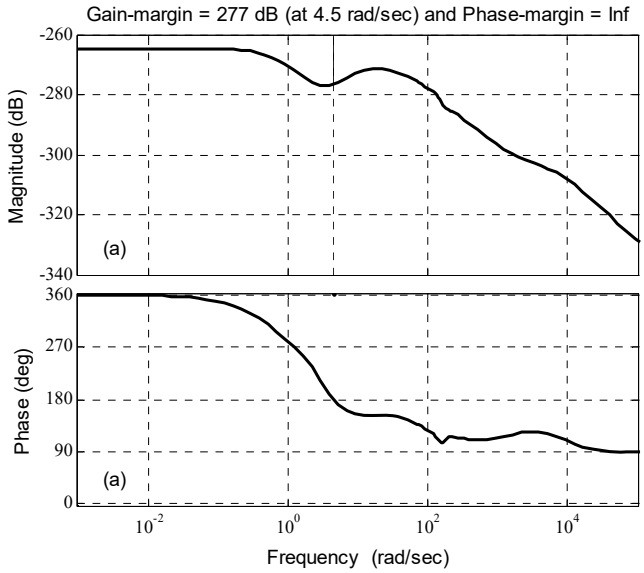

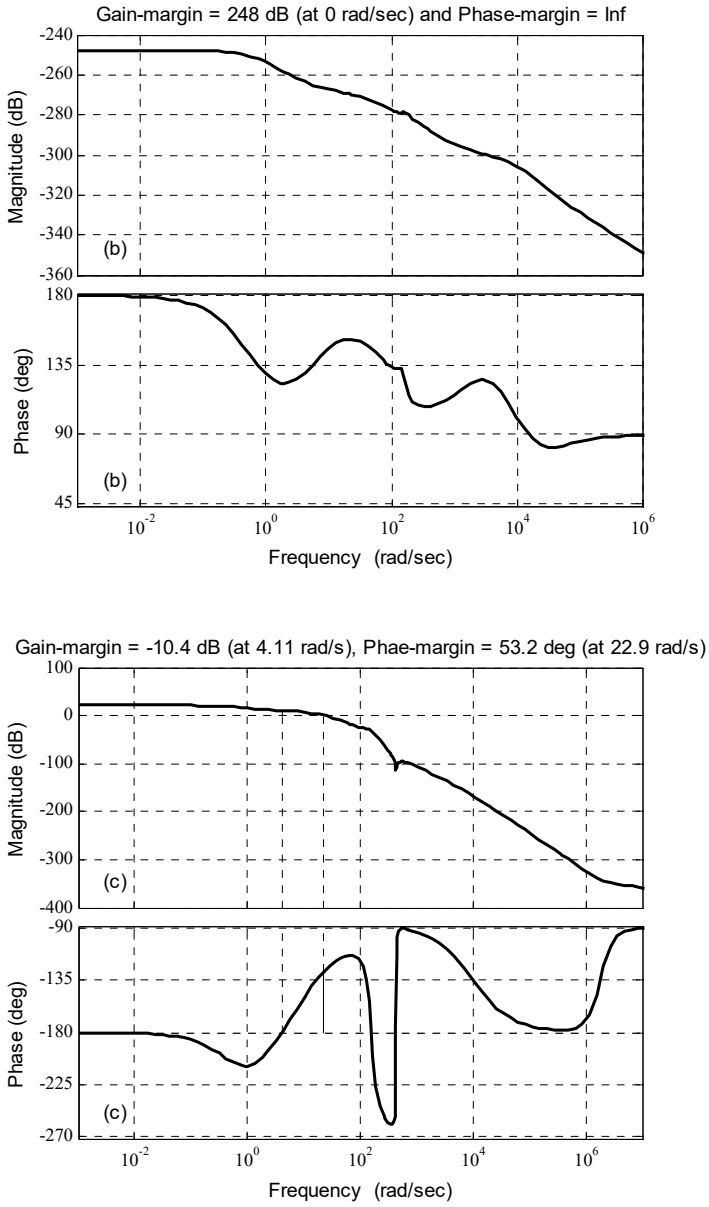

Figure 4.15: Bode plot for system open loop transfer function where ΔV is output and (a) Δa_{oltc}, (b) ΔB_c, and (c) DG excitation system ΔV_{ref} is input

After carefully analysing the results of the simulation case studies in sub-section 4.5.1 , it is noted that (a) the adverse effects caused by simultaneous responses can be mitigated by blocking the simultaneous responses in real-time using say a signal processing scheme, and (b) the adverse effects caused by non-simultaneous responses can be mitigated by operating the DG units and voltage control devices based on the topological details of the network i.e., interactions are inversely

proportional to the electrical distance between the DG units and voltage control devices. Moreover, the distinct detailed information (i.e., participation factors, mode shapes, observability and controllability matrices, and different phase and gain margins derived from the Bode plots of transfer functions $\Delta V/\Delta u$ where $u=a_{oltc}$, a_{vr}, B_{cb}, X_{ref}) extracted from the proposed small signal analysis gives an insight to understand the nature of associated dynamic interactions. Accordingly, the adaptive auxiliary controls can be designed for mitigating the dynamic impact of simultaneous and non-simultaneous responses of DG units and voltage control devices on voltage control process without leading to further interactions and *limit cycles* in the controllers. OLTC limit cycles in active distribution systems are investigated and analysed in Chapter 8 of this thesis.

Furthermore, after carefully analysing the simulation results in Section 4.5, it is noted that the coordinated operation of DG units and voltage control devices by assigning pre-defined time delays in their controllers followed by a time graded operation may not always be effective in case of generation rich distribution systems. Therefore, applying the *concept of virtual time delay* by distinctly mitigating the impacts of simultaneous and non-simultaneous responses of voltage control devices and DG units in real-time would be one of the feasible solutions to resolve the presented technical problem. Virtual time delay can characterise the effect of a pre-defined time delay that can be achieved through careful design of *control parameter tuning process*.

In the Sections 4.6 and 4.7 below, these aspects are further discussed.

4.6 Mitigating the Impact of Simultaneous Responses of DG Units and Voltage Control Devices

The simultaneous responses of multiple tap changers, CBs and DG units can result into cumulative effect on the voltage at any i^{th} node of the distribution system, V_i, which can be estimated using (14). The $\Sigma\Delta V_i^{tap}$, $\Sigma\Delta V_i^{cap}$ and $\Sigma\Delta V_i^{dg}$ denote steady-state voltage change by tap operations, CB switching operations and DG Volt/VAr controller operations, respectively at i^{th} bus.

$$\Delta V_i = \sum \Delta V_i^{tap} + \sum \Delta V_i^{cap} + \underbrace{\sum \Delta V_i^{dg}}_{V_{i/DG}} \quad \forall \quad t = t \tag{14}$$

In the worst case scenarios, V_i can be exceeded beyond maximum allowable voltage limit for the distribution system or vice versa, thereby violating the DB values of voltage control devices. Hence, as investigated by the preliminary simulation case studies in Section 4.5.1, the simultaneous responses of voltage control devices and the DG units can lead to conflicting operations under certain system operating conditions, and may exhaust total number of tap and CB switching operations resulting into voltage variations and transients. As outlined in Section 4.5, the impact of simultaneous responses can be eliminated or minimised by adopting the following technical aspects: (a) utilising DG for active voltage control on priority while maximising the DG voltage support using integrated DG controllers, (b) assigning on-line load center voltage measurements for voltage control device operation, and (c) implementing real-time control for avoiding simultaneous operations of DG controllers and voltage control devices. In case of the control aspect (a), the DG also operates as a voltage control device with its fast control action (for example, in case of synchronous machine based DG, with the aid of the excitation system operation). Accordingly, the associated time delay is smaller than the mechanical time delay of any voltage control device. Therefore, the voltage change by means of a DG response, $V_{i/DG}$ as given in (14), is now a control variable (defined as $V_{i/DGC}$), and the system voltage is quickly regulated by the DG under all system conditions. On the other hand, in case of the aspect (b) and (c), the simultaneous operations of voltage control devices and DG controllers are blocked in real-time preserving their local control action for which the ΔV_i can now be expressed by (15). Since, one of the terms in (15) is appropriately controllable; any violation in the system voltage due to simultaneous responses of multiple voltage control devices and DG, given by (14), can be avoided. It is noted that the *concept of virtual-time delay* outlined in Section of 4.5 is applied here by dynamically managing the control variable $V_{i/DGC}$ (i.e., through a sophisticated controller parameter tuning process as contributed by Chapter 5), since there is no other way to block the impact of simultaneous responses by a tap operation or a CB switching operation at a time and fast

excitation system operation (i.e., in case of synchronous machine based DG units) such as using pre-defined time delays. It also aids distribution system by enabling one control action of voltage control (by voltage control devices and DG controllers) at a time. The $\Delta V_i^{tap\ or\ cap}$ denotes the voltage change by one tap operation or CB switching operation at a time. This is the technical basis for contribution in Chapter 6 of this thesis.

$$\Delta V_i = \Delta V_i^{tap\ or\ cap} + V_{i/DGC} \tag{15}$$

4.7 Mitigating the Impact of Non-simultaneous Responses of DG Units and Voltage Control Devices

The DG impacts can not only be analysed under steady state conditions, but also under dynamic conditions as detailed in Section 4.5.2. Also, these impacts grow as DG proliferation in the network increases. Hence, in case of non-simultaneous responses, the impact of associated DG interactions cannot easily be eliminated as in the case of simultaneous responses. Therefore, coordinating voltage control devices and DG units according to some information based on system topology would be more feasible. However, it can be seen that the severity of the associated interactions is almost based on the electric distance between DG units and voltage control devices. Therefore, by operating voltage control devices farthest to DG units in terms of electric distance on priority and in real-time while utilising DG for active Volt/VAr control (i.e., as needed in the case of simultaneous responses), those impacts can also be eliminated or minimised. It is noted that the *concept of virtual time delay* is also applied here mainly through dynamically re-tuning the controller parameters using a sophisticated tuning algorithm as detailed in Chapter 05 when coordinating the voltage control devices and DG controllers based on the topological information, because there is no other way to address the limitations of topological based coordination utilising pre-defined time delays which may also be possible within some system states. This strategy is practically achievable in case of distribution systems with high penetration of DG where the voltages at all the buses can be regulated by dynamically updating the operation of voltage

control devices and Volt/VAr support DG units. This is the technical basis for contribution in Chapter 7 of this thesis.

4.8 Summary

In summary, in this chapter, the interactions between multiple DG units and voltage control devices are examined using a newly proposed generic approach applicable to any distribution system. In generation rich distribution systems, there can be both simultaneous and non-simultaneous operations involving OLTC and VR taps, CB switching and output power variations of the multiple Volt/VAr support DG units leading to significant interactions. The proposed analytical technique and small signal modelling approach can minimise such interactions by aiding distribution network planners and operators. Furthermore, the simulation results highlight the requirement of sophisticated coordinated voltage control mechanisms for normal-state operation of modern distribution networks embedded with renewable and non-renewable DG units.

CHAPTER 5: CONTROL SET-POINT RE-ADJUSTMENT IN VOLTAGE CONTROL DEVICES AND DG UNITS FOR VOLT/VAR CONTROL IN MODERN DISTRIBUTION SYSTEMS

This chapter proposes and details novel algorithm for dynamically tuning and updating the local control parameters of multiple voltage control devices and Volt/VAr support DG units in modern distribution systems. Also, the proposed strategy is designed with an aim to implement using DMS for real-time applications. This chapter is organised as below. Section 5.1 gives an introduction, while the proposed DMS based algorithm is detailed in Section 5.2. The test case study and simulation results are presented in Section 5.3, while Section 5.4 includes concluding remarks. Based on this chapter, a publication titled "Novel Volt/VAr Control Scheme using Voltage Regulating Devices and Renewable DG Units for Modern Distribution Systems," authored by D. Ranamuka, A. P. Agalgaonkar, and K. M. Muttaqi, has been submitted to the *IEEE Transactions on Smart Grid*.

5.1 Introduction

The objective of designing proposed algorithm for tuning control parameters of voltage control devices and multiple Volt/VAr support DG units is mainly based on the requirement of applying *virtual time delay* as detailed in Sections 4.5 – 4.7 in Chapter 4. Moreover, for optimal Volt/VAr control strategy proposed in Chapter 3, it is noted that (a) the number of control actions of Volt/VAr control devices for certain control states could be high and (b) voltage fluctuations may arise in the system during the time delayed operation of voltage control devices. This chapter proposes a new algorithm through facilitating the options for deriving and updating optimal controller settings of multiple Volt/VAr control devices with the due consideration of time delay sequence, variability associated with DG power output, voltage swings during the time delayed operation of voltage control devices, and voltage fluctuations. The proposed tuning algorithm can be implemented in substation centred DMS as a separate module for online voltage control. Hence, it is named as DMS tuning algorithm here onwards.

5.2 Proposed DMS Tuning Algorithm

In the proposed DMS tuning algorithm, the DG units are prioritised for voltage regulation support in the system, while tap changing devices are enacted only when required. Moreover, the DG voltage control mode operation, where in the voltage at the point of common coupling is maintained at a specific level by enacting reactive power capability can also be implemented when required instead of the reactive power control mode. The different operational modes of renewable and non-renewable DG units are discussed in detail in Section 2.3.1 of Chapter 2.

5.2.1 Impact of Reactive Power Generation by DG Units on System Voltage Regulation

For assessing the impacts of DG reactive power generation on system voltage regulation, the distribution feeder system shown in Figure 5.1 can be used. The phasor values of the nodal voltages are denoted by v_i where i is the number of nodes in the system. The magnitude of voltage at load bus is V_2. The tap ratio of the tap changing device is denoted using a. The feeder resistance and reactance values are given by R_L and X_L, respectively. The phasor value of substation voltage is v_0. The P_L and Q_L denote load active and reactive powers, respectively; and P_{DG} and Q_{DG} denote DG active and reactive powers, respectively. The reactive power injection by CB is Q_{CB}.

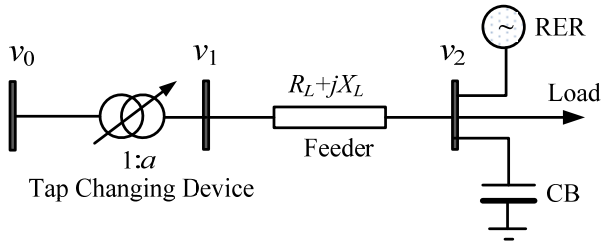

Figure 5.1: Example three bus distribution feeder system with DG

Assuming a small voltage angle between v_2 and v_1, the voltage drop on the feeder, ΔV can be approximated as given by (01) [5].

$$\Delta V = |v_1 - v_2|$$

$$\Delta V \approx \frac{R_L(P_L - P_{DG}) + X_L(Q_L - Q_{CB} \pm Q_{DG})}{V_2} \quad (01)$$

According to (01), the impact of *variable reactive power generation by the DG unit* in Figure 5.1 on the feeder voltage regulation can be explained using the four scenarios as follows.

- If the reactive power generation by the DG unit is zero, the feeder voltage drop can only be decreased with the reactive power injection by the CB.
- If the DG unit generates reactive power, it would further decrease the voltage drop along the distribution feeder. If the apparent power generated by DG unit and CB is larger than the feeder load, power will flow from the DG unit to the substation and can cause a voltage rise.
- If the DG unit absorbs reactive power, it can increase voltage drop based on the line *X/R* ratio and the amount of reactive power absorbed by the DG unit.
- If the DG unit is operated in voltage control mode (i.e., keeping V_2 constant), the DG unit actively involves in regulating the distribution voltage by controlling the reactive power output in commensurate with the reactive power capability limits. However, the reactive power capability of a DG unit may be limited due to the variability in its active power generation and DG capacity.

Therefore, it is clear that the control set-point re-adjustments of the CB, Volt/VAr controllers of the DG unit and the tap changing device have to be performed dynamically and accurately for effective voltage regulation in the distribution system. The dynamic co-generation mode is suggested for the VRs.

5.2.2 Proposed Tuning Algorithm

Figure 5.2 shows the topology of the proposed DMS tuning algorithm which has a hierarchical layered structure, where the Sub-sections 5.2.2.1, 5.2.2.2 and 5.2.2.3 detail the function of each control layer.

5.2.2.1 Control Layer-1

In control layer-1, the time series data sets of load demand, active power generation by DG units, initial tap and CB switching positions, and

initial VAr settings of DG units are executed. It is assumed that the derivation of these time series data sets and DG reactive power capability limits in each control state are carried out by an algorithm embedded in the DMS, and these settings are updated using the proposed tuning algorithm. The methodologies and models widely utilised for deriving such time series data sets incorporating load and generation uncertainties, and DG reactive power capability limits are detailed in [36], [48], [49].

In addition, the objective function and associated constraints including all variables are defined and initialised in this layer. The objective is to maximise the voltage regulation support by DG units and CBs within their reactive power capabilities in conjunction with LTC and VRs, where target is to find out the appropriate VAr reference values for the DG unit and the CB local controllers as well as the voltage set-point values for tap changing devices. The problem is formulated as given by (02), considering both voltage drop (VD) and voltage rise (VR) cases. It is assumed that the distribution system has m nodes. The VAr reference values of DG units and CBs are denoted as VAr_{DG} and VAr_{CB}, respectively, where the voltage set values of LTC and VRs are denoted as V_{LTC} and V_{VR}, respectively.

The required operational voltage level (i.e., reference voltage for each bus), V_{ri} is defined within maximum and minimum stipulated voltage limits of the system. The reference voltage, V_{ri} can be updated, if required, after deriving voltage magnitude profiles in the search method (Layer-2) by incorporating the required algorithm. Since the algorithm of updating V_{ri} also depends on the voltage control practice of DNO making it distinctive, it is not detailed in this chapter.

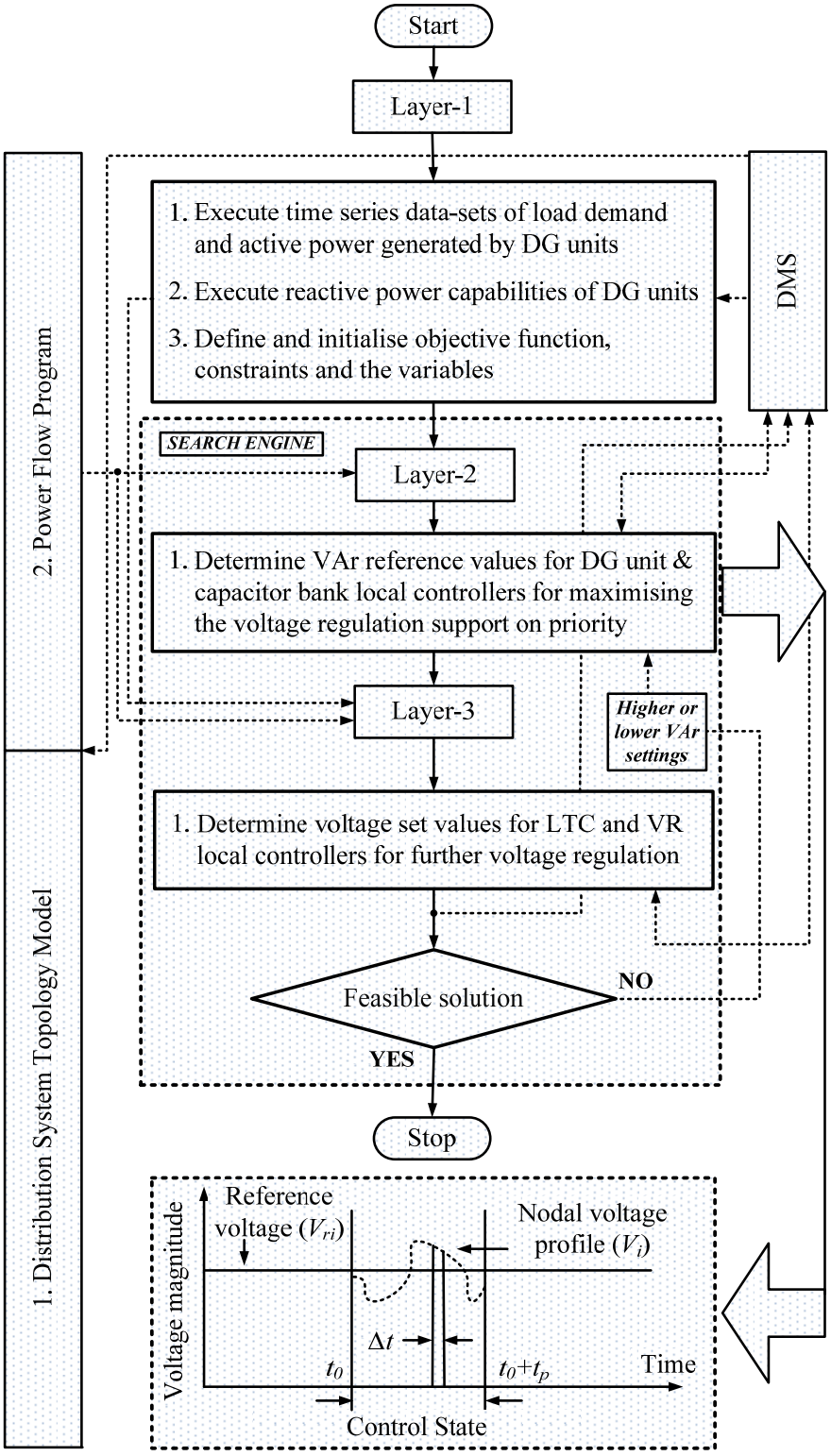

Figure 5.2: Diagrammatic representation of the proposed DMS algorithm

It is noted that the *modern voltage control* conceptualised in Sections 4.6 and 4.7 of Chapter 4 requires a fine mechanism for tuning control parameters of the

Volt/VAr control devices. It can be achieved via appropriately updating the V_{ri} in conjunction with the objectives of problem formulation and constraints, and accordingly deriving the control parameters while preserving the DNO voltage control practice. Also, the proposed tuning algorithm has the flexibility to be implemented on 15-minute/hourly/daily interval basis or mixture of them (i.e., 15-minute interval for peak time, and hourly interval for rest of the day) according to the requirements of DNO.

In (02), the t_{p1} denotes the cumulative time interval relevant to voltage drop cases within the considered control-state of time interval t_p, while t_{p2} denotes the cumulative time interval relevant to voltage rise cases. The DG active power is P_{DG}, and its rated value is $P_{DG/rated}$. The DG reactive power is Q_{DG}, and its rated value is $Q_{DG/rated}$, where DG capacity is S_{DG}, and its rated value is $S_{DG/rated}$. The CB reactive power is Q_{CB}, and its rated value is $Q_{CB/rated}$. The CB_{swt} denotes the CB switching position, where its nominal position is $CB_{swt,nominal}$ and maximum position is $CB_{swt,max}$. The tap operation of a LTC or a VR is denoted using Tap, where its maximum value is Tap_{high} and minimum value is Tap_{low}. Also, it is assumed that the constraints related to distribution line thermal limits and distribution transformer capacity limits are not violated under all the operational conditions. The time delay values of voltage control devices and DG units are denoted using T with respective subscript. The stipulated voltage limits of the distribution system are denoted by V_{min} and V_{max}, while bus voltage magnitude in i^{th} bus is denoted by V_i.

$$\text{Min } J_1\left(VAr_{DG}, VAr_{CB}, V_{LTC}, V_{VR}\right) = \sum_{i=i_1}^{m_1}\left(\left(V_{ri}\times t_{p1}\right)-\left(\int_{t_o}^{t_o+t_{p1}} V_i.dt\right)\right)_{VD} + \sum_{i=i_2}^{m_2}\left(\left(\int_{t_o}^{t_o+t_{p2}} V_i.dt\right)-\left(V_{ri}\times t_{p2}\right)\right)_{VR} \quad \in \Delta t$$

$$m = \left(m_1 + m_2\right) \text{ and } \left(t_{p1} + t_{p2}\right) = t_p \qquad (02)$$

Time delay sequence :

$$T_{DG} < T_{CB} < T_{upstream\ /VR} < \ldots < T_{downstream\ /VR} < T_{substation\ /LTC}$$

$\forall$

Generation limits of each DG unit

$$\sqrt{P_{DG}{}^2 + Q_{DG}{}^2} \leq S_{DG,rated}$$

Reactive power capability limits of each capacitor bank

$$Q_{CB} \leq Q_{CB,rated}$$

$$CB_{swt,no\min al} \leq CB_{swt} \leq CB_{swt,\max}$$

Steady state voltage limits of each bus

$$V_{\min} \leq V_i \leq V_{\max}$$

Tap limits of each tap changing device (LTC and VRs)

$$Tap_{low} \leq Tap \leq Tap_{high}$$

Moreover, since the substation LTC deals with voltage regulation at the substation bus-bar level using a coarse control and operates after a prolonged time delay by coordinating its operation with the upstream devices; some DNOs may not formulate the downstream distribution system Volt/VAr control problem incorporating the substation LTC operation as a control variable. Furthermore, the substation voltage will be assumed fixed for the considered time interval of the distribution system operation. In such case, the formulation given by (02) will be modified excluding the control variable V_{LTC} and its associated constraints i.e., tap limits of the substation LTC as given by (03).

The proposed search scheme is designed based on a heuristic method; because (a) conventional mathematical optimisation methods and associated solvers do not guarantee solution under all the system conditions, (b) application of intelligent search methods may also have limitations under certain system conditions according to the investigations and findings in [20], and (c) difficulty in handling multiple discrete variables with conventional optimisation methods. The proposed search engine has two control layers i.e., Layer-2 and Layer-3 as depicted in Figure 5.2. In Layer-2, the optimal VAr reference values for the DG unit and the CB local controllers are derived on priority for maximising the voltage regulation support. In this chapter, the proposed approach is named as *voltage-shaping*. In Layer-3, the optimal voltage set values for LTC and VRs are derived for

maximising the voltage regulation support, if required. This approach is named as *voltage-stepping*.

$$\text{Min } J_1\left(VAr_{RER}, VAr_{CB}, V_{VR}\right) = \sum_{i=i_1}^{m_1}\left(\left(V_{ri} \times t_{p1}\right) - \left(\int_{t_o}^{t_o + t_{p1}} V_i.dt\right)\right)_{VD} +$$

$$+ \sum_{i=i_2}^{m_2}\left(\left(\int_{t_o}^{t_o + t_{p2}} V_i.dt\right) - \left(V_{ri} \times t_{p2}\right)\right)_{VR} \quad \in \Delta t$$

$$m = \left(m_1 + m_2\right) \text{ and } \left(t_{p1} + t_{p2}\right) = t_p \qquad (03)$$

Time delay sequence :

$$T_{DG} < T_{CB} < T_{upstream\ /VR} < \ldots < T_{downstream\ /VR}$$

$$\forall$$

Generation limits of each DG unit

$$P_{DG} = P_{agrement}$$

$$\sqrt{P_{DG}^{\ 2} + Q_{DG}^{\ 2}} \leq S_{DG,rated}$$

Reactive power capability limits of each capacitor bank

$$Q_{CB} \leq Q_{CB,rated}$$

$$CB_{swt,no\ min\ al} \leq CB_{swt} \leq CB_{swt,max}$$

Steady state voltage limits of each bus

$$V_{min} \leq V_i \leq V_{max}$$

Tap limits of each tap changing device (VRs)

$$Tap_{low} \leq Tap \leq Tap_{high}$$

It is noted that the transition from control Layer-2 to Layer-3 is introduced for providing DNO a flexibility to operate (a) DG units and CBs when the distribution system is embedded with adequate DG units/CBs for Volt/VAr control, and (b) also VRs if needed, as per DNO's requirements. This strategy can also be utilised for voltage regulation in distribution systems subjected to structural changes, especially due to network reconfigurations. One of the salient features incorporated in the search engine is *searching-sequence,* which follows the time delay sequence of Volt/VAr control devices.

5.2.2.2 Control Layer-2

The proposed search method for deriving optimal VAr reference values for DG unit and CB local controllers is based on their Volt/VAr control capabilities. The application of nodal voltage magnitude profiles and voltage sensitivities (i.e., $\Delta V/\Delta Q_{DG}$ and $\Delta V/\Delta Q_{CB}$) for construction and traversals of search steps as outlined in the searching mechanism incorporated in Control Layer-2 (Appendix-IV), are major aspects. The derivations proposed in [50] are adopted for computing the voltage sensitivity values. Their mathematical formulations can be found in the Appendix-II; where the sensitivity values are based on the operating points and associated system Jacobian matrix determined by Newton-Raphson based power flow calculations. These voltage sensitivity values are used for estimating the nodal voltage change, ΔV for change in VAr supply from a DG unit, ΔV_{DG} and a CB, ΔV_{CB}. It is assumed that the nodal voltage magnitude profiles are derived using linear-model incorporated in the DMS and updated in the proposed tuning algorithm. The methodologies and models widely used for deriving linear variation for voltage between the time series data sets within a control-state are detailed in [51]. The construction and traversals of search steps are done using (02) and the linear variation (i.e., $V_i(t) = \underline{m}t+\underline{c}$) in each nodal voltage magnitude profile between the time series data sets with time interval, Δt as shown in Figure 5.2; while the changes in nodal voltage magnitudes due to DG and CB VAr support are estimated using the voltage sensitivity values.

Figure 5.3 shows the anatomy of the search-space with its different hierarchical levels. When defining the search space, first it is found the DG unit which is most capable of correcting the utmost nodal voltage variations compared to reference voltage considering both voltage sensitivity values and the reactive power capability limit of the DG unit, which is named as 'grand-parent' of the other DG units by adopting family anatomy. Using the same approach, the next level of family hierarchy i.e., 'parent', 'eldest-child' to 'youngest-child' and family friends can be found. CBs are treated as friends of the DG family; hence, no hierarchy is maintained. Therefore, within the search steps, the precision, p_j for each state of VAr reference values of each DG unit is defined i.e., the highest precision is

assigned for the grand-parent while the lowest precision is assigned for the youngest child. For friends (i.e., CB units), the VAr change per switching operation is considered as the precision, p_{cj} for each state of VAr reference values of each CB. At the post-optimisation stage, the power flow program is enacted to get the new state variables for updating the control layer-3 (as shown in Figure 5.2).

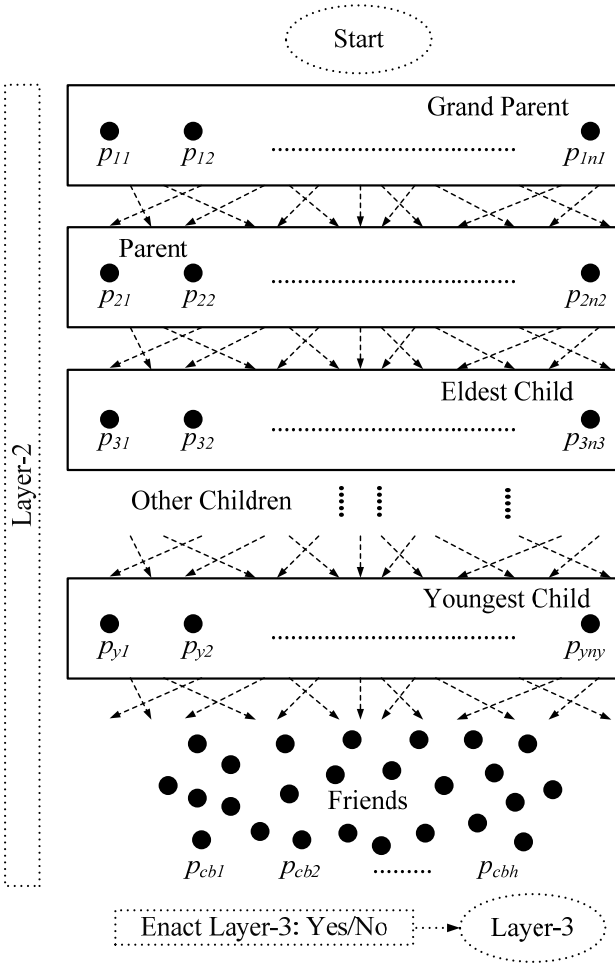

Figure 5.3: Anatomy of the search space of the proposed method (Layer-2)

The searching mechanism incorporated in Control Layer-2 is detailed in the Appendix-IV.

5.2.2.3 Control Layer-3

The proposed search method in this layer for deriving the optimal voltage set *values for LTC and VRs is based on their voltage control capabilities. First, the* new nodal voltage magnitude profiles, V_{ik}, incorporating the optimal VAr reference values of DG units and CBs (determined in Layer-2) are obtained. The construction and traversals of search steps are performed following (02) and linear variation (i.e., $V_i(t) = \underline{m}t+\underline{c}$) in each nodal voltage magnitude profile between the time series data sets with time interval, Δt; where the cumulative values of nodal voltage magnitudes changed by LTC and VR operations are estimated using (04). The relevant details can be found in [52], [53]. The $V_{LC(j)}^{ur}$ denotes unregulated voltage at LTC or VR target load centre in general, and V_{ik} denotes voltage magnitude at i^{th} node after assigning VAr_{DG} and VAr_{CB} support, while V_{ik}^{ur} denotes voltages at i^{th} node before LTC or VR action. The voltages at i^{th} node after LTC or VR action is denoted using V_{ik}^{rs}, while the respective equivalent tap ratio of LTC or VR is denoted using T^r_j. The $V_{SET/VR(j)or\ LTC}$ denotes voltage set value of VR or LTC. Figure 5.4 shows the anatomy of the search-space.

$$T_j^{\,r} = \frac{V_{SET/VR(j)\ or\ LTC}}{V_{LC(j)}^{\,ur}}, \qquad V_{ik}^{\,rs} = T_j^{\,r} \times V_{ik}^{\,ur} \tag{04}$$

Within the search steps, the precision, p_{tj} for each state of voltage set value is defined with the value of voltage change per tap operation. As shown in Figure 5.2, it is noted that the Layer-2 and Layer-3 communicate with each other by a separate embedded code for finalising the control parameters, while maintaining the system voltage within stipulated limits. At the post-optimisation stage, the power flow program is enacted to get the new state variables and thereby checking the feasibility of the final solution. Finally, the voltage set-point values for LTC and VR local controllers as well as VAr reference values for DG units and CBs are set. The searching mechanism incorporated in Control Layer-3 is also similar to the Layer-02 (Appendix-IV).

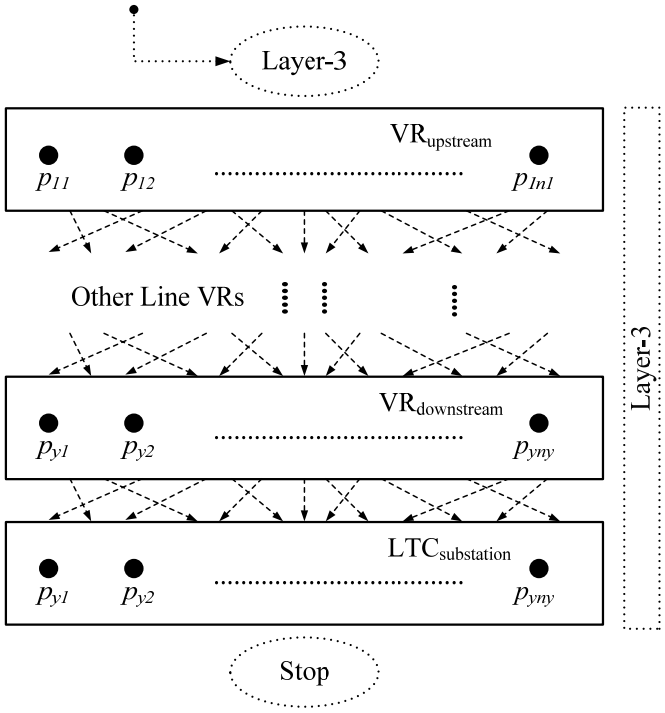

Figure 5.4: Anatomy of the search space of proposed method (Layer-3)

5.3 Test Case Study

Case Study-01: For the proof of concept, off-line simulations are carried out on selected control states of the MV distribution system topology shown in Figure 5.5, which is derived from the original version (Figure 2.1) in the Chapter 2. The simulated rated capacity of a CB is 0.600 MVAr. The rated capacities of DG1 and DG2 are 0.850 MVA. The acceptable voltage limits for the test system are 0.90 pu and 1.10 pu. The simulated representative aggregated load demand pattern, in which constant power loads are assumed at all nodes, is shown in Figure 5.6 (a); whereas the simulated active power generation patterns of DG1 and DG2 units are shown in Figures 5.6 (b) and (c), respectively. It is to be noted that the active power generation patterns of DG1 and DG2 are referred to a wind plant and solar-PV unit respectively, depicting worst case scenarios of variabilities associated with DG power generation. The simulations are carried out using MATLAB software. The case study presented in this chapter is based on one of the hourly simulated control states (8:00 am to 9:00 am) representing a higher power output variation for DG1 and DG2. The hourly operation is presented in order to clearly

demonstrate the merits of the proposed tuning algorithm. The formulation given by (02) is adopted. The unregulated nodal voltage magnitude profiles within the control state are shown in Figure 5.7.

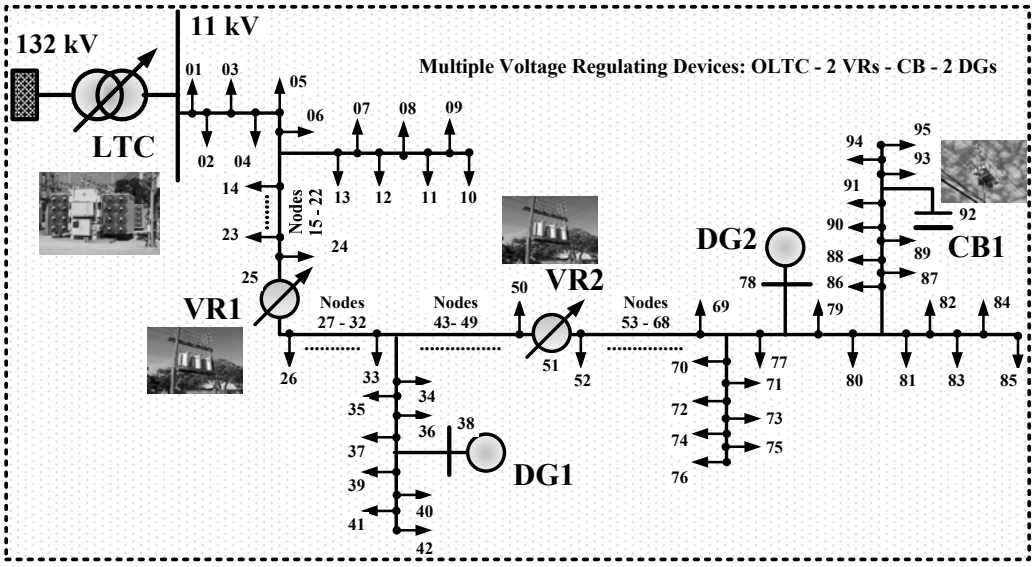

Figure 5.5: Topology of the test distribution system

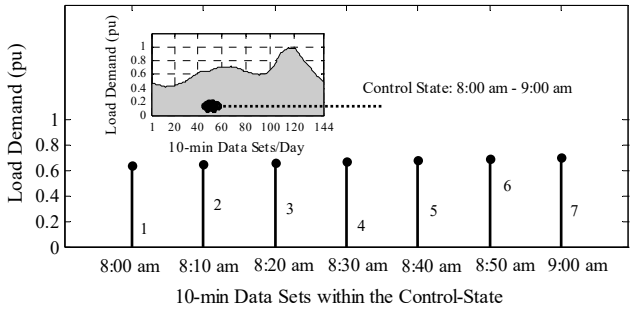

(a)

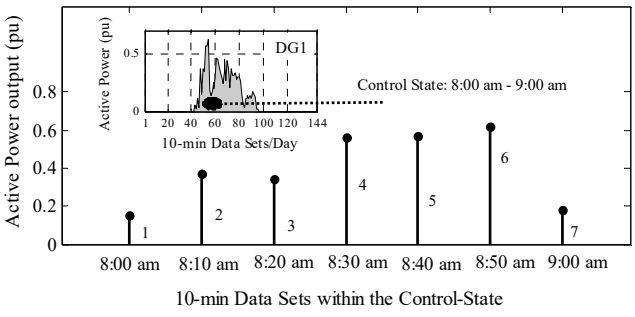

(b)

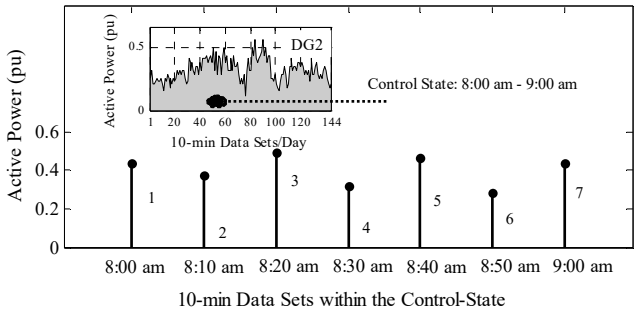

(c)

Figure 5.6: Simulated (a) load demand pattern, (b) active power generation pattern of DG1, and (c) active power generation pattern of DG2

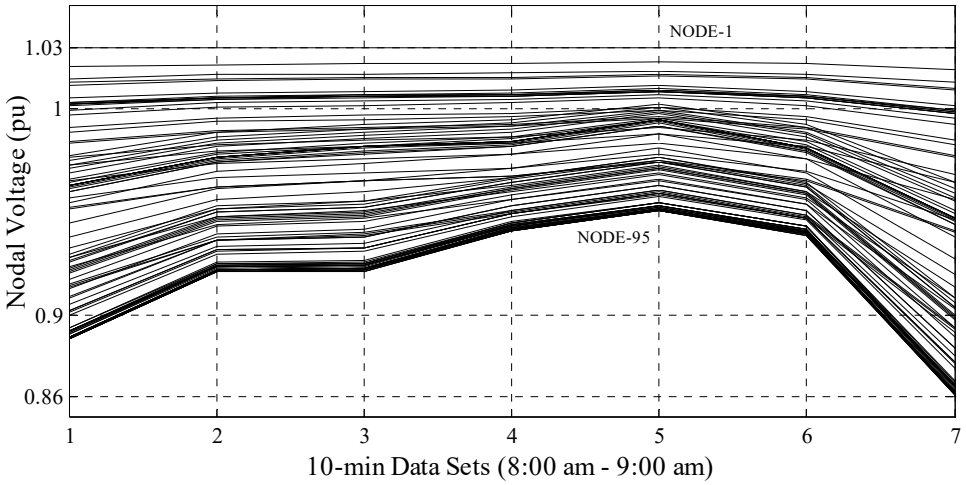

Figure 5.7: Unregulated nodal voltage magnitude profiles in the simulated control state

The simulated initial tap position of LTC is for correcting the substation secondary voltage to 1.03 pu. The initial tap positions of VR1 and VR2 are 5 and 3, respectively; whereas initial switching position of the CB is 2, supplying 0.200 MVAr. The initial VAr supply from DG1 and DG2 is assumed to be zero. If the DNO is interested in minimising the energy losses, the appropriate values for nodal reference voltage, V_{ri} have to be defined. The suggested method for updating V_{ri} in the proposed case study is based on contouring the variation of nodal voltages in the distribution system and accordingly, defining V_{ri} values by maintaining the same contour pattern while managing the nodal voltages to be at the expected level. The contours of the nodal voltage magnitudes can be obtained

from the output of the base case power flow simulation on 10-minutes time series data-sets within the hourly period (i.e., 8:00 am to 9:00 am) in the unregulated system. The respective time series data-sets are named as DS-1 (8:00am), DS-2 (8:10am), DS-3 (8:20am), DS-4 (8:30 am), DS-5 (8:40 am), DS-6 (8:50am), DS-7 (9:00am). Figure 5.8 shows the contours of nodal voltage magnitudes for this case study.

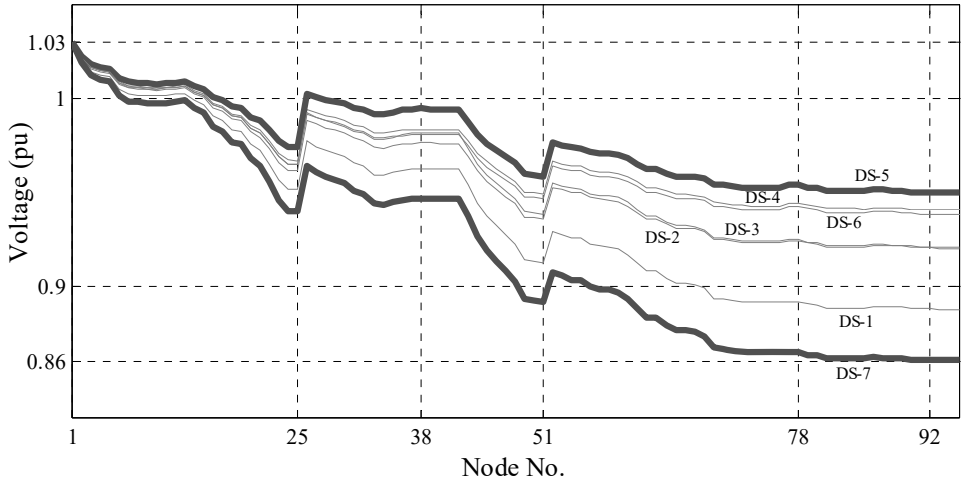

Figure 5.8: Contours of nodal voltage magnitudes

For the test simulations, VAr precisions assigned to the DG units are 0.005 MVAr (for grand-parent) and 0.01 MVAr (for parent), whereas the VAr precision assigned to the CB (family friend) is 0.1 MVAr. In case of LTC, total 16 tap positions (+8/-8) are modelled and hence, voltage change per tap (which is 0.01250 pu) is defined as the precision for voltage set value. For VRs, 32 tap positions (+16/-16) are modelled and voltage change per tap (i.e., 0.00625 pu) is defined as the precision for voltage set value considering a range between 0.90 pu to 1.10 pu for voltage correction. The selected V_{ri} values and nodal voltage magnitudes in the regulated system after control set-point re-adjustment are shown in Figure 5.9. The V_{ri} varies between 0.997 pu (i.e., at node 95) to 1.080 pu (i.e., at node 1) for the test case.

The nodal voltage magnitude profiles for the regulated system are shown in Figure 5.10. Figure 5.10 shows the reduction in voltage swings attributed to the DG1 and DG2 output power variations, with the application of proposed DMS

algorithm compared to the unregulated system as shown in Figure 5.7. Therefore, it is very clear that the proposed DMS algorithm is capable of damping the voltage swings in the distribution system.

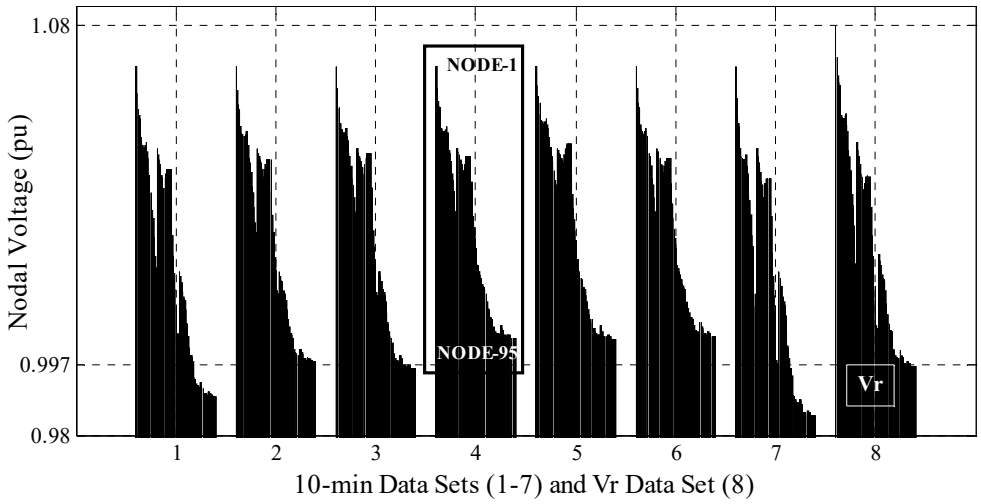

Figure 5.9: The nodal voltage reference values and voltage magnitudes in the regulated system after control set-point re-adjustment

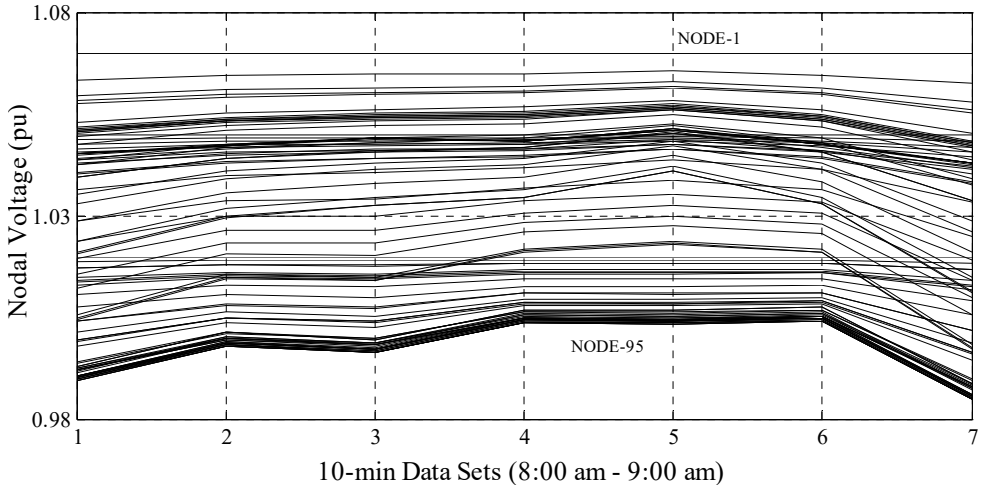

Figure 5.10: Nodal voltage magnitude profiles in the regulated system after control set-point re-adjustment

The optimal local controller parameter settings for DG1 and DG2, substation LTC, line VRs and CB local controllers are shown in Table 5.1. The nodal voltage error and total energy losses in the unregulated and regulated systems are shown in Table 5.2, while nodal voltage error after each stage of the tuning process is

shown in Table 5.3. The voltage error is calculated by integrating the hourly voltage profile, over and below the voltage reference value.

Table 5.1: Optimal controller settings for DG units, LTC, VRs and CB

DG1 VAr Setting/(MVAr)	DG2 VAr Setting/(MVAr)	CB1 VAr Setting/(MVAr)
0.56	0.42	0.20
LTC Voltage Set Value/(pu)	**VR1 Voltage Set Value/(pu)**	**VR2 Voltage Set Value/(pu)**
1.07	1.05	1.02

Table 5.2: Voltage error and energy losses in the regulated and un-regulated systems

	Total Voltage Error /(Volt pu.s)	Total System Losses/(MWh)
Unregulated system	364.63	0.20 (≈ 9 %)
Regulated system	23.08	0.14 (≈ 6 %)

Table 5.3: Voltage error at each stage of the tuning process

	Total Voltage Error /(Volt pu.s)
Unregulated system	364.62
Layer-2	156.95
Layer-3	23.08

According to the simulation results shown in Table 5.2, it is clear that the total nodal voltage error is significantly reduced by the application of the proposed DMS algorithm. Also, it can be seen that the total energy losses calculated by examining the power losses between 8:00 am to 9:00 am are reduced by 3% for the regulated system. Moreover, according to Table 5.3, it is very clear that the number of tap operations by LTC and VRs for voltage correction will be reduced when the proposed tuning algorithm is adopted. It is mainly because the prioritised and maximised voltage correction derived by the algorithm embedded in layer-2 leads to a significant reduction in voltage error. It is noted that the test distribution system also shows similar results for other control states.

Case Study-02: In the case study-02, an hourly time domain simulation is carried out for the test system in Figure 5.5 using MATLAB-SimuLink for observing the performance of the proposed control strategy in real-world operation. It is assumed that the load ramping within a 10-minute interval is negligible. Moreover, it is worth noting that the scenario with post-LTC tap operations is simulated; since the substation LTC deals with voltage regulation at the substation bus-bar level using a *coarse control* while coordinating with upstream voltage control devices. The simulated time delays for VR controllers (assuming Type-B type VRs) are 30 s for VR1 and 45 s for VR2. For LTC, 16 tap positions (+8/-8) are modelled including the nominal tap position and magnitude of voltage correction for one tap operation equals to 0.01250 pu considering a range of 0.90 pu to 1.10 pu for voltage correction. The simulated dead-band of tap changing devices is twice the per unit value of voltage change per tap operation. The total mechanical time delays for VR1 and VR2 are 5 s, and 10 s, respectively. The time delays are not assigned for CB operations and DG VAr controllers, since their operation is considered to be instantaneous with minimal time delay. Selected simulation results are presented in Figure 5.11. It can be seen that the results derived from time domain simulation studies validate the merits of the proposed strategy with limited tap operations and minimal voltage swings.

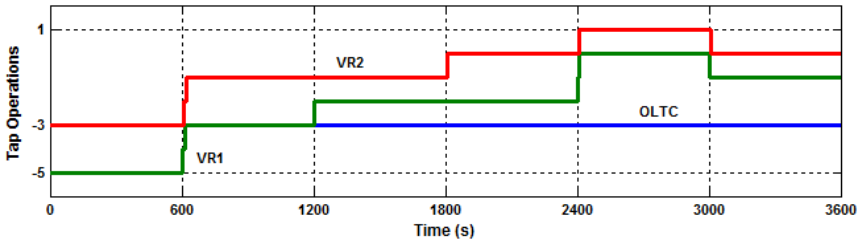

(a)

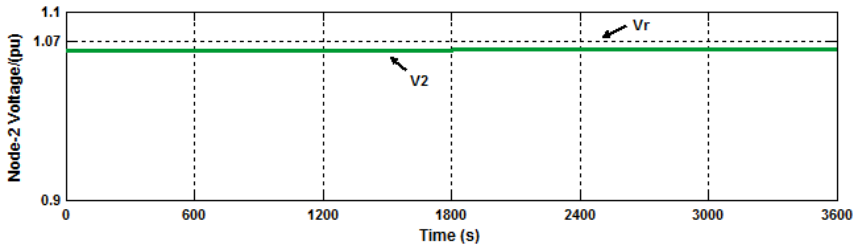

(b)

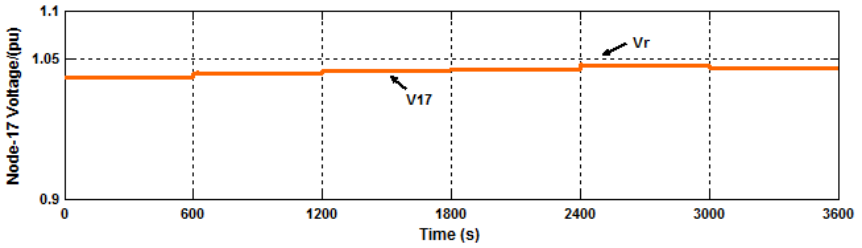

(c)

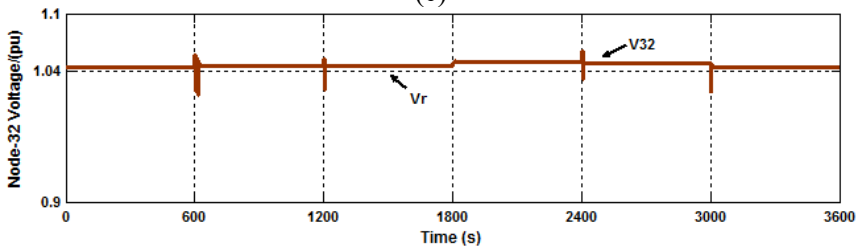

(d)

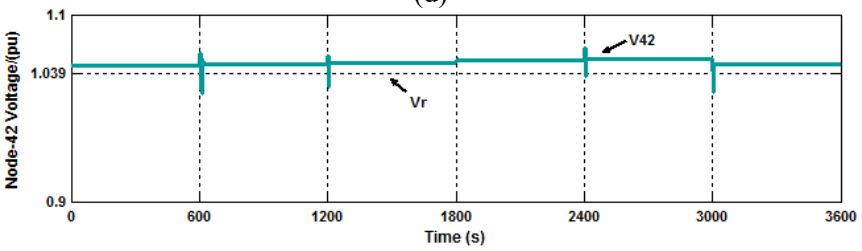

(e)

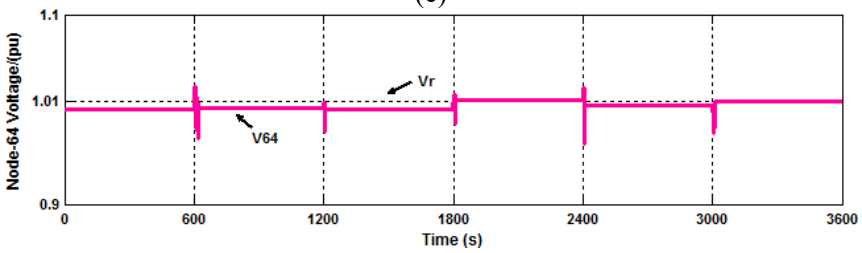

(f)

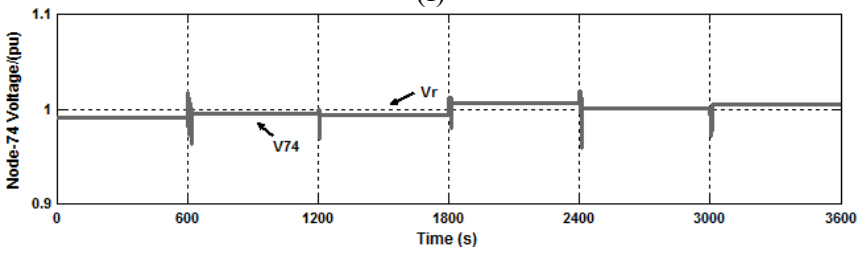

(g)

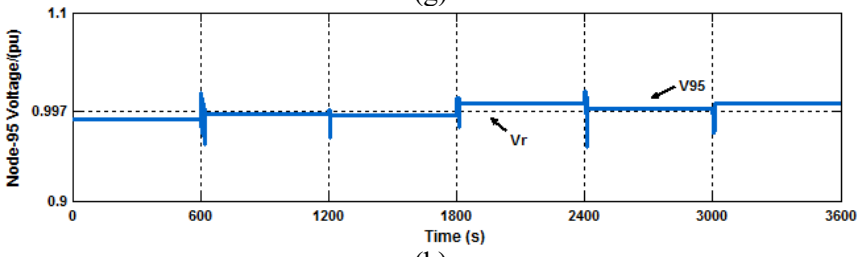

(h)

Figure 5.11: Results obtained from the hourly time domain simulation using the proposed control strategy: (a) tap operations by VR1 and VR2, and (b) – (h) regulated voltages at nodes-2, 17, 32, 42, 64, 74 and 95

5.4 Summary

In summary, this chapter proposes a DMS algorithm for tuning control parameters of multiple voltage control devices and Volt/VAr support DG units in distribution systems. It is shown that the proposed DMS algorithm is capable of optimising control actions of the multiple Volt/VAr control devices, and minimising both voltage fluctuations and voltage swings, especially on the nodes close to the DG units. Also, the techniques incorporated in the proposed formulation and search method following the time-graded operation of Volt/VAr control devices introduce a novel strategy for optimal Volt/VAr control in modern distribution systems. In the context of renewable energy resources, the non-utilisation of local energy-storage units and associated ramp-rate controls for mitigating the voltage swings would be beneficial to DNOs. Moreover, the proposed DMS algorithm can be implemented in a substation as a separate module and operated in real-time basis for effective voltage regulation.

The proposed tuning algorithm is invaluable as it exhibits the flexibility to implement varying DNO practices of optimal Volt/VAr control such as loss minimisation, conservation voltage reduction (CVR) and multi-objective Volt/VAR optimisation. It has also been found that a relatively flat voltage profile along the feeder is preferable to achieve an effective implementation of CVR.

CHAPTER 6: COORDINATED VOLTAGE CONTROL IN DISTRIBUTION SYSTEMS CONSIDERING THE IMPACT OF SIMULTANEOUS RESPONSES OF VOLTAGE CONTROL DEVICES AND DG UNITS

This chapter proposes and details a strategy for effective coordinated voltage control in distribution systems embedded with multiple voltage control devices and DG. This fulfils the requirement of mitigating the adverse effects of possible simultaneous responses of multiple voltage control devices and Volt/VAr support DG units as identified in the Chapter 4 through preliminary investigations. The proposed strategy is designed aiming to be implemented using substation centred DMS for online voltage control. This chapter is organised as follows. Section 6.1 gives a brief introduction to the chapter, while Section 6.2 includes a discussion on operation of multiple tap changing devices and DG units in a distribution system. Section 6.3 details the practical implementation strategy for proposed online voltage control, while the proposed control algorithm is detailed in Section 6.4. The test cases and simulation results are presented in Section 6.5 and Section 6.6 includes the concluding remarks. This chapter is based on the Journal Publication titled "Online Voltage Control in Distribution Systems with Multiple Voltage Regulating Devices," authored by D. Ranamuka, A. P. Agalgaonkar, and K. M. Muttaqi, *IEEE Transactions on Sustainable Energy*, vol. 5, no. 2, pp. 617-628, Apr. 2014.

6.1 Introduction

Voltage regulation in MV distribution feeder systems is typically performed with the aid of multiple voltage control devices, such as OLTC and SVRs, in addition to local CBs. These devices are conventionally tuned and locally coordinated using Volt/VAr optimisation strategies in accordance with the time graded operation. However, in case of distribution systems embedded with DG, there could be simultaneous responses of DG and multiple voltage control devices for correcting the target bus voltage thereby resulting into significant operational conflicts. This chapter proposes an on-line coordinated voltage control strategy for MV distribution systems containing DG and other voltage control devices. The

proposed strategy minimises the operational conflicts and resultant adverse effects on system voltage by prioritising the operations of different control devices, while maximising the voltage regulation support by the DG units. Since the proposed control logic preserves the existing design philosophies of DG local voltage controllers and other voltage control devices, and exhibits high computational efficiency, it can easily be implemented on a practical distribution system via a substation centred DMS. The simulation results have demonstrated that voltage control for a distribution feeder system can effectively be achieved on real-time basis through the application of the proposed control strategy. The test simulations are carried out using MATLAB-Simulink software for a detailed model of the test distribution system (feeder configuration–01 and 02) shown in Figure 2.1 of Chapter 2.

6.2 Operation of Multiple Tap changers and DG in a Distribution System

In case of long MV distribution feeder systems which are common throughout the Australian national electricity network, there could be significant drop in voltage towards the end of the feeders, especially due to the voltage drop across the line sections attributed by random variation in the load demands. It is essential to adopt necessary measures to maintain the voltage within stipulated limits throughout the feeder. Accordingly, multiple SVRs are commonly used in conjunction with the substation OLTC in order to regulate the voltage for long distribution feeder systems. A topology of such typical distribution system with multiple SVRs, OLTC and DG is shown in Figure 2.1 of Chapter 2. If Volt/VAr support DG is operated in an uncoordinated fashion, there is a possibility to introduce strong control interaction with other voltage control devices in the network, due to simultaneous responses of DG and other voltage control devices to correct the system voltage. The operation of such realistic distribution feeder systems has been investigated in [38], [39]. In summary, the findings are:

- Addition of DG further improvises the system voltage. The impact of voltage change by DG is significant, if the DG is connected at the end of a distribution feeder when the distribution system is lightly loaded.

- Total numbers of SVR tap operations are significantly increased (also leading to hitting tap limits and runaway) in the presence of DG installed between SVRs and end of the feeder system, because of the DG-SVR interactions and the resultant conflicting (against each other) operations. It is mainly due to the reverse power flow of DG followed by the DG responses at different system conditions. Also, the worst cases depend on operational mode of the SVR enacted with or without lined drop compensation.

  In case of DG unity power factor operation, there can be conflicting tap operations in SVRs which are operated with bi-directional mode under certain system conditions during the reverse power flow of DG. If the SVRs are operated with reactive bi-directional mode (mostly in loop distribution systems), there is not any significant impact of DG on operation of the SVRs. When the SVRs are operated with the co-generation mode; there can be conflicting tap operations due to the interactions between DG and the operation of LDC circuit under certain system conditions, if the R_L and X_L settings of LDC are not updated.

  In case of DG power factor control mode or VAr control mode, there is a higher possibility for conflicting tap operations in SVRs which are operated with bi-directional mode during the reverse power flow of DG operated without adaptive reference value for the power factor or VAr controller. If the SVRs are operated with reactive bi-directional mode, there is not any significant impact of DG on operation of the SVRs. When the SVRs are operated with the co-generation mode, there can be significant conflicting tap operations due to the interactions between DG and the operation of line drop compensation circuit under certain system conditions.

  In case of DG voltage control mode, there is a certain possibility for conflicting tap operations in SVRs which are operated with bi-directional mode during the reverse power flow of DG operated without adaptive voltage reference value for the DG voltage controller. If the SVRs are operated with reactive bi-directional mode, there can be impact of DG on operation of the SVRs under certain system conditions. When the SVRs are operated with the co-generation

mode, there can also be conflicting tap operations in SVRs due to the interactions between DG and the operation of LDC circuit.

- SVR and DG operation does not alter the OLTC tap operation, where far single large DG unit is connected to the system or few small DG units are distributed. If multiple DG units are distributed to a larger extent or single large DG unit connected closer to the OLTC and subjected to variable power injection, OLTC tap operations are altered.

- In addition to the steady-state voltage variations, each additional OLTC and SVR tap operation and DG response also introduce transients to the system. In case of online tap changing devices, a reactor or high speed resistance tap changing mechanism bridges the two taps temporarily while changing from one to the other introducing switching transients.

- Inclusion of a CB in the simulations (as detailed in Chapter 4) also shows the similar results, which are caused by further interactions among DG-SVR-CB under certain system conditions.

6.2.1 Substation On-Load Tap Changer and Step Voltage Regulators

As discussed in the Chapter 2, substation OLTC serves the core voltage regulation in distribution feeder systems fed by the substation. SVRs are used for voltage regulation, especially for regulating the voltage further at the downstream of a distribution feeder system. Most of the SVRs consist of an auto-transformer equipped with a load tap changing mechanism. The voltage change is obtained by changing taps on the series winding of the auto-transformer. SVRs are classified into several types according to their construction and mode of operation [1]. Typically, SVRs can be configured using a Type A or Type B connection. The more common type is Type B connection, where the input to the SVR is across the series and shunt windings. Therefore, when a change in taps is required, the autotransformer changes the number of turns on the series winding. The function of substation OLTC and SVR, with the application of an analog or digital LDC circuit, for estimating the voltage can generally be explained with the aid of voltage regulating device controller. It keeps the target load centre voltage V_{LC}

within a specified range. The set (reference) voltage, $V_{SET/VR}$ and dead-band voltage, V_{DB}, as shown in (01), are the controller parameters for the voltage regulating device where V_{LB} and V_{UB} are the lower boundary and upper boundary limits, respectively.

$$V_{LB} \le V_{LC} \le V_{UB}$$

$$V_{LB} = V_{SET/VR} - 0.5V_{DB}, \quad V_{UB} = V_{SET/VR} + 0.5V_{DB} \tag{01}$$

The function of a LDC based SVR in forward mode can be explained using the expression given by (02). It is assumed that R_L and X_L are the set values of resistance and reactance for LDC circuit respectively, and I is the measured current at the load side of SVR. It is assumed that the voltage at the voltage regulating device connection point is V_{VR}. For a lagging power factor $cos(\varphi)$, the remote end voltage can be given by (02).

$$V_{LC} \approx V_{VR} - I \times R_L \times cos(\varphi) - I \times X_L \times sin(\varphi) \tag{02}$$

The changes in active and reactive power flows between voltage control device and load centre will significantly affect the performance of a LDC based SVR. The performance will also be deteriorated, if the X_L/R_L ratio of LDC setting is poorly adjusted. This LDC error may cause additional tap operations of the SVR.

On the other hand, the effect of a tap changing device on its downstream nodal voltage profile can be estimated using the lossless linear regulator model given by (03), where $V_{LC(j)}^{ur'}$ is the unregulated voltage at its target load centre, $V_i^{ur'}$ and V_i^{rs} are the voltages at any i^{th} node before and after the voltage control action respectively, and Tr_j is the equivalent tap ratio of j^{th} device for regulating the load centre voltage defined by the voltage set value $V_{SET/VR(j)}$ [53]. This equation is also used in the Chapter 5 of this thesis for estimating the nodal voltage change by OLTC and SVRs.

$$T_j^r = \frac{V_{SET/VR(j)}}{V_{LC(j)}^{ur'}}, \quad V_i^{rs} = T_j^r \times V_i^{ur'} \tag{03}$$

The voltage control parameters of a substation OLTC i.e., set voltage and dead band are typically set to regulate the secondary voltage without violating the stipulated limits. The substation OLTC controller time delay can be set based on constant time variant or inverse time characteristics. In case of constant time variant characteristics, the time delay is constant. With inverse time characteristics, the time delay is inversely proportional to the voltage deviation and can dynamically be updated according to the network conditions. The set voltages and dead band settings of the SVRs are selected based on the total number of taps and the percentage value of voltage regulating range respectively. They are also operated with a time delay which can be assigned in the SVR controller. SVR farther from the substation has longer time delay than the SVR closer to the substation [8]. This time delayed operation of SVRs is based on constant time variant characteristics. Non sequential or sequential operational strategies are used for OLTC and SVR tap operations and to locally coordinate their operations with the upstream regulators. In non-sequential operation, the time delay is used for all the tap steps, while in sequential operation the time delay is used only for the first tap operation and the subsequent taps are operated with mechanical time delay.

6.2.2 Effect of DG on Nodal Voltage Profile of a Feeder System

Since, both active and reactive power injections from DG can change the distribution feeder voltage profile; impedance matrix (Z-matrix) of the distribution feeder can generally be used for estimating the respective voltage change [38]. If the DG current is I_g, then the voltage change by DG at k^{th} nodal bus, $V_{k/DG}$ can be estimated by using (04). It is assumed that the distribution feeder has n number of nodal buses (i.e., k = 1,…, n) and DG is connected at g^{th} node.

$$\left[\Delta V\right]_{n\times 1} = \left[Z\right]_{n\times n} \times \left[\Delta I\right]_{n\times 1}$$

$$\text{where } V_{k/DG} = Z_{k,g} \times I_g \qquad (04)$$

It is noted that the impact of DG on feeder voltage can be significant, if the DG is connected at the end of a lightly loaded long distribution feeder [38]. Also, the

synchronous machine based DG units are capable of responding instantaneously to meet the system load demand.

6.2.3 Effect of Simultaneous Responses of Tap Changing Devices and DG on Nodal Voltage Profile of a Feeder System

Based on the inherent operational characteristics of DG and SVRs, there is a potential of simultaneous responses between SVRs and DG under conventional decentralised and centralised voltage control as investigated and observed in the Chapter 4. If there are tap operations for multiple SVRs and a DG response at the same time then their cumulative effect on the voltage at i^{th} node, V_i can be estimated using (05). This is derived from the equation (14) shown in Section 4.6 of the Chapter 4, which considers multiple voltage control devices and DG units in general. The total voltage change by simultaneous tap operations is ΣV_i^{rs} and the voltage change by DG is $V_{i/DG}$. In this chapter, it is assumed that the substation OLTC is fixed based on the observation highlighted in section 6.2 i.e., SVR and DG operation does not alter the OLTC coarse voltage control at substation bus-bar level, where single large DG unit is connected to the system or few small DG units are distributed. However, if the operation of OLTC needs to be incorporated; it can easily be done when required. Moreover, it is noted that the integration of CBs shows further adverse effects under certain system conditions. However, it is not detailed in this chapter.

$$V_i = \Sigma V_i^{rs} + V_{i/DG} \qquad (05)$$

In the worst case scenario, V_i can be exceeded beyond V_{max} (maximum allowable voltage limit for the distribution system) or vice versa, thereby violating the dead-band values of tap changers in opposite direction. Hence, the simultaneous response of multiple tap changing devices and DG can also lead to conflicting operations under certain system operating conditions and may exhaust total number of tap operations resulting into voltage variations and transients, if there is not a real-time control mechanism to operationally avoid simultaneous responses of multiple SVRs and DG as identified by the research gap.

6.3 Practical Implementation Strategy for Proposed Online Voltage Control

The proposed control strategy described in Section 6.4 can effectively be implemented with the aid of a substation centred DMS. It mainly relies on three components, which are as follows:

- Control module for maximising voltage regulation support by the most capable DG
- Capability to capture on-line measurements of load centre voltage for SVR and DG voltage control module operation
- Control module for blocking simultaneous operations of DG voltage control module and multiple SVR taps

For implementing the proposed control system, the technical considerations and features related to commercially available DMS [55], [56] have been explored. A DMS is a real-time information system for all operational activities in a modern distribution control centre. The advanced DMS continually runs real-time analysis for various distribution system functionalities such as service restoration, Volt/VAR control, adaptable Volt/VAR optimisation, and equipment condition monitoring in addition to the state estimation. The state estimation algorithms applied for MV distribution systems may use network characteristics and data, estimated load and the power output by DG (pseudo-measurements). State estimation outputs are the controller inputs. A significant reduction in number of remote measurements can be obtained through optimal siting of measurement nodes. The substation centred advanced DMS schemes are well suited for waveform analysis and the signal processing, including relevant real-time monitoring and control [56]. Also, these DMS schemes are capable of utilising user-defined algorithms and customised software to determine best operating settings for voltage control devices such as Volt/VAr support DG units, tap changers and CBs in real-time [57].

The control system proposed in this chapter is based on updating the reference voltage of DG voltage controller (i.e., excitation control system in case of

synchronous machine based DG) and blocking the simultaneous operations between proposed DG voltage control module and SVR taps in real-time; in addition to tuning the voltage controller parameters as discussed in Chapter 5. The proposed control modules can easily be implemented in practical distribution systems containing not only multiple tap changers and DG, but also CBs. Accordingly, the newly designed control modules can be integrated into a substation centred DMS for enhancing real-time control operation. A substation centred DMS is proposed in this chapter for enacting the proposed control strategies. The topology of the proposed system implementation is shown in Figure 6.1.

Multiple voltage control device and DG voltage controller parameters are tuned and updated dynamically to ensure fine voltage control as highlighted in Chapter 5. The control settings of DG voltage control module and, control settings of SVR and substation OLTC local controllers are tuned by a tuning algorithm, which can also be embedded in the DMS (as discussed in Chapter 5). The time delay sequence of multiple voltage control devices in a feeder should be designed based on the condition given by (06), where SVRs are counted from the substation end. It is better to assign smaller time delay values for the voltage controllers in addition to dead-band, especially in case of distribution systems embedded with DG subjected to higher power output variations as discussed under problem formulation and solution method in the Chapter 5.

$$T_{DG} << T_{SVR(1)} < T_{SVR(2)} < \cdots T_{SVR(n)} < T_{OLTC} \qquad (06)$$

In (06), the T_{DG} and T_{SVR} are time delays for DG voltage control module and the SVRs respectively, which are assigned in this chapter with constant time variant characteristics for non-sequential operation. The sequential operation can also be assigned, if required. The DG voltage control module (DG-VCM) and control module for blocking simultaneous operations (CM-BSO) are integrated in the DMS as separate controls. The DG-VCM output is an input to the CM-BSO, where its output referred to the operation of DG-VCM is sent to the DG-VCM as an input. The respective control parameters are updated using separate modules as

shown in Figure 6.1. Additional two-way communication channels may be required for updating the control settings of SVRs and DG voltage controllers.

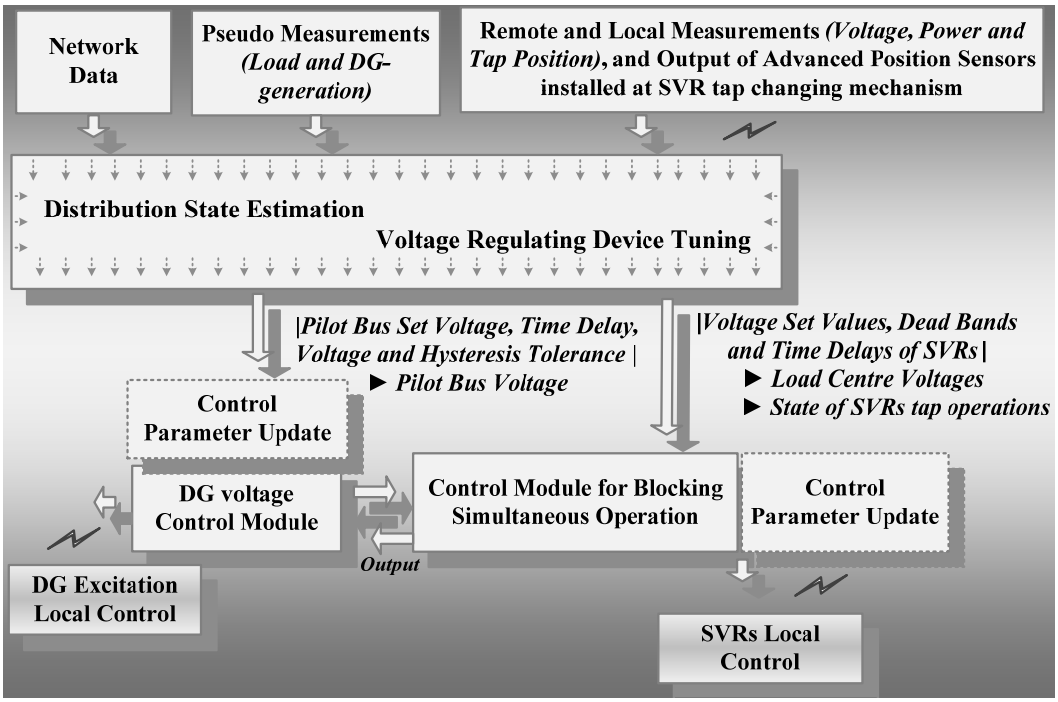

Figure 6.1: Topology of the on-line implementation for proposed control strategy

The proposed voltage control strategy enhances the system security due to its capability to update settings and enforce quick changeover to local control. It also helps to implement the proposed control scheme with minimum modification in the conventional control scheme as follows.

- DMS–tap changer control interface for updating control settings and assigning on-line target point voltage, and incorporating decision variables of CM-BSO
- Change-over facility to enable local control whenever required
- Advanced position sensors at the tap changing mechanism including associated interface for determining the state of progressive tap operation
- DMS-DG voltage control (i.e., excitation system in case of synchronous machine based unit) interface for updating the reference voltage of DG voltage controller, and incorporating decision variables of CM-BSO

6.4 Proposed Control Strategy

The proposed control strategy is based on the following three main control aspects managed by DMS in addition to tuning the regulating devices and prioritising their operations: (a) Maximising voltage regulation support by DG through DG-VCM, (b) On-line load centre voltage measurements for SVR operation, and (c) Real-time control for avoiding simultaneous operation of DG-VCM and multiple SVR taps.

In case of the control aspect (a), the DG operates as a voltage regulating device with its fast excitation control action (i.e., in case of synchronous machine based unit). Accordingly, the associated time delay is smaller than the mechanical time delay of a SVR where the typical values can be found in [5]. Also, the reference voltage for the excitation system is appropriately updated, by maintaining the time delay sequence given by (06), for maximising the voltage regulation support by DG through on-line DG-VCM. Therefore, the voltage change by means of a DG response, $V_{i/DG}$ as given in (05), is now a control variable (defined as $V_{i/DGC}$), and the system voltage is quickly regulated by the DG under all system conditions. On the other hand, in case of the aspect (c), the simultaneous operations of SVR taps and DG-VCM are blocked in real-time preserving their local control action for which the V_i can be expressed by (07).

$$V_i = V_i^{rs} + V_{i/DGC} \tag{07}$$

Since, one of the terms in (07) is appropriately controllable; any violation in the system voltage, given by (05), can be avoided by the proposed on-line voltage control strategy, while maximising and prioritising the voltage regulation support by the DG. It also aids distribution system by enabling one voltage control action (of DG-VCM or SVR tap) at a time. These aspects are detailed in the Section 4.6 of the Chapter 4.

6.4.1 DG Voltage Control Module (DG-VCM)

In the proposed DG voltage control module, the pilot bus (target bus) voltage is monitored in real-time, where pilot bus can be the weakest bus (or remote bus in

case of radial distribution feeder systems). In accordance with the magnitude of pilot bus voltage, reference voltage for the excitation system of DG (i.e., in case of synchronous machine based unit), V_{ref} will be updated by exploiting the reactive capability of the machine; thereby aiding voltage regulation. The lower and upper limits of reference voltage can be derived based on the capability chart of the synchronous machine in order to maximising the DG voltage regulation support. The selection of pilot bus and tuning of control parameters need to be carried out based on the DG capacity and standard voltage limits for the network. It is assumed that the initial exciter setting for the DG is at the nominal value of reference voltage. Subsequently, the proposed DG voltage control module (DG-VCM) embedded in the DMS is enabled. Its topology is shown in Figure 6.2.

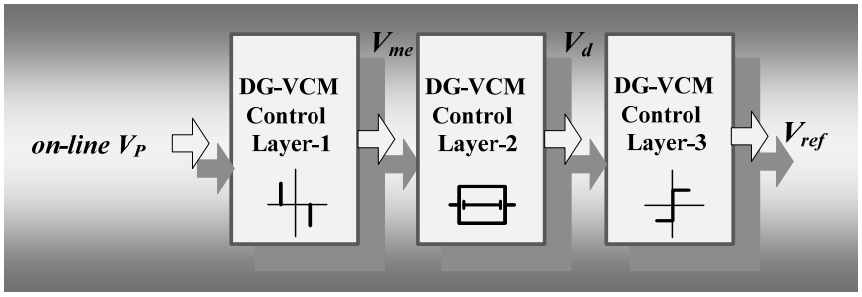

Figure 6.2: Topology of the DG voltage control module

The representative control logic for the model can be summarised as given by (08) to (12). The voltage set value $V_{SET/P,}$ voltage tolerance value V_t and hysteresis tolerance value ε_t are included in the DG-VCM control layer-1 which determines the state of the voltage error V_{err}. The difference between magnitude of pilot bus voltage V_p and the respective $V_{SET/P}$ is the voltage error V_{err}. The time delay T_{DG} is assigned in the DG-VCM control layer-2 which determines the time duration (T) of V_{err} exceeding the V_t. If the time duration T exceeds the assigned time delay value T_{DG}, the decision making layer (DG-VCM control layer-3) is enacted. The inputs of DG-VCM control layer-2 and DG-VCM control layer-3 are V_{me} and V_d, respectively. Accordingly, the DG excitation control scheme is updated with a new reference voltage by a voltage change (a_d) per control action. It is noted that the voltage at certain buses can also be regulated with the use of proposed control scheme, especially in the presence of synchronous machine based DG.

$$V_{err} = V_{SET/P} - V_P \tag{08}$$

$$V_{me} = \begin{cases} +1 & for\ V_{err} > \left(V_t + \in_t\right) \\ & for\ V_t < V_{err} \le \left(V_t + \in_t\right),\ V_{err} \downarrow \\ 0 & for\ -V_t \le V_{err} \le +V_t \\ & for\ V_t < V_{err} \le \left(V_t + \in_t\right),\ V_{err} \uparrow \\ & for\ -\left(V_t + \in_t\right) \le V_{err} < -V_t,\ V_{err} \downarrow \\ -1 & for\ V_{err} < -\left(V_t + \in_t\right) \\ & for\ -\left(V_t + \in_t\right) \le V_{err} < -V_t,\ V_{err} \uparrow \end{cases} \tag{09}$$

$$T = \begin{cases} T = \left(T + \Delta T\right) & if\ V_{me} \neq 0 \\ 0 & if\ V_{me} = 0 \\ & if\ V_{me} \pm \rightarrow \mp \\ & if\ V_{ref} \rightarrow \left(V_{ref}\right)_{new}\ transition\ state \end{cases} \tag{10}$$

$$V_d = \begin{cases} V_{me} & if\ T > T_{DG} \\ 0 & if\ T \le T_{DG} \end{cases} \tag{11}$$

$$V_{ref} = \begin{cases} V_{ref} & if\ V_d = 0 \\ V_{ref} + a_d & if\ V_d = +1 \\ V_{ref} - a_d & if\ V_d = -1 \end{cases} \tag{12}$$

The time delay, T_{DG} has been introduced to prevent unnecessary control actions in case of transient voltage variations. It is set to a small value with constant time variant characteristics in order to prioritise the voltage regulation support by DG as given in (06). Also, the values of a_d and V_t should be adequately large for stable operation, and should not lead to poor synchronising and damping torque coefficients in case of synchronous machine based DG units.

6.4.2 Online Voltage Measurements for Step Voltage Regulator Operation

The changes in active and reactive power flows between SVR and load centre may lead to a higher LDC error resulting into increased number of tap operations under certain system conditions. A methodology is proposed in Appendix-II for assessing the DG impact on operation of LDC in voltage control devices. If nodal voltage at the load centre is measured on-line, the conventional LDC scheme can be disabled. This chapter proposes a real-time monitoring scheme for SVRs. The topology of control model of such a SVR is shown in Figure 6.3.

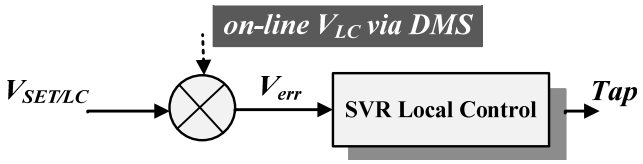

Figure 6.3: Topology of the model for SVR control with on-line load centre voltage measurements

6.4.3 Control Module for Blocking Simultaneous Operation (CM-BSO)

A control module is proposed for blocking simultaneous operations of DG-VCM and multiple SVR taps in real-time, which also ensures the prioritised action of the respective controllers. Since, substation OLTC deals with voltage regulation at the substation bus-bar level using a coarse control and operates after a prolonged time delay, it is not incorporated in the fine control strategy adopted in this section. Accordingly, the topology of the proposed control module (CM-BSO) embedded in the DMS is shown in Figure 6.4.

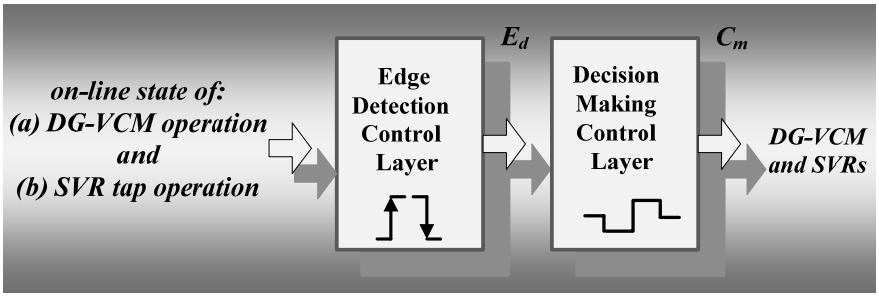

Figure 6.4: Topology of the control module for blocking simultaneous operations

The inputs for edge detection control layer are the state of DG-VCM operations and the tap operations of multiple SVRs. The position sensors can monitor transition state of a tap i.e., up or down operation with rising or falling edge at their output, respectively. Transition state of a DG-VCM operation can directly be monitored as rising or falling edge from its output. The edge detection control layer detects the state of progression for DG-VCM operations and each SVR tap operation by separate edge detection modules in order to enact the decision making control layer. Accordingly, rising or falling edge is referred to a transition state of a progressive tap operation or a DG-VCM operation. The two-dimensional (2D) step edge detection model, proposed in [58], is adopted in the proposed control module.

The decision making control layer is used for processing the outputs of edge detection control layer by summing up modules and comparator modules. The output of each summing up module is compared with the reference, assigned in a single input-inverting output comparator module prior to initiation of a control action for the DG-VCM or a tap operation for the respective SVR. The DG-VCM or the associated SVR tap operation will be enacted based on the outcome of the decision making control layer.

The representative control logic of CM-BSO for interpreting a DG-VCM operation can be summarised as given in (13) to (15). The output of the respective module for summing up the outputs of DG-VCM and SVRs edge detection modules is F_r (*DG-VCM*), and the output of the comparator module is C_m (*DG-VCM*). The respective modules for SVR are F_r (*SVR*) and C_m (*SVR*).

$$Edge\ \ det ection\ \ \ mod ule\ (DG-VCM/SVR)$$

$$E_d(DG-VCM/SVR)=\begin{cases} +1 & if\ \ ri sin g\ or\ falling\ edge\ is\ \ det ected \\ & \forall\ \ \ transition\ \ state\ \ of\ a\ DG\text{-}VCM\ /\ SVR\ operation \\ 0 & otherwise \end{cases} \tag{13}$$

$$Summing\ up\ module\ (DG-VCM/SVR)$$

$$F_r(DG-VCM/SVR)=\begin{cases} +1 & if\ output\ of\ an\ E_d(SVR)\ and/or\ E_d(DG-VCM)\ is\ +1 \\ & \forall \quad \sum E_d(SVR)+E_d(DG-VCM) \\ 0 & otherwise \end{cases} \tag{14}$$

$$Comparator\ module\ (DG-VCM/SVR)$$

$$C_m(DG-VCM/SVR)=\begin{cases} +1 & if\ output\ of\ F_r(DG-VCM)/F_r(SVR)\ is\ 0 \\ & \forall \quad Inverting\ output\ rule \\ 0 & otherwise \end{cases} \tag{15}$$

The diagrammatic representation of the proposed scheme in DG-VCM side for enacting a control action is shown in Figure 6.5.

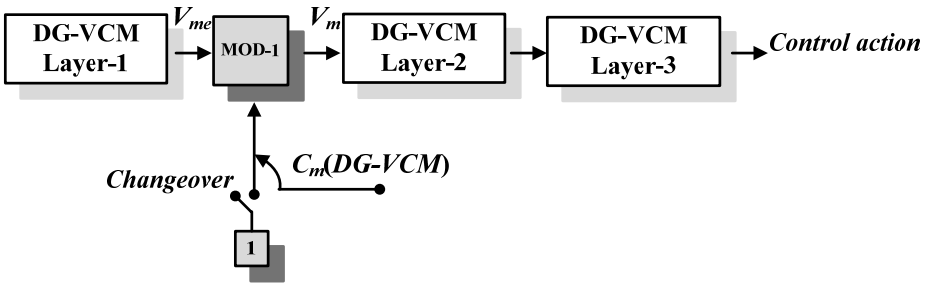

Figure 6.5: Modification required in the proposed DG-VCM

The representative control logic for the MOD-1 module is given by (16).

$$MOD\text{-}1\ \ module$$

$$V_m=\begin{cases} V_{me} & if\ V_{me}\neq 0\ \ and\ \ C_m(DG-VCM)=+1 \\ V_{me} & \\ \text{hold the action of DG-VCM layer-2 after the time delay until } C_m(DG-VCM)=+1, \text{ and} & \\ \text{then enact the DG-VCM layer-3} & \\ & if\ V_{me}\neq 0\ \ and\ \ C_m(DG-VCM)=0 \\ 0 & if\ V_{me}=0\ \ and\ \ C_m(DG-VCM)=0\ \ or\ \ +1 \end{cases} \tag{16}$$

The diagrammatic representation of the proposed control scheme for enacting a tap operation of SVR is shown in Figure 6.6. It is established with the aid of voltage regulator model proposed in [21]. The representative control logic for the MOD-2 module is given by (17).

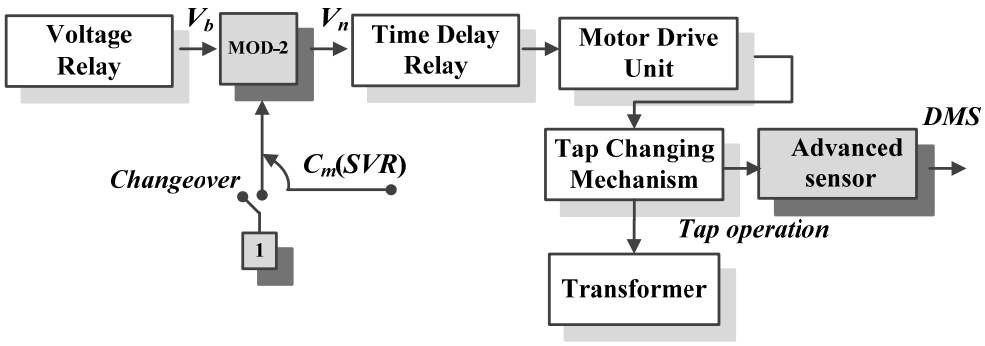

Figure 6.6: Modifications required in the SVR control

$$MOD\text{-}2 \quad module$$
$$V_n = \begin{cases} V_b \qquad if \;\; V_b \neq 0 \;\; and \;\; C_m(SVR) = +1 \\ V_b \\ hold\ the\ action\ of\ time\ delay\ relay\ after\ the\ time\ delay\ until\ C_m(SVR) = +1, and\ then\ \ enact \\ the\ SVR\ tap \\ \qquad if \;\; V_b \neq 0 \;\; and \;\; C_m(SVR) = 0 \\ 0 \qquad if \;\; V_b = 0 \;\; and \;\; C_m(SVR) = 0 \;\; or \;\; +1 \end{cases} \tag{17}$$

According to (16) and (17), no DG voltage control module and SVR tap operation can be initiated simultaneously. Hence, this scheme is capable of blocking any simultaneous operation in real-time, as it allows only one voltage control action (of DG-VCM or SVR tap) at a time, and accordingly enacts the next control action. The control algorithm of CM-BSO can be summarised as follows for the feeder system configuration–01 of the test distribution system as depicted in Figure 2.1 (Chapter 2):

- Step – 1 From on-line measurements and sensor information sent by DMS, the proposed and local voltage controllers are executed.
- Step – 2 (i) DG-VCM will update the reference voltage, V_{ref} of DG excitation -

control after time delay, T_{DG} if the pilot bus voltage magnitude is not within the stipulated limits and there is a confirmation from the CM-BSO; or

(ii) SVR2 will operate a tap after time delay, $T_{SVR(2)}$ if the target voltage magnitude is not within the stipulated limits and there is a confirmation from the CM-BSO; or

(iii) SVR3 will operate a tap after time delay, $T_{SVR(3)}$ if the target voltage magnitude is not within the stipulated limits and there is a confirmation from the CM-BSO; or

(iv) DG-VCM and SVR2 will be enabled after the associated time delays i.e., $T_{DG}<<T_{SVR(2)}$, if the target voltage magnitudes are not within the stipulated limits and there is a confirmation from the CM-BSO; or

(v) DG-VCM and SVR3 will be enabled after the associated time delays i.e., $T_{DG}<<T_{SVR(3)}$, if the target voltage magnitudes are not within the stipulated limits and there is a confirmation from the CM-BSO; or

(vi) SVR2 and SVR3 taps will be operated after the associated time delays i.e., $T_{SVR(2)}<T_{SVR(3)}$, if the target voltage magnitudes are not within the stipulated limits and there is a confirmation from the CM-BSO; or

(vii) DG-VCM, SVR2 and SVR3 will be operated after the associated time delays i.e., $T_{DG}<<T_{SVR(2)}<T_{SVR(3)}$, if their target voltage magnitudes are not within the stipulated limits and there is a confirmation from the CM-BSO.

Step – 3 For the subsequent instances of time (*i.e.,* $t = t + 1$), repeat the procedure from Step - 1.

The above procedure can be adjusted for a given network with a given number of SVRs and DG system as well as substation OLTC and CBs. If there are multiple DG units distributed to a larger extent in the MV distribution system, then the proposed method can easily be extended by establishing the relevant control logic to fully utilise the voltage support capabilities of the DG units and ensure coordinated operation of all the voltage control devices including multiple Volt/VAr support DG units on the distribution feeder system.

6.5 Test Case Study

In this section, simulation results and discussion associated with the proposed on-line voltage control in the realistic MV distribution system shown in Figure 2.1 are presented.

6.5.1 Test Distribution System Model

The performance of the proposed control algorithm is demonstrated through modelling the topology of the test distribution shown in Figure 6.7 in MATLAB-Simulink and conducting time domain simulations for different operational strategies of the feeder systems (feeder configuration – 01 and 02). Both the feeder systems have tie connection by means of ABS. Figure 6.7 is derived from Figure 2.1. It is to be noted that the stipulated operating voltage limits for the test system are within +/-10% from the nominal voltage.

The DG (synchronous machine based bio-diesel generator of 750 kVA rated capacity at node no. 78) is modelled to operate in a power factor control mode for depicting conventional operation as well as voltage control mode for signifying the proposed operation. The distribution network is assumed to be operated as a balance three phase system. The line impedance for 11 kV feeders is (0.802+j0.365) Ω/km. The type-B SVRs are modelled by incorporating 32 taps in the series winding. Two SVRs (Type-B type), SVR2 and SVR3 are installed in the test feeder system configuration-01, where one SVR (SVR1) which has been connected in feeder configuration-02 in addition to SVR3. A representative demand pattern depicting the realistic network conditions is considered to test the

effectiveness of the proposed on-line control strategy in managing the voltage regulation in the network.

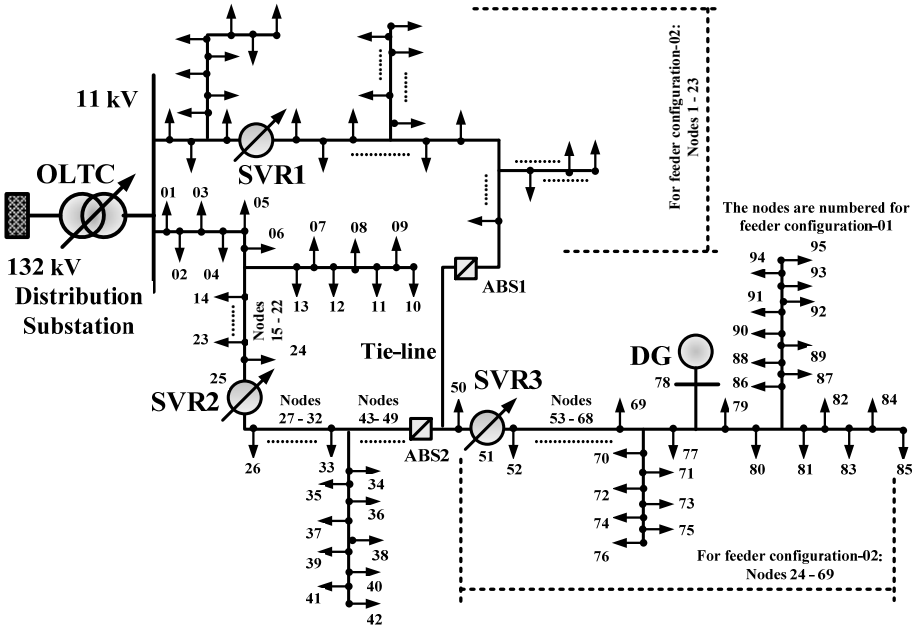

Figure 6.7: Topology of the test distribution system

Table 6.1 and 6.2 depict the simulated demand patterns at different time intervals. The feeder configuration – 01 is lightly loaded compared to the feeder configuration – 02.

Table 6.1: Simulated demand pattern for feeder configuration – 01

Time (s)	0	100	200	300	500	600
Load (kVA)	675	960	1140	1510	1270	995

Table 6.2: Simulated demand pattern for feeder configuration – 02

Time (s)	0	100	200	300	500	600
Load (kVA)	1234	1605	2082	2240	1890	1485

It is assumed that the OLTC is operated with a fixed tap position. The initial tap positions for SVR1/SVR2 and SVR3 are arbitrarily assumed to be at 3 and 4 respectively in the direction of increasing voltage. The total simulated time delays

for SVR1/SVR2 and SVR3 operation are assumed to be 4 s and 7 s, respectively. The total mechanical time delay assigned for voltage control devices is 1.0 s. Therefore, the total transition time for a tap operation is 1.0 s. The time delays are modelled with constant time variant characteristics and non-sequential tap operation. The voltage reference values are set at 1.05 pu and 1.01 pu for OLTC and SVRs, respectively. The dead-band values are set at +/- 1.5% and +/- 2.0% for OLTC and SVRs, respectively. The simulated control parameters of proposed DG voltage control module are $V_{SET/P}$ = 0.98 pu, a = 0.05 pu, V_t = 0.025 pu, ε_t = 0, and T_{DG} = 1.0 s, where nominal value of DG excitation reference voltage is 0.90 pu and pilot bus is the remote end bus of feeder configuration – 01 (node 95, i.e. *N95*). Based on the generator capability curve, the governor is tuned to supply an active power of 600 kW while the reactive power varies between +450 kVAr to -350 kVAr.

6.5.2 Simulation Results and Discussion

The proposed control modules are modelled using MATLAB and MATLAB-Simulink. The on-line information is assigned by '*Goto*' and '*From*' signal blocks without propagation delay. The total simulation time is assumed to be 750 s. The simulation results for the independent operation of the feeder configuration – 01 (by opening ABS-1 and closing ABS-2 in Figure 6.7) are shown below. Figure 6.8 shows the tap operations of multiple SVRs with conventional voltage control while Figure 6.9 (a) shows the tap operations with the proposed voltage control. Figure 6.9 (b) to (e) are the zoomed versions of Figure 6.9 (a) to clearly observe the tap operations.

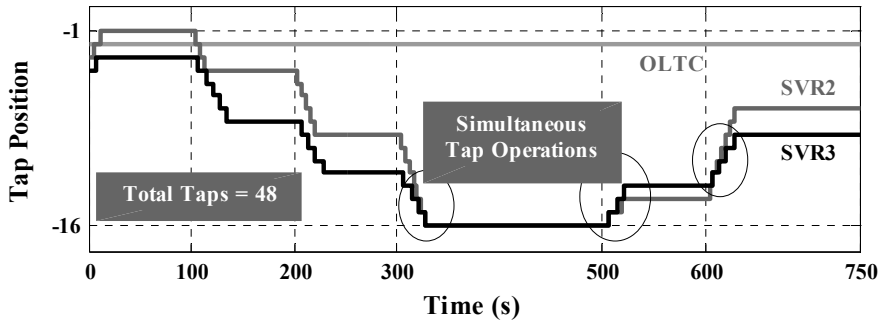

Figure 6.8: Tap operations for feeder configuration–01 operation with conventional voltage control

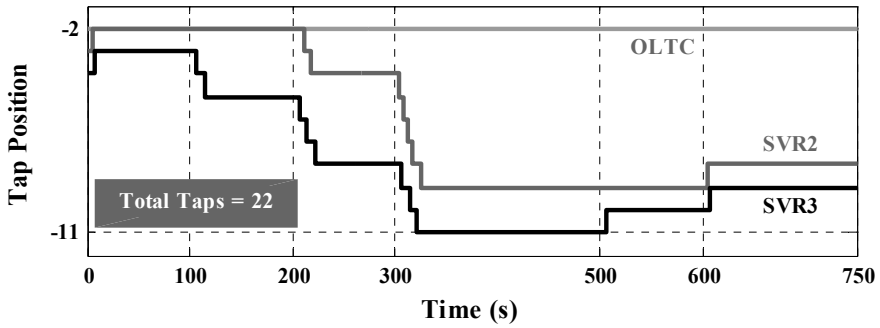
-2
-11
Tap Position
OLTC
SVR2
SVR3
Total Taps = 22
0
100
200
300
500
600
750
Time (s)

(a)

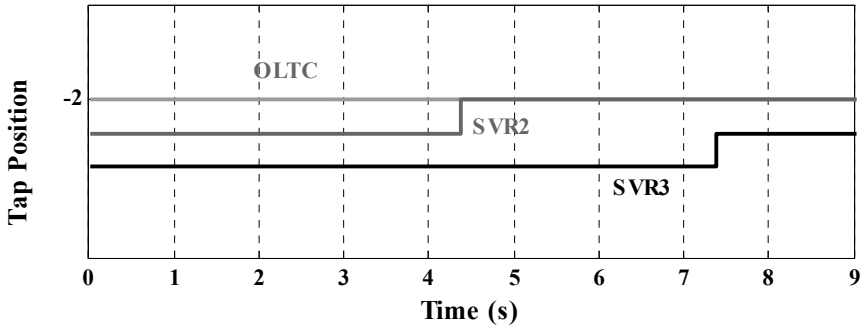
Tap Position
-2
OLTC
SVR2
SVR3
0
1
2
3
4
5
6
7
8
9
Time (s)

(b)

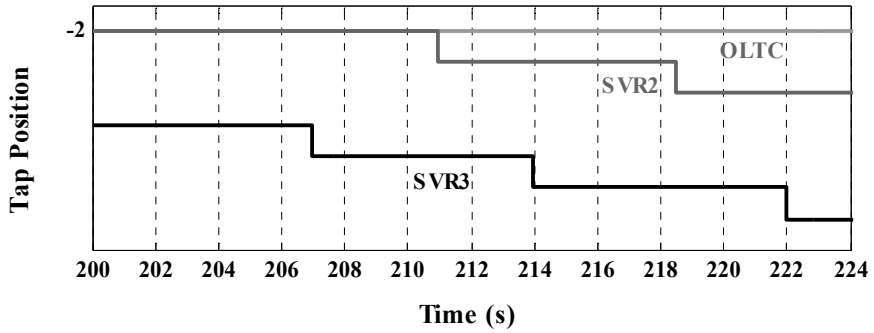
Tap Position
-2
OLTC
SVR2
SVR3
200
202
204
206
208
210
212
214
216
218
220
222
224
Time (s)

(c)

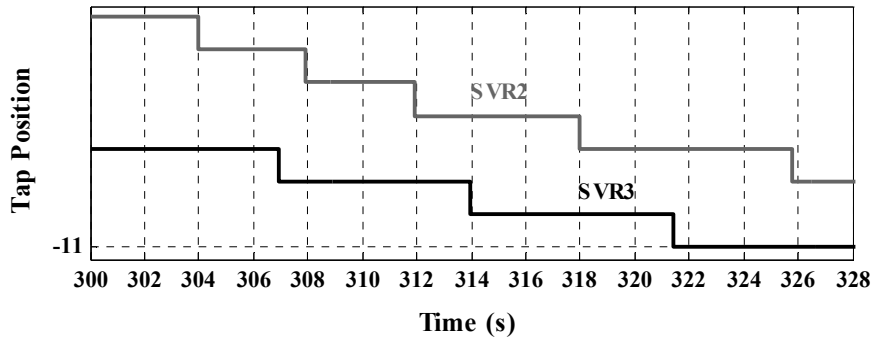
Tap Position
-11
SVR2
SVR3
300
302
304
306
308
310
312
314
316
318
320
322
324
326
328
Time (s)

(d)

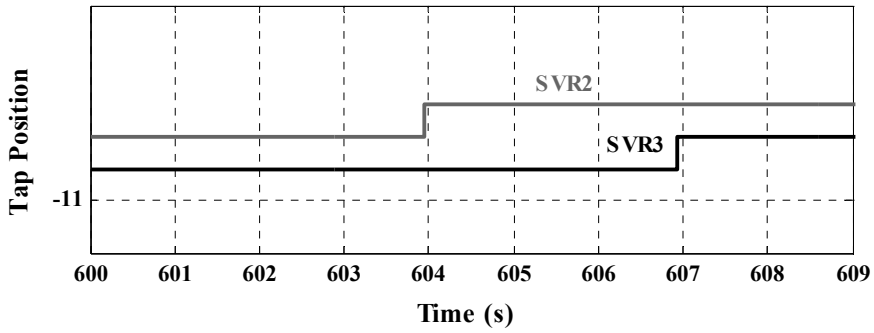

(e)

Figure 6.9: Tap operations for feeder configuration–01 operation with proposed voltage control (a) over the total simulation period (b) from t = 0 to 9 s (c) from t = 200 s to 224 s (d) from t = 300 s to 328 s (e) from t = 600 s to 609 s

Figure 6.8 shows simultaneous tap operations for SVRs at t = 328 s, 507 s, and 628 s with conventional voltage control. According to Figure 6.9 (a) to (e), there are no simultaneous tap operations (and DG-VCM actions) with the proposed control. It is because of the proposed CM-BSO based control action, which blocks the simultaneous operations in real-time. Its integrated operation with the modified local controllers also prioritises the operation of DG-VCM and SVRs. The DG-VCM and SVRs operate in accordance with the Step - 2 (vii) of the control algorithm as indicated in Sub-section 5.4.3. The DG-VCM operates at t = 1.0 s and V_{ref} is updated from 0.90 pu to 0.95 pu based on the pilot bus voltage (*N95*). It also operates at t = 2.0 s and V_{ref} is updated from 0.95 pu to 1.00 pu based on the pilot bus voltage. According to the DG-VCM control logic as given in (08) to (12), DG-VCM operates at t = 301 s. However, V_{ref} doesn't change due to the constrained operation of DG within the associated reactive power capability limits. The post-updated DG excitation controller regulates the voltage with its fast control action. This DG-VCM based operation may also support the feeder voltage regulation at the upstream nodes.

The first tap operation of SVR2 (at t = 4 s) and SVR3 (at t = 7 s) are initiated after DG-VCM control action followed by the time delay sequence given by (06). The 2nd (at t = 108 s) and 3rd (at t = 115 s) tap operations of SVR3 are initiated as given by Step - 2 (iii) of the control algorithm where there are no DG-VCM control action and/or SVR2 tap operation. Similarly, in response to the voltage

drop at t = 200 s and t = 300 s, SVR2 and SVR3 taps operate as given by Step - 2 (vi) of the control algorithm as indicated in Sub-section 5.4.3. Also, a SVR3 tap operates as given by Step - 2 (iii) in response to voltage change at t = 500 s, and SVR2 and SVR3 operate one tap each as given by Step – 2 (vi) at t = 600 s.

As the result of maximised DG voltage regulation support by DG-VCM and the real-time operation of CM-BSO, it can be seen that there is a significant reduction in tap operations for feeder configuration–01 operation with the proposed voltage control. This significant reduction in tap operations will obviously be beneficial to the DNO, as it directly correlates to the decrement in the regulator maintenance cost, increase in its life time expectancy, and the decrease in intermittent voltage variations attributed to the tap operations. The effect of proposed voltage control strategy to regulate the voltage of feeder configuration – 01 can be observed in the selected nodes denoted using *N*, which are *N95* (at the end of the feeder configuration – 01), *N09* (between substation and SVR2), *N34* (between SVR2 and SVR3), and *N62* (between SVR3 and DG) as shown in Figure 6.7. The respective nodal voltage profiles for feeder system operation with conventional voltage control and proposed voltage control are shown in Figure 6.10 to 6.12. The reduction in resulting voltage variations attributed to the tap operations is clearly observed in these figures.

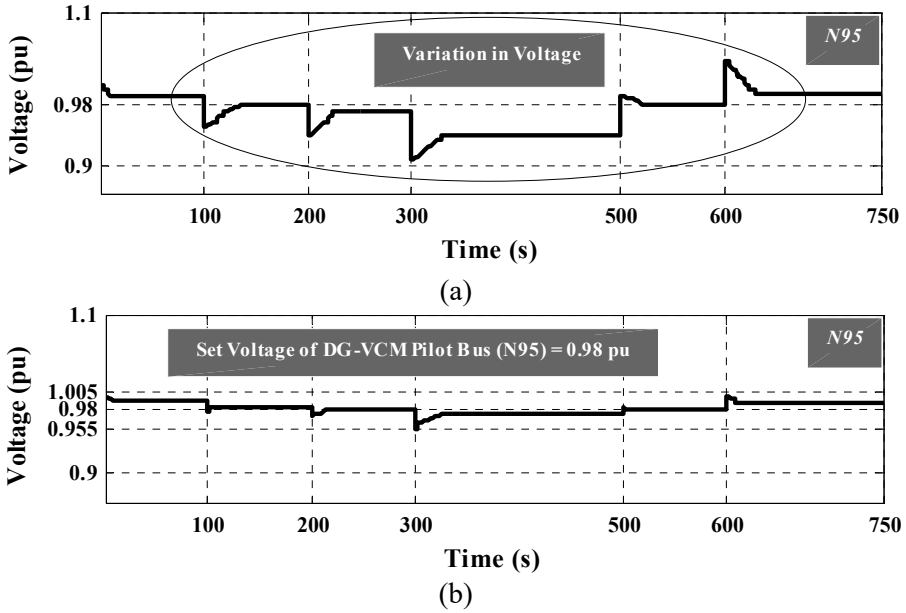

Figure 6.10: Voltage at node *N95* for feeder configuration–01 operation with (a) conventional voltage control (b) proposed voltage control

According to Figure 6.10 (a) and (b), it can be seen that the DG-VCM regulates the pilot bus voltage (which is the remote end of the feeder system, *N95*) within its stipulated limits of 1.005 pu and 0.955 pu for a set value of 0.98 pu, as outlined in the control logic given in (08) to (12). As shown in Figure 6.11 (b), the voltage regulation at the end of the feeder configuration – 01 is quite significant with the proposed control. Consequently, the proposed DG-VCM can support the feeder system voltage regulation at each node in accordance with (04).

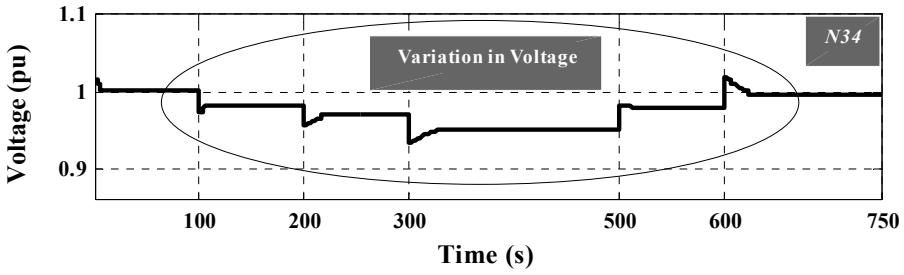

(a)

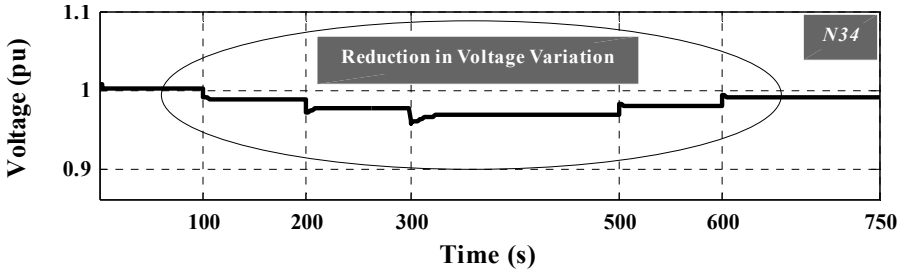

(b)

Figure 6.11: Voltage at node *N09* for feeder configuration–01 operation with (a) conventional voltage control (b) proposed voltage control

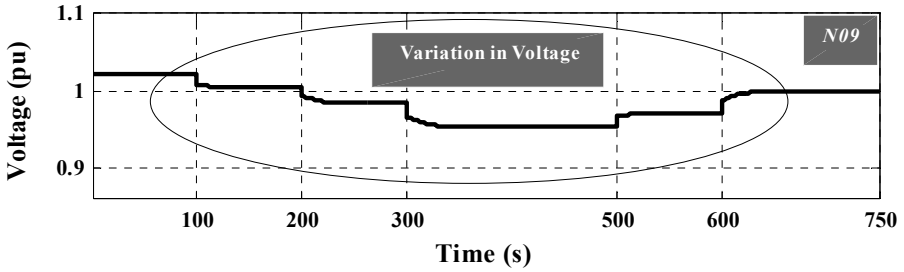

(a)

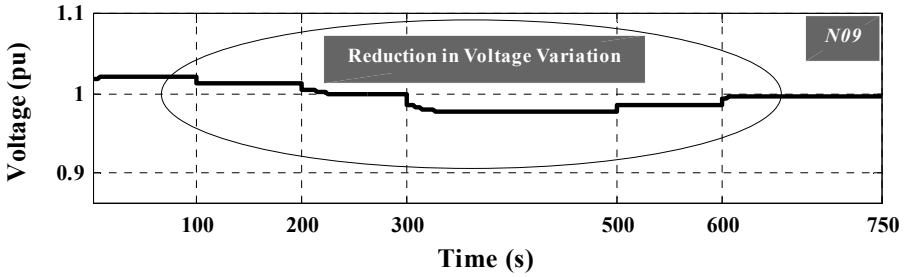

(b)

Figure 6.12: Voltage at node *N34* for feeder configuration–01 operation with (a) conventional voltage control (b) proposed voltage control

As seen in Figure 6.11 and 6.12, the voltages at various nodes along the feeder are significantly regulated even under reduced tap operations of the SVRs. The voltage variations also reduce with the adoption of proposed voltage control strategy. Moreover, the overall voltage profile of the feeder improvises. It is observed that the similar results can also be obtained for node *N62*. The active and reactive power outputs of the DG for feeder configuration – 01 operation are shown in Figure 6.13.

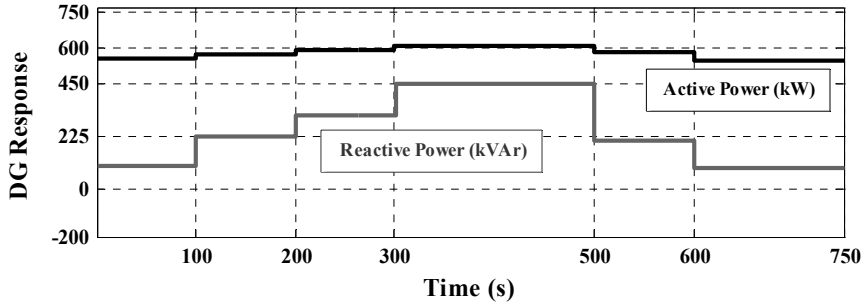

Figure 6.13: Active and reactive power outputs of DG in feeder configuration–01

The simulation results for the interconnected operation of feeder configuration–02 involving a feeder section of configuration–01 (by closing ABS-1 and opening ABS-2 in Figure 6.7) are shown below. Figure 6.14 shows the tap operations of multiple voltage control devices with conventional voltage control. Figure 6.15 (a) to (d) show the tap operations with proposed voltage control.

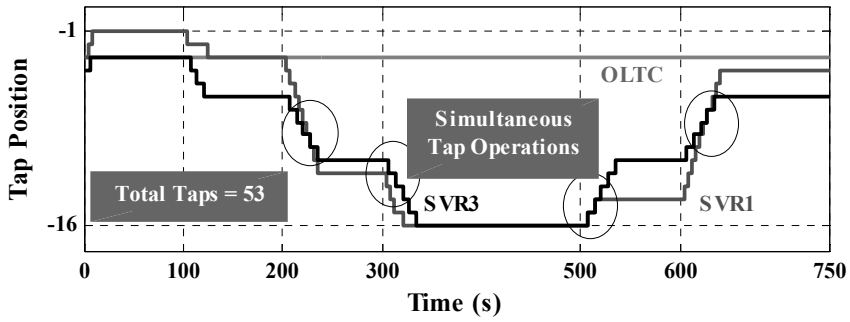

Figure 6.14: Tap operations for feeder configuration–02 interconnected operation with conventional voltage control

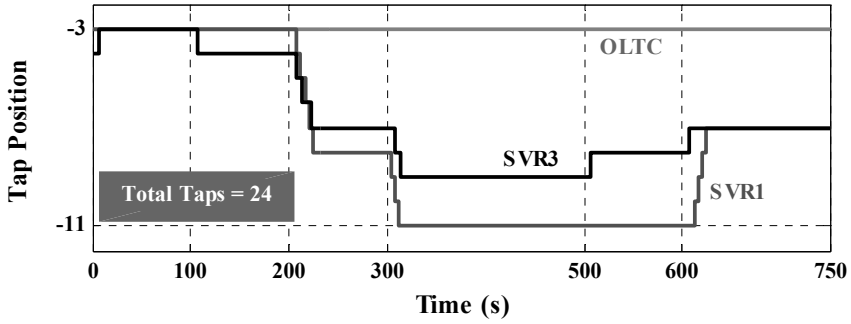

(a)

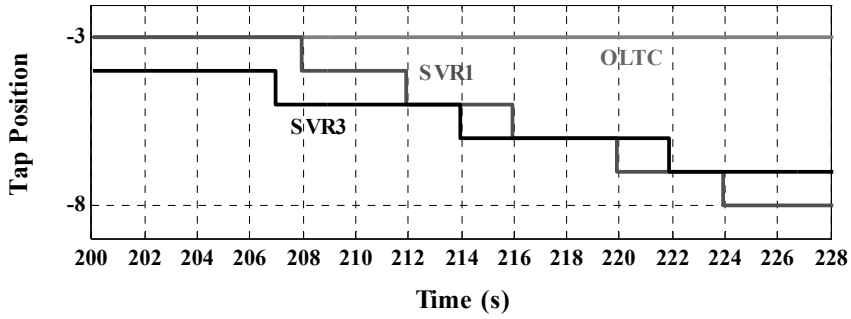

(b)

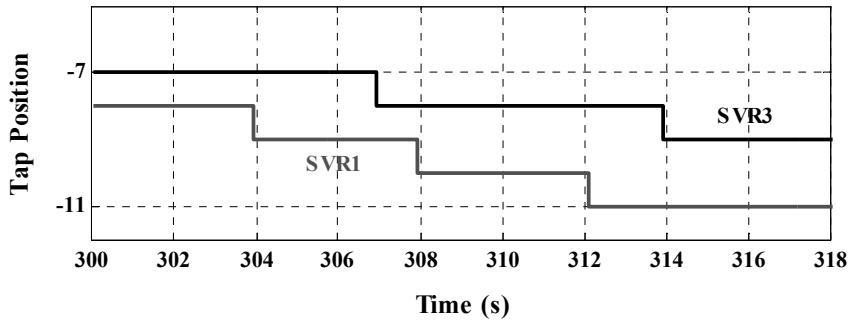

(c)

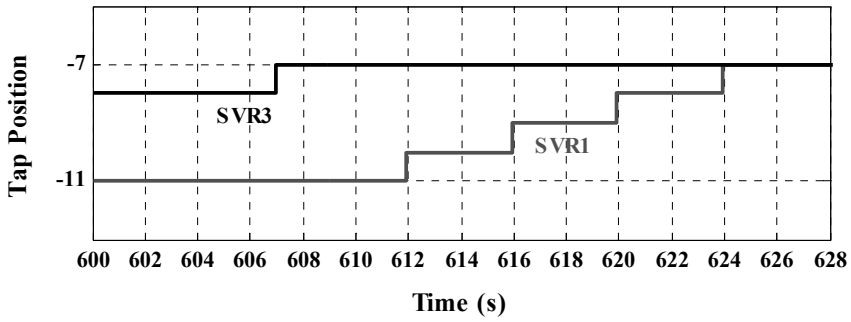

(d)

Figure 6.15: Tap operations for feeder configuration–02 interconnected operation with proposed voltage control (a) over the total simulation period (b) from t = 200 s to 228 s (c) from t = 300 s to 318 s (d) from t = 600 s to 628 s

Figure 6.14 shows simultaneous tap operations for SVRs at t = 228 s, 236 s, 321 s, 507 s, 514 s and 628 s with conventional voltage control. Figure 6.15 (b) to (d) are the zoomed versions of Figure 6.15 (a) to clearly observe the tap operations with the proposed voltage control. It is shown in Figure 6.15 (a) to (d) that there are no simultaneous tap operations (and DG-VCM actions) with the proposed control. The DG-VCM operates at (i) t = 1.0 s updating V_{ref} from 0.90 pu to 0.95 pu, (ii) at t = 2.0 s updating V_{ref} from 0.95 pu to 1.00 pu, and (iii) at t = 601 s updating V_{ref} from 1.00 pu to 0.95 pu based on the pilot bus voltage. The effect of proposed voltage control strategy to regulate the voltage of an interconnected feeder configuration–02 can also be observed in the selected nodes, which are *N95*, *N51* and *N17* as shown in Figure 6.16, 6.17 and 6.18 respectively. The results are very much similar to the previously simulated case of feeder configuration–01. The active and reactive power outputs of the DG for feeder configuration–02 operation are shown in Figure 6.19.

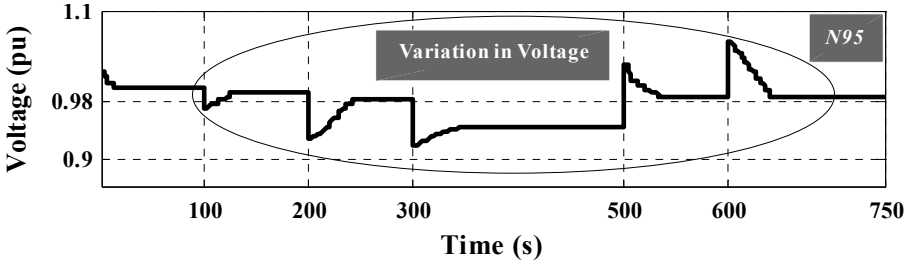

(a)

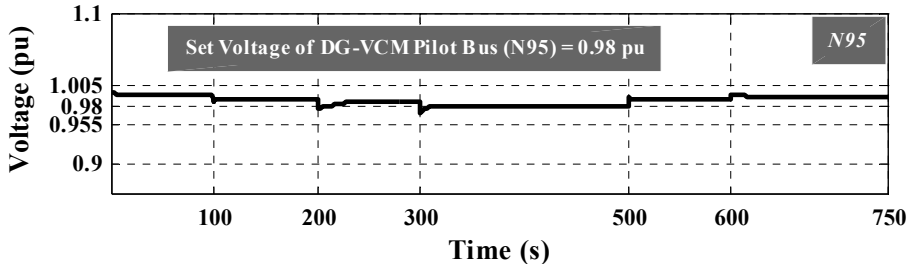

(b)

Figure 6.16: Voltage at node *N95* for feeder configuration–02 interconnected operation with (a) conventional voltage control (b) proposed voltage control

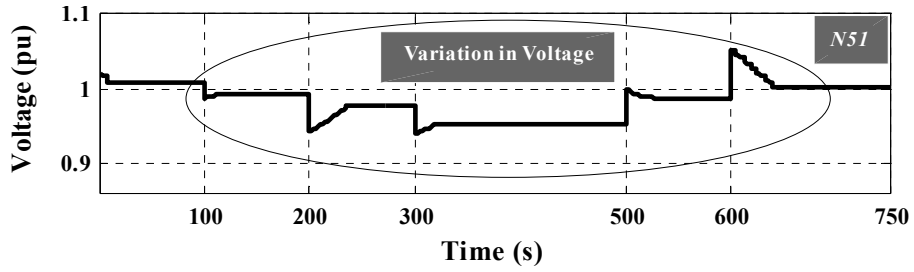

(a)

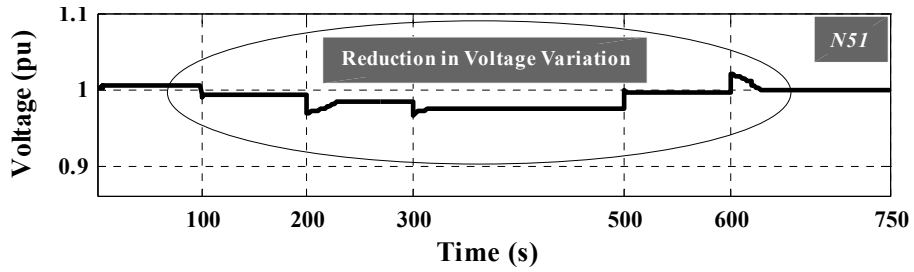

(b)

Figure 6.17: Voltage at node *N51* for feeder configuration–02 interconnected operation with (a) conventional voltage control (b) proposed voltage control

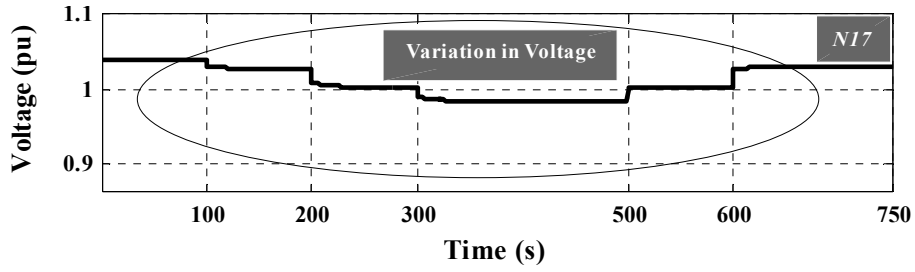

(a)

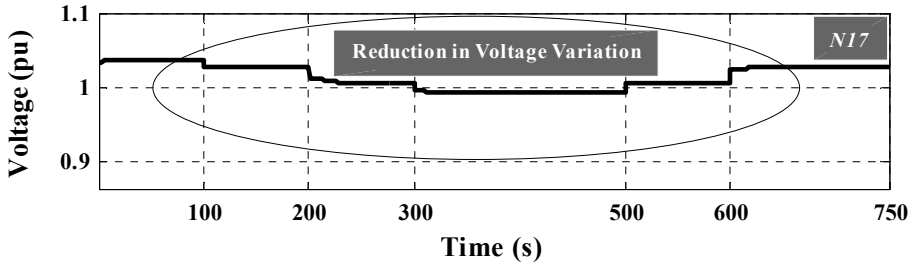

(b)

Figure 6.18: Voltage at node *N17* for feeder configuration–02 interconnected operation with (a) conventional voltage control (b) proposed voltage control

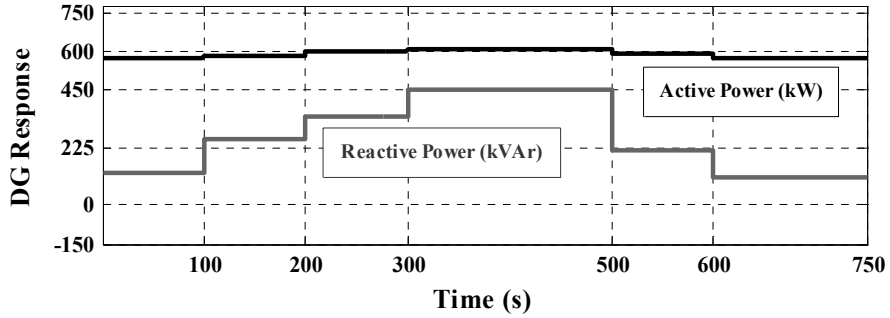

Figure 6.19: Active and reactive power outputs of DG in feeder configuration–02

Further, simulation results for the interconnected feeder configuration–02 are also indicative of the fact that the performance of proposed on-line voltage control supersedes the performance of the conventional voltage control strategy. Based on the simulation studies, it can be concluded that the proposed DG-VCM, CM-BSO based algorithm and its real-time implementation via substation cantered DMS can effectively improve the steady-state voltage profile of the distribution feeder containing SVRs and DG.

6.6 Summary

In summary, this chapter proposes a real-time coordinated voltage control strategy for voltage regulation in distribution system with multiple voltage control devices and DG considering simultaneous responses of the voltage regulating devices. The control design is based on three main aspects: (a) maximising voltage regulation support by DG through DG-VCM (b) procuring on-line load centre voltage measurements for SVRs, and (c) real-time control for avoiding simultaneous

operations of multiple voltage control devices and DG-VCM by means of CM-BSO. Based on the time domain simulation studies conducted for realistic 11 kV feeder system operations, it can be seen that the proposed control strategy minimises the total tap operations of SVRs while achieving voltage regulation by available voltage control devices and DG. It also exploits the reactive capability of DG in order to maximise the voltage regulation support. The proposed method reduces the resulting voltage variations attributed to the tap operations and improvises the feeder voltage. The simulation results have revealed that effective coordinated voltage control for modern distribution feeder system can be achieved in real-time through the application of the proposed voltage control strategy. This proposed voltage control strategy can also be implemented for MV distribution systems with asynchronous machine and inverter interface based DG units (i.e., DFIG and solar-PV) as well as local CBs utilising their reactive power capabilities.

CHAPTER 7: COORDINATED VOLTAGE CONTROL IN DISTRIBUTION SYSTEMS CONSIDERING THE IMPACT OF SIMULTANEOUS AND NON-SIMULTANEOUS RESPONSES OF VOLTAGE CONTROL DEVICES AND DG UNITS

This chapter proposes a strategy for coordinated voltage control in distribution systems which are subjected to structural changes and embedded with multiple voltage control devices and DG units for Volt/VAr control. Also, the proposed strategy can be embedded in a substation centred DMS for online voltage control. This chapter is organised as follows. Section 7.1 gives a brief introduction to the chapter; Section 7.2 describes the methodology proposed for determining voltage control zones for Volt/VAr support DG in distribution systems and Section 7.3 details mathematical proof for the proposed coordinated voltage control strategy. The proposed coordinated voltage control strategy is detailed in Section 7.4. The test cases and simulation results are presented in Section 7.5 and Section 7.6 includes the concluding remarks. This chapter is based on the Journal Publication titled "Online Coordinated Voltage Control in Distribution Systems Subjected to Structural Changes and DG Availability," authored by D. Ranamuka, A. P. Agalgaonkar, and K. M. Muttaqi, *IEEE Transactions on Smart Grid*, vol. 7, no. 2, pp. 580-591, Mar. 2016.

7.1 Introduction

Based on the inherent operational characteristics of DG units and voltage control devices for correcting the target bus voltage, both simultaneous and non-simultaneous responses of voltage control devices and DG units are existed. If there are tap operations for OLTC and SVRs, switching operations for CBs and DG responses occurring at the same time; then their cumulative effect can violate the allowable voltage limits for a distribution system. Hence, the simultaneous responses of voltage control devices and DG units can lead to conflicting operations under certain system operating conditions and may exhaust total number of tap operations resulting into voltage variations and transients as detailed in the Chapter 6. Similarly, the non-simultaneous responses of voltage control devices and DG units for correcting the target bus voltage can also lead to

the conflicting operations based on the impedance between voltage control devices and DG units, DG penetration level and their control parameters such as voltage set values, time delays and dead-band limits. This can be a more complex phenomenon, where the distribution systems are subjected to structural changes and the availability of DG units. It is worth noting that the system structural changes are resulted due to seasonal changes and line outages. Line outages or system faults may lead to the execution of network reconfiguration in the system. Also, availability of DG units depends on the active and reactive power dispatch requirements stipulated by the network operator, adequacy of generating resources, and preventive and breakdown maintenance of DG units, which may also lead to topological changes in the overall system. For example, significant topological changes may be occurred due to the shutdown or energising of DG units at multiple locations in distribution systems with considerably long feeders emerging out of the substation transformer.

One of the feasible ways of minimising the adverse effects of interactions among DG units and voltage control devices is control coordination. However, the research presented in the literature do not clearly address how the proposed control strategies operationally perform for minimising the impact of DG and voltage control device interactions, specifically when the distribution systems are subjected to structural changes and DG availability. There may be topology based limitations, which are clearly discussed in [14]. Accordingly, the proposed coordination strategy is designed with an objective of operationally achieving fine voltage control in modern distribution systems considering variabilities in system topology and DG availability; while eliminating or minimising the adverse effects of multiple DG units and voltage control device interactions. In the proposed voltage control scheme, the DG units and CBs are predominantly used for maximising the voltage support. The coordinated control decisions are mainly based on electric distance among the DG units and the voltage control devices. Therefore, the proposed strategy is able to effectively account for the impacts of structural changes in the network. Also, the interactions among DG units and voltage control devices are classified using simultaneous and non-simultaneous

responses, which are used for voltage control design purposes. Moreover, it exhibits a unique feature highlighting the use of substation centred DMS for practically implementing online voltage control. The control actions of the proposed coordination strategy are tested using MATLAB and MATLAB-Simulink software including detail models of the test distribution system topology (feeder configuration–01) shown in Figure 2.1 of Chapter 2; and results are reported. The simulation results have demonstrated that voltage control for a distribution feeder system can effectively be achieved on a real-time basis through the application of the proposed control strategy.

It is to be noted that the proposed strategy mainly considers synchronous machine based DG, since still the majority of embedded generation in Australian MV distribution systems is based synchronous machine based technologies. However, it can easily be extended to distribution systems which are also embedded with other DG technologies such as DFIG based wind generation and solar–PV as the proposed control algorithm is in the form of a generalised formulation applicable to all modern distribution systems.

7.2 Determination of Voltage Control Zones of DG in Distribution Systems

Modern distribution systems may contain multiple voltage control devices for voltage control and can be subjected to structural changes due to network reconfiguration and availability of DG units embedded in the network. A typical distribution system is shown in Figure 7.1. In accordance with the operation of tie-lines, with the aid of related ABSs, network reconfiguration can be performed in multiple feeder systems, which may be subjected to structural changes. Moreover, if such a feeder system contains multiple DG units, more topological changes are possible depending on the availability of the DG units.

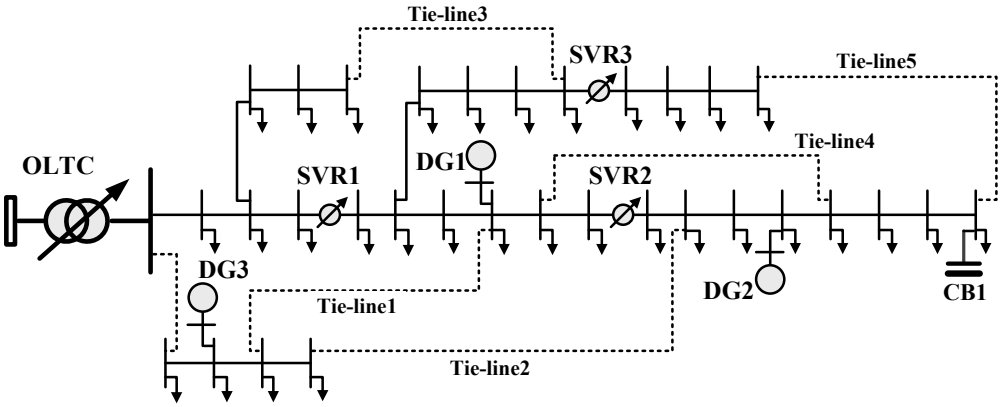

Figure 7.1: Topology of a distribution system capable of operating under structural changes with multiple voltage control devices and DG

In each system configuration, the voltage magnitude at i^{th} node of the distribution system for small changes in active and reactive power injections by a DG unit can be obtained using M_{sVP} and M_{sVQ} matrices which are derived from the system inverse Jacobian matrix, J^{-1} as given by (01). It is assumed that the DG unit is connected at k^{th} node for the MV distribution system with n number of nodes, which are numbered chronologically from the distribution substation-end.

$$\left[\frac{\Delta\alpha_s}{\Delta V_s}\right]_{2n\times 1} = \left[J^{-1}\right]_{2n\times 2n} \times \left[\frac{\Delta P_s}{\Delta Q_s}\right]_{2n\times 1}$$

$$\Delta\alpha_s \in \left(\Delta\alpha_{s1}, \Delta\alpha_{s2}, \ldots\ldots\ldots, \Delta\alpha_{si}, \ldots\ldots\ldots, \Delta\alpha_{sk}, \ldots\ldots\ldots, \Delta\alpha_{sn}\right)$$

$$\Delta V_s \in \left(\Delta V_{s1}, \Delta V_{s2}, \ldots\ldots\ldots, \underbrace{\Delta V_{si}}_{i^{th}\ node}, \ldots\ldots\ldots, \Delta V_{sk}, \ldots\ldots\ldots, \Delta V_{sn} \right)$$

$$\Delta P_s \in \left(\Delta P_{s1}, \Delta P_{s2}, \ldots\ldots\ldots, \Delta P_{si}, \ldots\ldots\ldots, \Delta P_{sDG}, \ldots\ldots\ldots, \Delta P_{sn}\right)$$

$$\Delta Q_s \in \left(\Delta Q_{s1}, \Delta Q_{s2}, ..., \Delta Q_{si}, ..., \underbrace{\Delta Q_{sDG}}_{k^{th}\ node\ (i=k)}, ..., \Delta Q_{sn} \right)$$

$$\left[J^{-1} \right]_{2n\times 2n} = \left[\begin{array}{c|c} M_{s\alpha P} & M_{s\alpha Q} \\ \hline M_{sVP} & M_{sVQ} \end{array} \right] \in \underbrace{\left[M_{sVP}\right]_{n\times n}, \left[M_{sVQ}\right]_{n\times n}}$$

$$\left[\Delta V_{s1/by\ DG} \quad ..... \quad \Delta V_{si/by\ DG} \quad ..... \quad ..... \quad \Delta V_{sn/by\ DG} \right]^T =$$

$$\underbrace{\left[\frac{\partial V_{s1}}{\partial P_{sDG}} \quad ..... \quad \frac{\partial V_{si}}{\partial P_{sDG}} \quad ..... \quad ..... \quad \frac{\partial V_{sn}}{\partial P_{sDG}} \right]^T}_{k^{th}\ column\ of\ \left[M_{sVP}\right]} \times \Delta P_{sDG} +$$

$$+ \underbrace{\left[\frac{\partial V_{s1}}{\partial Q_{sDG}} \quad ..... \quad \frac{\partial V_{si}}{\partial Q_{sDG}} \quad ..... \quad ..... \quad \frac{\partial V_{sn}}{\partial Q_{sDG}} \right]^T}_{k^{th}\ column\ of\ \left[M_{sVQ}\right]} \times \Delta Q_{sDG}$$

$$\Delta V_{si/by\ DG} = \left(\frac{\partial V_{si}}{\partial P_{sDG}} \right) \times \Delta P_{sDG} + \left(\frac{\partial V_{si}}{\partial Q_{sDG}} \right) \times \Delta Q_{sDG} \qquad (01)$$

$$i = j, \quad \Delta V_{sj/by\ DG} = \left(\frac{\partial V_{sj}}{\partial P_{sDG}} \right) \times \Delta P_{sDG} + \left(\frac{\partial V_{sj}}{\partial Q_{sDG}} \right) \times \Delta Q_{sDG}$$

The small changes in nodal voltage magnitudes, nodal voltage phasor angles, active and reactive powers at any system configuration, *s,* are denoted by $\Delta\alpha_s$, ΔV_s, ΔP_s and ΔQ_s sets respectively. The term associated with active power injection by a DG unit, $(\partial V_{si}/\partial P_{sDG})x\Delta P_{sDG}$ depends on the type of DG technology, primary energy source, the system topology and its operation. However, the term associated with reactive power injection, $(\partial V_{si}/\partial Q_{sDG})x\Delta Q_{sDG}$ can be controlled for the overall system voltage support. Also, voltage control zone for such a DG unit can be derived as follows. The magnitude of voltage coupling between any two buses of a power system can be quantified by the maximum attenuation of voltage variation between the two buses. The respective attenuations can be derived from $[M_{sVQ}]$ matrix by dividing the elements of each column by the diagonal term [59], [60].Therefore, the matrix of attenuations, $[\mu_{sij}]$ among all the buses of the power system can be derived as shown in (02). The electrical distance between nodes *i* and *j* is given by (03). The normalised electrical distance is given by (04). The

step by step methodology for deriving the voltage control zones for multiple DG units is given below. The μ_{sij}, D_{sij} and a_{ij} denote the attenuation of voltage variation between node i and j, electrical distance between nodes i and j and elements of M_{sVQ} matrix, respectively.

$$\left[M_{sVQ}\right] = \begin{bmatrix} \underbrace{\frac{\partial V_{s1}}{\partial Q_{s1}}}_{diagonal} & \cdots & \frac{\partial V_{s1}}{\partial Q_{si}} & \frac{\partial V_{s1}}{\partial Q_{sj}} & \frac{\partial V_{s1}}{\partial Q_{sDG}} & \frac{\partial V_{s1}}{\partial Q_{sn}} \\ \cdots & & \cdots & \cdots & \cdots & \cdots \\ \frac{\partial V_{si}}{\partial Q_{s1}} & \cdots & \underbrace{\frac{\partial V_{si}}{\partial Q_{si}}}_{diagonal} & \frac{\partial V_{si}}{\partial Q_{sj}} & \frac{\partial V_{si}}{\partial Q_{sDG}} & \frac{\partial V_{si}}{\partial Q_{sn}} \\ \frac{\partial V_{sj}}{\partial Q_{s1}} & \cdots & \frac{\partial V_{sj}}{\partial Q_{si}} & \underbrace{\frac{\partial V_{sj}}{\partial Q_{sj}}}_{diagonal} & \frac{\partial V_{sj}}{\partial Q_{sDG}} & \frac{\partial V_{sj}}{\partial Q_{sn}} \\ \cdots & \cdots & \cdots & \cdots & \cdots & \cdots \\ \frac{\partial V_{sk}}{\partial Q_{s1}} & \cdots & \frac{\partial V_{sk}}{\partial Q_{si}} & \frac{\partial V_{sk}}{\partial Q_{sj}} & \underbrace{\frac{\partial V_{sk}}{\partial Q_{sDG}}}_{diagonal} & \frac{\partial V_{sk}}{\partial Q_{sn}} \\ \cdots & \cdots & \cdots & \cdots & \cdots & \cdots \\ \frac{\partial V_{sn}}{\partial Q_{s1}} & \cdots & \frac{\partial V_{sn}}{\partial Q_{si}} & \frac{\partial V_{sn}}{\partial Q_{sj}} & \frac{\partial V_{sn}}{\partial Q_{sDG}} & \underbrace{\frac{\partial V_{sn}}{\partial Q_{sn}}}_{diagonal} \end{bmatrix}$$

$$\left[\Delta V_s\right]_{n\times 1} = \left[M_{sVQ}\right]_{n\times n} \times \left[\Delta Q_s\right]_{n\times 1} \quad and \quad \Delta V_{si} = \mu_{sij} \times \Delta V_{sj}$$

$$\mu_{sij} = \frac{\partial V_{si}}{\partial Q_{sj}} \Big/ \underbrace{\frac{\partial V_{sj}}{\partial Q_{sj}}}_{diagonal} \quad and \quad \mu_{sij} \neq \mu_{sji}, \quad j \in \underline{n} \tag{02}$$

$$For\ any\ DG\ \ node\ \ i.e.,\ i = k, \quad \mu_{skj} = \frac{\partial V_{sk}}{\partial Q_{sj}} \Big/ \underbrace{\frac{\partial V_{sj}}{\partial Q_{sj}}}_{diagonal}$$

$$D_{sij} = -Log\left(\mu_{sij}\right), \quad D_{sij} = D_{sji} = -Log\left(\mu_{sij}.\mu_{sji}\right) \tag{03}$$

$$Normalised \quad D_{sij} = D_{sij} / max\left(D_{si1}, D_{si2}, \ldots, D_{si\underline{n}}\right) \tag{04}$$

For any DG node i.e ., $i = k$,

$$D_{skj} = -Log\left(\mu_{skj}\right), \quad D_{skj} = D_{sjk} = -Log\left(\mu_{skj} \cdot \mu_{sjk}\right)$$

$$Normalised \quad D_{skj} = D_{skj} / max\left(D_{sk1}, D_{sk2}, \ldots, D_{sk\underline{n}}\right)$$

- Step – 1: Calculate the system Jacobian matrix, J and derive its inverse matrix, J^{-1}.
- Step – 2: Obtain $[M_{sVQ}]$ matrix, and the elements of this matrix are named as $a_{ij} = (\partial V_{si}/\partial Q_{sj})$.
- Step – 3: Obtain the attenuation matrix $[\mu_{sij}]$, and the elements of this matrix are written as $\mu_{sij} = (a_{sij} / a_{sjj})$.
- Step – 4: Calculate the electrical distance, D_{sij} array using (03).
- Step – 5: Normalise the electrical distance values using (04).
- Step – 6: For each DG unit bus (i.e., $i = k$), the normalised electrical distances from DG bus to all other buses (j, $j \neq i$) are classified into different pre-specified ranges such as $Range_1$, $Range_2$, $Range_3$, …, which are ranked in ascending order using R_1, R_2 and R_3 parameter values as given below. This is done for the sake of convenience in traversal and construction of the utmost voltage control zones of the DG units.

$$0 \leq Range_1 < R_1, R_1 \leq Range_2 < R_2, R_2 \leq Range_3 < R_3, \ldots. \quad \forall \; R_1 < R_2 < R_3 \ldots.$$

- Step – 7: Accordingly, the nodes within each range will determine the voltage control zone for a particular DG unit.
- Step – 8: The overlapping of voltage control zones can be avoided by appropriately classifying the overlapping nodes into each zone based on the respective electrical distance values.

For example, a typical variation of DG voltage control zones of a distribution feeder system configuration similar to a system depicted in Figure 7.1, where all

the tie-lines are opened, which has two DG units (i.e., DG1 and DG2), is shown in Figure 7.2. This is only a diagrammatic representation, which is based on the preliminary derivations of the case study. The end nodes of DG1 utmost voltage control zone are N_a and N_b, where the end nodes of DG2 utmost voltage control zone are N_c and N_d along the feeder. According to the Step-VI, $R_1 = e1$, $R_2 = e2$ and $R_3 = e3$. If conventionally operated voltage control devices are located inside the DG zones, the operational aspects of those devices may be significantly detrimental, even leading to conflicting operations under certain system conditions. A possible way of minimising those interactions is detailed below, which is the basis of the proposed coordination strategy.

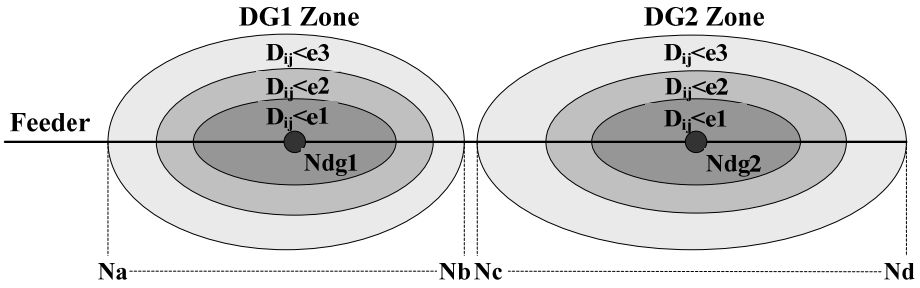

Figure 7.2: Diagrammatic representation of DG voltage control zones for the sample distribution system configuration with DG1 and DG2

The D_{ij} denotes the electrical distance between nodes *i* and *j*; where N_{dg1} and N_{dg2} denote DG1 and DG2 nodal buses, respectively. The N_a and N_b represent the end nodes of DG1 voltage control zone, where N_c and N_d represent end nodes of DG2 voltage control zone.

7.3 Mathematical Proof for the Proposed Coordinated Voltage Control

In this section, a mathematical proof for the proposed control strategy is established, which is fundamentally based on electrical distance theory in order to alleviate the adverse effects of non-simultaneous responses (in addition to simultaneous responses) of voltage control devices and DG units.

In each system configuration, operation of SVRs (for example, Type-B) in the forward mode can be demonstrated using their local control actions as given by

(05) [5], [8]. The more common connection for SVRs is the Type-B. In Type-B connection, the primary of the SVR is connected to the series winding via taps; where the series winding is connected to the shunt winding which is connected to the SVR secondary [1]. In the forward mode, when the target point voltage is less than the lower boundary voltage limit, the SVR taps down to raise the target point voltage within the upper and lower boundary voltage limits and vice versa. When the target point voltage is within the upper and lower boundary voltage limits, no further tap operation is enacted. The lower and upper boundary voltage limits are defined using voltage set value and dead band limit. The s, t, Tap_{st} and DB denote, state of any system configuration, time, SVR tap position and SVR dead-band limit, respectively. The V_{sLC}, V_{LB}, V_{UB} and $V_{SET/VR}$ denote SVR target point voltage, SVR lower boundary voltage, SVR upper boundary voltage and SVR voltage set value, respectively. Similar derivations can be obtained for substation OLTC, when it also needs to be incorporated in the control algorithm.

$$Tap_{s(t+1)} = \begin{cases} Tap_{st} + 1 & if\ V_{sLC} > V_{UB} \\ Tap_{st} & if\ V_{LB} \le V_{sLC} \le V_{UB} \\ Tap_{st} - 1 & if\ V_{sLC} < V_{LB} \end{cases}$$

$$V_{LB} = V_{SET/VR} - 0.5V_{DB} \quad and \quad V_{UB} = V_{SET/VR} + 0.5V_{DB} \tag{05}$$

The change of target point voltage of any m^{th} SVR for system configuration, s due to a small change in a DG unit reactive power response can be derived as given by (06). The $V_{sLC(m)}$ and $V_{sLC(m)/byDG}$ denote target point voltage of any m^{th} SVR and voltage change at target point of any m^{th} SVR by DG reactive power output, respectively.

$$\Delta V_{sLC(m)/by\,DG} = \left(\frac{\partial V_{sLC(m)}}{\partial Q_{sDG}} \right) \times \Delta Q_{sDG} \tag{06}$$

Similarly, in each system configuration, the operation of CBs can be demonstrated using their local control actions as given by (07) [5]. The SFC_{st}, V_{sFC}, V_{ON} and V_{OFF} denote CB switching position, target point voltage, switching *ON* voltage and switching *OFF* voltage, respectively.

$$SFC_{s(t+1)} = \begin{cases} ON & if \quad SFC_{st} = OFF \quad and \quad V_{sFC} < V_{ON} \\ SFC_{st} & if \quad V_{ON} \le V_{sFC} \le V_{OFF} \\ OFF & if \quad SFC_{st} = ON \quad and \quad V_{sFC} > V_{OFF} \end{cases} \tag{07}$$

The change of target nodal voltage of any g^{th} CB for system configuration, s due to a small change in a DG unit reactive power response can be derived as given by (08). The target point voltage of the CB is normally its connection nodal voltage. The $V_{sFC(g)}$, $V_{sCB(g)}$ and $V_{sFC(g)/byDG}$ denote target point voltage of any g^{th} CB, CB connection nodal voltage and voltage change at target point of any g^{th} CB by DG reactive power output, respectively.

$$\Delta V_{sFC(g)/by\ \ DG} = \left(\frac{\partial V_{sCB(g)}}{\partial Q_{sDG}} \right) \times \Delta Q_{sDG} \tag{08}$$

However, the following mathematical proof reveals that if the target node of a voltage control device is far from the node of a DG unit in terms of electrical distance, the impact of DG unit on the operation of the voltage control device is less and vice versa, under any system operation and any configuration or structure of the system.

$$\Delta V_{sk} = \mu_{skj} \times \Delta V_{sj} \quad and \quad D_{skj} = -Log\left(\mu_{skj} \right)$$

$$\Delta V_{sj/by\ DG} = \left(\frac{1}{Log^{-1}\left(D_{skj} \right)} \right) \times \Delta V_{sk/by\ DG} \tag{09}$$

$$If\ D_{skj} \to \infty,\ Log^{-1}\left(D_{skj} \right) \to \infty,\ then\ from\ (01),\ i = j$$

$$\Delta V_{sj/by\ DG} \to 0$$

$$From\ (06),\ (08)\ and\ (09):$$

$$\Delta V_{sLC(m)/by\ DG},\ \Delta V_{sFC(g)/by\ \ DG} \to 0,\quad if\ D_{skm}, D_{skg} \to \infty \tag{10}$$

7.4 Proposed Coordinated Voltage Control Strategy

The proposed coordination strategy is presented in this section. Section 7.4.1 outlines the proposed sequence of operation for Volt/VAr support DG units and voltage control devices and Section 7.4.2 presents the online implementation of the proposed strategy. The Section 7.4.3 elaborates the control algorithm of the proposed coordination strategy.

7.4.1 Sequence of Operation for DG units and Voltage Control Devices

As highlighted in Chapter 4, the seamless operation of distribution systems embedded with DG for effective voltage control is one of the challenging tasks, mainly because (a) DG units may interact with the conventional voltage control devices (i.e., tap changing devices and CBs) which are enacted with conventional time graded operation and (b) prioritised operation of different voltage control devices depends on the network topology. The interactions among multiple DG units and voltage control devices may lead to numerous conflicting operations and network oscillations, if they are not well coordinated. In this context, the multiple DG units with Volt/VAr support operation are identified and defined as the devices that have the greatest influence in voltage control. DG units can offer fast voltage correction compared to conventional voltage control devices. The proposed approach is similar to the conventional method for identifying the area that requires voltage support the most. As demonstrated in Section 7.3, the furthest voltage control device from the DG has low probability to introduce control interaction between DG and voltage control device. Accordingly DG units in the affected area are given the priority to maximise voltage support using VAr control.

It is proposed to operate the DG units in VAr control mode thereby maximising the voltage support. The VAr reference values of DG units are updated based on correcting the lowest nodal voltage (or highest voltage rise) by the most significant DG unit first, then by the next significant DG unit and so on. The most significant DG unit is identified by (a) using voltage control zones of the DG units and (b) electrical distance between DG units and the node which requires

immediate voltage correction. For example, in case of a distribution system in Figure 7.2, if the particular node which requires utmost voltage correction is within a particular DG zone (say DG2 zone), the VAr reference value of DG2 is updated first. If it is not adequate to maintain the voltage within the stipulated limits, the VAr reference value of next closer DG unit (in terms of electrical distance) i.e., DG1 is updated.

The sequence of operating voltage control devices (i.e., SVRs and CBs) in the affected area is determined by prioritising their operations based on the phenomenon demonstrated in (10) i.e., first operate the farthest voltage control device (with respect to DG units) in terms of electrical distance after updating the VAr reference values of the DG units; if the voltage is not within the stipulated limits. If the operation of farthest voltage control device is also not adequate to maintain the voltage within the stipulated limits; then operate the subsequent voltage control device, if available, which is the next furthest voltage control device out of the remaining voltage control devices in terms of electrical distance and so on. Since, substation OLTC operates after a prolonged time delay (coarse control), it is not incorporated in the feeder voltage control strategy proposed in this chapter. However, if needed, the operation of substation OLTC can also be incorporated in the proposed algorithm by incorporating the relevant upstream OLTCs and the voltage control devices in the MV distribution network with DG.

7.4.2 Online Implementation of the Proposed Coordination Strategy

It is proposed to implement the proposed coordination scheme with the aid of a substation centred advanced DMS for online voltage control [55], [56], [57]. The proposed control software and the hardware modules can be embedded in the DMS. The local control parameters of voltage control devices and DG units are tuned by a tuning algorithm embedded in the DMS as detailed in Chapter 5, which uses pseudo measurements of load and DG generation, and information on system structural changes as inputs. Since, network reconfiguration can be done online and availability of DG units can be monitored online with the aid of advanced DMS and associated infrastructure, the real-time status of structural changes is readily available. Also, the proposed voltage control strategy enhances the system

security due to its capability to update control settings and enforce quick changeover to the local control of respective voltage control devices. The detailed topology of the proposed coordination module is shown in Figure 7.3.

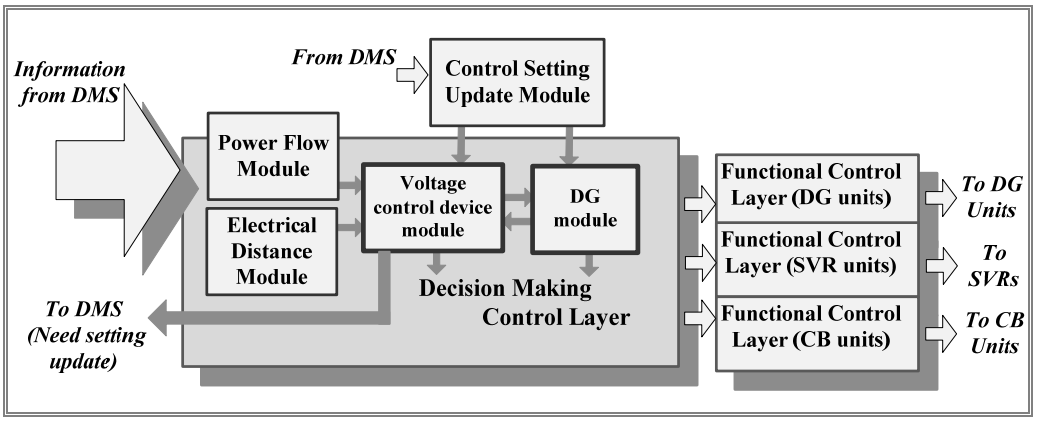

Figure 7.3: Topology of the designed coordination module

The complete coordination module contains embedded power flow module, electric distance module, control setting update module, voltage control device module, DG module and the decision making control layer with separate functional control layers for DG units, SVRs and CBs for enacting those devices according to the information provided by the decision making control layer. The electric distance module is for determining the required electrical distance values from DG units to the corresponding voltage control devices subject to structural changes and availability of the DG units, and accordingly the voltage control zones of DG units are determined. The DG module is for determining the sequence of updating VAr reference values for DG units and voltage control device module is for determining the sequence of operation for voltage control devices (i.e., SVRs and CBs). The control setting update-module is for updating the control parameters of voltage control devices and DG units when required (as indicated in Figure 7.4 flowchart) including VAr reference values of the DG units, which are derived by tuning algorithm also embedded in the DMS. Distribution system planning and operation by incorporating reactive power capabilities of different renewable and non-renewable DG units is discussed in [36].

The control panels (CPs) of DG units and voltage control devices are proposed to be equipped with SCADA facilities. This will have the functional capability of transmitting the real-time information about the status of VAr reference value update for DG units, SVR tap operations and CB switching operations to the coordination module via DMS. The edge-detection based methodology proposed in Chapter 6 is appropriately adopted for inferring real-time information about the status of voltage control devices and DG units. The voltage control devices and Volt/VAr support DG units are operated only after a confirmation from the coordination module i.e., by each functional control layer following the decision information taken by the decision making control layer. The control-algorithm embedded in the coordination module is presented in the following sub section.

7.4.3 Control Algorithm of the Proposed Coordination Strategy

The step by step procedure of the control algorithm of the proposed coordination strategy is described below:

- Step –1: System structural changes, state estimation and power flow information are executed with the aid of relevant embedded DMS modules.
- Step – 2: The VAr reference values for DG units are determined by the tuning algorithm embedded in the DMS and assigned to coordination module via control setting update-module.
- Step – 3: The sequence of operating DG units is determined by the DG module. The power flow and electric distance modules and updated VAr reference values for DG units are called by the DG module for this task. If there are no structural changes in the system, the electric distance values of the previous state are used instead of calling and executing the electric distance module again. The respective steps are outlined in the Section 7.4.1.
- Step – 4: The sequence of operation for voltage control devices (i.e., SVRs and CBs) is determined by voltage control device module. The respective procedure is outlined using a flowchart in Figure 7.4. The functions of power

flow and electric distance modules and updated VAr reference values for DG units are called by the voltage control device module whenever needed.

- Step – 5: Based on the information given by the DG module and the voltage control device module (i.e., sequence of operation of DG units and voltage control devices) and the real-time information on the status of DG unit and voltage control device operations, the decision making control layer is enacted. Accordingly, the functional control layers for DG units, SVRs and CBs are enacted after the information from decision making control layer in order to operate the required device, only if the status of operation of the voltage control devices and the DG units do not lead to simultaneous responses. The functional control layers will pass this information to the respective CPs of the DG units and voltage control devices online and update for every new operation.

- Step – 6: For the subsequent instances of time (i.e., $t = t + 1$), repeat the procedure from Step – 1.

It is assumed that the load forecasts are known with sufficient accuracy via relevant modules of the DMS. Accordingly, the sensitivity of the proposed algorithm for constant power and constant impedance loads could be notable only if the sampling time between two consecutive control states is significantly large. In case of constant current loads, the electric distance values can further be updated using the algorithm embedded in voltage control device module for higher accuracy.

7.5 Testing of the Proposed Coordinated Voltage Control Strategy

The proposed coordination strategy is tested using the interconnected MV distribution system topology model derived from the distribution network of the state of New South Wales, Australia, which is shown in Figure 2.1 of Chapter 2. This distribution system has long feeders, which are subjected to significant voltage drops. Balanced distribution feeder system operation (i.e., feeder configuration-01) with two DG units (DG1 and DG2) and feeder configuration-02 with one DG unit (DG2) are used as the test feeder systems, as shown in Figure 7.5.

In addition to substation OLTC, two SVRs (Type-B type), SVR1 and SVR2, are installed in the test feeder system configuration-01 for downstream voltage regulation. Moreover, a switched shunt CB of 0.50 MVAr capacity is connected at node-92. Synchronous machine based two bio-diesel generators (DG1 with 0.850 MVA capacity and DG2 with 1.000 MVA capacity) are connected to the distribution feeder system (one is at 38^{th} node and other is at 78^{th} node). There is one SVR (SVR3) which has been connected at node no. 12 (of feeder configuration-02) in addition to SVR2, CB and DG2 containing in the same feeder system. The representative simulated voltage limits of the 11 kV test system are 1.10 p.u. and 0.90 p.u. used as upper and lower limit respectively.

7.5.1 Test Simulation for Feeder Configuration-01 with Two DG Units

In this section, a MATLAB simulation is used to (a) demonstrate the phenomenon behind simultaneous and non-simultaneous responses of DG units and voltage control devices, and (b) implement the control action of the proposed coordination strategy to minimise their impacts. For this simulation, a system state (5 minute interval) with 3.0153 MVA representative total load demand with constant power characteristics and DG responses at different occasions of the test system are simulated. The simulated data of SVR1, SVR2 and CB are shown in Tables 7.1 and 7.2. The time delay (including the total mechanical time delay) is used only for the first tap operation of SVRs and the subsequent taps are operated with the mechanical time delay. The simulated time delay used for the SVR1/SVR3 is 6.0 s and SVR2 is 4.0 s. The initial tap position of SVR1 is 3 and tap position of SVR2 is 1 in the direction of increasing the secondary voltage. The simulated time delay used for the CB is 0.1 s.

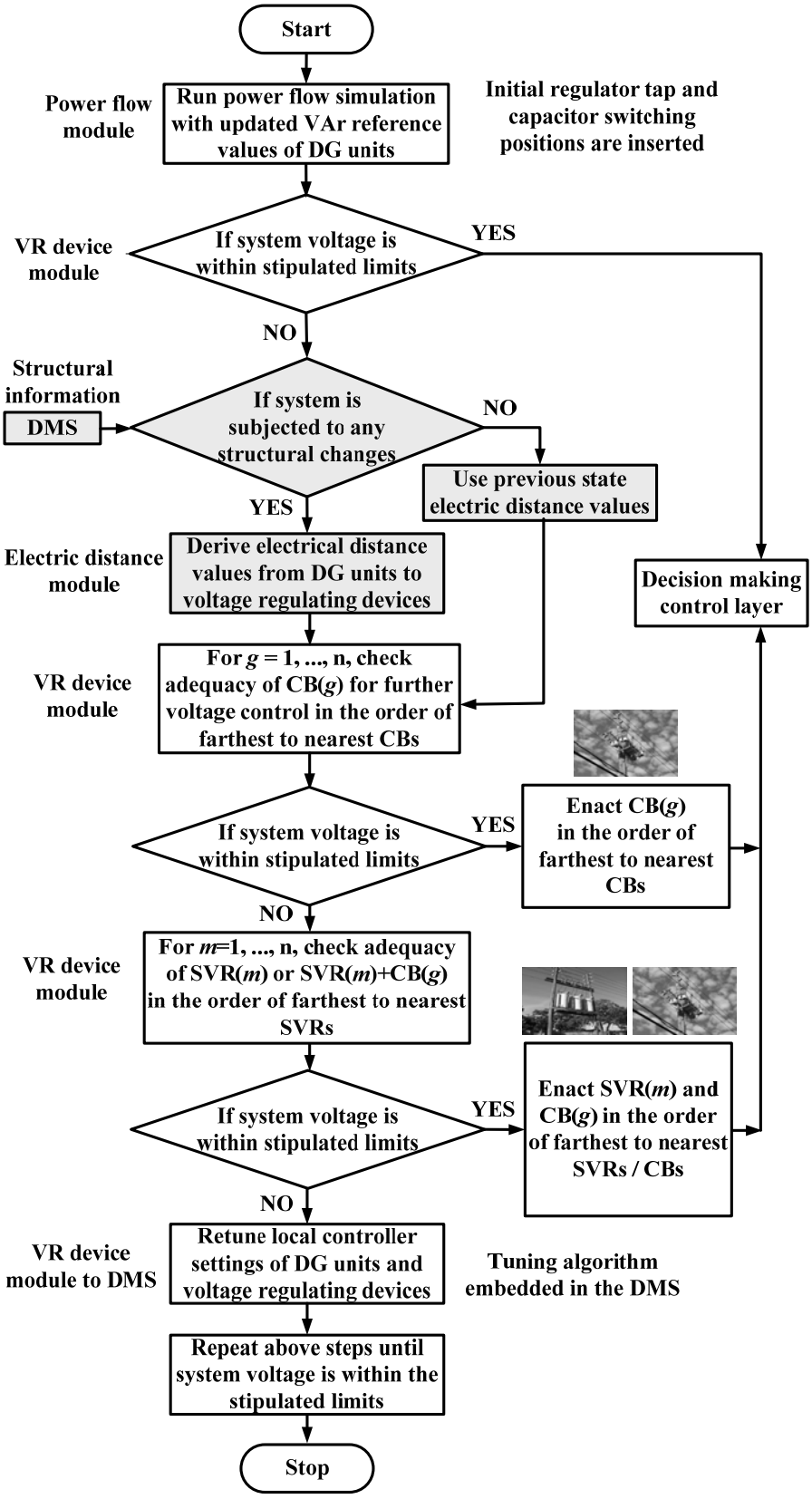

Figure 7.4: Flowchart of the voltage control device module

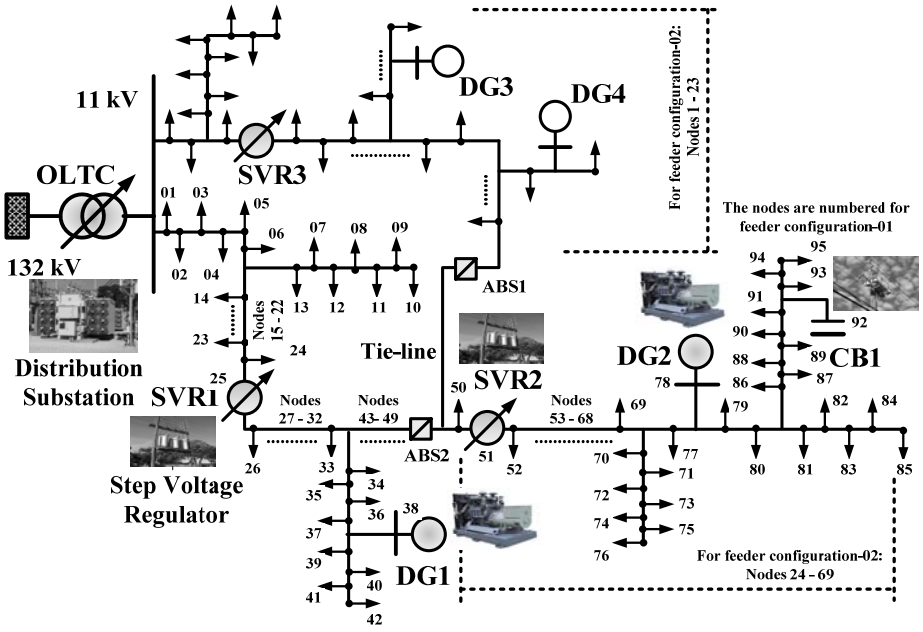

Figure 7.5: Topology of the test distribution system

The initial switching position of the CB is at its nominal position. The initial voltage reference value is set at 1.05 pu for OLTC.

The simulation study has been carried out for following two cases: variable DG output (Case-01) and fixed DG output (Case-02). Case-01 demonstrates the impacts of varying DG penetration levels on system voltage control compared to Case-02 where there is no change in the DG penetration level.

Table 7.1: Simulated data of step voltage regulators

SVR Unit	Voltage Set Value (pu)	Dead Band (%)	Time Delay (s)	Load Centre
SVR1/SVR3	1.0	$\pm$ 1.0	30	R_L=X_L=0
SVR2	1.0	$\pm$ 1.0	40	R_L=X_L=0

Table 7.2: Simulated data of CB on the feeder

CB	Capacity (MVAr)	Switch ON Voltage (pu)	Switch OFF Voltage (pu)	Time Delay (s)
CB1	0.50 (5 Steps of 0.10 MVAr)	0.900	1.010	0.10

The simulated active and reactive power responses (case–01) of available DG units (i.e., DG1 and DG2) for non-coordinated operation are P_{DG1} = 0.60 MW for t < 60 s, P_{DG1} = 0.74 MW for t $\geq$ 60 s, P_{DG2} = 0.70 MW for t < 48 s, P_{DG2} = 0.62 MW for t $\geq$ 48 s and no reactive power as the DG units are operated at unity power factor depicting conventional operation. The simulated power output responses of DG units for the proposed operation are Q_{DG1}= 0.37 MVAr, Q_{DG2} = 0.43 MVAr in addition to the same active power responses as indicated above.

The simulated results for the non-coordinated operation [23] of voltage control devices and DG units are shown in Figure 7.6. The Figure 7.6 (a) is for case-01 and Figure 7.6 (b) is for the case where there is no change in the DG response (case-02). The normalised values of electrical distances to each voltage control device (a) from the DG1 unit are 0.0761 for SVR1, 0.0812 for SVR2, 0.1790 for CB and (b) from the DG2 unit are 0.1938 for SVR1, 0.0568 for SVR2, 0.0292 for CB. According to the control logic as given by (02) and subsequent time delay, the CB is operated first, up to its maximum switching position, supplying 0.50 MVAr. The total operational time is 0.4 s (i.e., time, t = 0 to 0.4 s). Next, according to the control logic as given by (01) and after the requisite time delays, SVR1 is operated at t = 30 s and SVR2 is operated at t = 40 s. In this case (case-01, Figure 7.6 (a)), there are 8 tap operations for SVR1 and 13 tap operations for SVR2. Also, there are simultaneous tap operations at t = 48 s, 60 s and 72 s. The total number of operations for SVR and CB are 25. Moreover, the interactions caused by simultaneous responses of SVRs and DG units (i.e., 0.60 to 0.74 MW of DG1 at t = 60 s) lead to violation of dead band limit of SVR1 in opposite direction, because SVR1 is closer to the DG1 in terms of the electric distance. Hence tap operations (upward) are required for SVR1 to correct the voltage with respect to its voltage set value. In case of a light load scenario, this could be more significant. The impact of simultaneous responses of multiple voltage control devices and DG units on system voltage profile is thoroughly analysed and discussed in Chapter 6. Moreover, since DG1 is closer to the SVR1 and DG2 is closer to the SVR2 in terms of electric distance, the fast responses by DG1 and DG2 lead to a lesser number of tap operations in SVR1 and significantly a higher

number of tap operations in SVR2, respectively compared to the scenario where there is no change in DG responses at t = 48 s and 60 s (case-02) i.e., 9 tap operations by SVR1 (from 3 to 12) and 6 tap operations by SVR2 (from 1 to 7). This is an example for assessing the impact of non-simultaneous responses of DG units and voltage control devices. In the worst case scenario, if simultaneous and/or non-simultaneous responses of voltage control devices and DG units lead to such conflicting operations in each system configuration and system state of a day as well as throughout a year of 365 days, their impact on wear and tear of voltage control devices and the system voltage profile can be significant. For example, if there will be 6 tap operations more in each state as shown in the simulation (i.e., in Figure 7.6 (a) compared to Figure 7.6 (b)), there could be 630,720 additional tap operations as well as resultant voltage transients and voltage variations per year. The variations in the remote end voltage attributed to each operation of voltage control devices and DG responses for the case-01 (Figure 7.6 (a)) are shown in Figure 7.7.

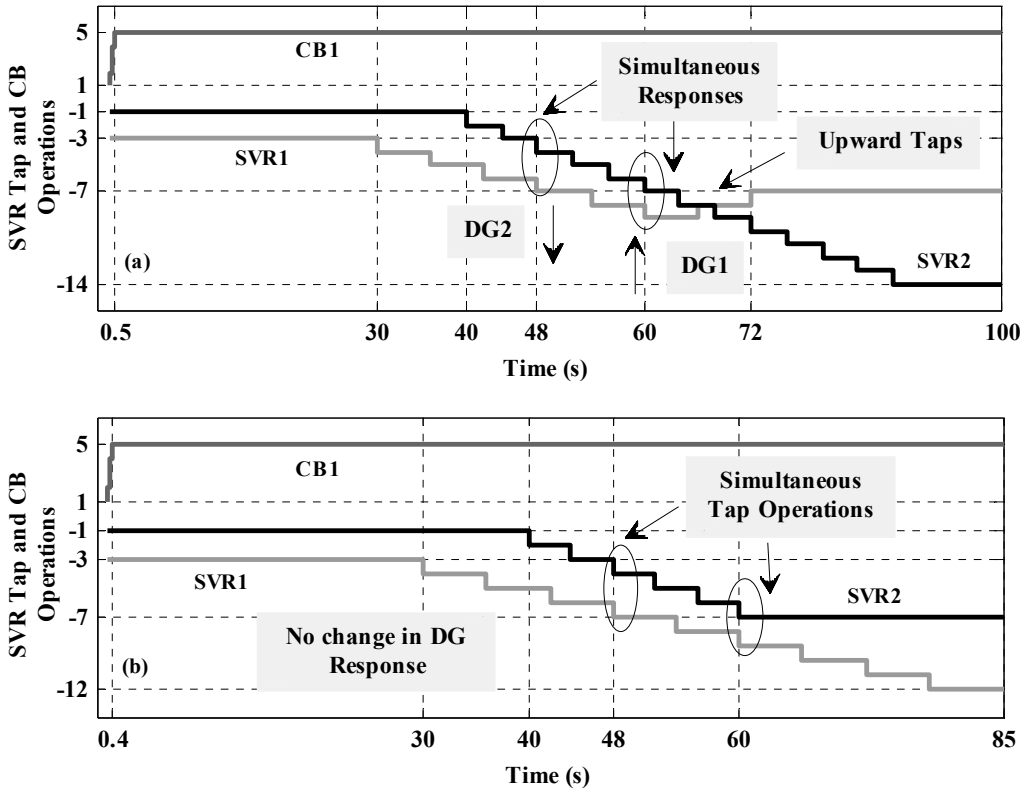

Figure 7.6: Non-coordinated operation of voltage control devices in presence of DG for the simulated (a) case-01 and (b) case-02

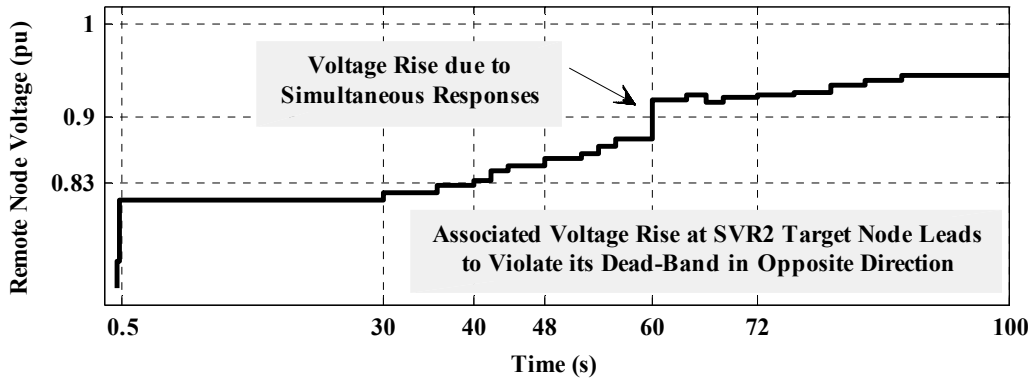

Figure 7.7: Remote end voltage for the simulated case-01

The simulated results for the coordinated operation of voltage control devices and DG units using the proposed algorithm, outlined in Section 7.4, are also shown, assuming zero propagation delay in communication channels, zero processing time of control software and hardware as well as zero error in load and DG forecasting. Figures 7.8 (a) and (b) show the operation of voltage control devices for case-01 and case-02 respectively, while Figure 7.9 shows the variations in remote end voltage attributed to each operation of voltage control devices and DG responses for case-01. The sequence of operating DG units and voltage control devices are in the order of DG2 followed by DG1, SVR1 and finally CB. The VAr reference value of DG2 is updated first after a time delay of 1 s (i.e., at t = 1 s) and next the VAr reference value of DG1 is updated after a subsequent time delay of 1 s (i.e., at t = 2 s).

In this case, the total number of SVR tap operations is less even compared to the scenario where there is no change in DG responses at t = 48 s and 60 s (case-02) i.e., 9 tap operations. It is mainly because of the DG1 active power response at t = 60 s, which significantly increases the feeder voltage. However, still there is one tap operation (upward) in SVR1, since DG1 is closer to the SVR1 in terms of electric distance. Compared to the non-coordinated operation, only one upward tap operation of SVR1 is enacted to correct the voltage rise, and CB is operated after the SVR1 according to the proposed coordinated control algorithm. In case of the proposed coordinated operation, there are also no simultaneous responses of DG units and voltage control devices. Moreover, the impact of interactions which

can be caused by non-simultaneous responses of DG units and voltage control devices on the voltage profile is minimised, since the voltage control devices farthest to the DG units (i.e., SVR1 and CB compared to SVR2) are operated on priority according to the electric distance.

The total number of SVR tap and CB switching operations (8 operations) is significantly less compared to the case of non-coordinated operation (25 operations) for the simulated state. If such an improvement is assumed in each system state throughout a year of 365 days, the annual reduction in voltage control device operations and resultant voltage variations would be 1,787,040.

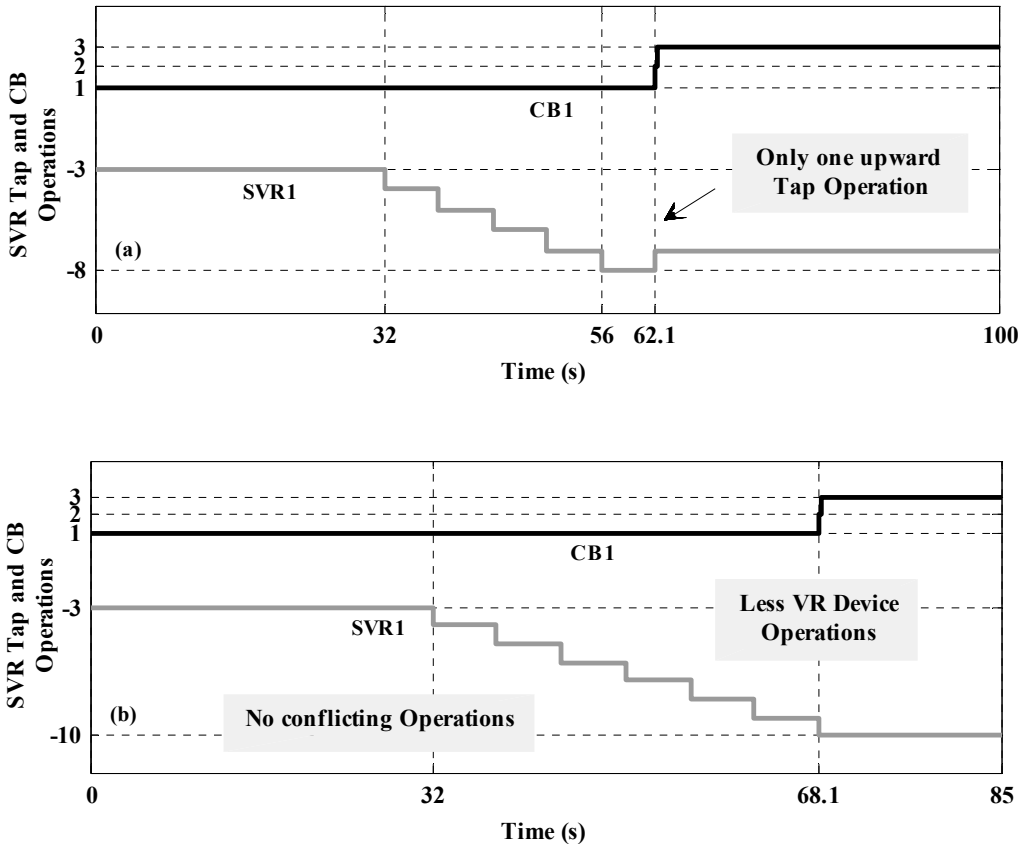

Figure 7.8: Operation of voltage control devices for the simulated (a) case-01 and (b) case-02, under proposed coordination strategy

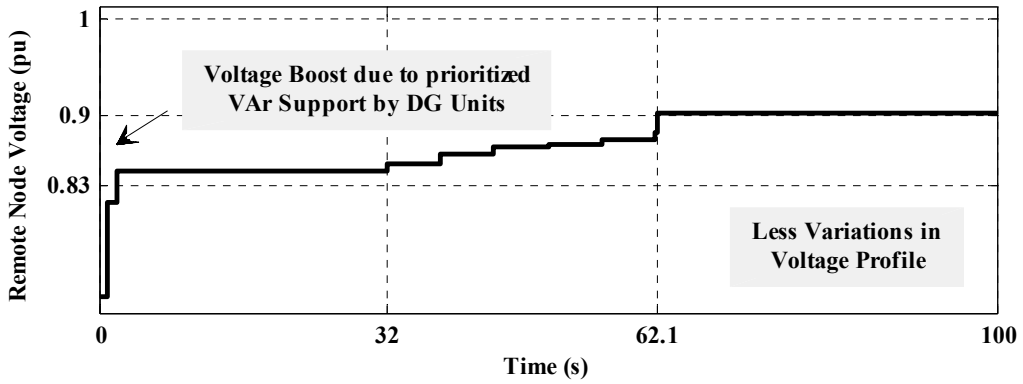

Figure 7.9: Remote end voltage for the simulated case-01(a)

Reduction in tap operations is indeed a key advantage of implementing the proposed voltage control strategy, which will obviously be beneficial to the DNO as it directly correlates to the decrement in the regulator maintenance cost, increase in its life time expectancy, and the decrease in intermittent voltage variations attributed to the SVR tap and CB switching operations. It is noted that the simulated voltage profile in remote node of the test distribution feeder system is below the minimum voltage limit. These simulations are representative only and used to show the merits of the proposed method in regulating the voltage of the feeder end nodes with the aid of voltage control devices and minimising the impact of their interactions on voltage profile where the system is also subjected to structural changes. These simulations show the benefits of using the proposed coordinated operations compared to the non-coordinated operation.

7.5.2 Test Simulation for Feeder Configuration-02 with One DG Unit

In this section, the control action of the proposed coordination strategy is further elaborated for above system configuration. The normalised values of electrical distances to each voltage control device from the DG2 unit are 0.3155 for SVR3, 0.1480 for SVR2 and 0.0360 for a CB. The simulated total load demand, P_{DG2} and Q_{DG2} are 3.4310 MW, 0.65 MVAr at t = 0 s and 0.80 MW and 0.43 MVAr at t = 64 s, respectively. The sequence of operation of DG2 unit and voltage control devices is in the order of DG2 followed by SVR3 and finally SVR2 under proposed control strategy. The non-coordinated operation and the proposed coordinated operation are shown in Figure 7.10 (a) and Figure 7.11 (a)

respectively, where the variations in the remote end voltage attributed to each operation of voltage control devices and DG responses are shown in Figure 7.10 (b) and Figure 7.11 (b), respectively. Under non coordinated voltage control, there are conflicting operations in SVR2 and CB, since DG2 is closer to those devices in term of electric distance.

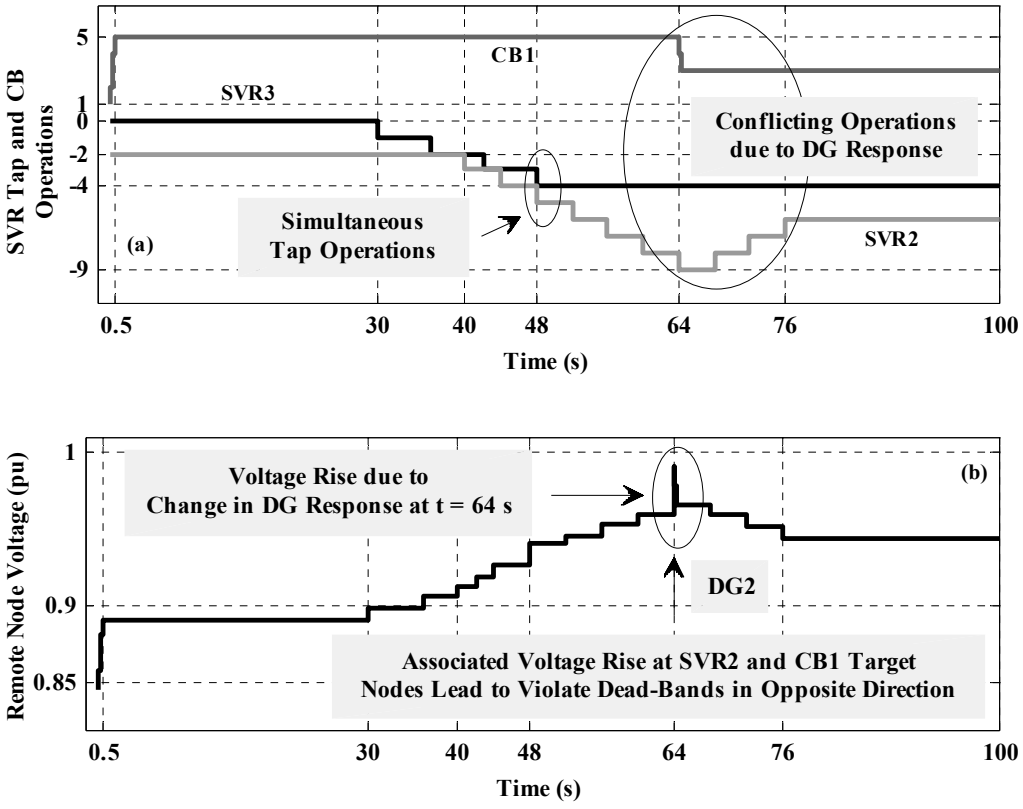

Figure 7.10: (a) Operations for voltage control devices and (b) remote node voltage, under conventional non-coordinated voltage control

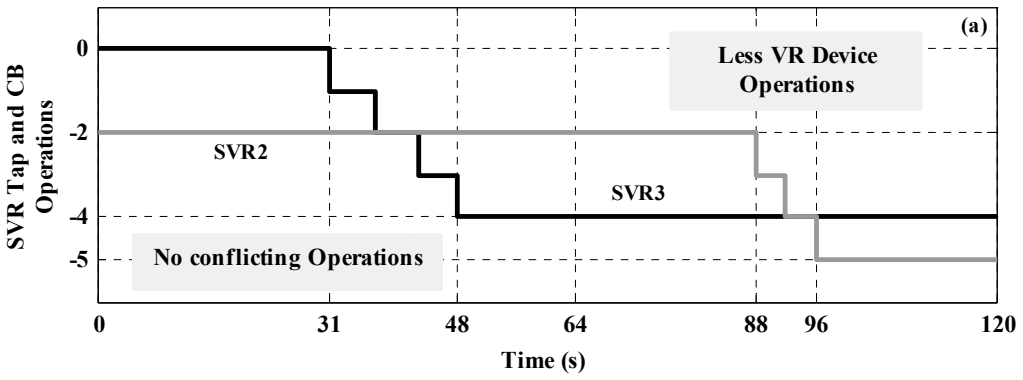

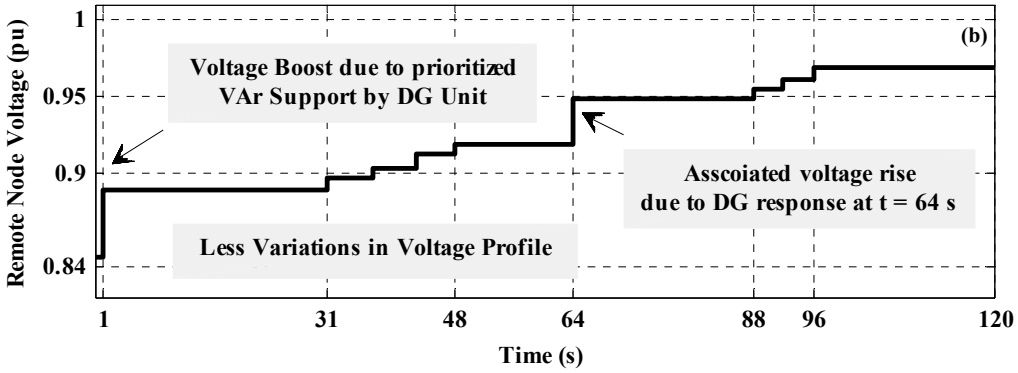

Figure 7.11: (a) Operations for voltage control devices and (b) remote node voltage, under proposed coordinated voltage control

In this simulated state, there is no requirement of operating CB under proposed coordinated voltage control, and the total number of SVR and CB maneuvers is significantly reduced from 20 operations to 7 operations. Also, there is no violation in the system voltage due to change in the DG2 response at t = 64 s and there are less SVR2 tap operations. Moreover, it is noted that if the SVR2 (which is located downstream of the feeder) has to be operated first based on the electric distance values with reference to DG units, it will be enacted first unless there is any violation in system voltage after the operation of SVR1 and/or CB. Otherwise, local controller settings of DG units and voltage control devices have to be re-tuned as mentioned in the flowchart of voltage control device module which is shown in Figure 7.4, while maintaining the stipulated limit of voltage recovery time.

7.5.3 Test Simulation under Real-time Environment for Feeder Configuration-01 with Two DG Units

In this section, the main aim is to test the real-time control action of the proposed strategy using separate online simulations for the different system states which are on 5-minute (i.e., 300 s) interval basis. Figure 7.12 shows the topology of the experimental setup. The real-world test distribution system topology is modeled using MATLAB-Simulink, where the system loads are modeled depicting variations in a daily load pattern. The local controllers of OLTC, SVRs, CB and DG units are modelled with preserving their real-time operations. The proposed

coordinated control model is implemented in MATLAB using separate MATLAB-functions for each module and the decision making control layer (as depicted in Figure 7.3), which exhibits higher computational efficiency. The functional control layers (as depicted in Figure 7.3), which give the appropriate signals to operate the required DG units and voltage control device local controllers are modeled with time delay embedded functions. The MATLAB script, ms.m is used for loading system parameters, setting up study conditions and plotting results. The proposed algorithm based information required for the functional control layers (i.e., confirmation to operate the device) is set by updating the time delay variable of each time delay embedded function (i.e., Embedded Function_1 to Embedded Function_4 as shown in Figure 7.12); after running the MATLAB functions and based on their outputs. The online information to and from DG units, voltage control devices and distribution system are assigned by '*Goto*' and '*From*' signal blocks without propagation delay, assuming zero communication delay.

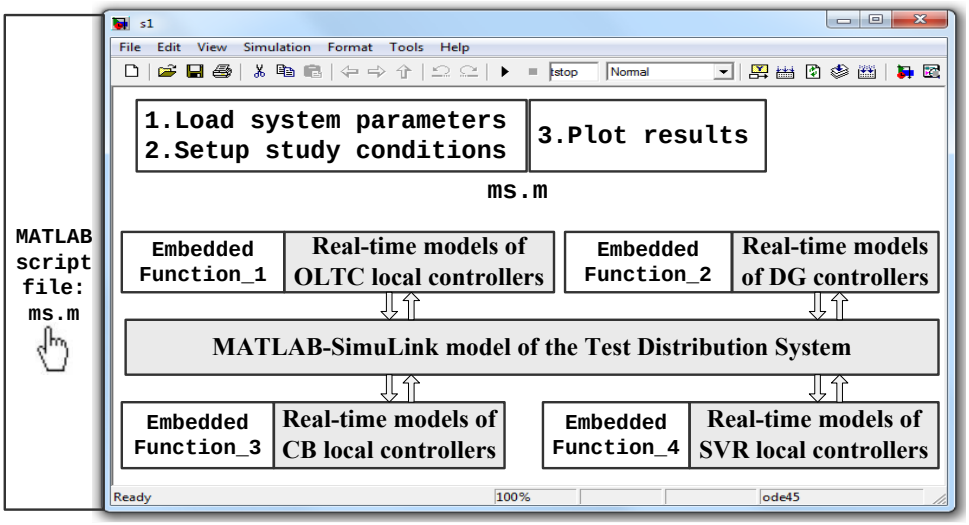

Figure 7.12: Topology of the experimental setup used for test simulation under real-time environment

Table 7.3 highlights the results obtained using one of the simulated demand patterns of the test distribution system for a system state at 300 s. The daily peak load demand is also reflected in this scenario. The DG units are initially operated at unity power factor mode. The initial tap positions of SVR1 and SVR2 are 5 and

8, respectively in the direction of increasing the voltage. The initial switching position of CB is 2. Other simulated data of SVRs and CB remain the same as used in the respective steady-state network simulation. The proposed coordinated controller is executed for total load demand of 3.5090 MVA, and active power generation of 761.6 kW for DG1 and 641.3 kW for DG2. The new VAr reference values of DG1 and DG2 are 300 kVAr and 450 kVAr, respectively and these values are updated with 1 s time delay. The operational sequence of DG units and voltage control devices under proposed coordinated control follows the sequential order of DG2, DG1, SVR1 and CB. It is noted that for the simulated operation of this test feeder system (configuration – 01), the operations of only SVR1 and CB are adequate for voltage control with respect to VAr reference values of the DG units used in the proposed coordination strategy.

Table 7.3: Simulated demand pattern for test distribution system

Time (s)	0	60	120	180	240
(%) Demand to peak value	89.8%	94.6%	97.8%	100%	96.4%

The SVR tap and CB switching operations under non-coordinated voltage control and proposed coordinated voltage control are shown in Figure 7.13 (a) and Figure 7.13 (b), respectively. The respective nodal voltage profiles for feeder operation with non-coordinated voltage control and proposed voltage control are shown in Figure 7.14 and Figure 7.15.

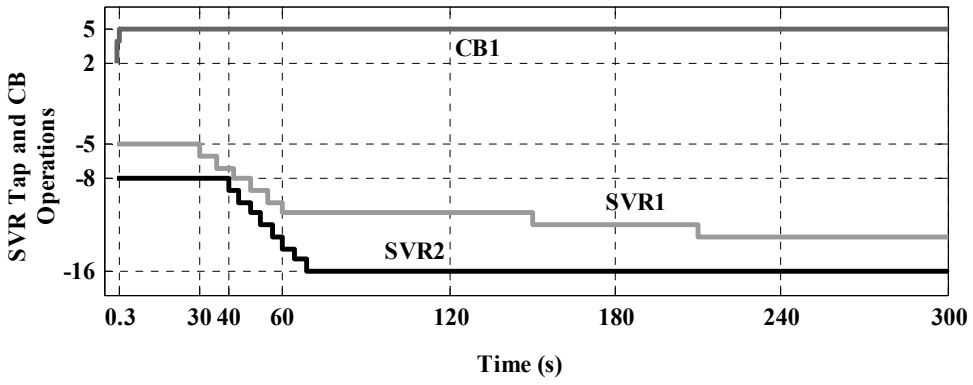

(a)

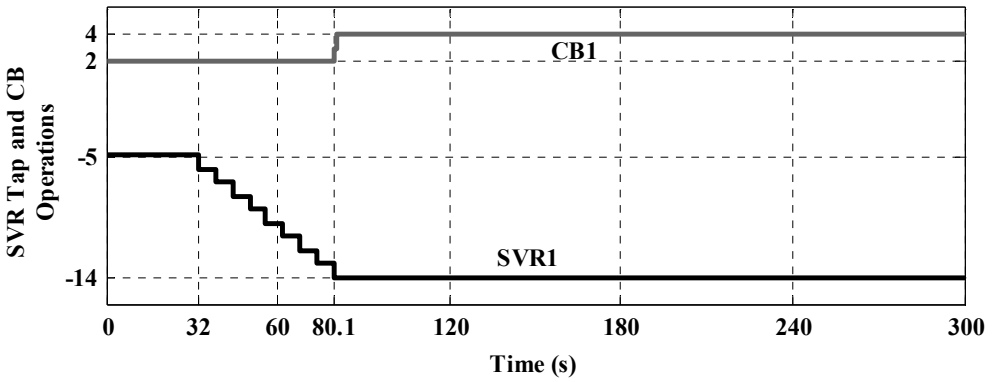

(b)

Figure 7.13: Operation of voltage control devices for the simulated state under (a) non-coordinated voltage control (b) proposed coordinated voltage control

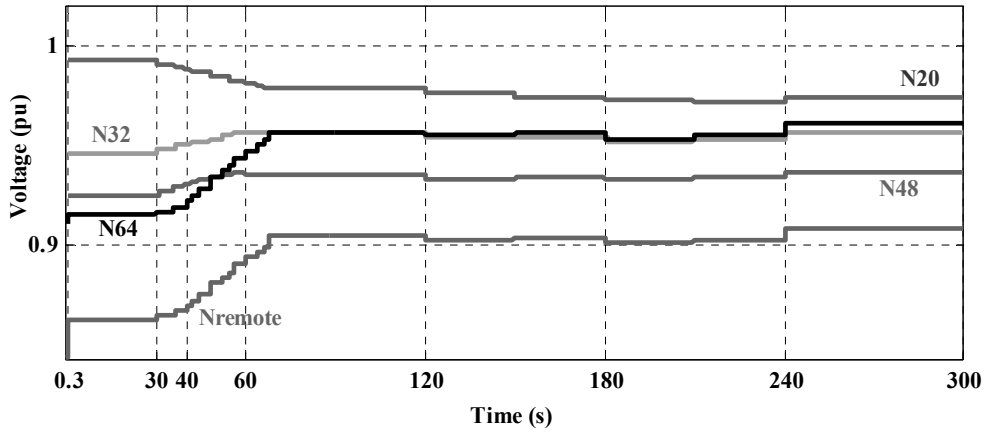

Figure 7.14: Voltage at selected nodes of the test distribution feeder operation using non-coordinated voltage control

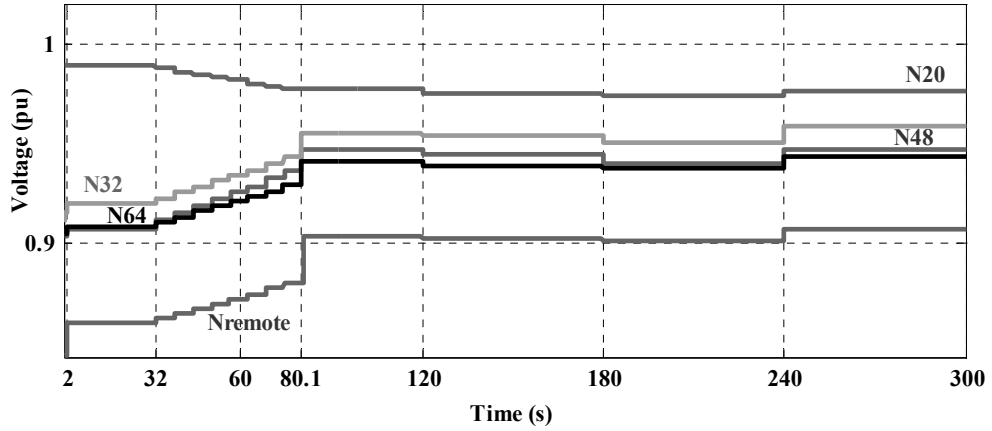

Figure 7.15: Voltages at selected nodes of the test distribution feeder operation using proposed coordinated voltage control

There are simultaneous tap operations at t = 48 s and t = 60 s, and SVR2 reaches its maximum tap position in the direction of increasing the voltage under non-coordinated operation. Also, there are additional tap operations of SVR1 at t = 150 s and t = 210 s for correcting the voltage. The performance of the proposed coordinated voltage control strategy to regulate the voltage of test distribution feeder system can be observed in the selected nodes, which are *node-20* (between substation and SVR1), *node-32* (between SVR1 and DG1), *node-48* (between DG1 and SVR2), *node-64* (between SVR2 and DG2), and *node-N95* (at the remote end). In this case, the total SVR tap operations and CB switching operations are reduced by 8 (from 19 to 11) with the application of proposed coordinated control strategy compared to the non-coordinated voltage control. Moreover, by the application of proposed strategy, the additional tap operations of SVR1 at t = 150 s and t = 210 s, which can be seen under non-coordinated voltage control, are eliminated. If such an improvement is achieved in each system state throughout a year (365 days), the annual reduction in voltage control device operations would be 840,960. Therefore, irrespective of the voltage variations attributed to load switching, the possible reduction in the associated voltage variations would also be 840,960. Hence, the test simulations under real-time environment have also demonstrated the merits of the proposed coordination strategy. The simulation results in other states of the test system are also showed the similar results. Therefore, it is very clear that the proposed coordination strategy is based on a novel mechanism to minimise the adverse effects (i.e., control interactions, resultant conflicting operations, voltage variations and voltage rise) caused by both simultaneous and non-simultaneous responses of multiple voltage control devices and DG units during any consecutive control states (i.e., $t = t$ to $t = t+1$) identified by the investigation studies carried out in Chapter 4. Since the control decisions are based on the electric distance among the DG units and the voltage control devices, the proposed strategy is also able to effectively account for the impact of structural changes associated with the distribution system. This is another salient feature of the proposed coordinated voltage control strategy.

7.6 Summary

This chapter proposes a strategy for coordinating multiple voltage control devices and DG units in MV distribution systems which are also subjected to structural changes and DG availability, thereby improving their overall voltage control performance. It coordinates the operation of multiple voltage control devices with DG units, and operates the DG units on a priority basis for maximising the voltage support by DG, in order to minimise the impact of interactions which can be occurred due to not only simultaneous but also non-simultaneous responses of voltage control devices and DG systems. The proposed priority scheme can improve the system voltage profile by eliminating uncoordinated operation of voltage control devices and DG, thereby reducing possible conflicting operations and resulting voltage variations in the system. The proposed coordination algorithm is based on the structural information derived by adopting electrical distance estimation, which is used to determine the sequence of operation for DG units and voltage control devices. Therefore, it can also effectively assess the impact of structural changes in the network on the control interactions. Results which are derived from the test simulation case studies further highlight the merits of proposed voltage control strategy in terms of voltage control device maneuvers. Based on the simulation case studies, it can be concluded that up to 32% annual increase in tap changing device and CB maneuvers is possible if specified structural changes and varying DG responses are assumed for each state of the test distribution system. With the similar assumptions, it can be concluded that a 42% to 68% annual reduction in tap changing device and CB maneuvers is possible in the test distribution system by the application of the proposed coordination strategy. Also, this leads to improved power quality in the system by reducing associated voltage variations and voltage transients in the network.

CHAPTER 8: OSCILLATIONS IN MODERN DISTRIBUTION SYSTEMS SUBJECTED TO NORMAL-STATE VOLTAGE CONTROL AND MITIGATING TAP CHANGER LIMIT CYCLES

This chapter discusses the short-term and long-term oscillations which can commonly be possible in modern MV distribution systems subjected to normal-state voltage control, when the DG is utilised for Volt/VAr support in the system. Typically, short-term oscillations occur due to interactions among different DG units and their controllers, long-term oscillations occur due to DG-Volt/VAr control device interactions, and sustained oscillations are induced by tap changer limit cycles. Consequently, it emphasises the requirement of supplementary control and mitigating strategies for damping these oscillations in modern MV distribution systems. This chapter is organised as follows. Section 8.1 gives an introduction to the possible short-term and long-term oscillations in modern MV distribution systems whereas Section 8.2 details the sustained oscillations induced by OLTC limit cycles due to interactions among OLTC control, load and local generation. Section 8.3 includes concluding remarks. This chapter is based on the Journal Publication titled "Mitigating Tap-changer Limit Cycles in Modern Electricity Networks Embedded with Local Generation Units," authored by D. Ranamuka, A. P. Agalgaonkar, K. M. Muttaqi, and M. J. E. Alam, *IEEE Transactions on Industrial Applications*, vol. 52, no. 1, pp. 455-465, Jan. 2016.

8.1 Introduction

In Australian MV distribution systems, as indicated earlier, majority of localised generation uses synchronous machine based technology. These small to medium scale synchronous machine based generators, which normally have low inertia coefficient, are used for active voltage control in the system with the aid of excitation systems [52]. However, the occurrence of significant and frequent inter-unit electro-mechanical oscillations in nearby synchronous machine based DG units is one of the dominant phenomenon, which is influenced by (a) low inertia coefficient associated with the small machines and (b) the operation of excitation system which deteriorates the damping of electro-mechanical oscillations that follow the first rotor swing after the perturbation, because a fast responding

excitation system can reduce the damping torque component [62]. The detail modelling of electric power systems, machines and excitation systems using MATLAB-Simulink for observing the electro-mechanical oscillations and associated interactions is presented in [63]-[65]. It is indicative of the fact that certain supplementary control would be required for modern active MV distribution systems in order to mitigate these inter-unit electro-mechanical oscillations which are specifically possible among Volt/VAr support DG units. However, it may require a different design criteria compared to the conventional design criteria used for transmission systems, since the modern distribution system electric variables are inherently subjected to varying system conditions. Also, the application of process control strategies such as model predictive control, adaptive tuning based control and fuzzy rule based control would not be suitable with the same reason. Fundamentally, process control follows a pattern of the particular process which is more or less definite in space and time; where the nature of electric distribution systems is entirely variable.

The other possible oscillations are phenomenally long-term and mainly caused by the DG-Volt/VAr control device interactions. Such long-term oscillations caused by OLTC-switched capacitor interactions and associated limit cycles were observed in an 11 kV distribution system in [66]. Theoretically, trajectory sensitivities are used to analyse the observed oscillations and identify the most influential variables and parameters. The details on application of trajectory sensitivity analysis are available in [67]-[69]. It was found that existence of the observed oscillations was mainly dependent upon the system fault level, capacitor rating, and OLTC dead-band limits. Also, it has been found that grazing-type conditions separated oscillatory behaviour from the steady-state behavior in all cases. Moreover, it was identified that variation of certain control parameters results in structurally different forms of oscillatory behavior. These pivotal situations are almost all related to the grazing bifurcations i.e., a system trajectory just touches a switching hypersurface.

Moreover, the sustained oscillations induced by OLTC limit cycles due to interactions among load, OLTC controls and the local generation operation would

be another common phenomenon. In electric power systems, there are various potential sources for the system long-term oscillatory behaviour. One of the common sources is OLTC limit cycles resulted due to interactions between OLTC and load dynamics. It can be observed that the power systems with OLTC limit cycles are likely to experience sustained long term oscillations under certain operating conditions. On the other hand, the research on voltage behaviour reveals that the dynamics of voltage collapse are closely related to the dynamic interactions among OLTCs and system loads. It is because OLTCs maintain load voltages within stipulated limits though transmission system voltages may be reduced. Therefore in case of long term voltage collapse, OLTC limit cycles play a key role. One of the findings in this section is that the OLTC limit cycles can occur frequently in case of electricity networks embedded with local generation units due to interactions among load, OLTC control and the local generation unit operation. In this section, in general, the DG is named as local generation (LG). The recurrence of OLTC limit cycles in the presence of LG under any practical system operation can be high, as predicted, compared to the system operation without LG. The OLTC limit cycles may sustain for a longer time especially under flat load profiles or load profiles with slow ramp variations. Also, it would adversely affect the system Volt/VAr control mechanisms and objectives. Moreover, it leads to (a) numerous tap operations (up and down) causing rapid wear and tear in tap changing devices, and (b) interactions among voltage control devices in the system. In [70], the existence of OLTC limit cycles is investigated and analysed. The system load level, degree of reactive power compensation and the load-voltage dependency are identified as the key parameters for initiation and avoidance of the OLTC limit cycles. The nature of limit cycles caused by the interaction between transformer tap changer and load dynamics is analysed in [71]. A linearisation of Poincar´e map is used to analyse the local stability in the system under OLTC limit cycles. In [72], voltage oscillations in power systems with cascaded multiple OLTC units have been studied, where the focus is on the limit cycles due to interactions among tap changers and system loads. Also, a control strategy is proposed in [72] to mitigate the OLTC limit cycles. It is based on adjusting the dead-band (DB) of the tap changer, which typically depends on

the load characteristics. It has been found that the existing limit cycles can be avoided and a steady-state condition is reached given a sufficiently large DB in case of stable load dynamics when tap ratios are fixed. The existing limit cycles will not be removed by increasing DB in case of unstable load dynamics wherein tap ratios are fixed. Moreover, it has been found that adjusting OLTC control parameters such as time delay and/or DB size may not have any effect on the existence of limit cycles under certain system conditions [70]. Hence, it may not be possible to avoid limit cycle behaviour simply by retuning the OLTC dead-band limit and/or time delay. However, none of the studies in the literature have investigated and analysed the OLTC limit cycle phenomena in electricity networks with higher penetration of renewable and non-renewable local generation. For such networks, OLTC limit cycles can occur frequently due to interactions among load, OLTC control and the local generation operation.

8.2 Mitigating OLTC Limit Cycles in Modern Distribution Systems

In this section, OLTC limit cycle phenomena in case of MV electricity networks with higher penetration of LG is investigated and analysed thoroughly. The small signal model and describing function method used in [70] for OLTC limit cycle analysis in a two-bus system have been extended for analysing and predicting OLTC limit cycles in multi-bus system topology with LG. Also, a strategy based on coordinated VAr support from LG units and shunt CBs is explored in order to mitigate the OLTC limit cycles in the presence of LG units. It is easily implementable with a typical voltage control scheme.

8.2.1 Background Theory

Eigen value analysis is used to predict the existence of OLTC limit cycles, and the results are compared with describing function analysis. For large MV power systems, network reduction methods can be applied to minimise the computational burden [43].

8.2.1.1 Modelling Aspects

The model described by the dead band-ordinary differential equation (DB-ODE) is used for modelling OLTC as given by (01) [73]. It is noted that discrete tap steps are not taken into account in this OLTC model. While analysing OLTC limit cycles using the proposed small-signal analysis, it was noted that the overall behaviour of the moderately loaded power systems is largely similar for continuous as well as discrete OLTC models. However, it could be otherwise under heavy loading conditions, which is insignificant in presence of LG units as the local load is supplied by the LG. Under heavy load conditions, the systems with discrete OLTC model exhibits a limit cycle that will arrest oscillatory voltage instability predicted by small-signal analysis, whereas the system with the continuous models shows voltage collapse after a few cycles. These aspects are detailed in [70]. However, the prediction of OLTC limit cycles in power systems using the proposed small-signal analysis is accurate for both cases. Also, it is to be noted that the limit cycles in the power system are associated with its mathematical model and not with the numerical problems in the simulation. In this section, small-signal model and analysis is used to predict the occurrence of OLTC limit cycles in power systems embedded with LG units and a new control strategy is proposed to mitigate long term sustained oscillations in the system.

The V_{LC} denotes regulated voltage at the regulating point, V_{set} is the voltage set value, T is the OLTC controller time delay and a is the transformer tap-ratio.

$$\frac{da}{dt} = \begin{cases} (-)\ \frac{1}{T}.\left(V_{LC} - V_{set} - DB/2\right) & if\ \left(V_{LC} - V_{set}\right) > DB/2 \\ (-)\ \frac{1}{T}.\left(V_{LC} - V_{set} + DB/2\right) & if\ \left(V_{LC} - V_{set}\right) < (-)\,DB/2 \\ 0 & if\ \left|V_{LC} - V_{set}\right| < DB/2 \end{cases} \quad (01)$$

Accurate modelling of different load characteristics is one of the key requirements of analysing and predicting OLTC limit cycles. In this section, the loads are modelled as exponential recovery loads as given by (02) and (03) [43].

$$\dot{x}_p = \frac{1}{T_p}\left(-x_p + P_s(V) - P_t(V)\right), \qquad P_s(V) = k_L.P_0(V)^{\alpha s}$$
$$P_t(V) = k_L.P_0(V)^{\alpha t}, \qquad P_d = x_p + P_t(V) \tag{02}$$

$$\dot{x}_q = \frac{1}{T_q}\left(-x_q + Q_s(V) - Q_t(V)\right), \qquad Q_s(V) = k_L.Q_0(V)^{\beta s}$$
$$Q_t(V) = k_L.Q_0(V)^{\beta t}, \qquad Q_d = x_q + Q_t(V) \tag{03}$$

where, x is an internal state which models the load recovery dynamics. The recovery time constants are T_p and T_q, and α_s, α_t, β_s, β_t are the exponents of the voltage. The steady-state nodal voltage dependency of loads is denoted using $P_s(V)$ and $Q_s(V)$, where the transient (instantaneous) nodal voltage dependency is denoted using $P_t(V)$ and $Q_t(V)$ respectively. The P_d and Q_d denote actual loads where the rated load values are denoted using P_0 and Q_0. The load scale factor is k_L. Moreover, it is assumed that the LG units respond instantaneously to the system changes. The respective power injections of LG units have been incorporated in the power balance equations. The active power response of LG unit is P_{LG} whereas the reactive power response is Q_{LG}.

The describing function ($N(A)$) in the DB-ODE model of the OLTC can be derived as given by (04) [70], [74]. The amplitude of any sinusoidal input is A_s, where periodic OLTC limit cycles are assumed to be approximately sinusoidal. The condition associated with the occurrence of OLTC limit cycle phenomenon is given by (05), where the small signal model of the power system is given by (06). The limit cycle phenomenon under each operation is predicted using the proposed small signal model and the associated eigen value analysis. This is an extended version of the analysis done in [70].

$$N(A_s) = \begin{cases} 1 - \frac{2}{\pi}\left(sin^{-1}\left(\frac{DB}{2A_s}\right) + \frac{DB}{2A_s}\sqrt{1-\left(\frac{DB}{2A_s}\right)^2} \right) & if\ A_s > DB/2 \\ 0 \quad if\ A_s < DB/2 \end{cases} \tag{04}$$

Condition for limit cycle phenomenon :

$$G(j\omega) = (-)\left\{\frac{1}{N(A_s)}\right\} \quad \forall \ G(j\omega) = (-)G_n(j\omega) \times G_c(j\omega) \tag{05}$$

$G_n(s) \rightarrow$ transfer function of the power system model, which is derived from the state space model given by (06)
$G_c(s) \rightarrow$ transfer function of the ODE part of DBODE model

The proposed mathematical model used for analysing and predicting OLTC limit cycles is given below, for the example two bus power system shown in Figure 8.1.

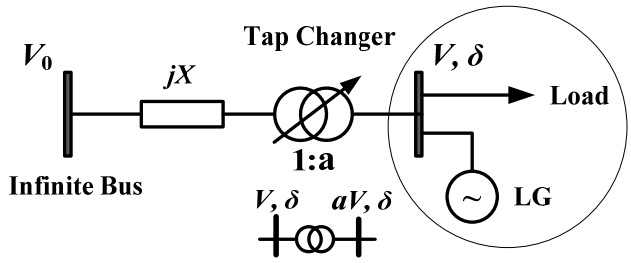

Figure 8.1: Two bus system model

System equations including dynamics :

$$\dot{x} = f(x, v), \quad g(x, v, P_{LG}, Q_{LG}, u) = 0$$

δ = voltage phasor angle, V = voltage magnitude

State space model :

$$\Delta \dot{x} = \left(\frac{\partial f}{\partial x}\right)\Delta x + \left(\frac{\partial f}{\partial v}\right)\Delta v$$

$$\left(\frac{\partial g}{\partial x}\right)\Delta x + \left(\frac{\partial g}{\partial v}\right)\Delta v + \left(\frac{\partial g}{\partial u}\right)\Delta u = 0$$

$$\Delta \dot{x} = (A)\Delta x + (B)\Delta a$$
$$\Delta v = (C)\Delta x + (D)\Delta a \tag{06}$$

State matrix : $x = \begin{bmatrix} x_p & x_q \end{bmatrix}^T$, Input matrix : $u = [a]$

a = tap ratio, Output matrix : $v = [V \quad \delta]^T$

$$A = \left(\frac{\partial f}{\partial x}\right) - \left(\frac{\partial f}{\partial v}\right)\left(\frac{\partial g}{\partial v}\right)^{-1}\left(\frac{\partial g}{\partial x}\right), \qquad C = (-)\left(\frac{\partial g}{\partial v}\right)^{-1}\left(\frac{\partial g}{\partial x}\right)$$

$$B = (-)\left(\frac{\partial f}{\partial v}\right)\left(\frac{\partial g}{\partial v}\right)^{-1}\left(\frac{\partial g}{\partial u}\right), \qquad D = (-)\left(\frac{\partial g}{\partial v}\right)^{-1}\left(\frac{\partial g}{\partial u}\right)$$

8.2.1.2 Predicting Existence of OLTC Limit Cycles

In this section, predicting OLTC limit cycles using the proposed model is elaborated using simulation case studies conducted using MATLAB software.

8.2.1.2.1 Case Study for a Two-Bus System

Firstly, the two bus system shown in Figure 8.1 is used for investigating and analysing OLTC limit cycle phenomenon under different system operational states, and some of the selected cases are presented. The transformer equivalent impedance is jX [43]. The existence of OLTC limit cycles in the presence of the LG unit has been tested for different load demand levels, and the key results of some example simulations are summarised below. The Nichols plots of both left and right hand side functions are used to solve the equation (05). The sample load and system data, used for simulation purposes, are P_0 = 106.8 MW, Q_0 = 43.2 MVAr, X = 0.10641 pu, α_s = 1, β_s = 0, α_t = 1, β_t = 4 and $T_p = T_q$= 60 s. The tap changer controller time delay (T) is 30 s. The simulated voltage change per tap operation is 0.0010 pu. The initial tap position of the OLTC is set at its nominal position for all simulations. The peak load demand is 96.005 MVA, where k_L = 1, 0.9, 0.8, 0.7, 0.6, 0.5, 0.4 and 0.3. The sending end bus voltage is 1.01 pu. Figure 8.2 shows the respective Nichols plots for two bus system operation without LG unit (case-01). According to the Nichols plots (Gki, where i = 1, …, 8), it can be seen that the plots do not intersect the Nichols plot of –1/N(A) function for different values of k_L, which demonstrates that OLTC limit cycles do not exist for the test system without LG. The plot (GA), shown by the (orange colour) vertical line, represents the Nichols plot of 1/N(A).

According to the investigations, it can be seen that there can be OLTC limit cycles where active power generation level of the LG unit exceeds 26.5 MW and k_L = 0.3 as shown in Figure 8.3 (case-02). Figure 8.4 illustrates an example for OLTC limit

cycles in real-time for the limit cycle phenomenon predicted in case-02 (Figure 8.3). This is obtained by solving the first order differential equations of x-states which models the load recovery dynamics. In this case, the power output of the LG unit is assumed to be constant, where mechanical time delay of OLTC is assumed to be 6 s. The time domain simulation studies highlight the applicability of describing function method for predicting OLTC limit cycles in electric power systems with local generation, when utilising a simplified version of the power system following network reduction methods.

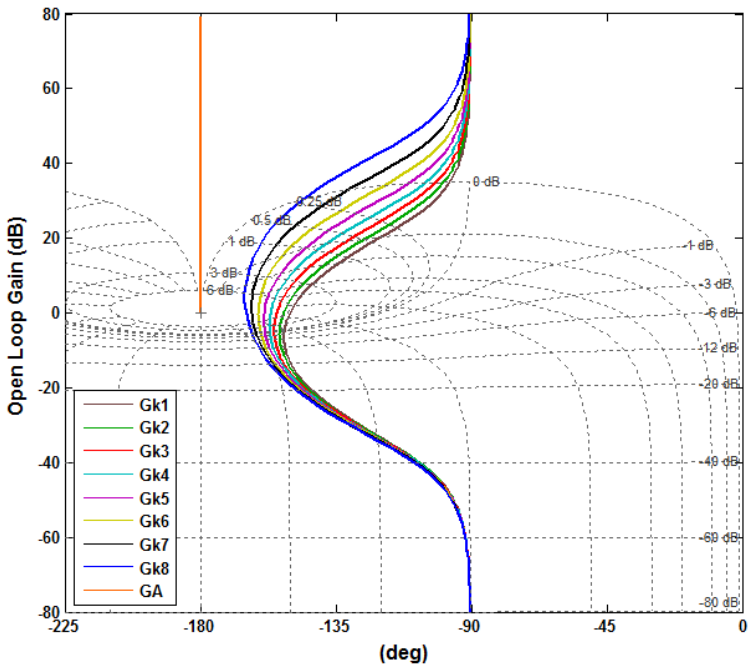

Figure 8.2: Nichols plots of G($j\omega$) function for different values of k_L in case of system operations without LG and Nichols plot of –1/N(A) (case-01)

Figure 8.5 shows that the OLTC limit cycles may recur frequently, if active power generation level of the LG unit exceeds 87.5 MW (case-03). It is indicative of the fact that compared to the system operation without LG, recurrence of OLTC limit cycles in the presence of a LG unit under any system operation can be high, as predicted. Also, after predicting for a particular load factor (k_L), the limit cycles may sustain for a longer time especially under flat load profiles or load profiles with slow ramp variation. Therefore, an implementation strategy for mitigating

OLTC limit cycles in the presence of LG units may be essential for networks with high penetration of LG.

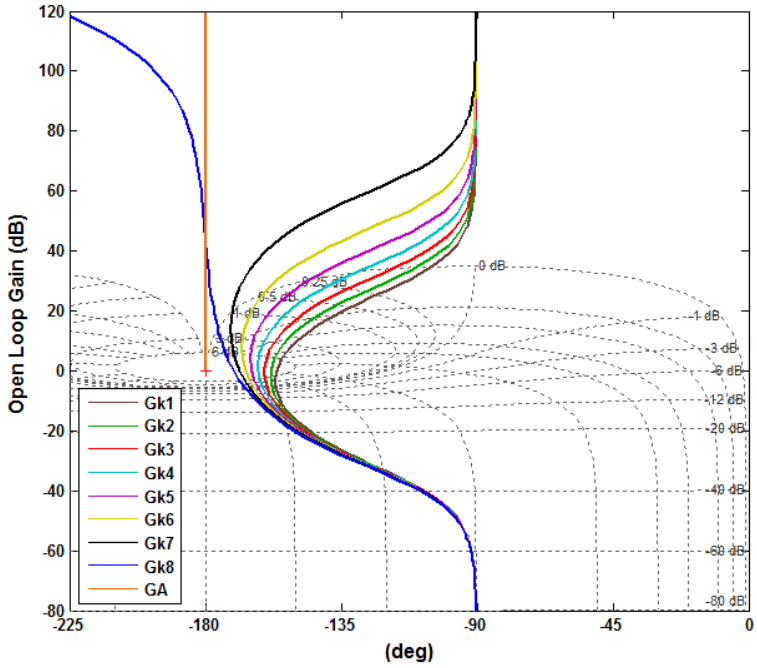

Figure 8.3: Nichols plots of G($j\omega$) function for different values of k_L in case of system operations with P_{LG} = 26.5 MW (case-02)

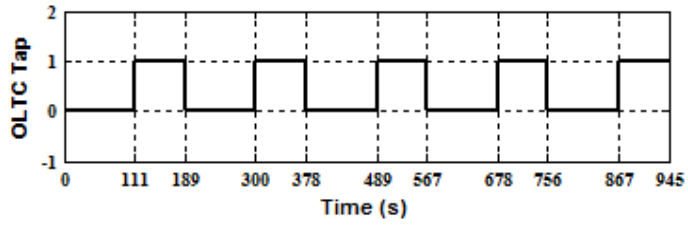

(a)

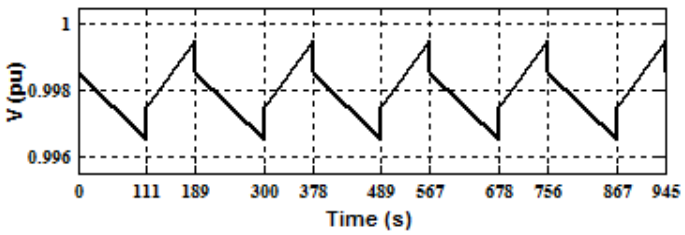

(b)

Figure 8.4: Simulated (a) OLTC tap operations and (b) resultant voltage oscillations, which can occur due to OLTC limit cycle phenomenon predicted in case-02

The reactive power support (export) of 13.5 MVAr by the LG unit in Figure 8.1 can prevent the system from an oscillatory response, attributed to OLTC limit cycles, which can occur when the real power output of the LG unit is 26.5 MW and k_L = 0.3 as shown in Figure 8.6 (case-04). It is indicative of the fact that OLTC limit cycles may be mitigated by considering degree of reactive power compensation and accordingly implementing a coordinated VAr management scheme in the system, comprising of Volt/VAr support by the LG unit.

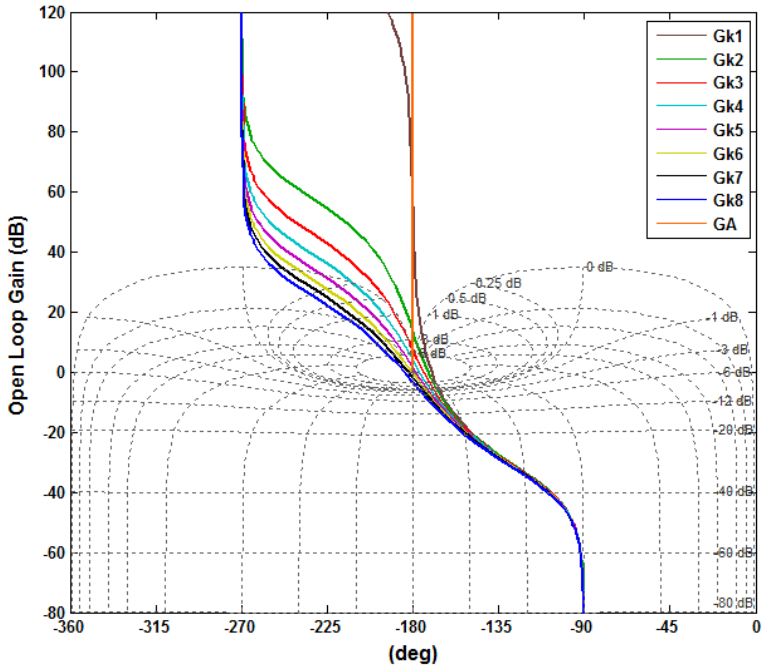

Figure 8.5: Nichols plots of G($j\omega$) function for different values of k_L in case of system operations with P_{LG} = 87.5 MW (case-03)

When the LG unit absorbs (import) reactive power of 9.6 MVAr (case-05), it is noted that the intersection point of the associated Nichols plots i.e., Gki (where k_L = 0.3) shifts downwards as shown in Figure 8.7 along the GA curve to a lower open loop gain compared to the case-02. It means that the absorption of reactive power by the LG unit affects G($j\omega$) function. Consequently, the amplitude of limit cycles is changed, but not the frequency. Moreover, shifting the curve below the point (0 dB, -180^0) can eliminate the limit cycle, but it may lead to instability of the closed loop system. In summary, it is clear that there would be a certain LG

penetration level which can create OLTC limit cycles, and also which can mitigate OLTC limit cycles for each operational state of the system.

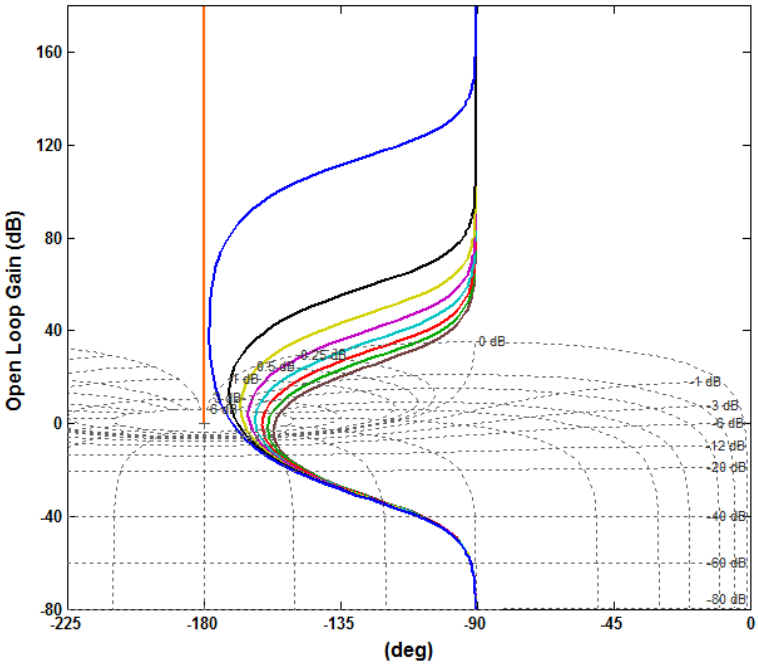

Figure 8.6: Nichols plots of G($j\omega$) function for different values of k_L in case of system operations with P_{LG} = 26.5 MW and Q_{LG} = 13.5 MVAr (case-04)

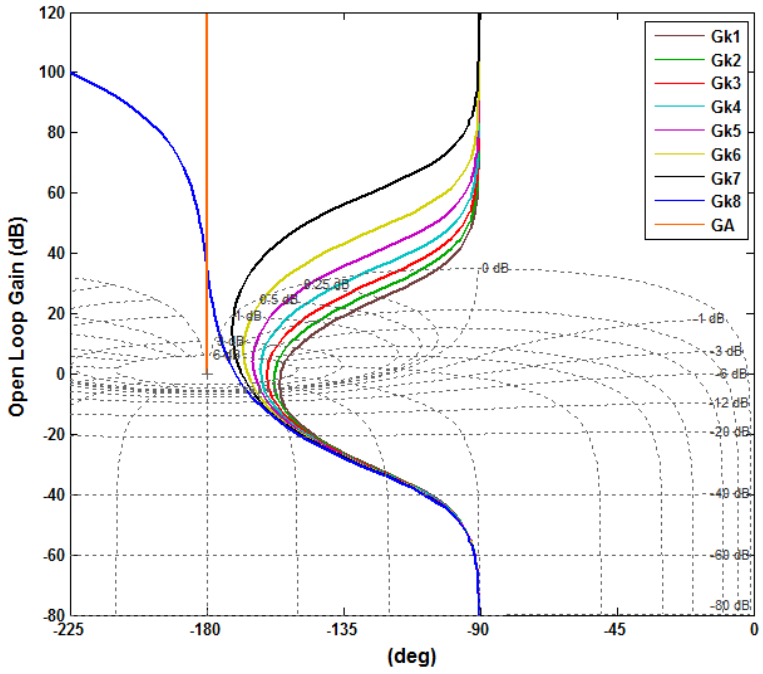

Figure 8.7: Nichols plots of G($j\omega$) function for different values of k_L in case of system operations with P_{LG} = 26.5 MW and Q_{LG} = – 9.6 MVAr (case-05)

According to the simulation case study discussed above, the rating of the system, S_{LG} /$S_{Load\text{-}Rated}$ and existence of OLTC limit cycles can be summarised as given in the Table 8.1. It is indicative of the fact that implementing an OLTC limit cycle mitigation strategy in an alert-state would be more reliable as the occurrence of OLTC limit cycles also depends on the rating of the system, S_{LG} /$S_{Load\text{-}Rated}$ for an initial tap position of the OLTC. Finally, the eigen values of overall system state matrix for the above mentioned different operational states (case-01 to case-05) are derived and shown in Table 8.2. The unstable scenarios with OLTC limit cycles, where at least one of the eigen values has a positive real part are highlighted. The results of the eigen value analysis are very much in agreement with the results obtained using the describing function method which has been used for predicting the existence of OLTC limit cycles. Moreover, a modal analysis can be done using the proposed small signal model in order to identify the oscillatory modes referred to OLTC limit cycle instability especially in case of long term voltage collapse phenomenon; which is out of the scope of this section.

Table 8.1: Existence (√=YES, ×=NO) of OLTC limit cycles

S_{LG} /$S_{Load\text{-}Rated}$	k_L = 1.0	k_L = 0.9	k_L = 0.8	k_L = 0.7
0 S_{LG} = 0 (No LG)	×	×	×	×
0.23 Q_{LG} = 0	×	×	×	×
0.24 Q_{LG} = - 9.6 MVAr	×	×	×	×
0.26 Q_{LG} =13.5 MVAr	×	×	×	×
0.76 Q_{LG} = 0	√ Case-03	√ Case-03	√ Case-03	√ Case-03
S_{LG} /$S_{Load\text{-}Rated}$	k_L = 0.6	k_L = 0.5	k_L = 0.4	k_L = 0.3
0 S_{LG} = 0 (No LG)	×	×	×	×
0.23 Q_{LG} = 0	×	×	×	√ Case-02
0.24 Q_{LG} = - 9.6 MVAr	×	×	×	√ Case-05
0.26 Q_{LG} =13.5 MVAr	×	×	×	×
0.76 Q_{LG} = 0	√ Case-03	√ Case-03	√ Case-03	√ Case-03

Table 8.2: Results of eigen value analysis (real part of the eigen values) for the two bus system operation

Case Study	$k_L = 1.0$	$k_L = 0.9$	$k_L = 0.8$	$k_L = 0.7$
Case-01	- 0.0010 - 0.0167	- 0.0009 - 0.0167	- 0.0008 - 0.0167	- 0.0007 - 0.0167
Case-02	- 0.0007 - 0.0167	- 0.0006 - 0.0167	- 0.0005 - 0.0167	- 0.0004 - 0.0167
Case-03	+ 0.0000 - 0.0167	+ 0.0001 - 0.0167	+ 0.0002 - 0.0167	+ 0.0003 - 0.0167
Case-04	- 0.0007 - 0.0167	- 0.0006 - 0.0167	- 0.0005 - 0.0167	- 0.0004 - 0.0167
Case-05	- 0.0007 - 0.0167	- 0.0006 - 0.0167	- 0.0005 - 0.0167	- 0.0004 - 0.0167
Case Study	$k_L = 0.6$	$k_L = 0.5$	$k_L = 0.4$	$k_L = 0.3$
Case-01	- 0.0006 - 0.0167	- 0.0005 - 0.0167	- 0.0004 - 0.0167	- 0.0003 - 0.0167
Case-02	- 0.0003 - 0.0167	- 0.0002 - 0.0167	- 0.0001 - 0.0167	+ 0.00000 - 0.0167
Case-03	+ 0.0004 - 0.0167	+ 0.0005 - 0.0167	+ 0.0006 - 0.0167	+ 0.0007 - 0.0167
Case-04	- 0.0003 - 0.0167	- 0.0002 - 0.0167	- 0.0001 - 0.0167	- 0.0000 - 0.0167
Case-05	- 0.0003 - 0.0167	- 0.0002 - 0.0167	- 0.0001 - 0.0167	+ 0.00001 - 0.0167

8.2.1.2.2 Case Study for a Multi-Bus System

The multi bus (single OLTC) system shown in Figure 8.8 is used for investigating and analysing OLTC limit cycle phenomenon under different system operational states, and one of the selected case is presented. The describing function analysis and eigen value analysis are carried out, and compared for the multi bus system in order to further test the applicability of the mathematical model derived under Sub-section 8.2.1.1 for predicting the OLTC limit cycles.

Multi-bus system of Figure 8.8 is derived from [77] and modified by adding load dynamics, control data and the line data (i.e., R_5 = 0.00192 pu and X_5 = 0.04256 pu) related to connecting the LG unit. The bus voltage magnitudes are V_0, V_1, V_2, V_3, V_4 and V_5 form grid to the LG bus, where the voltage phasor angles are *zero*, δ_1, δ_2, δ_3, δ_4 and δ_5, respectively. The tap ratio of the substation transformer equipped with OLTC is '*a*' for particular instance of time. The line impedances

are jX_0, (R_2+jX_2), (R_3+jX_3), (R_4+jX_4) and (R_5+jX_5) from grid to the LG bus, respectively. The substation transformer equivalent impedance is (R_1+jX_1) [43]. The respective admittance values are denoted using *Y,* where their phasor angles are denoted using γ.

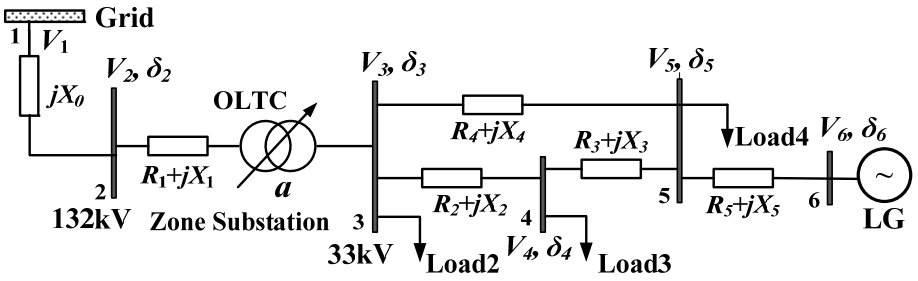

Figure 8.8: Multi bus system model with single OLTC

The small signal model of the multi bus power system is given by (07). If there is a CB in the system, it can be modelled using its susceptance value, *B* as shown below.

System equations including dynamics :

$$\dot{x} = f(x, v), \quad g\left(x, v, P_{LG}, Q_{LG}, B, u\right) = 0, \quad Q_{CB} = B.V^2$$

State space model :

$$\Delta \dot{x} = \left(\frac{\partial f}{\partial x}\right)\Delta x + \left(\frac{\partial f}{\partial v}\right)\Delta v$$

$$\left(\frac{\partial g}{\partial x}\right)\Delta x + \left(\frac{\partial g}{\partial v}\right)\Delta v + \left(\frac{\partial g}{\partial u}\right)\Delta u = 0$$

$$\Delta \dot{x} = \left(A_1\right)\Delta x + \left(B_1\right)\Delta a$$

$$\Delta v = \left(C_1\right)\Delta x + \left(D_1\right)\Delta a \qquad (07)$$

State matrix : $x = \left[x_{p3} \;\; x_{q3} \;\; x_{p4} \;\; x_{q4} \;\; x_{p5} \;\; x_{q5}\right]^T$

Input matrix : $u = [a]^T$ Output matrix :

$$v = \left[V_3 \;\; V_4 \;\; V_5 \;\; \delta_3 \;\; \delta_4 \;\; \delta_5\right]^T$$

$$A_1 = \left(\frac{\partial f}{\partial x}\right) - \left(\frac{\partial f}{\partial v}\right)\left(\frac{\partial g}{\partial v}\right)^{-1}\left(\frac{\partial g}{\partial x}\right), \quad C_1 = (-)\left(\frac{\partial g}{\partial v}\right)^{-1}\left(\frac{\partial g}{\partial x}\right)$$

$$B_1 = (-)\left(\frac{\partial f}{\partial v}\right)\left(\frac{\partial g}{\partial v}\right)^{-1}\left(\frac{\partial g}{\partial u}\right), \quad D_1 = (-)\left(\frac{\partial g}{\partial v}\right)^{-1}\left(\frac{\partial g}{\partial u}\right)$$

For the tap changer model, input is the transformer secondary bus voltage magnitude, V_3 whereas output is the tap ratio, a. The OLTC limit cycles can be predicted as shown in Figure 8.9, where the simulated load and system data are as below: total P_0 = 94.0 MW, total Q_0 = 21.0 MVAr, $\alpha_s = \beta_s = 1$, $\alpha_t = 2$, $\beta_t = 4$, T_p = 120 s, T_q= 60 s and OLTC controller time delay, T = 30 s. The total active and reactive power outputs (export) by the LG unit are 34.6 MW and 5.3 MVAr, respectively. Initial tap position of OLTC is '1' in the direction of increasing voltage, where taps are incorporated in the primary winding of the substation transformer. The total peak load demand is around 90.0 MVA, where k_L = 0.85 and the grid voltage is 1.0 pu. In this case, the rating of the system, S_{LG} /$S_{Load\text{-}Rated}$ is 0.36.

The eigen values derived using overall system state matrix with the VAr support by the LG unit are shown in Table 8.3. They are also indicative of the fact that OLTC limit cycles can also exist with the LG unit operating in voltage control mode, especially when the Volt/VAr control action of the LG unit has not been coordinated with the operation of other voltage control devices.

Also, this simulation and other associated simulation shows the applicability and suitability of the proposed eigen value analysis for predicting OLTC limit cycle instability even in multi bus systems. Therefore, the Sub-section 8.2.2 which discusses mitigation of OLTC limit cycles is mainly based on the proposed mathematical model and the associated eigen value analysis which can be used for predicting OLTC limit cycles and associated instability in electricity networks with LG.

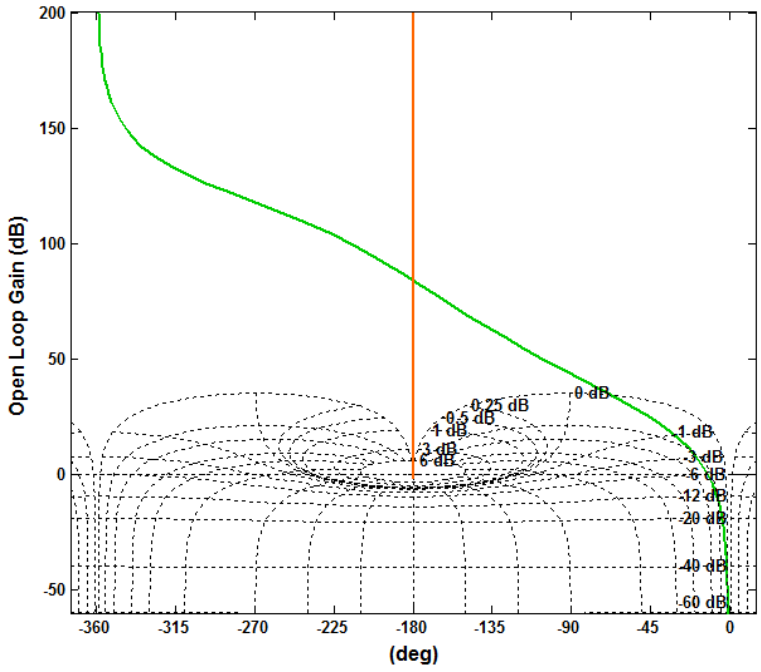

Figure 8.9: Nichols plots of G($j\omega$) for an existence of OLTC limit cycles in the multi bus system when k_L = 0.85, P_{LG} = 34.6 MW and Q_{LG} = 5.3 MVAr

Table 8.3: Results of eigen value analysis (real part of the eigen values) for the multi bus (single OLTC) system operation with VAr support of the LG unit

+ 0.0010	+ 0.0010	- 0.0186	- 0.0174	- 0.0078	- 0.0081

Secondly, the multi bus (cascaded OLTCs) system shown in Figure 8.10 is used for investigating and analysing OLTC limit cycle phenomenon under different system operational states, and one of the selected cases is presented. In this test system, OLTC limit cycles can be induced not only due to interaction among load, OLTC control and the power generated by LG units, but also due to the interaction of the CB connected at 132 kV bus.

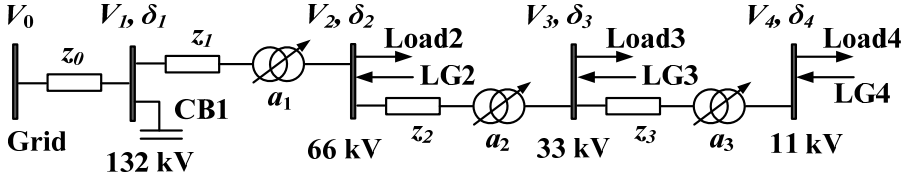

Figure 8.10: Multi bus system model with cascaded OLTCs

The bus voltage magnitudes are V_0, V_1, V_2, V_3, and V_4 from grid to the 11 kV bus, where the voltage phasor angles are zero, δ_1, δ_2, δ_3, and δ_4, respectively. The tap ratios of the substation transformers equipped with OLTC are a_1, a_2, and a_3, respectively for particular instance of time. The line impedances are z_0, z_1, z_2, and z_3 including the respective transformer equivalent impedances [43] from grid to the 11 kV bus. The small signal model of the system can be derived similar to (07) and defining state, input and output matrices as given by (08). The linear state-space modelling of complex and large electric systems is referred to [75], [76].

$$\text{State matrix} : x = \begin{bmatrix} x_{p2} & x_{q2} & x_{p3} & x_{q3} & x_{p4} & x_{q4} \end{bmatrix}^T$$

$$\text{Input matrix} : u = \begin{bmatrix} a_1 & a_2 & a_3 \end{bmatrix}^T$$

$$\text{Output matrix} : v = \begin{bmatrix} V_2 & V_3 & V_4 & \delta_2 & \delta_3 & \delta_4 \end{bmatrix}^T \quad (08)$$

In the simulated state, a possibility of limit cycles in OLTC (a_1) and OLTC (a_2) is predicted and the results of the eigen value analysis which predicts OLTC limit cycles are shown in Figure 8.11 and Table 8.4, respectively. In Figure 8.11 legend; n1, n2 and n3 represent the Nichols plots related to OLTC (a_1), OLTC (a_2) and OLTC (a_3), respectively. The predicted OLTC limit cycles may or may not be sustained in case of cascaded OLTCs, because of the hunting phenomenon [70]. However, enacting a mitigating strategy would be essential in a realistic network, as emulated for the above test system, with a significant penetration of local generation; because there is a higher possibility of sustaining the predicted OLTC limit cycle phenomena due to variability in power outputs of the LG units and associated changes in system dynamics.

The simulated load scale factors for loads 2, 3, and 4 are k_{L2} = 0.8, k_{L3} = 0.9, and k_{L4} = 0.9, respectively. The total peak load demands for loads 2, 3, and 4 are 80 MVA, 12.800 MVA and 3.128 MVA, respectively; where P_{02} = 86.4 MW, Q_{02} (export) = 41.8454 MVAr, P_{03} = 13.824 MW, Q_{03} (export) = 6.6953 MVAr, P_{04} = 3.456 MW and Q_{04} (export) = 1.6738 MVAr. The rating of the CBs is 40 MVAr and simulated VAr support is 20 MVAr. The simulated initial tap positions of

OLTC, a_1, a_2 and a_3, are 2, 4 and 4 respectively in the direction of increasing voltage, where the controller time delays are 30 s, 45 s and 60 s respectively. The simulated active and reactive power generations of LG1, LG2 and LG3 units are (33.000 MW, 9.300 MVAr (export)), (6.500 MW, 0 MVAr) and (1.600 MW, 0 MVAr), respectively.

The simulated load parameters of loads 2, 3 and 4 are (α_{s2} = 1.5, β_{s2} = 4.5, α_{t2} = 8, β_{t2} = 3, T_{p2} = 174 s, T_{q2} = 84 s), (α_{s3} = 2.5, β_{s3} = 5.5, α_{t3} = 4, β_{t3} = 1.5, T_{p3} = 201 s, T_{q3} = 48 s) and (α_{s4} = 1, β_{s4} = 3.5, α_{t4} = 6, β_{t4} = 2, T_{p4} = 121 s, T_{q4} = 64 s), respectively. The line data as shown in Figure 8.10 are z_0 = (0.0129 + j0.0550) pu, z_1 = (0.0011 + j0.0950) pu, z_2 = (0.1510 + j0.6721) pu, and z_3 = (0.1989 + j2.6565) pu, respectively. The simulated grid voltage is 1.010 pu. The voltages at buses 1, 2, 3, and 4 are 1.002 pu, 0.990 pu, 0.964 pu and 0.951 pu, respectively.

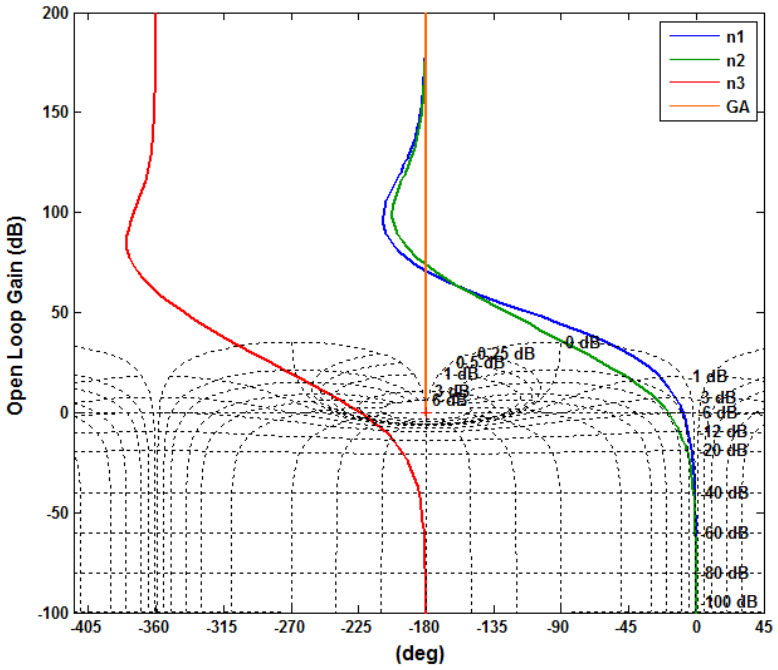

Figure 8.11: Nichols plots of G($j\omega$) for existence of limit cycles in OLTC1 and OLTC2 under simulated test conditions

Table 8.4: Results of eigen value analysis (real part of the eigen values) for the multi bus (cascaded OLTC) system operation with LG

+ 0.0140	- 0.0227	- 0.0139	- 0.0086	- 0.0010	- 0.0036

8.2.2 Proposed Control Strategy for Mitigating OLTC Limit Cycles

From power system control perspective, the system-operating conditions are normally classified into five states such as normal, alert, emergency, extreme emergency and restorative [8]. In the proposed strategy for mitigating OLTC limit cycles, the control transition is between normal and the alert states. The system enters the alert-state form the normal-state, if existence of OLTC limit cycles is predicted. Then, the preventive control action based on the proposed control strategy is activated to mitigate the OLTC limit cycles while controlling the system voltage. Since, (a) the objectives of normal-state voltage control can be different and incorporating those objectives with mitigating OLTC limit cycles may not always be effective and (b) the possibility of occurring OLTC limit cycles also dependant on the rating of the system, $S_{LG}/S_{Load\text{-}Rated}$; transition based voltage control is used. This is a key feature of the proposed control strategy applicable to power systems embedded with LG units, because normal-state voltage control is not an easy task in presence of high penetration of local generation.

The system load level, penetration level of LG, degree of reactive power compensation and the load-voltage dependency are identified as the key parameters for mitigating the OLTC limit cycles. On the other hand, it may not be possible to avoid limit cycle behavior under certain system operating conditions simply by retuning the OLTC control parameters. For example, an increase of the DB size will only increase the amplitude of a limit cycle but will not remove it. Similarly, the different time delays in the OLTC control system have no influence on the existence of limit cycles, only on the amplitude and period time. The only parameters which can affect the existence of limit cycles are load and network parameters [70], [72]. The level of reactive power compensation can effectively be used as one of the key parameters for mitigating OLTC limit cycles in the electricity networks embedded with LG based on dynamic VAr management in the network using reactive power capability of available LG units and shunt CBs.

Therefore, the proposed strategy is mainly based on exploring the impact of degree of reactive power compensation on OLTC limit cycles, and accordingly coordinated VAr control in the system using reactive power capabilities of LG units and CBs for avoiding the conditions which have to be satisfied for the existence of OLTC limit cycles. From (07) and for particular system operation, it can be seen that the *A*-matrix is also a function of nodal voltage magnitudes and phase angles as given by (09).

$$A = \left(\frac{\partial f}{\partial x}\right) - \left(\frac{\partial f}{\partial v}\right)\left(\frac{\partial g}{\partial v}\right)^{-1}\left(\frac{\partial g}{\partial x}\right)$$

$$\left(\frac{\partial f}{\partial v}\right) = f(V), \quad \left(\frac{\partial g}{\partial v}\right) = f(V,\ \delta) \quad \rightarrow \quad A = f(V,\ \delta) \tag{09}$$

Hence, by means of voltage control through coordinated VAr management in the system, a stable system operation without system oscillations, typically induced by OLTC limit cycles, can also be achieved. Accordingly, the proposed mitigation strategy is developed. The step-by-step algorithm of the proposed strategy is outlined below.

- Step-01: From the on-line measurements and information sent by DMS, the control module is executed.
- Step-02: For the current state of the system, the overall system state matrix is updated and the respective eigen values are derived.
- Step-03: If all the eigen values have negative real part, the normal-state voltage control module is enacted.
- Step-04: If at least one eigen value has a positive real part, the alert-state voltage control module is enacted.
- Step-05: The sensitivity matrix, S_M given by (10) is derived with the aid of analytical strategy proposed by authors in [50]. The sensitivity values for VAr support by the LG unit and the CB are S_{MQLG} and S_{MQCB}, respectively, where ΔV is voltage deviation for small change of the LG unit's reactive power (import/export), ΔQ_{LG} and CB's reactive power (export), ΔQ_{CB}.

$$\Delta V = \left[S_{MQLG} \mid S_{MQCB} \right] \begin{bmatrix} \Delta Q_{LG} \\ \Delta Q_{CB} \end{bmatrix}, \qquad S_M = \left[S_{MQLG} \mid S_{MQCB} \right] \tag{10}$$

- Step-06: The operational sequence of VAr support devices (i.e., LG units and CBs) which are going to be utilised for coordinated VAr support is determined based on the amount of voltage correction offered by each device (i.e., maximum to minimum in order), which is derived using two parameters. They are (i) the sensitivity values derived in Step-05, and (ii) capability of the VAr devices for supporting the system voltage. The generalised sequence in terms of time delays, *T* is given by (11). The control logic adopted for local control of CB is given by (12); where *t, V_{CB}, SCB_t*, V_{ON} and V_{OFF} denote time, CB target point voltage, switching position, switching *ON* voltage and switching *OFF* voltage, respectively. The local controllers of LG unit VAr control and OLTCs are discussed in [52].

$$T_{LG-larger} < T_{LG-smaller} < T_{CB-larger} < . < T_{CB-smaller} < OLTC_{upstream} < OLTC_{downstream} \tag{11}$$

$$SCB_{(t+1)} = \begin{cases} ON & \text{if } SCB_t = OFF \text{ and } V_{CB} < V_{ON} \\ SCB_t & \text{if } V_{ON} \le V_{CB} \le V_{OFF} \\ OFF & \text{if } SCB_t = ON \text{ and } V_{CB} > V_{OFF} \end{cases} \tag{12}$$

- Step-07: The new VAr reference values for selected VAr support devices (i.e., LG units and CBs) are identified subject to operational sequence derived under Step-06, system constraints and capability limits of the LG units and CBs, where objective is to ensure stable system operation without OLTC limit cycles and maintain the system voltage within stipulated limits.

- Step-08: The updated VAr reference values are assigned for local controllers of the LG units and CBs.

- Step-09: The OLTC local controllers are enabled.

- Step-10: For the subsequent instances of time (i.e., $t = t + 1$), repeat the procedure starting from Step-01.

Flow chart of the proposed voltage control algorithm prior to enacting OLTC tap operations is shown in Figure 8.12.

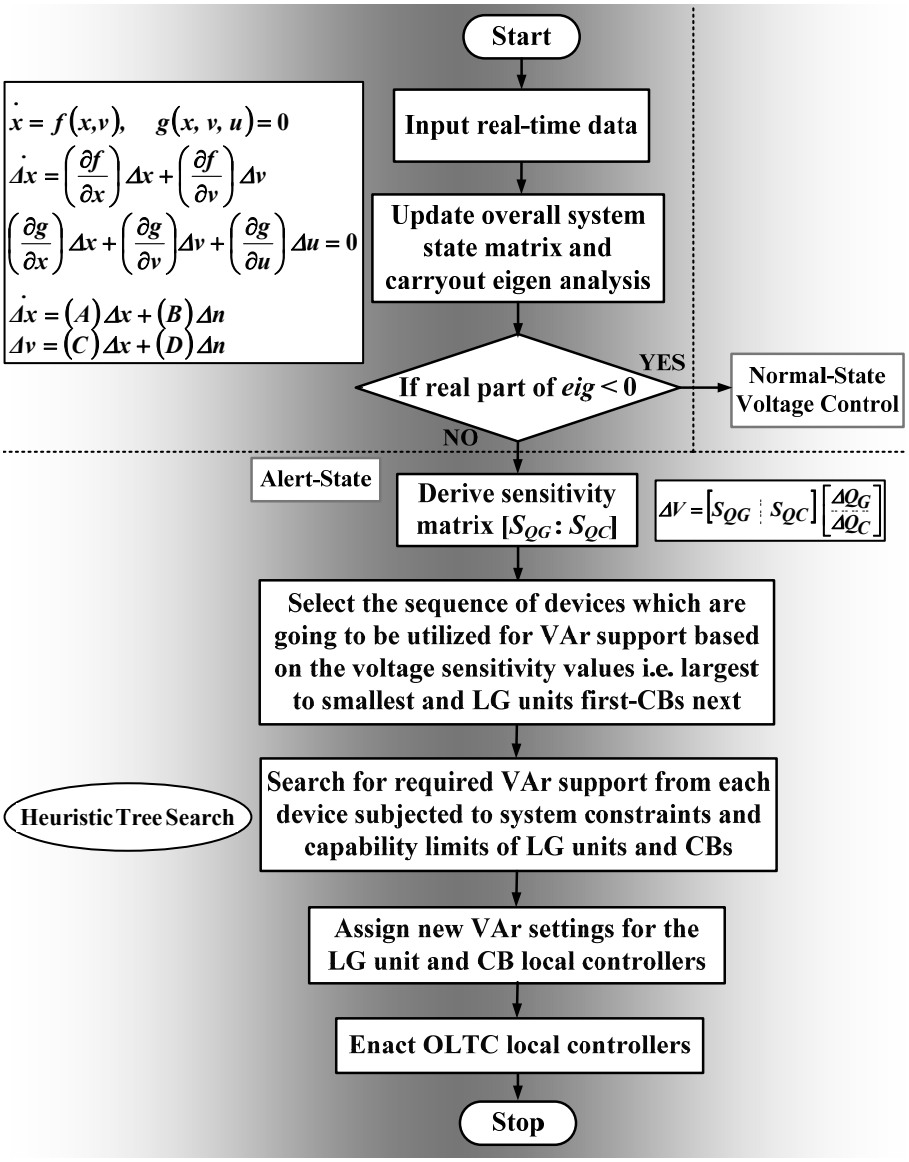

Figure 8.12: Flow chart of the proposed voltage control algorithm with capability of mitigating OLTC limit cycles

The voltage control strategy proposed in Chapter 7 can be used for normal-state voltage control in conjunction with the proposed strategy of mitigating OLTC limit cycles. It is an online voltage control strategy which is designed and tested for correcting the system voltage with control-coordination ascertaining voltage support by LG units in the system. Also, it ensures prioritised voltage support operation of LG units and the voltage control devices, and aids in blocking simultaneous operations, thereby minimising the adverse effects of DG-voltage

control device interactions. However, even with this voltage control, there could be a possibility of recurrence of OLTC limit cycles in presence of LG; since there is not any mechanism to avoid OLTC limit cycles.

Design of the proposed control module contains the embedded mathematical model of the power system, model of the proposed control logic, search engine and the decision making control layer for enacting the VAr controllers of LG units, CBs and the tap operations of OLTCs. The search engine based on the proposed control algorithm, as detailed in the flow chart in Figure 8.12, is adopted in order to determine the control parameters of LG units and CBs.

The practical implementation strategy for proposed control is outlined in Figure 8.13 for the example electricity network with cascaded OLTCs shown in Figure 8.10. The proposed control modules are embedded in a grid substation centered DMS for on-line voltage control. The control panels of LG units and voltage regulating devices are proposed to be equipped with SCADA facilities.

The proposed control module is implemented to act as a separate module embedded in to a standard DMS, and it only utilises information from the DMS where control functions are independent from the outputs of the DMS. Also, substation centered advanced DMS schemes are capable of utilising user-defined algorithms and customised software/hardware to determine best operating settings for voltage control devices and LG units in real-time. It is to be noted that no major modifications are required to be implemented in the DMS for adopting the proposed voltage control scheme.

The proposed strategy is tested using different case studies, and performance analysis of the algorithm under different system operating conditions (i.e., states) is given in Sub-section 8.2.3.

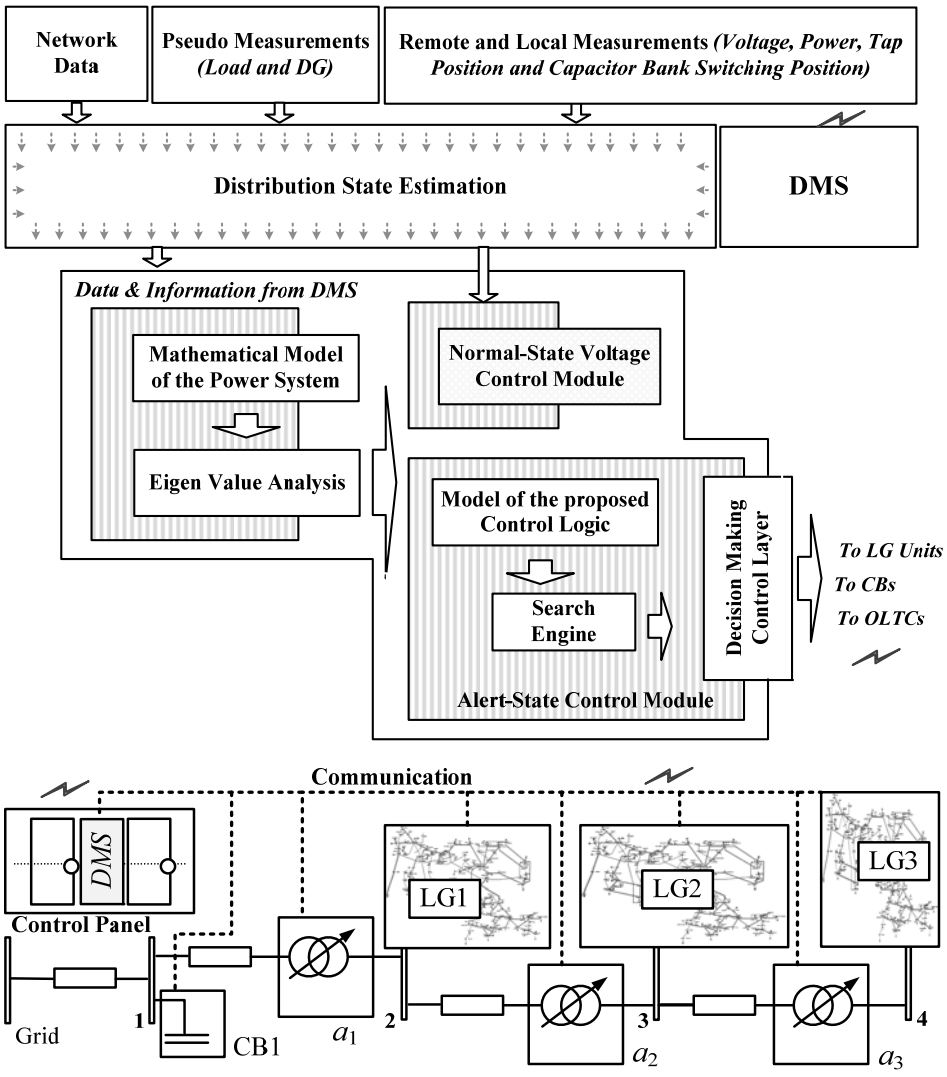

Figure 8.13: Topology of the on-line implementation of proposed control strategy for an electricity network with cascaded OLTCs, CB and multiple LG units

8.2.3 Test Case Study

In this sub-section the test case studies carried out for evaluating the performance of proposed OLTC limit cycle mitigation strategy, and the simulation results are presented.

8.2.3.1 Test Case Study-1

In this case study, the multi-bus test system shown in Figure 8.8 is considered. Data of some of the simulated operating points where OLTC limit cycles are predicted, are summarised in Table 8.5. For the OLTC, 32 taps are assumed with

+/- 0.1 pu voltage correction capacity. The proposed eigen value analysis which predicts OLTC limit cycles in each state is performed according to Step-01 to Step-03 of the proposed control strategy detailed in Sub-section 8.2.2. Results of the eigen value analysis are shown in Table 8.6.

Table 8.5: Simulated Test Data for the Multi-Bus System with Single OLTC

Simulated State-01	Simulated State-02	Simulated State-03
k_L = 1.00	k_L = 0.60	k_L = 0.85
P_L = 38.0 MW	P_L = 25.3 MW	P_L = 34.6 MW
Q_L = 0 MVAr	Q_L = (-) 2.3 MVAr	Q_L = (+) 5.3 MVAr
n_{start} = 0.98750	n_{start} = 1.0000	n_{start} = 0.99375

Table 8.5: Bus Voltage and Results of Eigen Value Analysis (Real Part of the Eigen Values) for the Multi-Bus System with Single OLTC

Simulated State-01	Simulated State-02	Simulated State-03
Bus Voltages/(pu)	Bus Voltages/(pu)	Bus Voltages/(pu)
V_1= 1.000 V_2= 0.984 V_3= 0.970 V_4= 0.963 V_5= 0.971 V_6= 0.972	V_1= 1.000 V_2= 0.989 V_3= 0.972 V_4= 0.966 V_5= 0.971 V_6= 0.970	V_1= 1.000 V_2= 0.990 V_3= 0.981 V_4= 0.979 V_5= 0.997 V_6= 1.000
Real Part-Eigen Values	Real Part-Eigen Values	Real Part-Eigen Values
+ 0.0044	+ 0.0003	+ 0.0010
- 0.0188	+ 0.0003	+ 0.0010
- 0.0174	- 0.0180	- 0.0186
- 0.0011	- 0.0171	- 0.0174
- 0.0078	- 0.0079	- 0.0078
- 0.0081	- 0.0082	- 0.0081

Subsequently, as in the Step-04 of the proposed algorithm, voltage control is moved to an alert state if OLTC limit cycle is predicted. Accordingly, as in the Step-05, the sensitivity matrix, S_M is derived. The sensitivity matrix for each state (i.e., $S_{M(i)}$, i=01 to 03) where OLTC limit cycles are predicted is shown in (13).

The buses of the test system are counted from the substation-grid (slack bus) as shown in the Figure 8.8.

$$S_{M(01)} = \begin{bmatrix} 0.0762 \\ 0.1969 \\ 0.2748 \\ 0.4296 \\ 0.4733 \end{bmatrix}, \quad S_{M(02)} = \begin{bmatrix} 0.0733 \\ 0.1902 \\ 0.2671 \\ 0.4228 \\ 0.4670 \end{bmatrix}, \quad S_{M(03)} = \begin{bmatrix} 0.0706 \\ 0.1828 \\ 0.2556 \\ 0.4011 \\ 0.4426 \end{bmatrix} \tag{13}$$

Next, the sequence of VAr support devices which are going to be utilised for coordinated VAr support is determined as in Step-06 (in this case only LG unit). According to Step-07, the new VAr reference value for LG unit is derived. The simulation results are shown in Table 8.7. The eigen value analysis is also performed with the new VAr settings in order to compare the results in respective pre alert-state control (Table 8.5). Next, only in the alert-states, the updated VAr reference values are assigned to the local controller of LG unit according to Step-08, where the OLTC local controller is enacted according to Step-09 of the proposed algorithm. In other states of the system, the voltage control is in normal-state after the Step-03 of the proposed control. In the Step-10, next control-state is counted and enacted.

8.2.3.2 Test Case Study-2

In this case study, the multi-bus test system shown in Figure 8.10 is considered, including the same simulation data. In the presented simulated control state, a possibility of limit cycles in OLTC (a_1) and OLTC (a_2) is predicted according to Step-01 to Step-03 of the proposed control algorithm detailed earlier in Sub-section 8.2.2. The results of the proposed eigen value analysis which predicts OLTC limit cycles are shown in Table 8.7. Subsequently (as in the Step-04 of the proposed algorithm), voltage control is moved to an alert-state. According to Step-05, the sensitivity matrix, S_M is derived. The sensitivity matrix where OLTC limit cycles are predicted is shown in (14). Next, the sequence of VAr support devices (i.e., LG units and CB) which are going to be utilised for coordinated VAr support is determined as in Step-06, and it is shown in (15). According to Step-07, the new VAr reference values (export) for selected VAr support devices are derived and they are 10.200 MVAr, 1.900 MVAr, 0.300 MVAr and 25 MVAr, for LG2,

LG3, LG4 and CB respectively. In this case, the voltages at buses 1, 2, 3, and 4 are 1.007 pu, 0.998 pu, 0.988 pu and 0.985 pu, respectively. The results of the respective eigen value analysis are shown in Table 8.8. Finally, the updated VAr reference values are assigned to the local controllers of the LG units and CB, and the OLTC local controllers are enabled according to Step-08 and Step-09, respectively of the proposed algorithm. For the subsequent instance of time, $t=t+1$, the procedure is repeated starting from Step-01.

Table 8.7: VAr Reference Values, Bus Voltages and Results of Eigen Value Analysis (Real Part of the Eigen Values) under Proposed Control for the Multi-Bus System with Single OLTC

State-01	State-02	State-03
VAr Reference the LG Unit	VAr Reference the LG Unit	VAr Reference for the LG Unit
4.7 MVAr	1.8 MVAr	0.50 MVAr
Bus Voltages/(pu)	Bus Voltages/(pu)	Bus Voltages/(pu)
V_1= 1.000 V_2= 0.987 V_3= 0.979 V_4= 0.975 V_5= 0.991 V_6= 0.994	V_1= 1.000 V_2= 0.992 V_3= 0.980 V_4= 0.977 V_5= 0.988 V_6= 0.989	V_1= 1.000 V_2= 0.987 V_3= 0.979 V_4= 0.977 V_5= 0.987 V_6= 0.988
Real Part-Eigen Values	Real Part-Eigen Values	Real Part-Eigen Values
- 0.0189	- 0.0000	- 0.0003
- 0.0189	- 0.0000	- 0.0001
- 0.0089	- 0.0181	- 0.0185
- 0.0008	- 0.0172	- 0.0173
- 0.0078	- 0.0079	- 0.0078
- 0.0081	- 0.0082	- 0.0081

$$S_M = \left[S_{MQLG2} \mid S_{MQLG3} \mid S_{MQLG4} \mid S_{MQCB1} \right], \quad S_M = \begin{bmatrix} 0.0690 & 0.0639 & 0.0578 & 0.0548 \\ 0.1893 & 0.1753 & 0.1591 & 0.0571 \\ 0.9873 & 0.9144 & 0.1727 & 0.0620 \\ 0.9995 & 0.9770 & 0.1845 & 0.0662 \end{bmatrix} \tag{14}$$

$$T_{LG2} < T_{LG3} < T_{LG4} < T_{CB1} < OLTC_1 < OLTC_2 < OLTC_3 \tag{15}$$

Table 8.8: The Results of Eigen Value Analysis (Real Part of the Eigen Values) under Pre Alert-State and Alert-State for the Multi-Bus System with Cascaded OLTCs

Pre Alert-State					
+ 0.0140	- 0.0227	- 0.0139	- 0.0086	- 0.0010	- 0.0036
Alert-State					
- 0.0097	- 0.0200	- 0.0094	- 0.0094	- 0.0023	- 0.0037

According to the above analyses and simulation case studies, it is very clear that the proposed methodology of mitigating OLTC limit cycles is applicable to any network, after carefully simplifying and modeling the system and the associated control logic, compatible to implement the proposed algorithm.

8.3 Summary

This chapter discusses some of the short-term and long-term oscillations which can commonly be possible in active MV distribution systems subjected to normal-state voltage control, when the DG units are also utilised for Volt/VAr support in the system. Also, it presents an analysis detailing OLTC limit cycle phenomena and explores a mitigation strategy in the presence of local generation units. The OLTC limit cycles normally occur in electricity networks due to interactions among load dynamics and OLTC controls, resulting into sustained long term oscillations. The OLTC limit cycles due to interactions among different loads, OLTC controls and local generation operation have been thoroughly investigated. The level of reactive power compensation is used as one of the key parameters for mitigating OLTC limit cycles. The proposed mitigating strategy is developed based on dynamic VAr management in the network using reactive power capability of local generation units and CBs. The main contributions are (a) development of small signal model and application of describing function method for analysing OLTC limit cycles for power systems embedded with LG, (b) investigation and analysis of OLTC limit cycle phenomenon in presence of LG equipped with voltage control capabilities, and (c) development of a new strategy

for mitigating OLTC limit cycles in presence of LG, which is designed for *alert-state voltage control* in conjunction with conventional voltage control. On-line application of the proposed control strategy will effectively mitigate the sustained oscillations attributed to OLTC limit cycles in distribution networks embedded with LG.

CHAPTER 9: CONCLUSIONS AND RECOMMENDATIONS FOR FUTURE WORK

The concept of voltage and reactive power control is a fundamental requirement for delivering electric power (a) within appropriate voltage limits (stipulated by technical standards) in such a way that consumers' equipment operate flawlessly; and (b) by minimising power losses and maintaining load power factor close to unity. The relationship between voltage and reactive power varies based on the type of load, system topology, voltage and reactive power controllers' settings and their mode of operation, generation level, and the location of distributed energy resources. Energy storage and electric vehicle charging centres may also introduce significant impacts affecting distribution voltage and reactive power control. Therefore, it is clear that the complex and dynamic nature of these phenomena make the task of managing and operating electrical distribution systems more challenging thereby adversely affecting conventional voltage control. In this research project, the challenges associated with voltage control in MV distribution systems which also utilise DG for Volt/VAr control have been investigated, and mitigation strategies have been proposed.

The smart grid concept has dramatically changed the design and operation of voltage control systems in modern distribution systems. The objectives of voltage control have expanded considerably beyond simply maintaining acceptable voltage and power factor. The overall objective has now become *voltage and reactive power optimisation*, which has evolved over a period of time through stand-alone control, SCADA rule-based control, advanced analytics-based control, and DMS model-driven control. Consequently, the main objectives in modern distribution systems are to increase overall system efficiency, improve coordinated operation, implement demand side management, promote energy conservation, and improve power quality and the voltage stability margin. On the other hand, modern voltage control systems must also accommodate distributed energy resources, responding automatically when changes occur in the status or output level of these resources. In addition, these control systems should operate effectively following feeder reconfigurations which will happen more frequently

in a modern distribution grid due to optimal network reconfiguration, automatic service restoration, DG availability and other applications involving smart switching.

In the stand-alone controller approach, the voltage and reactive power are managed by individual, independent and stand-alone voltage and reactive power control devices based on local measurements. The advantages of such a system are: (a) zero or low cost (b) minimal learning curve (c) operation without field communications and (d) scalability (i.e. it can work with one feeder system or many). The weaknesses are: (a) operation without self-monitoring features (b) non optimal and coordinated operation under almost all conditions owing to larger built safety margin as a consequence of lack of visibility in remote conditions (c) lack of feasibility to respond to changing conditions in feeder systems (d) poor capability of handling scenarios with a high penetration of DG and (e) no option for overriding normal operation during power system emergencies.

In SCADA rule-based control, the voltage and reactive power control devices are operated based on distribution system measurements and fixed rules. This type of control has the following strengths: (a) self-monitoring capabilities (b) control actions based on feeder-level and system-level measurements (c) capability of coordinating distinct voltage and reactive power controls and (d) moderate operational cost when operated through distribution level SCADA (DSCADA). The possible weaknesses are (a) difficulty in handling highly meshed distribution systems with frequent switching and (b) poor performance in handling scenarios with a high penetration of DG and associated coordinated operations.

In the case of advanced analytics-based control, the voltage and reactive power control devices are operated based on the combination of measurement analysis, topology analysis and heuristics. Heuristics generally provide an alternative to computationally intensive mathematical formulations and analysis. The major strengths are (a) control actions not based on full blown impedance and/or topology based model (b) capability of adapting feeder reconfigurations and (c) capability of coordinating distinct voltage and reactive power controls. However,

advanced analytics-based control also has certain weaknesses, namely (a) requirement of a learning curve for control room operators (b) high cost of field equipment such as substation processors and measurement equipment, and (c) poor adaptation in scenarios with high penetration of DG under certain system conditions.

On the other hand, optimal voltage and reactive power controls, as with advanced analytics-based control, require a learning curve for control room operators. The cost for implementing, operating and sustaining these controls is potentially higher. They may also adopt highly complex mathematical models to achieve certain objectives. These controls have strengths such as (a) capability of coordinating distinct voltage and reactive power controls (b) capability of assigning various objectives (such as demand side management, reduction in power losses, reactive power area support and weighted combination of different objectives); (c) adaptive to feeder reconfigurations, and (d) capability of handling a high penetration of DG (i.e. handling reverse power flow and utilising DG for voltage and reactive power support). However, it is still unclear whether or not they can achieve fully coordinated operations under all system conditions. The solution for this case would be the adaptation of DMS model-based voltage and reactive power control which is an entirely new concept at the moment. This research project examined the above mentioned technical aspect for voltage control in MV distribution systems embedded with DG. The specific thesis contributions are summarised below.

9.1 Summary of Contributions

In Chapter 3, possibility for DG-voltage control device interactions under optimal Volt/VAr control in modern distribution systems utilising DG for Volt/VAr support, is examined. In the optimisation formulations, operating the fast responding Volt/VAr support DG units on priority appears to be a strategy for minimising the maneuvers of tap changing devices and CBs while achieving other objectives of the optimal Volt/VAr control. However, in reality, it would not always be the case due to the possibilities for DG - voltage control device interactions. It has been identified that the optimal control set-point re-adjustment

in different Volt/VAr control devices needs to be carried out in conjunction with the proposed coordinated operation of multiple voltage control devices (i.e., by modifications in the optimisation formulation and search method while minimising the effects of variability in the DG power output), in order to minimise the DG-voltage control device interactions and adverse effects of the resultant conflicting operations.

In Chapter 4, the theory of the proposed novel voltage control strategy is established. The theory is fundamentally based on the concepts of *simultaneous and non-simultaneous responses* of voltage control devices and DG units, and *virtual time delay*. Typically, these responses can be OLTC and SVR tap operations, CB switching operations, the operation of other voltage control devices and updations in the DG controllers. In addition, a small signal model was proposed in Chapter 4 for analysing the impact of simultaneous and non-simultaneous responses of voltage control devices and DG units while preserving the system dynamics. Moreover, the concept of virtual time delay was introduced and has been proposed to apply mainly through dynamically re-tuning the voltage controller parameters using a sophisticated tuning algorithm for coordination of voltage control devices and DG units.

In Chapter 5, the proposed algorithm for tuning control parameters of Volt/VAr control devices has been detailed. It is mainly based on the requirement of applying virtual time delay through facilitating the options for (a) deriving and updating local controller settings for voltage control devices and Volt/VAr support DG units (b) maintaining minimal tap and CB switching operations (c) reducing voltage swings (up and down) mainly on feeder buses closer to DG units during time-delayed operation of voltage control devices, and (d) eliminating cases of voltage fluctuations on feeder buses. It was shown that the proposed tuning algorithm is capable of achieving the technical aspects highlighted above for implementing voltage control in modern distribution systems. Also, the techniques incorporated in the proposed problem formulation and search method lead to a novel approach for optimal voltage and reactive power control in distribution systems embedded with multiple voltage control devices and

Volt/VAr support DG units. Moreover, the proposed tuning algorithm can be implemented in substation-centred DMS as a separate module for online voltage control.

In Chapter 6, the proposed coordinated voltage control strategy, which considers simultaneous responses of multiple voltage control devices and DG units, has been detailed. In the proposed strategy, the control design is based on three main aspects (a) maximising voltage regulation support by DG through the DG voltage control module (DG-VCM) (b) procuring online load centre voltage measurements for SVRs and CBs, and (c) real-time control to avoid simultaneous operations of multiple voltage control devices and DG-VCM by means of the control module for blocking simultaneous responses (CM-BSO). The algorithm embedded in DG-VCM also exploits the reactive capability of DG in order to maximise the voltage regulation support. In addition, advanced position sensors are introduced at each voltage control device physical mechanism to determine the state of progressive tap or CB switching operation. Moreover, the edge detection technology is incorporated in CM-BSO to detect the state of progression for each DG-VCM and voltage control device operation. Furthermore, a practical implementation strategy for the proposed voltage control has been detailed, which utilises the substation centred DMS for real world operation.

In Chapter 7, the proposed coordinated voltage control strategy, which considers non-simultaneous responses (in addition to simultaneous responses) of multiple voltage control devices and Volt/VAr support DG units, has been described. This strategy is capable of coordinating the operation of multiple voltage control devices and the DG units, and operates the DG units on a priority basis to maximise their voltage support, in order to minimise the adverse effects of interactions which can occur not only due to simultaneous but also to non-simultaneous responses of voltage control devices and DG systems. The control actions are fundamentally based on the structural information derived by adopting electrical distance estimation, which is used to determine the sequence of operation for DG units and voltage control devices. Therefore, it can also effectively assess the impact of control interactions in presence of structural

changes and DG availability in a network. A practical implementation strategy for the proposed voltage control has also been detailed, which utilises the substation-centred DMS for real-world operation. Moreover, a test system based on MATLAB® and SimuLink has been proposed for effectively and simplistically testing the coordinated voltage control algorithm at the design stage.

In Chapter 8, oscillations which can occur in modern MV distribution systems subjected to normal-state voltage control have been investigated and analysed. The occurrences of these oscillations are possible when DG is also utilised for system Volt/VAr support. Through the associated case studies in Chapter 8, it has been found that significant and frequent inter-unit electro-mechanical oscillations can occur in nearby synchronous machine-based DG units, influenced by (a) the low inertia coefficient associated with small machines and (b) the operation of the excitation system, which deteriorates the damping of oscillations that follow the first rotor swing after the perturbation where a fast responding excitation system reduces the damping torque component. In addition, it has been found that the recurrence of sustained oscillations induced by OLTC limit cycles due to interactions between load, OLTC controls and the local DG operation could be a concern. The proposed research in Chapter 8 has outlined ways of mitigating these oscillations through supplementary control and alert-state control for modern distribution systems.

In Appendix-I, the possible Volt/VAr management issues under CVR is elaborated. In Appendix-II, a static tool has been developed and tested for estimating the impact of DG on the operation of voltage control devices enacted with LDC modes. The development of this tool was motivated by the requirement of the DNO to have a unique method for assessing the impact of DG on the operation of LDC modes in different voltage control devices, rather than running multiple power flow cases and carrying out the associated recurrence calculations. The proposed mathematical model, which is fundamentally based on deriving first-order voltage sensitivity at the load centre defined for the LDC, helps in devising a static tool to estimate the impact of DG on the operation of voltage control devices enacted with LDC modes. In Appendix-III, a typical testing

methodology, which is used for testing and validating newly designed voltage controllers is outlined.

9.2 Recommendations for Further Work

Majority of future distribution systems in developed countries will be fully automated in the same manner as that of the distribution systems in the state of Alabama, USA (as indicated earlier). In addition, these smart distribution systems will be embedded with a higher level of renewable energy resources, energy storage systems, micro-grids, DMSs, advanced sensors and metering equipment, and sophisticated real-time controls and monitoring. On the other hand, distribution systems in rural areas, isolated communities and developing countries may not be greatly improved compared to their present state. However, in such locations, significant integration of renewable energy resources could be achieved with the aid of energy storage systems and satisfactory improvements in decentralised controls. Moreover, current distribution system planning and operational guidelines need to be revised to encompass the integration of electric vehicle charging centres. Therefore, distribution system operation will continue to pose challenges and will also require dedicated research in the area of voltage control. Some of the future research directions are as below:

- Testing the performance of proposed voltage control strategy incorporating the models of micro-grids, different renewable energy resources, energy storage systems and fast Volt/VAr support devices such as distributed static compensators into the test distribution systems
- Testing the proposed voltage control strategy incorporating the models of multiple electric-vehicle battery-charging stations including variable charging patterns
- Altering the proposed voltage control strategy considering upstream as well as downstream voltage controls in LV distribution feeder systems

- Testing and evaluating dynamic performance of the proposed controllers in the presence of large perturbations, and accordingly designing appropriate dynamic-state voltage control strategies
- Developing detailed models of different distribution systems for investigating the dynamic interactions subjected to voltage control in the presence of renewable and non-renewable energy resources
- Developing distribution level auxiliary and alert-state controls for mitigating the network oscillations thereby examining dynamic aspects associated with modern distribution systems

REFERENCES

[1] W. H. Kersting. *Distribution System Modelling and Analysis*. CRS Press, 2002.

[2] A. Pahwa, G. Simard, G. L. Clark, B. Uluski, B. J. Deaver, E. Boardman, J. R. Aguero, G. Gilchrist, and T. Saxton. *Smart Distribution Systems*. Tutorial at the IEEE/PES Annual General Meeting and Conference, 2014.

[3] J. J. Erbrink. *On-load Tap Changer Diagnosis on High-Voltage Power Transformers using Dynamic Resistance Measurements*. Ph.D. dissertation, Delft University of Technology, 2011.

[4] A. Prieto, M. Cuesto, P. Pacheco, M. Oliva, L. Prieto, A. Fernandez, L. Navarro, H. Gago, and M. Burgos. Optimisation of power transformers based on operative service conditions for improved performance. In *Proc. CIGRE*, 2012.

[5] F. A. Viawan. *Voltage Control and Voltage Stability of Power Distribution Systems in the Presence of Distributed Generation*. Ph.D. dissertation, Chalmers University, 2008.

[6] R. A. Walling, R. Saint, R. C. Dugan, J. Burke, and L. A. Kojovic. Summary of distributed resources impact on power delivery system. *IEEE Trans. on Power Delivery*, 23(3):1636–1644, Jul. 2008.

[7] A. Einfalt, F. Kupzog, H. Brunner, and A. Lugmaier. Control Strategies for Smart Low Voltage Grids. In *Proc. CIRED*, 2012.

[8] P. Kundur. *Power System Stability and Control*. McGraw-Hill, 1994.

[9] G. M. Masters. *Renewable and Efficient Electric Power Systems*. John Wiley & Sons, 2004.

[10] T. T. Quoc, L. L. Thanh, C. Andrieu, N. Hadjsaid, C. Kieny, J.C. Sabonnadière, K. Le, O. Devaux, and O. Chilard. Stability Analysis for the Distribution Networks with Distributed Generation. In *Proc. IEEE/PES Transmission and Distribution Conference*, pages 289-294, 2006.

[11] W. Freitas, J. C. M. Vieira, A. Morelato, and W. Xu. Influence of Excitation System Control Modes on the Allowable Penetration Level of Distributed Synchronous Generators. *IEEE Trans. on Energy Conversion*, 20(2):474–480, Jun. 2005.

[12] Y. J. Kim, S.J. Ahn, P.I. Hwang, G. C. Pyo, and S. I. Moon. Coordinated Control of a DG and Voltage Control Devices Using a Dynamic Programming Algorithm. *IEEE Trans. on Power Systems*, 28(1):42-51, Feb. 2013.

[13] F. A. Viawan, *and* D. Karlsson. Combined Local and Remote Voltage and Reactive Power Control in the Presence of Induction Machine Distributed Generation. *IEEE Trans. on Power Systems*, 22(4):2003-2012, Nov. 2007.

[14] A. Kulmala, S. Repo, and P. Jarventausta. Coordinated Voltage Control in Distribution Networks Including Several Distributed Energy Resources. *IEEE Trans. on Smart Grid,* 5(4):2010-2020, Jul. 2014.

[15] K. Alobeidli, and M. S. E. Moursi. Novel Coordinated Secondary Voltage Control Strategy for Efficient Utilisation of Distributed Generations. *IET Renewable Power Generation,* 8(5):569-579, Jan. 2014.

[16] M. S. E. Moursi, H. H. Zeineldin, J. L. Kirtley, and K. Alobeidli. A Dynamic Master/Slave Reactive Power-Management Scheme for Smart Grids with Distributed Generation. *IEEE Trans. on Power Delivery,* 29(3):1157-1167, Jun. 2014.

[17] L. Yu, D. Czarkowski, and F. D Leon. Optimal Distributed Voltage Regulation for Secondary Networks with DGs. *IEEE Trans. on Smart Grid,* 3(2):959-967, Jun. 2012.

[18] S. C. E. Jupe, P.C. Taylor, and A. Michiorri. Coordinated Output Control of Multiple Distributed Generation Schemes. *IET Renewable Power Generation,* 4(3):283-297, Jan. 2010.

[19] T. Senjyu Y. Miyazato, A. Yona, N. Urasaki, and T. Funabashi. Optimal Distribution Voltage Control and Coordination with Distributed Generation. *IEEE Trans. on Power Delivery,* 23(2):1236-1242, Apr. 2008.

[20] Y. Yamamoto, S. Yoshizawa, J. Yoshinaga, and Y. Hayashi. Verification of Efficiency of Searching Methods Determining Optimal Control Parameters of Advanced SVRs. In *Proc. IEEE International Energy Conference*, pages 1076-1082, 2014.

[21] X. Liu, A. Aichhorn, L. Liu, and H. Li. Coordinated Control of Distributed Energy Storage System with Tap Changer Transformers for Voltage Rise Mitigation Under High Photovoltaic Penetration. *IEEE Trans. on Smart Grid,* 3(2):897-906, Jun. 2012.

[22] M. E. Elkhatib, R. E. Shatshat, and M. M. A. Salama. Novel Coordinated Voltage Control for Smart Distribution Networks with DG. *IEEE Trans. on Smart Grid,* 2(4):598-605, Dec. 2011.

[23] F. Bignucolo, R. Caldon, and V. Prandoni. Radial MV Networks Voltage Regulation with Distribution Management System Coordinated Controller. *Electric Power Systems Research*, 78(4):634-645, Apr. 2008.

[24] F. A. Viawan and D. Karlsson. Voltage and reactive power control in distribution systems with synchronous machine-based distributed generation. *IEEE Trans. on Power Delivery*, 23(2):1079–1087, Apr. 2008.

[25] P. H. Nguyen, J. M. A. Myrzik, and W. L. Kling. Coordination of Voltage Regulation in Active Networks. In *Proc. IEEE/PES Transmission and Distribution Conference,* 2008.

[26] F. A. Viawan, and D. Karlsson. Coordinated Voltage and Reactive Power Control in the Presence of Distributed Generation. In *Proc. Power and Energy Society General Meeting and Conference*, 2008.

[27] A. Augugliaro, L. Dusonchet, S. Favuzza, and E. R. Sanseverino. Voltage Regulation and Power Losses Minimization in Automated Distribution Networks by an Evolutionary Multi-objective Approach. *IEEE Trans. on Power Systems*, 19(3):1516-1527, Aug. 2004.

[28] A. D.T. Le, M. A. Kashem, M. Negnevitsky, and G. Ledwich. Optimal Distributed Generation Parameters for Reducing Losses with Economic Consideration. In *Proc. IEEE Power Engineering Society General Meeting and Conf*erence, 2007.

[29] M. A. Kashem, V. Ganapathy, G. B. Jasmon, and M. I. Buhari. A Novel Method for Loss Minimization in Distribution Systems. In *Proc. Electric Utility Deregulation and Restructuring and Power Technologies Conference*, pages 251-256, 2000.

[30] A. Chanhome, S. Phichaisawat, and S. Chaitusaney. Voltage Regulation in Distribution System by Considering Uncertainty from Renewable Energy. In *Proc. IEEE Electrical Engineering/Electronics, Computer, Telecommunications and Information Technology Conference,* 2012.

[31] J. H. Choi, and J. C. Kim. Advanced Voltage Regulation Method of Power Distribution Systems Interconnected with Dispersed Storage and Generation Systems. *IEEE Trans. on Power Delivery,* 16(2):329-334, Apr. 2001.

[32] Y. Kubota, T. Genji, S. Takayama, and F. Fukuyama. Influence of Distribution Voltage Control Methods on Maximum Capacity of Distributed Generators. *Electrical Engineering in Japan*, 150(1):8-17, Jan. 2005.

[33] A. Borghetti, M. Bosetti, S. Grillo, S. Massucco, C. A. Nucci, M. Paolone, and F. Silvestro. Short-term Scheduling and Control of Active Distribution Systems with High Penetration of Renewable Resources. *IEEE Systems Journal*, 4(3):313-322, Sep. 2010.

[34] J. Zhu. *Optimization of Power System Operation*. John Wiley & Sons, 2009.

[35] R. Caldon, F. Rossetto, and A. Scala. Reactive Power Control in Distribution Networks with Dispersed Generation: A Cost based Method. *Electric Power Systems Research*, 64(1):209-217, Jan. 2003.

[36] K. Zou, A. P. Agalgaonkar, K. M. Muttaqi, and S. Perera. Distribution System Planning with Incorporating DG Reactive Capability and System Uncertainties. *IEEE Trans. on Sustainable Energy*, 3(1):112-123, Jan. 2012.

[37] M. Bakr. *Nonlinear Optimisation in Electrical Engineering with Applications in MATLAB*. IET Press, 2013.

[38] D. Ranamuka, A. P. Agalgaonkar, and K. M. Muttaqi. Investigating the Operation of Multiple Voltage Regulators and DG in a Distribution Feeder. *Energy Procedia*, 14(1):1945-1950, Mar. 2012.

[39] R. A. Walling, R. Saint, R. C. Dugan, J. Burke, and L. A. Kojovic. Summary of distributed resources impact on power delivery system. *IEEE Trans. on Power Delivery,* 23(3):1636–1644, Jul. 2008.

[40] D. Ranamuka, A. P. Agalgaonkar, and K. M. Muttaqi. Mitigating Tap-changer Limit Cycles in Modern Electricity Networks Embedded with Local Generation Units. In *Proc. IEEE/IAS Annual Meeting and Conference,* 2014.

[41] K. E. Yeager, and J. R. Willis. Modelling of Emergency Diesel Generators in an 800 Megawatt Nuclear Power Plant. *IEEE Trans. on Energy Conversion*, 8(3):433–441, Sep. 1993.

[42] M. R. R. Mojumdar, P. Arboleya, and C. G. Moran. Step-Voltage Regulator Model Test System. In *Proc. IEEE/IAS Annual Meeting and Conference*, 2015.

[43] R. Lind, and D. Karlsson. Distribution System Modelling for Voltage Stability Studies. *IEEE Trans. on Power Systems*, 11(4):1677-1682, Nov. 1996.

[44] M. L. Crenshaw, K. E. Bollinger, R. T. Byerly, R. L. Cresap, L. E. Eilts, D. E. Eyre, F. W. Keay, P. Kundur, E. V. Larsen, D. C. Lee, J. F. Luini, R. G. Pillote, and P.L. Dandeno, Others contributing to the work of this group are K.C. Bess, H.H. Chen and D.G. Ramey. Excitation System Models for Power System Stability Studies. *IEEE Trans. on Power Apparatus and Systems*, 100(2):494-509, Feb. 1981.

[45] T. Theubou, R. Wamkeue, and I. Kamwa. Dynamic Model of Diesel Generator Set for Hybrid Wind-Diesel Small Grids Applications. In *Proc. IEEE Canadian Electrical and Computer Engineering Conference*, 2012.

[46] D. G. Ramey, and J. W. Skooglund. Detailed Hydro-governor Representation for System Stability Studies. *IEEE Trans. on Power Apparatus and Systems*, 89(1):106-112, Jan. 1970.

[47] W. B. Gish. Small Induction Generator and Synchronous Generator Constants for DSG Isolation Studies. *IEEE Trans. on Power Systems*, 1(2): 231-239, Apr. 1986.

[48] T. Lund, P. Sorensen, and J. Eek. Reactive Power Capability of a Wind Turbine with Doubly Fed Induction Generator. *Wind Energy*, 10(1):379–394, Apr. 2007.

[49] F. Delfino, G. B. Denegri, M. Invernizzi, R. Procopio, and G. Ronda. A P-Q Capability Chart Approach to Characterize Grid Connect PV-Units. In *Proc. CIGRE/IEEE PES Joint Symposium*, Jul. 2009.

[50] D. Ranamuka, A. P. Agalgaonkar, and K. M. Muttaqi. Dynamic Adjustment of OLTC Parameters using Voltage Sensitivity while utilising DG for Volt/VAr Support. In *Proc. IEEE/PES Annual Meeting and Conference*, 2014.

[51] M. V. V. S. Yalla, B. Uluski, M. Simms, V. Dabic, L. Conrad, M. Baran, B. Stephens, P. Powell, and B. Milosevic. *Distribution Volt-VAr Control and Optimization*. Tutorial at the IEEE/PES Annual General Meeting and Conference, 2016.

[52] D. Ranamuka, A. P. Agalgaonkar, and K. M. Muttaqi. On-line Voltage Control in Distribution Systems with Multiple Voltage Regulating Devices. *IEEE Trans. on Sustainable Energy*, 5(2):617-628, Apr. 2014.

[53] J. J. Grainger, and S. Civanler. Volt/VAr Control on Distribution Systems with Lateral Branches Using Shunt Capacitors and Voltage Regulators Part I: The Overall Problem. *IEEE Trans. on Power Apparatus and Systems*, 104(1):3278-3283, Nov. 1985.

[54] N. Mwakabuta, and A. Sekar. Comparative Study of the IEEE 34 Node Test Feeder under Practical Simplifications. In *Proc. NAPS Conference*, pages 484-491, 2007.

[55] NR Electric. Distribution Management System. http://www.nrelect.com

[56] B. Uluski. *Distribution Management Systems*. Presented at the CRN Summit, Cleveland Ohio, 2011.

[57] ABB. Network Manger SCADA/DMS Distribution Network Management. http://www.abb.com

[58] S. Ghosal, and R. Mehrotra. Detection of Composite Edges. *IEEE Trans. on Image Processing*, 3(1):14-25, Jan. 1994.

[59] J. Zhong, E. Nobile, and K. Bhattacharya. Localized Reactive Power Markets Using the Concept of Voltage Control Areas. *IEEE Trans. on Power Systems*, 19(3):1555-1561, Aug. 2004.

[60] P. Lagonotte, J. C. Sabonnadiere, J. Y. Leost, and J. P. Paul. Structural analysis of the electrical system: Application to secondary voltage control in France. *IEEE Trans. on Power Systems*, 4(2):479-486, May 1989.

[61] R. H. Salim, M. Oleskovicz, and R. A. Ramos. Power Quality of Distributed Generation Systems as Affected by Electromechanical Oscillations – Definitions and Possible Solutions. *IET Generation, Transmission & Distribution*, 5(11):1114-1123, Jan 2011.

[62] M. Basler, and R. C. Schaefer. Understanding Power System Stability. *IEEE Trans. on Industry Applications*, 44(2):463-474, Mar. 2008.

[63] C. M. Ong. Dynamic Simulation of Electric Machinery Using MATLAB-Simulink. Prentice-Hall, 1998.

[64] D. Ranamuka, A. P. Agalgaonkar, and K. M. Muttaqi. Simulink Model for Examining Dynamic Interactions Involving Electro-Mechanical Oscillations in Distribution Systems. In *Proc. Australasia Power Engineering Conference (AUPEC)*, 2015.

[65] MathWorks. Simulink User Guide. http:// www.mathworks.com

[66] V. Donde, and I. A. Hiskens. Analysis of Tap-Induced Oscillations Observed in an Electrical Distribution System. *IEEE Trans. on Power Systems*, 22(4):1881-1887, Nov. 2007.

[67] I. Hiskens and M. Pai. Trajectory sensitivity analysis of hybrid systems. *IEEE Trans. on Circuits and Systems*, 47(2):204–220, Feb. 2000.

[68] R. Seydel. *Practical Bifurcation and Stability Analysis*. Springer, 1994.

[69] P. Reddy and I. Hiskens. Limit-induced stable limit cycles in power systems. In *Proc. Power Tech Conference*, Jun. 2007.

[70] M. Larsson, D. H. Popovic, and D. J. Hill. Limit Cycles in Power Systems due to OLTC Deadbands and Load-Voltage Dynamics. *Electric Power Systems Research,* 47(3):181-188, Nov. 1998.

[71] V. Donde, and I. A. Hiskens. Analysis of Limit Cycle Stability in A Tap-Changing Transformer. In *Proc. IEEE Circuits and Systems Conference*, pages 693-696, 2002.

[72] Q. Wu, D. H. Popovic, and D. J. Hill. Avoiding Sustained Oscillations in Power Systems with Tap Changing Transformers. *International Journal of Electrical Power & Energy Systems*, 22(8):597-605, Nov. 2000.

[73] J. Medanic, M. Ilic-Spong, and J. Christensen. Discrete Models of Slow Voltage Dynamics for Under Load Tap-Changing Transformer Coordination. *IEEE Trans. on Power Systems*, 2(4):873-880, Nov. 1987.

[74] J. C. Hsu, and A. U. Meyer. *Modern Control Principles and Applications*. McGraw-Hill, 1968.

[75] L. L. Grigsby. *Power System Stability and Control*. Taylor & Francis, 2007.

[76] R. Graham. *Power System Oscillations*. Kluwer Academic, 1994.

[77] N. Jenkins, R. Allan, P. Crossley, D. Kirschen and G. Strbac. *Embedded Generation.* Cambridge University Press, 2000.

[78] D. K. Khatod, V. Pant, and J. Sharma. A Novel Approach for Sensitivity Calculations in the Radial Distribution System. *IEEE Trans. on Power Delivery*, 21(4):2048-2057, Oct. 2006.

[79] SimPowerSystems, T. M. "Reference, Hydro-Québec and the MathWorks." Inc., Natick, MA (2010).

[80] [Online]. Available: http://www.abs.gov.au

[81] M. D. Aguilo, J. Sandraz, R. Macwan, F. D. Leon, D. Czarkowski, C. Comack, and D. Wang. Field-Validated Load Model for the Analysis of CVR in Distribution Secondary Networks: Energy Conservation. *IEEE Trans. Power Delivery*, 28(4): 2428–2436, Oct. 2013.

[82] H. Ravindra, M. O. Faruque, K. Schoder, R. Meeker, M. Steurer, and P. McLaren. Modeling and Validation of a Utility Feeder for Study of Voltage Regulation in the Presence of High PV Penetration. In *Proc. IEEE T&D Conference and Exposition*, pages 1-5, 2014.

APPENDIX-I: CASE STUDY ON CONSERVATION VOLTAGE REDUCTION AND VAR MANAGEMENT

Modern distribution systems are mainly characterised by behaviour of non-linear consumer loads, stochastic nature of load variations and voltage dependency, intermittency of distributed generation (DG) especially roof-top and distributed solar-PV; and thereby frequent operation of Volt/VAr control devices. Conservation voltage reduction (CVR) has been adopted by most of the distribution utilities as a viable technique for peak-demand reduction and long-term energy savings. However, because of diversified and inherent characteristics associated with the modern distribution system operation, achieving high CVR factor, high power factor, minimum number of tap changer operations and low power losses could be a challenging task when solar-PV penetration level is high. In this Appendix, the issues associated with VAr management in urban distribution systems while implementing CVR in presence of highly intermittent solar-PV are analysed. This is not explicitly addressed in the literature in greater detail. Three conventional Volt/VAr control strategies were used to identify the specific technical aspects associated with CVR and VAr management in distribution power grids in the presence of high solar-PV penetration. A case study on urban distribution system operation with high penetration of solar PV has been carried out. It is revealed that a carefully design of Volt/VAr control strategy is required for successful implementation of CVR under high penetration of solar PV. It is worth noting that the research-work associated with this Appendix has been carried out in conjunction with the investigation studies in Chapter 3. The contents in this Appendix lead to the publication titled "Conservation Voltage Reduction and VAr Management Considering Urban Distribution System Operation with Solar-PV," authored by D. Ranamuka, A. P. Agalgaonkar, and K. M. Muttaqi, has been submitted to the *Renewable Energy Journal*.

AI.1 CVR Implementation Strategy

This section summarises the factors considered with CVR, and presents a strategy of CVR implementation.

AI.1.1 Factors Considered with CVR

The solar-PV profiles are selected depicting the possible causes shown in Figure AI.1(a). Conventional stand-alone Volt/VAr management schemes have been considered i.e., (a) a stand-alone control comprising substation OLTC, (b) a stand-alone control comprising substation OLTC with a CB, and (c) a stand-alone control comprising substation OLTC with multiple line CBs. The topologies of those control schemes are shown in Figure AI.1(b) for an example 3-bus distribution system, where feeder resistance and reactance values are given by R_L and X_L, respectively. It is noted that the variation in CVR factor as well as variations in power factor, losses, bus voltage magnitudes, operation of Volt/VAr control devices and reactive power drawn from the transmission system during the CVR period as well as CVR effects on specific consumer loads have been examined under normal-state operation.

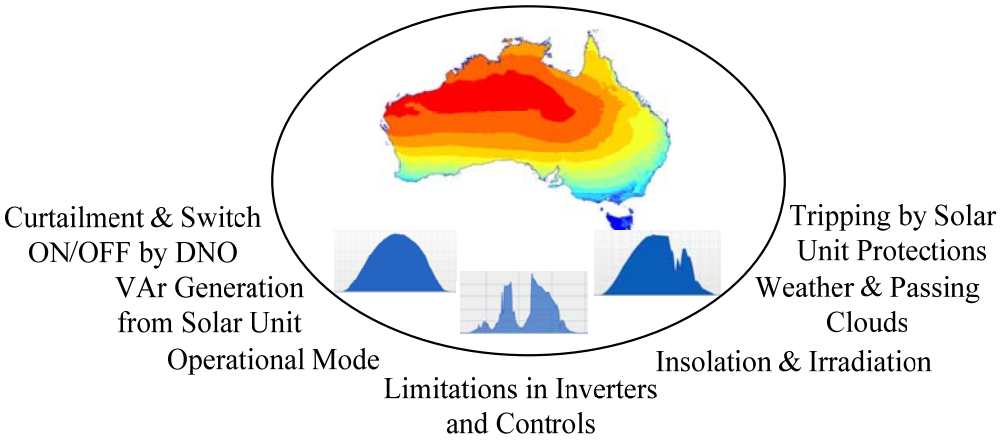

Figure AI.1: (a) Factors which can affect the power generation pattern of a solar unit, and (b) a typical network topology

AI.1.2 CVR Implementation Strategy

In this sub-section, the CVR implementation using: *1)* substation OLTC control, *2)* user defined model developed for incorporating time-series data of solar-PV and load profiles, and *3)* ZIP factors is briefly discussed.

The HV/MV substation OLTC controls have primarily been used for implementing CVR for the case study. The HV/MV substation analogy of the distribution system incorporating the stand-alone OLTC controls used for implementing CVR is shown in Figure AI.2. When implementing normal operation and operation under CVR; the stand-alone controller is enacted and updated with required control-parameters.

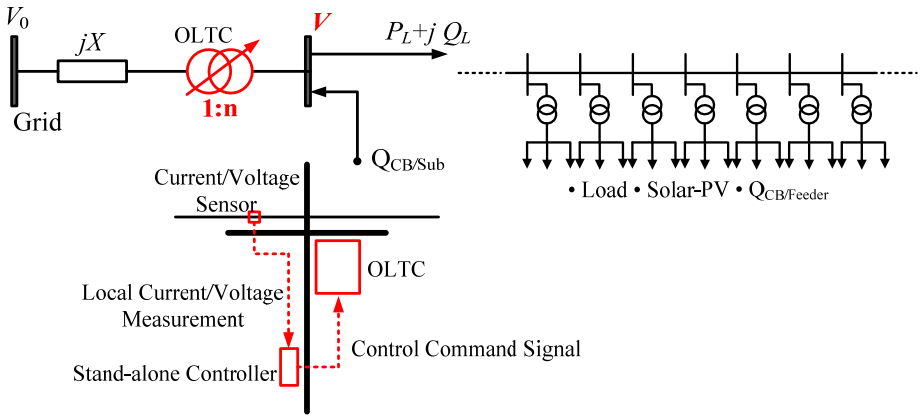

Figure AI.2: Substation analogy incorporating OLTC controls

Figure AI.3 shows the topology of user-defined model developed for incorporating time-series data of solar-PV and ZIP-load profiles. In the Load block shown in Figure AI.3, ZIP models are incorporated. The Load and Solar-PV blocks are interfaced with Meter block in order to obtain the real-time values of voltages, and thereby computing the real-time values of currents in Load and Solar-PV blocks. Both balanced/un-balanced 3-wire MV/4-wire LV systems can be modelled using this method. The transformers, distribution lines, OLTC, CBs, grid and transmission line can be modelled using the modelling approach discussed in [79].

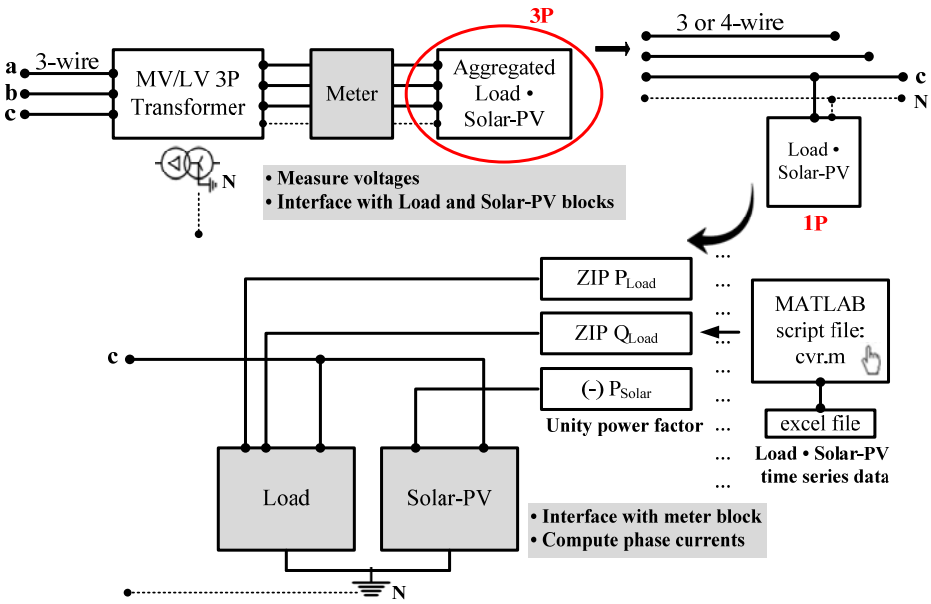

Figure AI.3: Topology of user defined load model

For load ZIP Factors, the ZIP-data of residential distribution feeder system are considered. Numerical values of the load-ZIP factors are given below [80]. These ZIP-factors are executed in the ZIP load model (Figure AI.3). The equipment ZIP factors and summarised load survey data are shown in Table AI.I and Table AI.II. The strategies for Deriving and testing load ZIP factors are detailed in [81].

$$Z_p = 0.92 \qquad I_p = 0.11 \qquad P_p = -0.03$$
$$Z_q = -3.15 \qquad I_q = 5.97 \qquad P_q = -1.82$$

TABLE AI.1
LOAD FACTORS OF CONSUMER EQUIPMENT

Equipment Type	*Zp*	*Ip*	*Pp*	*Zq*	*Iq*	*Pq*
Space heater	1.00	0.00	0.00	0.00	0.00	0.00
Water heater	1.00	0.00	0.00	0.00	0.00	0.00
Air Conditioner	0.85	-1.40	1.56	22.92	-40.39	18.47
Lighting (Incandescent)	1.00	0.00	0.00	0.00	0.00	0.00
Lighting (Fluorescent)	0.14	0.77	0.09	0.06	0.34	0.60
Refrigerator	1.19	-0.26	0.07	0.59	0.65	-0.24
Clothes dryer	1.91	-2.23	1.33	2.51	-2.34	0.83
Computer	0.08	0.07	0.85	0.00	0.00	0.00
Cooking stove	1.00	0.00	0.00	0.00	0.00	0.00
Dishwasher	0.05	0.31	0.63	-0.56	2.20	-0.64
Exhaust Fan	0.98	0.02	0.00	0.69	0.25	0.06
Freezer	1.19	-0.26	0.07	0.59	0.65	-0.24
Hair Dryer	0.98	0.02	0.00	0.69	0.25	0.06
Iron	1.00	0.00	0.00	0.00	0.00	0.00

Microwave	-2.78	6.06	-2.28	0.00	0.00	0.00
Oven	1.00	0.00	0.00	0.00	0.00	0.00
Stereo system	1.00	0.00	0.00	0.00	0.00	0.00
TV set	1.00	0.00	0.00	0.00	0.00	0.00
Vacuum cleaner	0.98	0.02	0.00	0.69	0.25	0.06
Washing machine	0.05	0.31	0.63	-0.56	2.20	-0.64
Answer machine	0.08	0.07	0.85	0.00	0.00	0.00
Fax machine	0.08	0.07	0.85	0.00	0.00	0.00
Bread maker	1.00	0.00	0.00	0.00	0.00	0.00
Coffee machine	1.00	0.00	0.00	0.00	0.00	0.00
Kettles	1.00	0.00	0.00	0.00	0.00	0.00
Lamp	0.98	-0.03	0.06	-29.84	45.26	-14.42

TABLE AI.2
SUMMARISED LOAD SURVEY DATA

Equipment Type	**Household own One Unit/(%)**	**No. of Equipment in a House**	**No. of Working Hours**	**Rated Power/(W)**
Space heater	46.00%	4	1.5	2000
Water heater	96.00%	1	1	3600
Air Conditioner	10.00%	1	0	3450
Lighting (Incandescent)	100.00%	7	1.5	100
Lighting (Fluorescent)	100.00%	3	1.5	36
Refrigerator	74.70%	1	1	210
	25.00%	2	0.5	210
Clothes dryer	55.00%	1	0	2400
Computer	36.20%	1	0.5	400
Cooking stove	94.00%	1	0.25	1500
Dishwasher	26.00%	1	0	2400
Exhaust Fan	99.60%	1	0.5	100
Frezzer	60.00%	1	7	160
Hair Dryer	98.00%	1	0.125	1500
Iron	98.00%	1	0.125	1000
Microwave	78.90%	1	0.25	1300
Oven	94.00%	1	0	2400
Stereo system	82.30%	1	0.125	78
TV set	43.40%	1	0.25	200
	55.80%	2	0.125	200
Vacuum cleaner	78.90%	1	0	1000
Washing machine	97.00%	1	0	500
Answer machine	40.00%	1	0.1	10
Fax machine	10.00%	1	0.1	15
Bread maker	94.00%	1	0.15	850
Coffee machine	70.00%	1	0.2	800
Kettles	94.00%	1	0.2	2200
Lamp	98.00%	2	1.5	60
No. of houses in the urban area = 200000				

AI.2 Case Study and Discussion

A practical MV test distribution system topology is shown in Figure AI.4. It depicts a distribution feeder system in a *modern-planned* urban area. Moreover, high solar-PV penetration level is considered depicting a possible futuristic scenario. The network reduction and un-balanced to balanced conversion methods proposed in [54], [82] have been adopted to optimise the model and thereby

enhance the simulation effort. Among the various case-study cases carried out, only the results of some selected cases are presented and discussed.

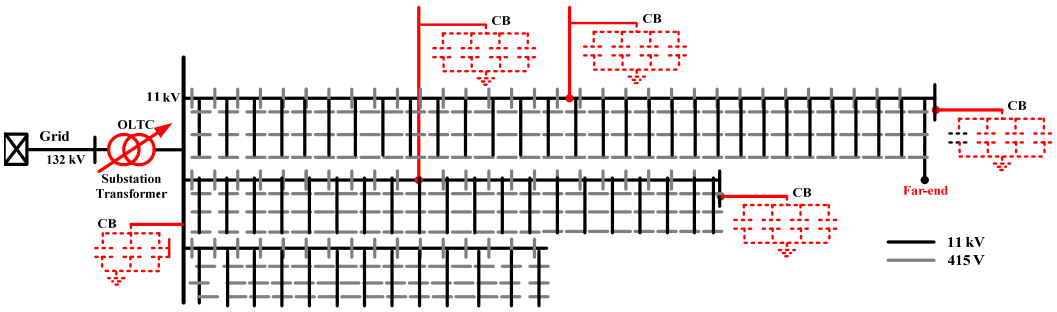

Figure AI.4: Test distribution system topology

The simulated load and solar-PV generation patterns at a neighbourhood (cluster of houses) is shown in Figure AI.5 and Figure AI.6 respectively. The solar generation pattern is mostly smooth and un-interrupted, but with some high intermittency incidents. It depicts a common solar-PV profile in a day with clear weather conditions and smooth power system operation (Figure AI.1(a)). The load profiles emulate modern life style of consumers in an urban area.

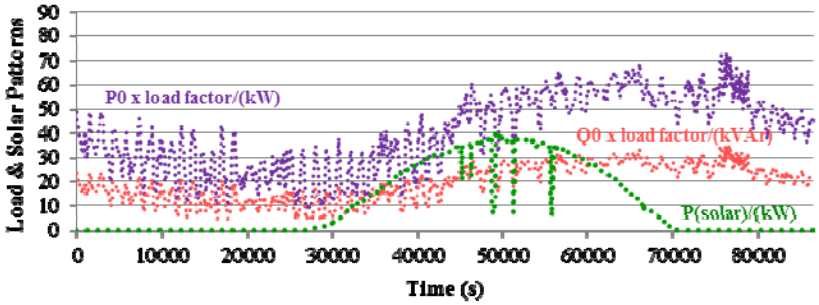

Figure AI.5: Simulated load and solar-PV penetration patterns in a neighbourhood

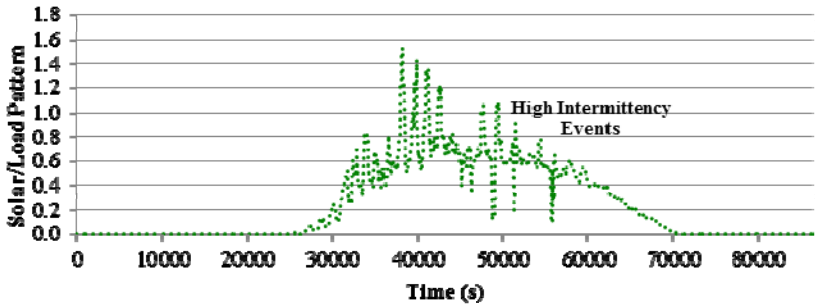

Figure AI.6: Simulated solar-PV penetration pattern in a neighbourhood in terms of solar**:** load ratio

AI.2.1: Case-1: a stand-alone control comprising substation OLTC

As mentioned in Section-AI.1, a stand-alone control comprising substation OLTC is considered for this case. The OLTC is modelled with 60 s time delay based on constant time-variant characteristics and non-sequential operation, (+8/-8) tap operations, 0.01250 pu voltage correction per tap (0.90 - 1.10) pu of system voltage limits), and 5^{th} tap position at start. The real-time controls of OLTC are modelled in detail for its operation without enacting line-drop compensation (LDC). The simulated dead-band for OLTC controls is twice the per unit value of voltage change per tap operation. The target voltage reduction for daily operation, ΔV is 10% at the substation level; and it aims peak-demand reduction as well as energy savings. According to Section-AI.1, the simulation results are analysed. In Figure AI.7, the variation of CVR factor for active power is presented, where the variation of CVR factor for reactive power is shown in Figure AI.8. The variation of reactive power imported from transmission system is shown in Figure AI.9; where Figure AI.10 shows the daily variation of power factor at substation level.

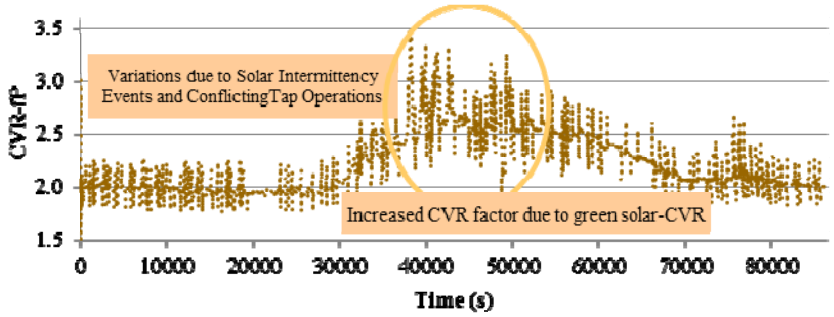

Figure AI.7: CVR factor for active power

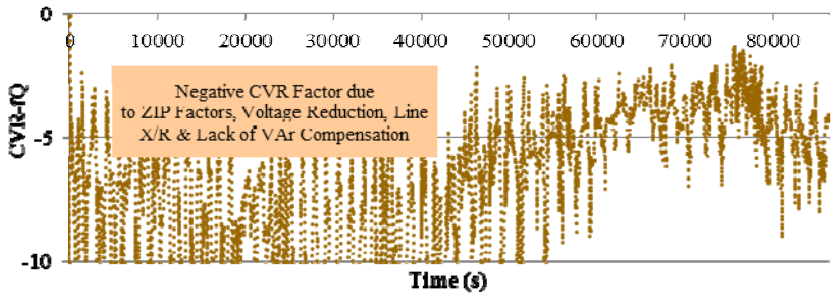

Figure AI.8: CVR factor for reactive power

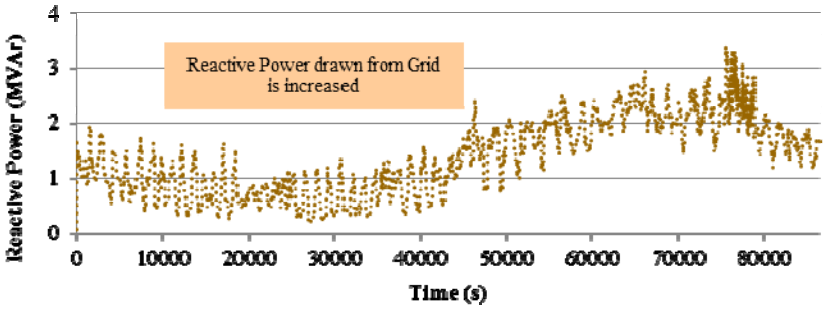

Figure AI.9: Reactive power imported from transmission system

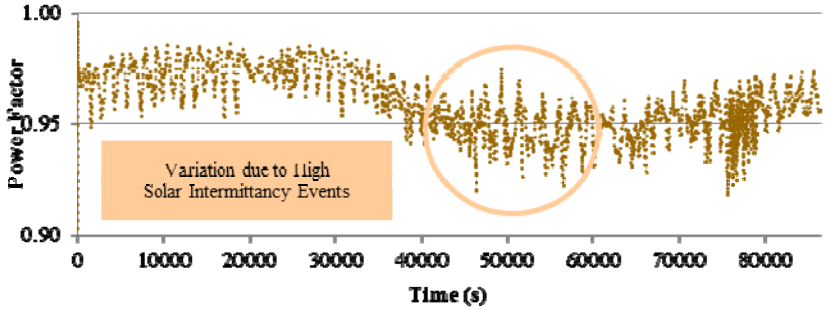

Figure AI.10: Power factor at the substation level

Monitored lowest voltage in MV feeder level, 0.8323 pu is experienced during CVR at the far end (Figure AI.4).

AI.2.2: Case-2: a stand-alone control comprising substation OLTC with a CB

According to Figure AI.1(b), in addition to the substation OLTC operation simulated in Case-1, a substation CB operation (i.e., with 0.5 MVA off-peak supply and 1.0 MVA peak supply) is considered.

In Figure AI.11, the variation of CVR factor for active power is presented, where the variation of CVR factor for reactive power is shown in Figure AI.12. The variation of reactive power imported from transmission system is shown in Figure AI.13; where Figure AI.14 shows the daily variation of power factor at substation level.

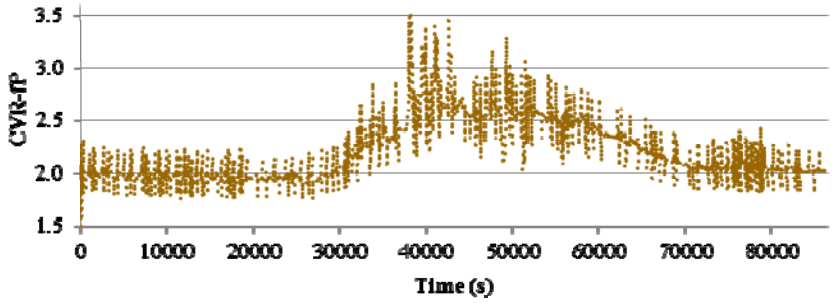

Figure AI.11: CVR factor for active power

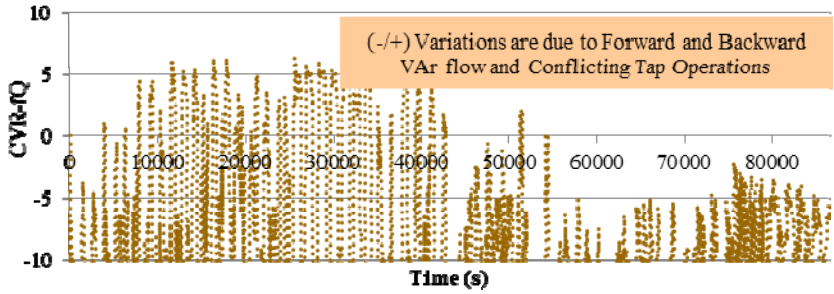

Figure AI.12: CVR factor for reactive power

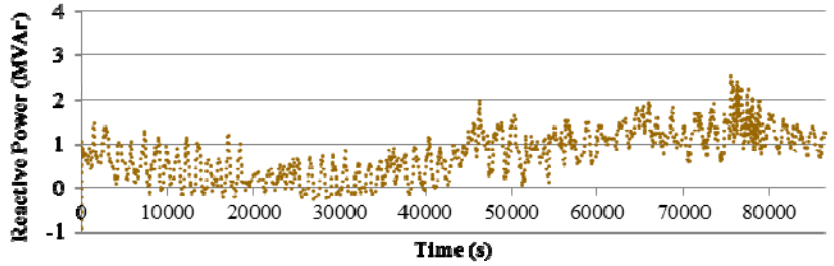

Figure AI.13: Reactive power imported from transmission system

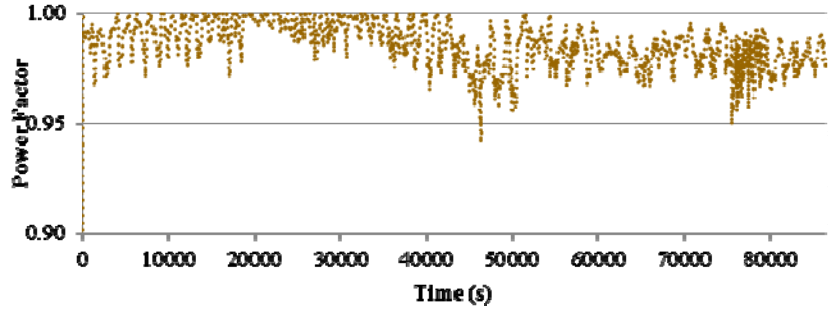

Figure AI.14: Power factor at the substation level

Monitored lowest voltage in MV feeder level, 0.8292 pu is experienced during CVR at the far end. The results of CVR analyses are compared with the results of CVR analyses of other case-study cases and presented in Figure AI.19.

AI.2.3: Case-3: a stand-alone control comprising substation OLTC with multiple line CBs

According to Figure AI.1(b), in addition to the substation OLTC operation simulated in Case-1, operation of multiple line CBs (i.e., each with 0.1 MVA off-peak supply and 0.2 MVA peak supply) are considered. These CBs are shown in Figure AI.4.

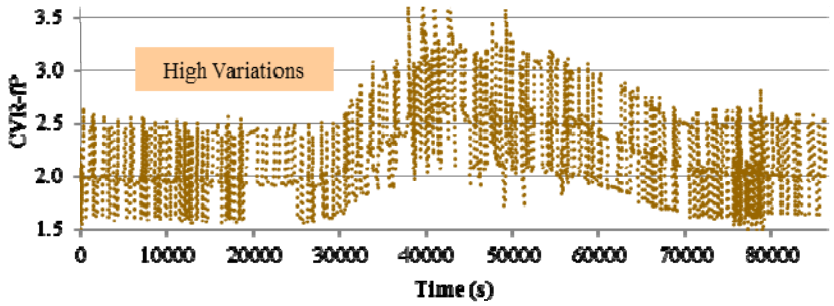

Figure AI.15: CVR factor for active power

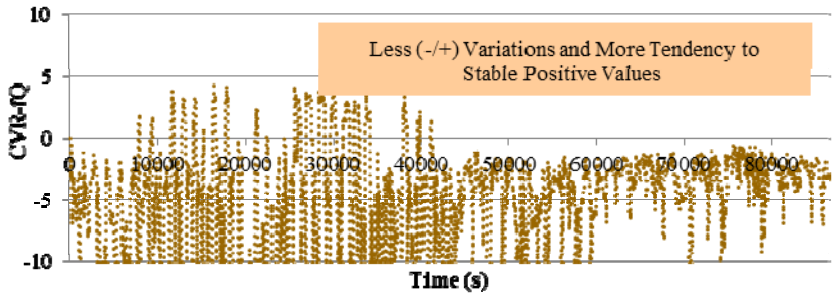

Figure AI.16: CVR factor for reactive power

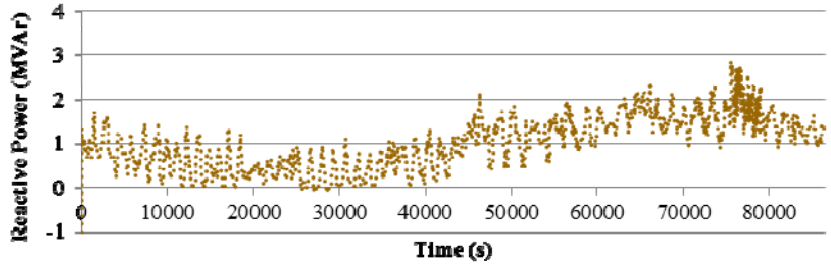

Figure AI.17: Reactive power imported from transmission system

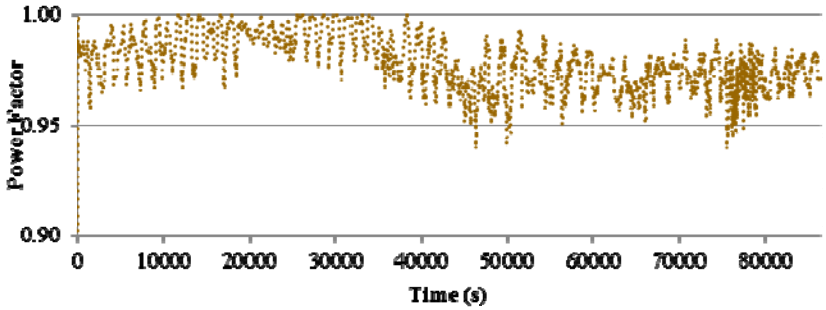

Figure AI.18: Power factor at the substation level

Monitored lowest voltage in MV feeder level, 0.8576 pu is experienced during CVR at the far end. The results of CVR analyses are shown in Figure AI.19. In each bar-chart, the vertical axis denotes Case-1 to 3.

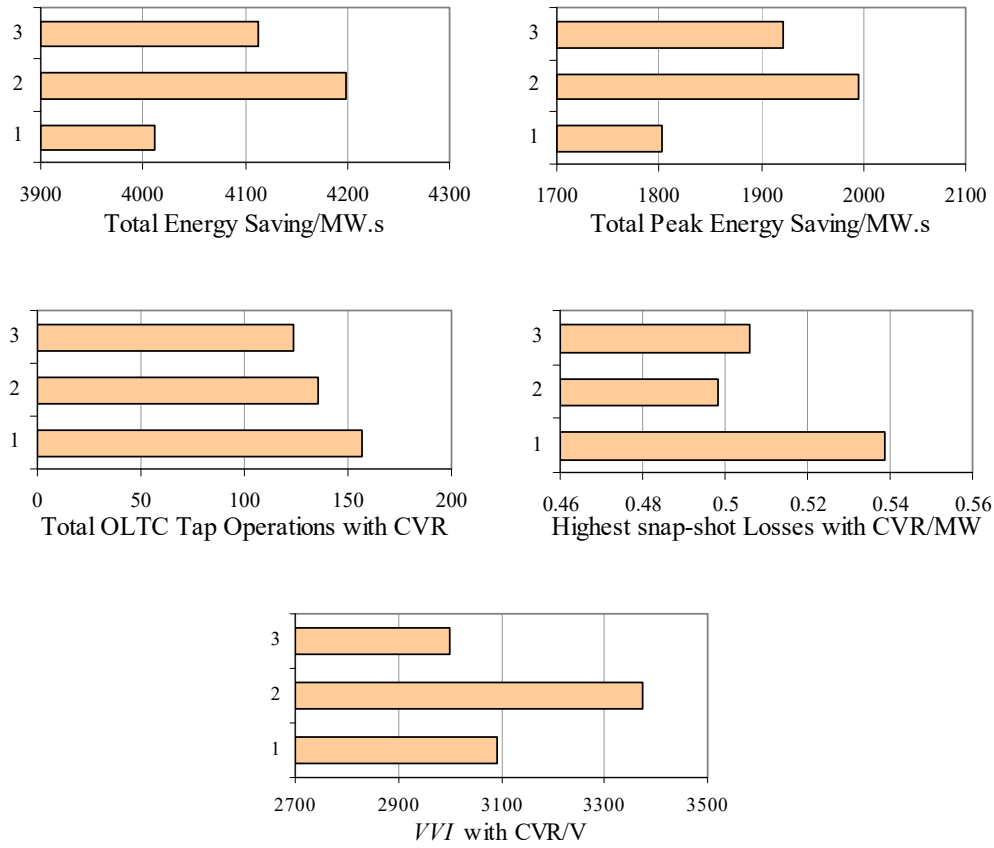

Figure AI.19: Results of CVR analyses: Case-1, 2 and 3

AI.3: Discussion on Case Study Findings

• Simulation Case-1: According to Figure AI.7, it can be seen that the solar-PV generation can improvise MW targets of CVR (from 2.0 to 2.5 CVR factor) during the period of solar-PV availability. This is called green solar-CVR, and it will have a significant impact in distribution systems which have peak load profiles also at the day time. High variations in the CVR factor can be seen due to high intermittency events in solar-PV power output. It can deteriorate the expected outcome from CVR. The number of OLTC tap operations is high (Figure AI.19), which is not the case in most of the present substations. However, this can be an issue in modern and planned urban distribution systems, where consumers have life styles leading to load variations and higher penetration of solar-PV. It would be further worsen in presence of highly intermittent and sudden loss of solar-PV as shown in Figure AI.1(a). The reactive power drawn from grid (Figure AI.8) is high with CVR mainly based on load ZIP factors, level of VAR support and line *X/R* ratio. Accordingly, the VAr CVR factor stays negative (Figure AI.9). Also, there is a tendency in lowering the power factor with CVR (Figure AI.10). This can be worst with further voltage reduction aiming to achieve higher MW CVR factor. According to the results of CVR analyses shown in Figure AI.19; the total energy savings is less compared to other cases. Moreover, the losses and tap-operations are high. However, lower *VVI* is experienced.

• Simulation Case-2: There is no significant change in MW CVR factor compared to Case-1 (Figure AI.11). However, VAr CVR factor varies from negative to positive values (Figure AI.12) due to forward and backward VAr-flow resultant from substation CB operation and system VAr requirements. On the other hand, the reactive power drawn from grid is significantly reduced (Figure AI.13), and the power factor is improvised except some variations (Figure AI.14). According to the results of CVR analyses shown in Figure AI.19, the highest energy savings by CVR are experienced. The number of OLTC tap operations is less compared to Case-1, while the lowest amount of losses is experienced. However, *VVI* is increased reducing the voltage at remote end bus, compared to Case-1 and Case-3.

• Simulation Case-3: In this case, it can be seen that there is a significant tendency for having positive and stable VAr CVR factor (Figure AI.15), compared to Case-1 and 2. The reactive power drawn from grid is also reduced, with improved power factor comprising lesser variations (Figure AI.16–Figure AI.18), compared to Case-1. According to the results of CVR analyses shown in Figure AI.19, the OLTC tap operations are further reduced compared to both Case-1 and Case-2; while remote end bus voltage is improvised and *VVI* is reduced due to the local and fast VAr support from multiple line CBs. The losses are also reduced compared to Case-1. However, after careful observations, it can be seen that there is a tendency for occurring high voltages in bus locations away from substation with the application of multiple CBs in presence of variations in high solar-PV (that are also difficult to forecast); which can deteriorate CVR factor. Moreover, there are significant variations in MW CVR factor (Figure AI.15), which intern can reduce the expected outcome (i.e., energy saving targets) from CVR.

In summary, it can be seen that there are possibilities for both positive and negative effects under each simulated conventional stand-alone Volt/VAr control method; while opportunities also exist for having high MW CVR factor in presence of high solar-PV penetration. However, achieving higher and stable MW CVR factor together with at least positive VAr CVR factor, higher power factor, minimum tap changer operations and voltage variations, lower losses, lower reactive power drawn from grid; and voltages within the stipulated limits including far end consumer locations can be a challenging task under stand-alone Volt/VAr control in modern urban distribution networks which on the other hand have best candidate substations and feeder systems for CVR. *Moreover, there can also be possibilities for significant interactions among Volt/VAr regulating devices and Volt/VAr support DG units (Figure AI.7) as highlighted in Chapter 3.* This can be more complicated in presence of stochastic nature of solar-PV and loads, and timely variations in load ZIP factors. Dynamic VAr management under CVR (i.e., subjected to large perturbations) will also be critical in certain system conditions. In such a scenario, adding dynamic VAr compensating devices (i.e., DSTATCOMs) will be one of the technical solutions; but it may lead to economic

considerations affecting wide implementation of CVR. Therefore, a precise techno-economical VAr management scheme will be required for addressing those issues, and thereby assuring the stable and reliable operation of the distribution grid under implementation of CVR program national-wide. Accurate derivation of load ZIP factors; fine mapping of VAr adequacy in each control-state; designing and implementing auto-adaptive optimal Volt/VAr control with *assured coordinated operation among Volt/VAr control devices* will pave the way for it.

APPENDIX-II: STATIC TOOL FOR ASSESSING DG IMPACT ON LINE DROP COMPENSATION IN VOLTAGE CONTROL DEVICES

This appendix presents a methodology for assessing the DG impact on operation of voltage control devices enabled with line drop compensation (LDC) modes, using first order voltage sensitivities of the regulating point voltage, V_{LC} estimated by LDC scheme to DG active and reactive power responses. Therefore, the assessment tool is $\Delta V_{LC}/\Delta Q_{PG}$ and $\Delta V_{LC}/\Delta Q_{DG}$, respectively. However, it is challengeable, because the *load centre* defined for a LDC scheme is normally a *fictitious point in space*. The derived mathematical formulations are tested using nodal voltage sensitivities proposed in [78] and multiple power flow (MPF) simulations. It is shown that the proposed methodology is capable of accurately estimating the DG impact on operation of voltage control devices enabled with LDC modes, which is indeed a useful static-tool to DNOs. The contents in this appendix are based on the publication [50] originated from this research project.

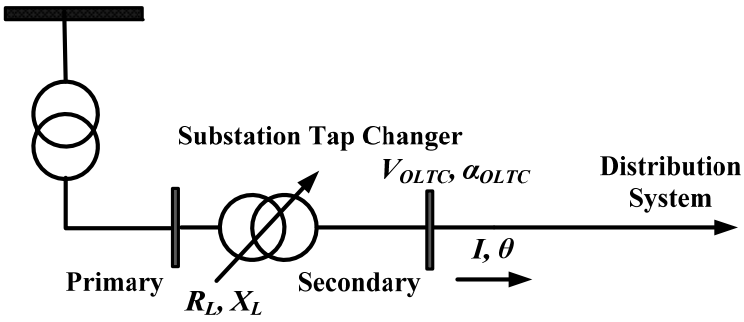

Figure AII.1: Substation transformer OLTC operated with LDC

$$V_{LC} = f\left(V_{OLTC}, \alpha_{OLTC}, I, \theta, R_L, X_L\right)$$

$$\Delta V_{LC} = \left(\frac{\partial V_{LC}}{\partial V_{OLTC}}\right)\Delta V_{OLTC} + \left(\frac{\partial V_{LC}}{\partial \alpha_{OLTC}}\right)\Delta \alpha_{OLTC} + \left(\frac{\partial V_{LC}}{\partial I}\right)\Delta I + \left(\frac{\partial V_{LC}}{\partial \theta}\right)\Delta \theta$$

$$\Delta V_{LC} = (LC1)\Delta V_{OLTC} + (LC2)\Delta \alpha_{OLTC} + (LC3)\Delta I + (LC4)\Delta \theta \qquad (01)$$

$$LC1 = \left(\frac{\partial V_{LC}}{\partial V_{OLTC}}\right), \quad LC2 = \left(\frac{\partial V_{LC}}{\partial \alpha_{OLTC}}\right), \quad LC3 = \left(\frac{\partial V_{LC}}{\partial I}\right), \quad LC4 = \left(\frac{\partial V_{LC}}{\partial \theta}\right)$$

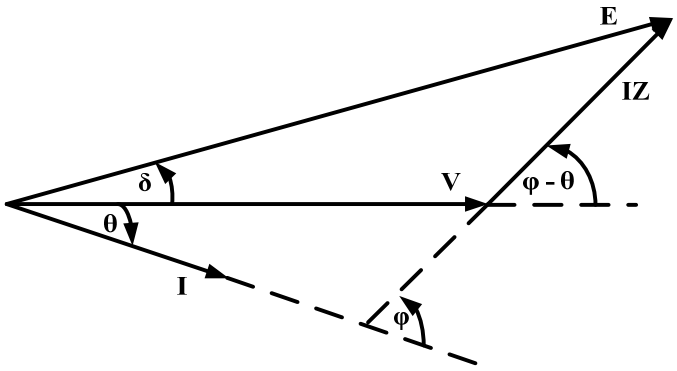

(a)

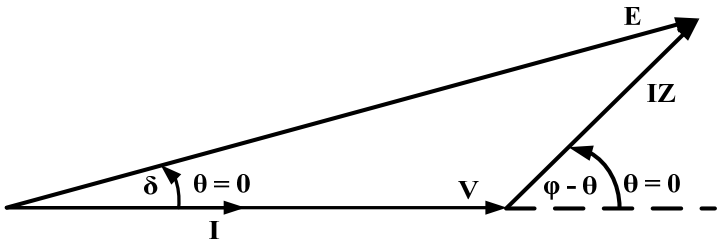

(b)

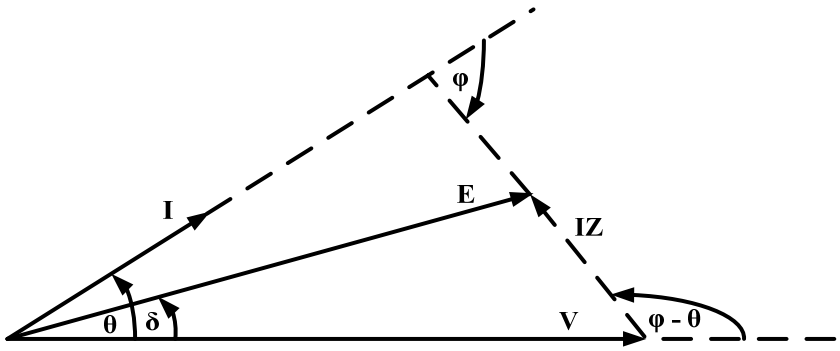

(c)

Figure AII.2: Phasor diagrams for θ: (a) negative, (b) zero and (c) positive cases

$$V_{LC} = \sqrt{\left(V_{OLTC}^{2} + I^{2} Z^{2} - 2V_{OLTC}\, IZ_{L} \times cos\left(\theta - \varphi_{L} + \alpha_{OLTC}\right)\right)} \qquad (02)$$

$$\varphi_{L} = tan^{-1}\left(\frac{X_{L}}{R_{L}}\right), \qquad Z_{L} = \sqrt{\left(R_{L}^{2} + X_{L}^{2}\right)}$$

$$LC1 = \left(\frac{\partial V_{LC}}{\partial V_{OLTC}}\right) = \frac{\left(V_{OLTC} - IZ_{L} \times cos\left(\theta - \varphi_{L} + \alpha_{OLTC}\right)\right)}{\sqrt{\left(V_{OLTC}^{2} + I^{2} Z_{L}^{2} - 2V_{OLTC}\, IZ_{L} \times cos\left(\theta - \varphi_{L} + \alpha_{OLTC}\right)\right)}}$$

$$LC2 = \left(\frac{\partial V_{LC}}{\partial \alpha_{OLTC}}\right) = \frac{V_{OLTC}\, IZ_L \times \sin\left(\theta - \varphi_L + \alpha_{OLTC}\right)}{\sqrt{\left(V_{OLTC}{}^2 + I^2 Z_L{}^2 - 2V_{OLTC}\, IZ_L \times \cos\left(\theta - \varphi_L + \alpha_{OLTC}\right)\right)}}$$

$$LC3 = \left(\frac{\partial V_{LC}}{\partial I}\right) = \frac{\left(IZ_L{}^2 - V_{OLTC}\, Z_L \times \cos\left(\theta - \varphi_L + \alpha_{OLTC}\right)\right)}{\sqrt{\left(V_{OLTC}{}^2 + I^2 Z_L{}^2 - 2V_{OLTC}\, IZ_L \times \cos\left(\theta - \varphi_L + \alpha_{OLTC}\right)\right)}}$$

$$LC4 = \left(\frac{\partial V_{LC}}{\partial \theta}\right) = \frac{V_{OLTC}\, IZ_L \times \sin\left(\theta - \varphi_L + \alpha_{OLTC}\right)}{\sqrt{\left(V_{OLTC}{}^2 + I^2 Z_L{}^2 - 2V_{OLTC}\, IZ_L \times \cos\left(\theta - \varphi_L + \alpha_{OLTC}\right)\right)}}$$

$\theta < 0$ Case :

$$I^2 Z^2 = E^2 + V^2 - 2EV \times \cos(\delta)$$

$$I = \frac{1}{Z}\sqrt{\left(E^2 + V^2 - 2EV \times \cos(\delta)\right)}, \qquad \Delta I = \left(\frac{\partial I}{\partial E}\right)\Delta E + \left(\frac{\partial I}{\partial V}\right)\Delta V + \left(\frac{\partial I}{\partial \delta}\right)\Delta\delta$$

$$\Delta I = (I1)\,\Delta E + (I2)\,\Delta V + (I3)\,\Delta\delta \qquad (03)$$

$$I1 = \left(\frac{\partial I}{\partial E}\right), \qquad I2 = \left(\frac{\partial I}{\partial V}\right), \qquad I3 = \left(\frac{\partial I}{\partial \delta}\right)$$

$$I1 = \left(\frac{\partial I}{\partial E}\right) = \frac{E - V.\cos(\delta)}{Z \times \sqrt{\left(E^2 + V^2 - 2EV \times \cos(\delta)\right)}}$$

$$I2 = \left(\frac{\partial I}{\partial V}\right) = \frac{V - E.\cos(\delta)}{Z \times \sqrt{\left(E^2 + V^2 - 2EV \times \cos(\delta)\right)}}$$

$$I3 = \left(\frac{\partial I}{\partial \delta}\right) = \frac{EV.\sin(\delta)}{Z \times \sqrt{\left(E^2 + V^2 - 2EV \times \cos(\delta)\right)}}$$

$$V^2 = I^2 Z^2 + E^2 - 2IZE \times \cos(\theta - \varphi + \delta), \qquad \varphi = \tan^{-1}\left(\frac{X}{R}\right) \text{ and } Z = \sqrt{\left(R^2 + X^2\right)}$$

$$V = \sqrt{\left(I^2 Z^2 + E^2 - 2IZE \times \cos(\theta - \varphi + \delta)\right)}, \qquad \pi/2 < \left|(\theta - \varphi + \delta)\right| < \pi$$

$$\Delta V = \left(\frac{\partial V}{\partial I}\right)\Delta I + \left(\frac{\partial V}{\partial E}\right)\Delta E + \left(\frac{\partial V}{\partial \theta}\right)\Delta\theta + \left(\frac{\partial V}{\partial \delta}\right)\Delta\delta \ , \qquad \Delta\theta = \frac{\Delta V - \left(\frac{\partial V}{\partial I}\right)\Delta I - \left(\frac{\partial V}{\partial E}\right)\Delta E - \left(\frac{\partial V}{\partial \delta}\right)\Delta\delta}{\left(\frac{\partial V}{\partial \theta}\right)}$$

$$\Delta\theta = \left(\frac{1-\theta 1 I 2}{\theta 3}\right)\Delta V - \left(\frac{\theta 2 + \theta 1 I 1}{\theta 3}\right)\Delta E - \left(\frac{\theta 4 + \theta 1 I 3}{\theta 3}\right)\Delta\delta \qquad (04)$$

$$\theta 1 = \left(\frac{\partial V}{\partial I}\right), \quad \theta 2 = \left(\frac{\partial V}{\partial E}\right), \quad \theta 3 = \left(\frac{\partial V}{\partial \theta}\right), \quad \theta 4 = \left(\frac{\partial V}{\partial \delta}\right)$$

$$\theta 1 = \left(\frac{\partial V}{\partial I}\right) = \frac{Z\left(IZ - E.\cos(\delta)\right)}{\sqrt{\left(I^2 Z^2 + E^2 - 2IZE \times \cos(\theta - \varphi + \delta)\right)}}$$

$$\theta 2 = \left(\frac{\partial V}{\partial E}\right) = \frac{E - IZ.\cos(\delta)}{\sqrt{\left(I^2 Z^2 + E^2 - 2IZE \times \cos(\theta - \varphi + \delta)\right)}}$$

$$\theta 3 = \left(\frac{\partial V}{\partial \theta}\right) = \frac{IZE.\sin(\theta - \varphi + \delta)}{\sqrt{\left(I^2 Z^2 + E^2 - 2IZE \times \cos(\theta - \varphi + \delta)\right)}}$$

$$\theta 4 = \left(\frac{\partial V}{\partial \delta}\right) = \frac{IZE.\sin(\theta - \varphi + \delta)}{\sqrt{\left(I^2 Z^2 + E^2 - 2IZE \times \cos(\theta - \varphi + \delta)\right)}}$$

$\theta = 0$ Case :

$$I^2 Z^2 = E^2 + V^2 - 2EV \times \cos(\delta)$$

$$I = \frac{1}{Z}\sqrt{\left(E^2 + V^2 - 2EV \times \cos(\delta)\right)}, \qquad \Delta I = \left(\frac{\partial I}{\partial E}\right)\Delta E + \left(\frac{\partial I}{\partial V}\right)\Delta V + \left(\frac{\partial I}{\partial \delta}\right)\Delta\delta$$

$$\Delta I = (I1)\Delta E + (I2)\Delta V + (I3)\Delta\delta \qquad (05)$$

$$I1 = \left(\frac{\partial I}{\partial E}\right), \qquad I2 = \left(\frac{\partial I}{\partial V}\right), \qquad I3 = \left(\frac{\partial I}{\partial \delta}\right)$$

$$I1 = \left(\frac{\partial I}{\partial E}\right) = \frac{E - V.\cos(\delta)}{Z \times \sqrt{\left(E^2 + V^2 - 2 \times E \times V \times \cos(\delta)\right)}}$$

$$I2 = \left(\frac{\partial I}{\partial V}\right) = \frac{V - E.cos(\delta)}{Z \times \sqrt{\left(E^{2} + V^{2} - 2 \times E \times V \times cos(\delta)\right)}}$$

$$I3 = \left(\frac{\partial I}{\partial \delta}\right) = \frac{EV.sin(\delta)}{Z \times \sqrt{\left(E^{2} + V^{2} - 2 \times E \times V \times cos(\delta)\right)}}$$

$$V^{2} = I^{2}Z^{2} + E^{2} - 2IZE \times cos(\theta - \varphi + \delta), \qquad \varphi = tan^{-1}\left(\frac{X}{R}\right) \quad and \quad Z = \sqrt{\left(R^{2} + X^{2}\right)}$$

$$V = \sqrt{\left(I^{2}Z^{2} + E^{2} - 2IZE \times cos(\theta - \varphi + \delta)\right)},$$

$\theta = 0$

$\Delta\theta = \neg\ \exists$ (06)

$\theta > 0$ Case :

$$I^{2}Z^{2} = E^{2} + V^{2} - 2EV \times cos(\delta)$$

$$I = \frac{1}{Z}\sqrt{\left(E^{2} + V^{2} - 2EV \times cos(\delta)\right)}, \qquad \Delta I = \left(\frac{\partial I}{\partial E}\right)\Delta E + \left(\frac{\partial I}{\partial V}\right)\Delta V + \left(\frac{\partial I}{\partial \delta}\right)\Delta\delta$$

$$\Delta I = (I1)\Delta E + (I2)\Delta V + (I3)\Delta\delta \qquad (07)$$

$$I1 = \left(\frac{\partial I}{\partial E}\right), \qquad I2 = \left(\frac{\partial I}{\partial V}\right), \qquad I3 = \left(\frac{\partial I}{\partial \delta}\right)$$

$$I1 = \left(\frac{\partial I}{\partial E}\right) = \frac{E - V.cos(\delta)}{Z \times \sqrt{\left(E^{2} + V^{2} - 2 \times E \times V \times cos(\delta)\right)}}$$

$$I2 = \left(\frac{\partial I}{\partial V}\right) = \frac{V - E.cos(\delta)}{Z \times \sqrt{\left(E^{2} + V^{2} - 2 \times E \times V \times cos(\delta)\right)}}$$

$$I3 = \left(\frac{\partial I}{\partial \delta}\right) = \frac{EV.sin(\delta)}{Z \times \sqrt{\left(E^{2} + V^{2} - 2 \times E \times V \times cos(\delta)\right)}}$$

$$V^2 = I^2 Z^2 + E^2 - 2IZE \times \cos(\theta - \varphi + \delta), \qquad \varphi = \tan^{-1}\left(\frac{X}{R}\right) \quad and \quad Z = \sqrt{\left(R^2 + X^2\right)}$$

$$V = \sqrt{\left(I^2 Z^2 + E^2 - 2IZE \times \cos(\theta - \varphi + \delta)\right)}, \qquad \left|(\theta - \varphi + \delta)\right| < \pi / 2$$

$$\Delta V = \left(\frac{\partial V}{\partial I}\right)\Delta I + \left(\frac{\partial V}{\partial E}\right)\Delta E + \left(\frac{\partial V}{\partial \theta}\right)\Delta\theta + \left(\frac{\partial V}{\partial \delta}\right)\Delta\delta\ , \qquad \Delta\theta = \frac{\Delta V - \left(\frac{\partial V}{\partial I}\right)\Delta I - \left(\frac{\partial V}{\partial E}\right)\Delta E - \left(\frac{\partial V}{\partial \delta}\right)\Delta\delta}{\left(\frac{\partial V}{\partial \theta}\right)}$$

$$\Delta\theta = \left(\frac{1 - \theta 1 I 2}{\theta 3}\right)\Delta V - \left(\frac{\theta 2 + \theta 1 I 1}{\theta 3}\right)\Delta E - \left(\frac{\theta 4 + \theta 1 I 3}{\theta 3}\right)\Delta\delta \qquad (08)$$

$$\theta 1 = \left(\frac{\partial V}{\partial I}\right), \quad \theta 2 = \left(\frac{\partial V}{\partial E}\right), \quad \theta 3 = \left(\frac{\partial V}{\partial \theta}\right), \quad \theta 4 = \left(\frac{\partial V}{\partial \delta}\right)$$

$$\theta 1 = \left(\frac{\partial V}{\partial I}\right) = \frac{Z(IZ - E.\cos(\delta))}{\sqrt{\left(I^2 Z^2 + E^2 - 2IZE \times \cos(\theta - \varphi + \delta)\right)}}$$

$$\theta 2 = \left(\frac{\partial V}{\partial E}\right) = \frac{E - IZ.\cos(\delta)}{\sqrt{\left(I^2 Z^2 + E^2 - 2IZE \times \cos(\theta - \varphi + \delta)\right)}}$$

$$\theta 3 = \left(\frac{\partial V}{\partial \theta}\right) = \frac{IZE.\sin(\theta - \varphi + \delta)}{\sqrt{\left(I^2 Z^2 + E^2 - 2IZE \times \cos(\theta - \varphi + \delta)\right)}}$$

$$\theta 4 = \left(\frac{\partial V}{\partial \delta}\right) = \frac{IZE.\sin(\theta - \varphi + \delta)}{\sqrt{\left(I^2 Z^2 + E^2 - 2IZE \times \cos(\theta - \varphi + \delta)\right)}}$$

Single DG at bus − k :

$$\begin{bmatrix}\Delta\alpha \\ \Delta V\end{bmatrix}_{2n\times 1} = \left[J^{-1}\right] \times \begin{bmatrix}\Delta P \\ \Delta Q\end{bmatrix}_{2n\times 1} \quad \forall \quad J^{-1} = \begin{bmatrix}M_{\alpha P} & M_{\alpha Q} \\ M_{VP} & M_{VQ}\end{bmatrix}_{2n\times 2n}, \quad J \equiv Jacobian\ \ matrix$$

$$\frac{\Delta V_{OLTC}}{\Delta P_{DG}} = \left(M_{VP}\right)_{oltc,k}, \qquad \frac{\Delta\alpha_{OLTC}}{\Delta P_{DG}} = \left(M_{\alpha P}\right)_{oltc,k} \qquad (09)$$

$$\frac{\Delta V_{OLTC}}{\Delta Q_{DG}} = \left(M_{VQ}\right)_{oltc,k}, \qquad \frac{\Delta\alpha_{OLTC}}{\Delta Q_{DG}} = \left(M_{\alpha Q}\right)_{oltc,k} \qquad (10)$$

$$\frac{\Delta I}{\Delta P_{DG}} = (I1)\times\left(M_{VP}\right)_{oltc,k} + (I3)\times\left(\left(M_{\alpha P}\right)_{oltc,k} - \left(M_{\alpha P}\right)_{(oltc+1),k}\right) + \\ + (I2)\times\left(M_{VP}\right)_{(oltc+1),k}$$

$$\frac{\Delta I}{\Delta Q_{DG}} = (I1)\times\left(M_{VQ}\right)_{oltc,k} + (I3)\times\left(\left(M_{\alpha Q}\right)_{oltc,k} - \left(M_{\alpha Q}\right)_{(oltc+1),k}\right) + \\ + (I2)\times\left(M_{VQ}\right)_{(oltc+1),k}$$

$$\frac{\Delta\theta}{\Delta P_{DG}} = \left(\frac{1-\theta1.I2}{\theta3}\right)\times\left(M_{VP}\right)_{(oltc+1),k} - \left(\frac{\theta2+\theta1.I1}{\theta3}\right)\times\left(M_{VP}\right)_{oltc,k} - \\ - \left(\frac{\theta4+\theta1.I3}{\theta3}\right)\times\left(\left(M_{\alpha P}\right)_{oltc,k} - \left(M_{\alpha P}\right)_{(oltc+1),k}\right)$$

$$\frac{\Delta\theta}{\Delta Q_{DG}} = \left(\frac{1-\theta1.I2}{\theta3}\right)\times\left(M_{VQ}\right)_{(oltc+1),k} - \left(\frac{\theta2+\theta1.I1}{\theta3}\right)\times\left(M_{VQ}\right)_{oltc,k} - \\ - \left(\frac{\theta4+\theta1.I3}{\theta3}\right)\times\left(\left(M_{\alpha Q}\right)_{oltc,k} - \left(M_{\alpha Q}\right)_{(oltc+1),k}\right)$$

$$\frac{\Delta V_{LC}}{\Delta P_{DG}} = (LC1)\times\left(M_{VP}\right)_{oltc,k} + (LC2)\times\left(M_{\alpha P}\right)_{oltc,k} + \\ + (LC3)\times\left((I1)\times\left(M_{VP}\right)_{oltc,k} + (I2)\times\left(M_{VP}\right)_{oltc+1,k} + (I3)\times\left(\left(M_{\alpha P}\right)_{oltc,k} - \left(M_{\alpha P}\right)_{oltc+1,k}\right)\right) + \\ + (LC4)\times\begin{pmatrix}\left(\frac{1-\theta1.I2}{\theta3}\right)\times\left(M_{VP}\right)_{oltc+1,k} - \left(\frac{\theta2+\theta1.I1}{\theta3}\right)\times\left(M_{VP}\right)_{oltc,k} - \\ -\left(\frac{\theta4+\theta1.I3}{\theta3}\right)\times\left(\left(M_{\alpha P}\right)_{oltc,k} - \left(M_{\alpha P}\right)_{oltc+1,k}\right)\end{pmatrix} \qquad (11)$$

$$\frac{\Delta V_{LC}}{\Delta Q_{DG}} = (LC1)\times\left(M_{VQ}\right)_{oltc,k} + (LC2)\times\left(M_{\alpha Q}\right)_{oltc,k} + \\ + (LC3)\times\left((I1)\times\left(M_{VQ}\right)_{oltc,k} + (I2)\times\left(M_{VQ}\right)_{oltc+1,k} + (I3)\times\left(\left(M_{\alpha Q}\right)_{oltc,k} - \left(M_{\alpha Q}\right)_{oltc+1,k}\right)\right) + \\ + (LC4)\times\begin{pmatrix}\left(\frac{1-\theta1.I2}{\theta3}\right)\times\left(M_{VQ}\right)_{oltc+1,k} - \left(\frac{\theta2+\theta1.I1}{\theta3}\right)\times\left(M_{VQ}\right)_{oltc,k} - \\ -\left(\frac{\theta4+\theta1.I3}{\theta3}\right)\times\left(\left(M_{\alpha Q}\right)_{oltc,k} - \left(M_{\alpha Q}\right)_{oltc+1,k}\right)\end{pmatrix} \qquad (12)$$

Multiple DG case :

$$\frac{\Delta V_{LC}}{\Delta P_{DG}} = \frac{\Delta V_{LC}}{\Delta P_{DG1}} + \frac{\Delta V_{LC}}{\Delta P_{DG2}} + \frac{\Delta V_{LC}}{\Delta P_{DG3}} + \frac{\Delta V_{LC}}{\Delta P_{DG4}} + \ldots\ldots + \frac{\Delta V_{LC}}{\Delta P_{DG(g\text{-}1)}} + \frac{\Delta V_{LC}}{\Delta P_{DGg}} \tag{13}$$

$$\frac{\Delta V_{LC}}{\Delta Q_{DG}} = \frac{\Delta V_{LC}}{\Delta Q_{DG1}} + \frac{\Delta V_{LC}}{\Delta Q_{DG2}} + \frac{\Delta V_{LC}}{\Delta Q_{DG3}} + \frac{\Delta V_{LC}}{\Delta Q_{DG4}} + \ldots\ldots + \frac{\Delta V_{LC}}{\Delta Q_{DG(g\text{-}1)}} + \frac{\Delta V_{LC}}{\Delta Q_{DGg}} \tag{14}$$

APPENDIX-III: TESTING METHODOLOGY FOR VOLTAGE CONTROLLERS

This appendix outlines typical testing methodology which is also suitable for voltage controllers. During the design and development of a controller, there are many consecutive stages and corresponding validation methods which have to be used in the different processes. The main stages are (a) concept algorithm, (b) prototype and (c) realisation as illustrated in Figure AIII.1 [7].

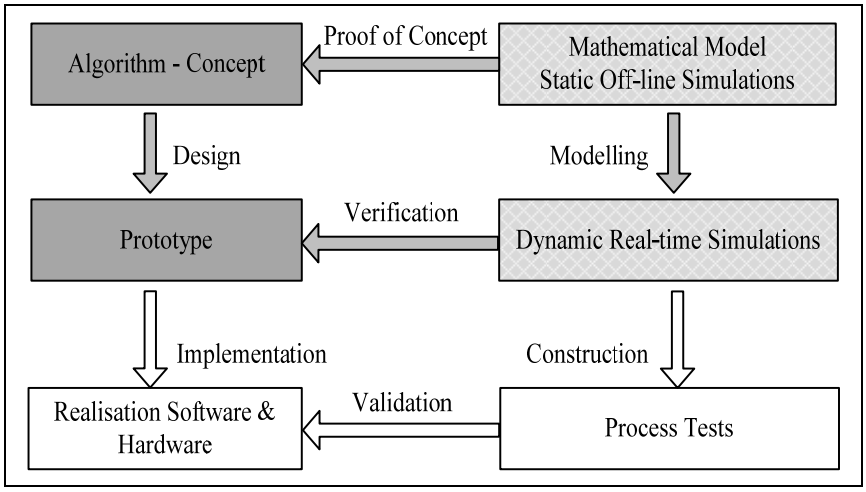

Figure AIII.1: Diagrmatic representation of the process of testing control algorithms

During the first stage of a development process (i.e., concept-algorithm), the method or algorithm is drawn up and elaborated. When the concept has taken a more specific form, it is important to prove its functionality and feasibility i.e., the proof of concept are needed. Practically this is achieved by a mathematical model and scenario based static off-line simulations. After the conceptual design has been proofed, the prototype is developed for verification. The process of transforming a concept to a prototype may introduce issues, for example related to communication time delays and interfacing that are not considered during the proof of concept. Next, the scenario based dynamic simulations by coupling the prototype with the co-simulation environment are carried out. During the development of a prototype, iterative refinements of the algorithm are often

necessary and having a dynamic real-time simulation set-up would be an added advantage. In the realisation stage, the validation process is commenced. The related software development for hardware is commonly guided by different methods i.e. agile methods, extreme programming and test driven development. Field test cases are used to validate the behaviour of software parts from unit to integration and system test; and next the required hardware is built. At this stage, it is important to test the controller in the real environment acting on the real process. This is usually done in some kind of demo application if possible i.e., a copy of the real process is either implemented. The controller is often tested in two steps i.e. (a) open loop test and (b) final closed loop tests. In open loop tests, the controller is connected to the real process and receives the inputs from the process. Since the outputs of the controller are not connected to the process, the controller has no influence on the behaviour of the process. However, the controller responses can be measured and validated before the closed loop tests. In the closed loop tests, the controller is tested in real controlled environment. The commissioning of the controller in the closed loop real world setup completes the validation process. However, in most of the field applications, the controller parameters have to be readjusted and experience can give feedback for further improvement and development in the control algorithm. Moreover, it is better to test the controller performance under different scenarios of distribution system operation i.e., under (a) normal operation, (b) step voltage response, (c) load excursion, (d) system fault and (e) availability of DG (i.e., DG connection, disconnection and response change). In this research project, the proposed control algorithms are tested by (a) proof of concept using mathematical models and scenario based off-line simulations with static models of the test distribution systems, and (b) prototype verification using scenario based on-line simulations with dynamic model of the test distribution systems.

APPENDIX-IV: SEARCHING MECHANISM INCORPORATED IN CONTROL LAYER-2 OF CHAPTER 5

This appendix presents the searching mechanism, which has been developed for implementing the control layer-2 and control layer-3 of Chapter 5. The Chapter 5 is based on tuning the controller parameters of voltage control devices and Volt/VAr support DG units in modern distribution systems.

Step-I: Derive the required voltage sensitivities as follows, and define p_{kj} and p_{cbx} values within the DG and CB constraints. Please note that the derivations are based on the operating points and associated system Jacobian matrix, [J] determined by Newton-Raphson based power flow calculations. J_{VP} and J_{VQ} denote matrix of partial derivatives, $\delta V/\delta P$ where V is voltage magnitude and P is active power; and matrix of partial derivatives, $\delta V/\delta Q$ where Q is reactive power; respectively. $J_{\alpha P}$ and $J_{\alpha Q}$ denote matrix of partial derivatives, $\delta\alpha/\delta P$ where α is phasor angle of nodal voltages; and matrix of partial derivatives, $\delta\alpha/\delta Q$. These voltage sensitivity values are used for estimating the nodal voltage change, ΔV_i (i.e., i=1, …, m) for change in VAr supply from a DG unit, ΔV_{DG} and a CB, ΔV_{CB}.

$$\left[\frac{\Delta P}{\Delta Q}\right]_{2m\times 1} = [J]_{2m\times 2m}\left[\frac{\Delta\alpha}{\Delta V}\right]_{2m\times 1}, \qquad J^{-1} = \left[\begin{array}{c|c} J_{\alpha P} & J_{\alpha Q} \\ \hline J_{VP} & J_{VQ} \end{array}\right]_{2m\times 2m}$$

$$[\Delta V]_{m\times 1} = \left[J_{VQ}\right]_{m\times m} \times [\Delta Q]_{m\times 1}$$

$$\Delta V \in \left(\Delta V_1,\ \Delta V_2,\ \Delta V_x,\ .....,\ \underbrace{\Delta V_i}_{node-i},\ .....,\ \Delta V_k,\ .....,\ \Delta V_m\right)$$

$$\Delta Q \in \left(\Delta Q_1,\ \Delta Q_2,\ \underbrace{\Delta Q_{CB}}_{node-x\ (i=x)},\ ...,\ \Delta Q_i, ...,\ \underbrace{\Delta Q_{DG}}_{node-k\ (i=k)},\ ...,\ \Delta Q_m\right)$$

$$\left[J_{VQ}\right] \in \left[\Delta V / \Delta Q_{DG}\right]_{i\times k},\ \left[\Delta V / \Delta Q_{CB}\right]_{i\times x}$$

Step-II:

1. Start search with only [grand-parent] combinations and the state of VAr reference values referred to p_{1j} (i.e., j=1, …, n1) in the search space. The voltage sensitivity values are used for estimating the ΔV_i values as follows.

$$\Delta V_i = \Delta V / \Delta Q_{DG}\Big|_{i,k} \times p_{kj} \quad \forall \quad k = 1$$

2. Search for states of VAr reference values referred to p_{1j} data set of the grand-parent (i.e., from j=1 to j=n1) until the value of objective function given by (2), J_1 = 0 or $J_1 \approx 0$ (Figure AIV.1).

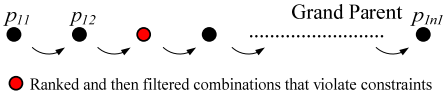

Figure AIV.1: Search space partitioned for grand-parent combinations

if J_1 = 0 or $J_1 \approx 0$ is reached, ***stop***

else continue the search as done in Step-II and orderly with only [parent] combinations, next only **[**eldest-child] combinations, ……, next only **[**youngest-child] combinations, and next only [family-friends] combinations (Figure AIV.2).

$$\Delta V_i = \Delta V / \Delta Q_{DG}\Big|_{i,k} \times p_{kj} \quad \forall \quad k = 2, ..., y$$
$$\Delta V_i = \Delta V / \Delta Q_{CB}\Big|_{i,x} \times p_{cbx} \quad \forall \quad x = 1, ..., h$$

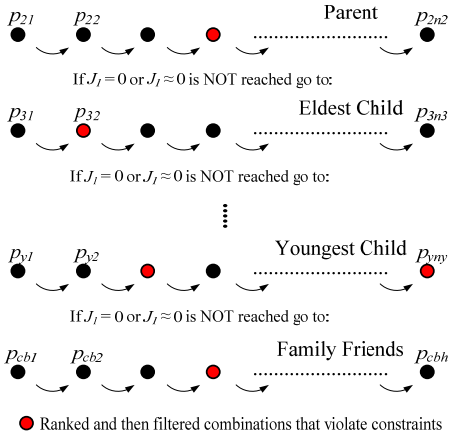

Figure AIV.2: Search spaces partitioned for parent, eldest-child, youngest-child and friends

if $J_1 = 0$ or $J_1 \approx 0$ is reached, ***stop***

else go to **Step-III.**

3. Rank all the combinations that violate the constraints (i.e. nodal voltage constraints), from j=1 to j=nk following the lowest (-) value to the highest (+) value of p_{kj} and from x=1 to x=h of p_{cbx}. The (-) and (+) values of p_{kj} denote the possible combinations of DG reactive power import and export based on reactive power capability.

Step-III:

1. Start the search with only [grand-parent]-[parent] combinations and the respective state of VAr reference values referred to p_{1j} (i.e., j=1, …, n1) and p_{2j} (i.e., j=1, …, n2). The ΔV_i values are estimated as follows.

$$\Delta V_i = \underbrace{\Delta V / \Delta Q_{DG}\big|_{i,k} \times p_{kj}}_{k=1\,(\text{Step}-\text{I})} + \underbrace{\Delta V / \Delta Q_{DG}\big|_{i,k} \times p_{kj}}_{k=2\,(\text{Step}-\text{I})}$$

2. Search for the states of VAr reference values in the combinations referred to p_{1j} and p_{2j} data sets (excluding the combinations ranked in Step-II(3), p_{1j} and p_{2j}; which are with the same sign (i.e., +/-) where associated voltage sensitivities are also with the same sign), until the value of objective function given by (2), $J_1 = 0$ or $J_1 \approx 0$ is achieved (Figure AIV.3).

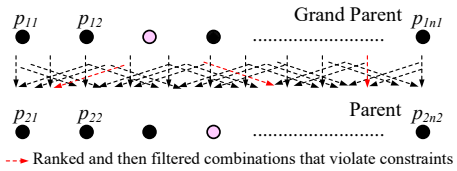

Figure AIV.3: Search space partitioned for grand-parent-parent combinations

if $J_1 = 0$ or $J_1 \approx 0$ is reached, ***stop***

else continue the search as done in Step-III and orderly with only [grand-parent]-[eldest-child] combinations, ……, next only [grand-parent]-[youngest-child] combinations, and next only [grand-parent]-[friends] combinations (Figure AIV.4).

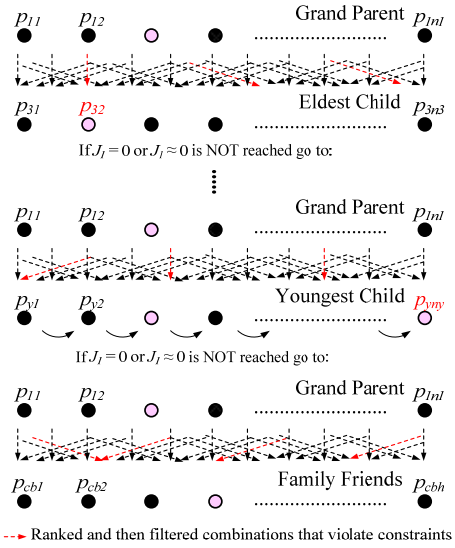

Figure AIV.4: Search spaces partitioned for grand-parent-eldest-child,…, grand-parent-youngest-child and grand-parent- friends combinations

if $J_1 = 0$ or $J_1 \approx 0$ is reached, ***stop***

else continue the search similarly and orderly with only [parent]-[eldest-child] combinations, ….., up to only **[**youngest-child]-[friends] combinations

if $J_1 = 0$ or $J_1 \approx 0$ is reached, ***stop***

else go to **Step-IV.**

3. Rank all the combinations that violate the constraints, as done in Step-II(3).

Step-IV: Continue the search with same methodology and orderly with *other possible combinations* from [grand-parent] to [friends] in the search space up to [grand-parent]-[parent]-[eldest-child]-....-[youngest-child]-[friends] combinations.

Step-V: If $J_1 = 0$ or $J_1 \approx 0$ is not reached in all steps, select the solution which gives the utmost minimum value for J_1 as the final solution for *Control Layer-2*.